Codimension-Two Free Boundary Problems

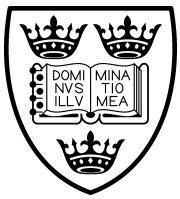

Keith Gillow
St Catherine's College
University of Oxford

A thesis submitted for the degree of
Doctor of Philosophy

November 1998

To my Parents
for their unending support and encouragement

Acknowledgements

I would like to thank Dr S.D. Howison and Dr J.R. Ockendon for their encouragement and guidance as my supervisors, Dr S.J. Chapman for all his advice and assistance and the Engineering and Physical Sciences Research Council for their continued support. I would also like to thank the DH9 crew and the computing support staff for providing several sanity preserving distractions. Finally I would like to thank my Parents and Kathryn for all their support, faith and interest.

Abstract

Over the past 30 years the study of free boundary problems has stimulated much work. However, there exists a widely occurring, but little studied subclass of free boundary problems in which the free boundary has dimension two fewer than that of the underlying space rather than the more commonly studied case of one less. These problems are called *codimension-two* free boundary problems.

In Chapter 1 the typical geometries required for such problems, the main mathematical techniques and the methodology used are discussed. Then, in Chapter 2, the techniques required to solve them are demonstrated using the particular example of the water entry problem. Further results for the water entry problem are then derived including an analysis of the relatively poorly understood water exit problem. In Chapter 3 a review is given of some classical contact and crack problems in solid mechanics. The inclusion of a cohesive zone in a dynamic type-III crack problem is considered. The Muskhelishvili potential method is presented and used to solve both a contact and crack problem. This enables the solution of a type-I crack problem relating to an ink delivery system to be found. In Chapter 4 a problem posed by car windscreen forming is addressed. A local solution near a corner is analysed to explain when and how point forces occur at the corners of the frame on which the simply supported windscreen rests. Then the full problem is solved numerically for different types of boundary condition. Chapters 5 and 6 deal with several sintering problems in viscous flow highlighting the value of the methodology introduced in Chapter 1. It will be shown how the Muskhelishvili potential method also carries over to Stokes flow problems. The difficulties of matching to an inner as opposed to an outer region are investigated. Lastly two interface problems between immiscible liquids are considered which show how the solution procedure is adapted when the field equation in the thin region is non-trivial. In the final chapter results are summarised, open problems listed and conclusions drawn.

Contents

1 Introduction **1**

1.1 Typical geometry required for a codimension-two problem 2

1.2 Where codimension-two problems occur 3

1.2.1 Water entry 4

1.2.2 Viscous sintering 5

1.3 One-phase and two-phase problems 6

1.4 Outline of the general methodology 7

1.5 Mathematical techniques 8

1.5.1 Matched asymptotic expansions 8

1.5.1.1 A note on log matching 8

1.5.2 The Riemann problem 9

1.5.3 Variational formulations 10

1.6 Layout and aims 12

1.7 Statement of originality 14

2 The water entry problem **16**

2.1 The two dimensional water entry model 17

2.1.1 The outer problem 18

2.1.1.1 The codimension-two free boundary problem 19

2.1.1.2 Determination of the surface elevation 23

2.1.1.3 The law of motion of the free point 23

2.1.2 The inner and jet regions 25

2.1.3 The leading order pressure and force on the body 25

2.2 Variational formulation of the outer problem 26

2.3 Stability and water exit 29

2.3.1 A local stability analysis of the water entry problem 29

2.3.1.1 The local space and time model 30

2.3.1.2 Comparison with other types of stability analysis . . 36

2.3.2 A linearised initial value problem 36
2.3.2.1 Determination of the velocity potential 38
2.3.2.2 Derivation of the free surface elevation 40
2.3.2.3 The law of motion of the free boundary 44
2.3.3 Water exit problems 46
2.3.4 Conjectures on how to pose an exit problem 47
2.3.5 The Basilisk lizard 47
2.4 Extensions to the model 48
2.4.1 Bodies initially in contact with the fluid 48
2.4.2 Non-constant body velocity 48
2.4.2.1 Three-dimensional axisymmetric problem 51
2.4.2.2 The 'bouncing' bomb 53
2.4.3 Non-symmetric body shape 54

3 Solid contact and crack problems 56
3.1 Equations of linear elasticity 60
3.1.1 Airy stress function 62
3.1.2 The Muskhelishvili potential 63
3.2 A dynamic type-III crack moving at a constant velocity 67
3.2.1 Solution when the crack face is stress free along its entire length 68
3.2.2 Inclusion of a cohesive zone 72
3.3 Two-dimensional contact of two identical elastic bodies 75
3.3.1 Normal contact force 76
3.3.1.1 Solution of the codimension-two model 78
3.3.1.2 Alternative solution procedure using the Muskhelishvili potential 82
3.3.1.3 Determination of the normal traction 84
3.3.1.4 Parameters determining the contact region 85
3.3.2 Application of a shearing force after initially applying a normal force 86
3.3.2.1 Determination of the traction with no slip 87
3.3.2.2 Determination of the traction with slip 88
3.3.3 Simultaneous variations of normal and shearing forces 90
3.4 A static type-I crack problem 91
3.4.1 An ink delivery problem 92

4 Contact of an elastic plate supported by a frame **100**
4.1 Thin plate equations . . . 101
4.1.1 Variational formulation . . . 106
4.1.2 Nondimensional thin plate model . . . 107
4.2 Behaviour near a corner . . . 108
4.2.1 Asymptotics of the solution near a critical angle . . . 113
4.3 Consideration of the problem for a rectangular plate . . . 115
4.3.1 The codimension-two free boundary problem . . . 116
4.3.1.1 Local analysis near a free point . . . 117
4.3.1.2 Numerical solution . . . 118

5 Stokes flow problems **127**
5.1 Point sources in Stokes flow . . . 130
5.1.1 The outer problem . . . 134
5.1.2 The codimension-two problem . . . 135
5.1.2.1 A local analysis at a free point . . . 136
5.1.2.2 Solution of the codimension-two problem . . . 138
5.1.2.3 Determination of the free surface . . . 141
5.1.2.4 The law of motion of the free point . . . 141
5.2 Stokes flow with non-zero surface tension . . . 142
5.2.1 The full problem . . . 142
5.2.2 The codimension-two problem . . . 143
5.2.3 The inner region . . . 144
5.2.4 Matching difficulties . . . 145
5.2.5 Reassessment of the codimension-two region . . . 146
5.2.6 Matching revisited . . . 148
5.2.7 Minimising the effort and maximising the results . . . 149
5.2.8 Extension to different initial free boundary shapes . . . 151
5.3 Ice Closure . . . 153
5.3.1 Rigid impermeable bed . . . 154
5.3.2 Inclusion of sediment creep . . . 156

6 Hele–Shaw problems **158**
6.1 Point sources in a Hele-Shaw cell . . . 159
6.2 The three discs problem . . . 163
6.2.1 The first outer problem . . . 164
6.2.2 The first codimension-two problem . . . 165

6.2.2.1 Determination of the free surface position 167
6.2.2.2 The law of motion of the free point 167
6.2.3 The second outer problem 168
6.2.4 The second codimension-two region 169
6.2.4.1 Determination of the free surface position 171
6.2.4.2 The law of motion of the free point 171
6.2.5 The third outer problem 172
6.2.6 The third codimension-two region 172
6.2.6.1 Determination of the free surface position 174
6.2.6.2 The law of motion of the free point 174
6.2.7 Extension to n discs 175
6.3 Muskat problems 177
6.3.1 Problem 1: Circular source at infinity 180
6.3.2 Problem 2: Contact and non-contact regions interchanged . . 181

7 Conclusions and further work **183**
7.1 Summary 183
7.2 General remarks 187
7.3 Two open problems 188
7.3.1 Hele-Shaw flow with non-zero surface tension 188
7.3.2 A note on inviscid sintering 190
7.4 Further work 191

A Sobolev and Hilbert spaces **193**

B Riemann boundary value problems and index **197**
B.1 The Riemann problem for a simply connected domain 198
B.1.1 Solution of the homogeneous problem 199
B.1.2 Solution of the non-homogeneous problem 201
B.2 Solution of the Riemann problem with discontinuous coefficients . . . 203
B.2.1 Reduction to a problem with continuous coefficients 204
B.2.2 Solution of the homogeneous problem 206
B.2.3 Solution of the non-homogeneous problem 207
B.3 The Riemann problem for open contours 208
B.4 Inversion of a Cauchy integral 212
B.5 The Riemann problem for a non-Hölder free term 213

C The Stokes flow sintering matching condition **215**
C.1 Solution of Stokes flow with a cusp 215
C.1.1 Solution following the procedure suggested by Morgan 215
C.1.2 Direct method of obtaining the same result 219

D The Ivantsov parabola **220**

Bibliography **224**

List of Figures

1.1 Typical geometry leading to a two-dimensional codimension-two problem. 3
1.2 The water entry problem. 4
1.3 The Stokes flow viscous sintering problem. 5
1.4 The one-dimensional obstacle problem. 10

2.1 The geometry of the water entry problem. 16
2.2 The codimension-one water entry problem. 17
2.3 The codimension-two free boundary problem. 20
2.4 The free surface shape for a wedge. 24
2.5 The free surface shape for a parabola. 24
2.6 The perturbed problem for the velocity potential ϕ. 37
2.7 The domain of definition of the free surface elevation for the water entry and water exit problems. 46
2.8 The position of the free point $d(t)$ in the case $d(0) = 0.5$. 49
2.9 The free surface shape for a wedge initially in contact with the fluid. . 49
2.10 The free surface shape for a dropped parabolic body. 51

3.1 The three types of solid mechanics problems to be considered. 56
3.2 Schematic of three types of crack. 58
3.3 The initial configuration of the crack. 68
3.4 The codimension-two type-III dynamic crack problem. 69
3.5 The codimension-two type-III dynamic crack problem in the moving frame. 70
3.6 The domain of the crack problem in the z, $\tilde{s}$ and s planes. 71
3.7 The inner crack problem with a cohesive zone. 73
3.8 The positions of the deformed and undeformed bodies. 76
3.9 The codimension-two free boundary problem. 79
3.10 The geometry of the additional shearing force problem. 87
3.11 The type-I crack problem. 92

3.12 The industrial requirement. 93
3.13 The first aperture shape. 95
3.14 The second aperture shape. 97
3.15 The third aperture shape. 98

4.1 The geometry of a simplified plate glass problem. 100
4.2 An element of an elastic plate. 101
4.3 The moments and forces per unit length on the middle plane of an elastic plate. 102
4.4 Representation of how a point force occurs at the corner. 105
4.5 The simplified problem for a single corner. 108
4.6 The further simplified problem for a single corner. 109
4.7 The edge reaction for different values of α. 113
4.8 The codimension-two laterally loaded plate problem. 116
4.9 The local problem near a free point. 117
4.10 The application of (4.20)–(4.40). 121
4.11 The points of reference and keys for Figures 4.12–4.14. 122
4.12 1×1 plate : (a) Displacement w, (b) Cross sections of the displacement w, (c) Reactions along the edge. See Figure 4.11 for keys. 123
4.13 1×2 plate : (a) Displacement w, (b) Cross sections of the displacement w, (c) Reactions along the edge. See Figure 4.11 for keys. 124
4.14 1×4 plate : (a) Displacement w, (b) Cross sections of the displacement w, (c) Reactions along the edge. See Figure 4.11 for keys. 125

5.1 The geometry of the two-point Stokes flow injection problem. 127
5.2 The free surface shape for the injection problem. 142
5.3 The free surface shape for the sintering problem. 149
5.4 The free surface shape for the sintering problem with initial shape $|x|^3$. 153
5.5 The geometry of the ice closure problem. 153
5.6 The codimension-two ice closure problem. 154
5.7 The codimension-two ice and till closure problem. 156

6.1 The geometry of the two point Hele-Shaw injection problem. 159
6.2 The free surface shape for the injection problem. 162
6.3 The geometry of the three discs problem. 163
6.4 The full problem near the first codimension-two region. 165
6.5 The first codimension-two problem. 166

6.6 The free surface shape for the first codimension-two problem. 168
6.7 The full problem near the second codimension-two region. 169
6.8 The second codimension-two problem. 170
6.9 The free surface shape for the second codimension-two problem. . . . 172
6.10 The full problem near the third codimension-two region. 173
6.11 The third codimension-two problem. 174
6.12 The free surface shape for the third codimension-two problem. 175
6.13 The Muskat problem. 178
6.14 The codimension-two Muskat problem. 179
6.15 The geometry of the second Muskat problem. 181

7.1 The inviscid sintering problem. 190

C.1 The geometry of the cusp problem. 216
C.2 The general geometry to explain the force at the cusp. 217

D.1 The Ivantsov parabola problem. 220
D.2 The Ivantsov parabola problem with two fluids. 222

Chapter 1

Introduction

The mathematical theory of free boundary problems has been extensively researched over the last thirty years. An indication of this can be seen from the vast array of material now available on the subject in the form of books [12, 17, 23, 67], proceedings [8, 10, 18, 31, 64, 68, 101] and bibliographies [13, 91]. Free boundary problems are defined as a set of differential equations which must be solved in a domain of dimension n whose boundary, of dimension $(n-1)$, is unknown *a priori*. An example is the classical Stefan problem [12] of determining the position of the free boundary between melting ice and water. The boundaries between the regions of ice and water are known as *free boundaries* as they are free to lie anywhere in the domain and are only determined as part of the solution. As stated above the free boundary has one dimension fewer than that of the underlying domain and so the boundary could be termed the 'codimension-one free boundary'. The inherent nonlinearity of these problems has prompted theoretical investigations into questions of existence, uniqueness, regularity of the boundary, numerical algorithms, stability and asymptotic behaviour.

The techniques that have been used to try to answer these and other questions include numerical analysis, asymptotic expansions and weak solutions. Asymptotic expansions involve the exploitation of small parameters which occur in the model under certain circumstances, whilst weak solutions, although rarely available, satisfy an integrated formulation of the problem and are not required to be as smooth as solutions to the original differential equations. When they exist, weak solutions can sometimes be closely related to the equally rare variational formulations of certain special free boundary problems and hence great unification can be achieved both analytically and numerically. At the opposite extreme, when very irregular or unstable free boundary morphology can occur in practice, none of these techniques is usually available even to demonstrate existence of the solution and much theoretical work remains to be done.

Despite all this mathematical activity, there remains a widely-occurring, but little-studied, subclass of free boundary problems in which the free boundary has dimension $(n-2)$. Two early attempts at unification were made by Howison [35] and Ockendon [67] and more recently by Morgan [58] and together they have produced a review [36] in order to stimulate further discussion. The number of case studies of this type that have appeared in the literature is now very large. We have termed these problems *codimension-two* free boundary problems, since the free boundary has two fewer dimensions than that of the underlying space in which the field equations are to be solved. In a two-dimensional problem the codimension-two free boundary is a collection of 'free points', and in three dimensions it is a collection of 'free curves'.

We remark that the term codimension-two free boundary problem is also applied to models of a free curve in $\mathbb{R}^3$ as is the case for fluid and superconducting vortex dynamics. However, in these cases the global attribute of the free boundary problem may be lost since to lowest order the dynamics of the free curve are often purely governed by a local problem. This thesis deals with a subset of codimension-two free boundary problems which are not of the vortex dynamics type but occur when the codimension-one free boundary is uniformly close to a known boundary. This will enable us to exploit a naturally occurring small parameter and often these problems will be susceptible to formulation as Riemann problems from which a solution can be systematically obtained.

1.1 Typical geometry required for a codimension-two problem

A codimension-two free boundary problem is usually (although not always — see Chapter 4) obtained as a particular limit of its corresponding codimension-one problem. To illustrate this point consider a codimension-one problem with a two dimensional geometry as in Figure 1.1. The curve $\Gamma(x, y, t) = 0$ is a prescribed boundary, that is its position is known. The position of the codimension-one free boundary $h(x, y, t) = 0$ which separates the two regions is unknown *a priori* and so must be solved for as part of the problem. In regions I and II, sets of partial differential equations are given which satisfy given boundary conditions on h and Γ, one more boundary condition being required on h than Γ in order to determine its position. For a codimension-two problem to arise, the free boundary must be uniformly close to the known boundary and the extent of the contact region II along the known boundary must be large compared to its width (their ratio is known as the aspect

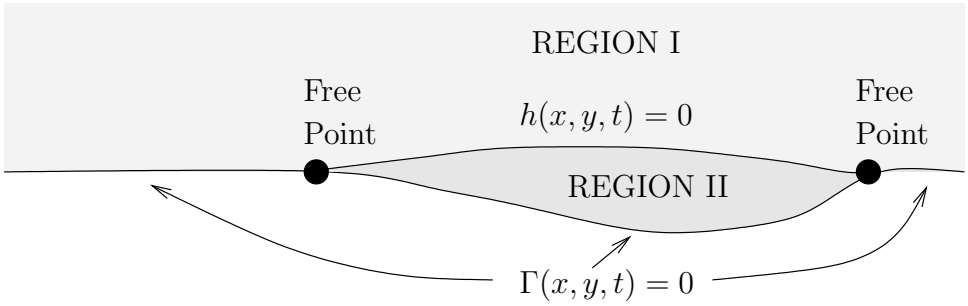

Figure 1.1: Typical geometry leading to a two-dimensional codimension-two problem.

ratio). The points at which the free boundary meets the fixed boundary are known as the free points. The majority of the problems considered in this thesis will only have two free points but, in general, there may be any number of them (of course the intersection of the free boundary with the prescribed boundary will be a curve in the three dimensional case).

If these conditions are met, the limit is taken as the aspect ratio tends to infinity. Then, any equations which formerly held in region I, which was of unknown extent, now hold in the known region 'above' $\Gamma(x, y, t) = 0$ and the only unknown parts of the geometry are the free points. The region of the fixed boundary between the free points is known as the 'non-contact' region because there is no contact between the fixed boundary and region I. Likewise, the region of the fixed boundary outside this region is known as the 'contact' region. This terminology is taken from that used in contact or obstacle problems in mechanics (such a problem is considered in Chapter 3).

1.2 Where codimension-two problems occur

A wide range of problems exhibit the characteristic type of geometry discussed above making them amenable to a codimension-two analysis. We list below just a few:

- Contact problems and crack problems in linear elasticity;
- Entry of a uniformly nearly flat body into a fluid (water entry) [47, 58, 102];
- Flow over a shallow step [70];
- Patch cavitation on a bluff head form [9, 36];
- Steady electropainting of a workpiece [58];

- Percolation in a sand bank [1];
- Viscous sintering of two cylinders under the action of surface tension [33, 36, 58].

Of the examples listed it is crack problems in solid mechanics that could be considered to be the progenitors of all codimension-two problems. We shall consider contact and crack problems in solid mechanics in more detail in Chapter 3. To expand upon the list, to give more of an idea of the type of problem that can be considered in a codimension-two framework, we shall now briefly describe two of those problems, the water entry problem and the viscous sintering problem.

1.2.1 Water entry

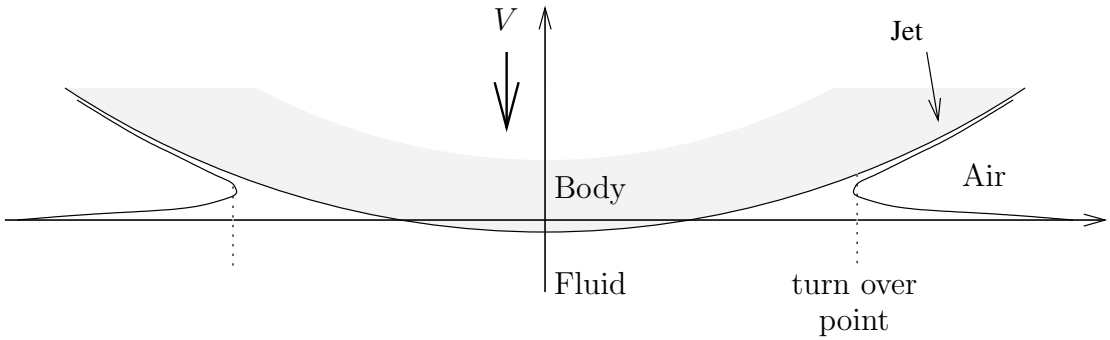

Figure 1.2: The water entry problem.

The water entry problem is the study of the normal impact of a nearly flat rigid convex body on an idealised fluid surface as shown in Figure 1.2. In terms of the discussion above region I is the fluid and region II is the air. The boundary of the body is known and the free boundary is the fluid surface. Since the body is nearly flat the free surface lies close to the body and to the undisturbed fluid level. Thus the problem has the required geometry described in Section 1.1 and both the free surface and fixed boundary can be linearised onto the prescribed undisturbed fluid level. One complication of this problem is the jets which are shown to form up the sides of the body. However, it has been shown [37] that these jets are thin and thus to leading order in the codimension-two problem they can be neglected such that to leading order the free surface does not turn over but rises to meet the body. The free points are where the free surface meets the body. The solution to this problem breaks down into three regions. There is the outer codimension-two region, this then drives inner regions around the turnover points, which in turn drive the thin jet regions. This problem will be reviewed in more detail in Chapter 2.

1.2.2 Viscous sintering

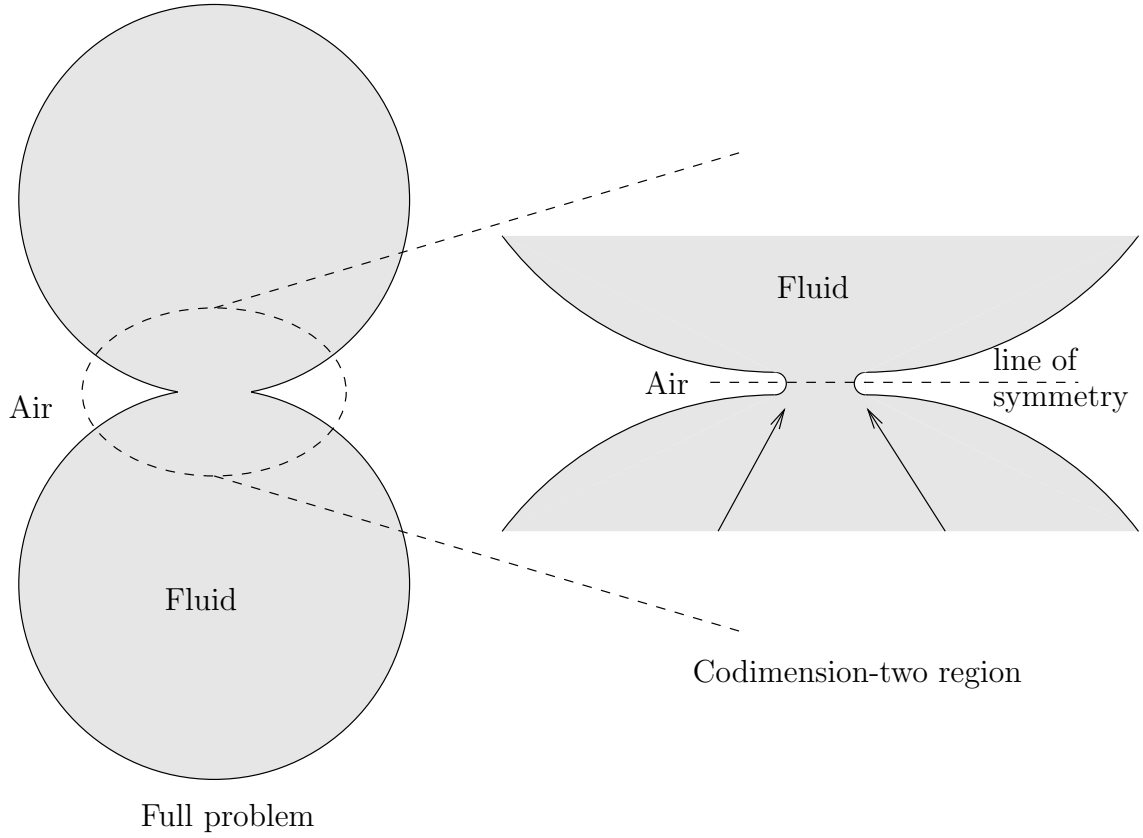

Figure 1.3: The Stokes flow viscous sintering problem.

Two identical cylinders of viscous fluid, which initially touch along a common generator, will coalesce purely under the action of surface tension to eventually form one large cylinder. This process is known as sintering and will be discussed in more detail in Chapter 5. For small times after the initial contact and in the region near to the contact the fluid flow problem can be formulated as a codimension-two problem. Region I for this problem is the fluid and region II is the air. The known boundary is the line of symmetry and the free boundary is the fluid boundary. For these small times and near to the contact region the free boundary is close to the line of symmetry. Hence in this region the problem exhibits the necessary geometry as described in Section 1.1. The free points are the points at which the fluid boundary meets the line of symmetry. This problem also exhibits three regions. However this problem is driven by the inner regions around the free points since the free boundary curvature is large. These inner regions then drive the codimension-two region indicated and then this drives an outermost region.

There are essentially two different ways in which codimension-two problems can arise. The first is as a local space and time analysis of a larger problem (such as in sintering). These problems often occur as the contact region grows, having initially zero extent. The codimension-two problem then gives a valuable insight into the nature of the solution at what is a crucial stage in the evolution. The second possibility is if the free boundary is close to the fixed boundary for all times. Such examples include the water entry problem (although the water entry problem can also occur as a local in time and space problem as will be discussed in Chapter 2).

1.3 One-phase and two-phase problems

In general the field equation will take a different form in regions I and II. If neither of the field equations in these regions is trivial, the problem is known as *two-phase*. In this case the field equation in region II has to be solved and substituted into the boundary conditions on the free boundary. The largeness of the aspect ratio can be exploited to simplify the field equation in this region enabling an approximate solution to be obtained. If the equations are trivial in region II (for example, it may be a vacuum), but not so in region I, the problem is known as *one-phase*.

Lastly, if the equations in region I are trivial, a different type of problem is realised which will not be considered in this thesis. The linearisation procedure in this case effectively causes region II to vanish. Since this was the only region with a non-trivial field equation there are now no equations remaining to solve. For this reason the problem is typically rescaled in such a way as to produce a partial differential equation for h the free surface shape. An example of this is the spread of a viscous drop on a solid surface where the free boundary thickness is described by a partial differential equation (for example, see [6]).

Generally, a codimension-one problem is nonlinear and cannot be solved analytically. Thus a major motivation for considering a codimension-two formulation of such a problem (even if only for a short time) is to obtain an approximate solution to an otherwise intractable problem. The codimension-two formulation has the key benefit that it is 'only' a mixed boundary value problem (admittedly over a domain where the position of the free points, at which the boundary conditions switch, are unknown) rather than a free boundary problem. Mixed boundary value problems are often quite well understood with well-developed techniques available for their solution, an example for Laplace's equation being the theory of Riemann problems. Another

benefit to accrue from a codimension-two analysis for small times is the generation of accurate initial conditions for a full numerical solution which would otherwise have suffered from having to contend with ill-defined initial singularities.

1.4 Outline of the general methodology

The linearisation procedure described in Section 1.1 is only part of the whole solution procedure. As described above the codimension-two solution usually only represents the solution on some particular length scale and the whole problem can be broken down into several different regions. If the problem can be broken up in this way then we can follow the flow of information through the problem. Thus as described above for the sintering problem it is the innermost regions that drive the codimension-two region which in turn drives an outer region. The different regions of the solution must 'match' together, that is, for this flow of information, we solve the problem in the inner region and the solution when expanded in codimension-two region variables gives the matching condition (driving mechanism) for the codimension-two region. In turn expanding the codimension-two solution in outer variables gives the matching condition (driving mechanism) for the outer problem. A crucial step in solving these problems is to, therefore, identify how the information is flowing through the problem. According to the particular sequence of regions through which the information flows the solution procedure should be modified. However, as with any problem in asymptotics to say that the information is purely flowing in one direction would be misleading. In order to solve the problem in any one region assumptions are generally made which can only be verified at the matching stage. The assumptions we make are often made by applying Van Dyke's maxim of taking the minimum allowable singularity at the free points. An example of this is when we solve the codimension-two water entry problem. The solution in the codimension-two region relies upon making certain assumptions about its behaviour near the free points. This assumption is only verified once the inner problem is solved and the two problems are found to match showing that the assumed behaviour was indeed correct.

The general procedure has been applied in a wide variety of physical situations, some of which are reviewed in [35, 36, 58]. The procedure can be broken down into three clear steps:

1. Identify the expected different regions of the solution and how the information will flow between them.

2. Solve the model in each region in turn following the flow of information using the solution to each previous region to drive the next one by means of the matching condition.

3. Perform any necessary matching between the regions to confirm the regions all match up and any assumptions that were made were correct.

1.5 Mathematical techniques

Three of the main techniques we will use in this thesis are matched asymptotic expansions, Riemann problems and variational formulations.

1.5.1 Matched asymptotic expansions

As discussed above the codimension-two solution is often only valid over some particular region of the full codimension-one problem, the codimension-one problem being broken down into two or more regions where the different regions of the solution must 'match' together. A key tool we will call upon is the Van Dyke Matching Principle [99]. Van Dyke's matching principle can be written concisely as

$$mti(nto) \quad = \quad nto(mti) \quad .$$

This notation is to be interpreted as follows:

$mti(nto)$:	Take the n-term outer expansion, write it in inner variables, and expand it to m-terms.
$nto(mti)$:	Take the m-term inner expansion, write it in outer variables, and expand it to n-terms.

Having calculated these two expressions they are written in common variables (either outer or inner). The above rule then states that the two expressions must be equal if they are to match. For a given $m = M$ and $n = N$ all possible matches must hold, for all combinations of $m = 1 \ldots M$ and $n = 1 \ldots N$, if we are to say the two expansions match up to these orders.

1.5.1.1 A note on log matching

Let us consider inner and outer expansions of the following function

$$f(x) \quad = \quad 1 + \frac{\log x}{\log \epsilon} \quad .$$

Assume that $x = O(1)$ is the outer expansion and $x = \epsilon X$, $X = O(1)$ is the inner expansion, then the outer and inner expansions are simply

$$\begin{aligned} f_{out} &\sim 1 + \frac{\log x}{\log \epsilon} \\ f_{in} &\sim 2 + \frac{\log X}{\log \epsilon} \quad . \end{aligned}$$

If we now apply the basic Van Dyke matching principle then we have

$$\begin{aligned} 1ti(1to) &= 1 \\ 1to(1ti) &= 2 \end{aligned}$$

which clearly shows the principle failing to work. But if we treat $\log \epsilon$ as $O(1)$ for the purposes of matching then all terms in both expansions above comprise the one term expansions and when we apply the matching principle everything now works as it must since they are simply expansions of one function on different scales.

Although in the limit $\epsilon \to 0$, $\epsilon^n \ll \epsilon^n \log 1/\epsilon$, which by the basic Van Dyke matching principle would say that they match at different orders, the above suggests that we should in fact consider them at the same time. In essence it suggests one should interpret the $\log \epsilon$ as being $O(1)$ for the purposes of applying the matching principle. This modification of the principle is discussed in more detail by Fraenkel [21].

1.5.2 The Riemann problem

We will use Riemann problems time and time again in this thesis as a means of formulating the codimension-two problem and hence finding the solution. In its general form a Riemann problem is to find an analytic function $\Phi(z)$, where $z = x + iy$, which satisfies the condition

$$\Phi^+(t) - G(t)\Phi^-(t) = g(t)$$

on L, a closed smooth curve where t is a variable denoting the position on L. The curve L divides the complex plane, on one side Φ takes the limiting value Φ^+ and on the other Φ^-. The function $G(t)$ is called the coefficient of the Riemann problem and $g(t)$ is called the free term. In the simplest form $G(t)$ and $g(t)$ satisfy Hölder conditions. The theory of the Riemann problem is discussed in detail in Appendix B in which the solution for the above problem is derived along with more complicated cases such as when G or g have discontinuities or when the curve L is open.

1.5.3 Variational formulations

As mentioned earlier, variational formulations are rare, but when they exist they can be extremely useful both analytically and numerically. Analytically they can often be used to prove uniqueness and existence of a solution. Numerically they can be used for a finite element solution. A simple example would be the one-dimensional obstacle problem shown in Figure 1.4.

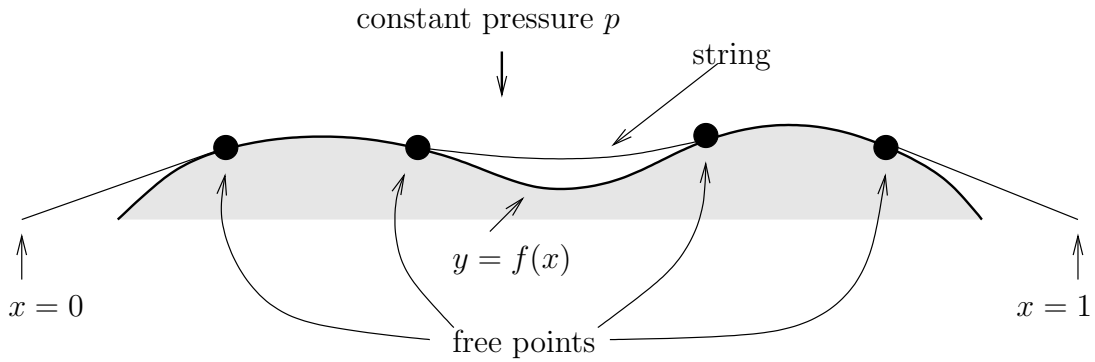

Figure 1.4: The one-dimensional obstacle problem.

This is the problem of determining the shape of an elastic string under constant pressure $p > 0$ when it is stretched over a rigid body $y = f(x)$. On the non-contact region the displacement is governed by the equation for an elastic string under constant load, whilst on the contact region the displacement coincides with the body shape. At the free points the contact is smooth (if it were not it would lead to an infinite force on a point). At the end points the string is fixed. Lastly, we have two inequalities which state that the string lies above the rigid body and the downward force per unit length on the string is not greater than p. In summary this gives the model

$$
\begin{aligned}
u_{xx} &= p && \text{on the non-contact region} \\
u &= f && \text{on the contact region} \\
u &= f && \text{at the free points} \\
u_x &= f_x && \text{at the free points} \\
u &\geq f && \text{for } \; x \in [0,1] \\
u_{xx} &\leq p && \text{for } \; x \in [0,1] \\
u &= 0 && \text{at } \; x = 0, 1 \; .
\end{aligned}
$$

As an intermediary step in formulating a variational inequality, from the above equations, we can write the complementarity problem

$$\begin{aligned} u &\geq f \\ -u_{xx} + p &\geq 0 \\ (u-f)(u_{xx}-p) &= 0 \\ u(0) = u(1) &= 0 \ . \end{aligned}$$

We now define a Hilbert space (see Appendix A for more details on Sobolev and Hilbert spaces)

$$\mathcal{V} = \left\{ v \in \mathcal{H}^1[0,1] \ : \ v(0) = v(1) = 0 \ , \ v \geq f \right\} \ .$$

We further define, for $u, v \in \mathcal{V}$, a bilinear form

$$a(u,v) = \int_0^1 u_x v_x dx$$

and a linear mapping

$$l(u) = -\int_0^1 pu dx \ .$$

Then for any $v \in \mathcal{V}$

$$\begin{aligned} a(u, v-u) &= \int_0^1 u_x (v-u)_x dx \\ &= -\int_0^1 u_{xx}(v-u)dx \qquad \text{using integration by parts} \\ &\geq -\int_0^1 p(v-u)dx \\ &\geq l(v-u) \end{aligned}$$

which is the *variational inequality* for the problem. As stated above this could now be used to prove the existence and uniqueness of a solution using the theorem of Appendix A or for a finite element numerical solution. See Elliott and Ockendon [17] for a proof that the variational inequality implies the complementarity problem and in turn the classical problem, provided we assume the solution to the variational inequality has continuous first derivatives. Furthermore, using a projected SOR method to solve the finite element problem, which can be generated from this variational inequality, the procedure naturally determines the position of the free boundary without the need to explicitly track it.

1.6 Layout and aims

In Chapter 2 a theory is reviewed for the water entry of a uniformly nearly flat rigid convex body. The body is nearly parallel to the free surface and the effects of gravity, fluid viscosity, surface tension, air pressure and air entrapment are all neglected. This has previously been formulated and analysed by many including Wagner [100], Korobkin [47], Wilson [102] and Morgan [58] and is formulated here as a clear example of how a codimension-two free boundary problem is derived and to demonstrate the techniques and arguments that are required to address such a problem. In Section 2.2 the variational formulation of the model as first proposed by Korobkin [45] is discussed. A detailed analysis of the stability of the codimension-two free boundary, to small perturbations along its length, is undertaken. The initial value problem for small disturbances to the free surface and codimension-two free boundary are then considered. The implications of the stability analysis and initial value problem to one particular formulation of the exit problem, namely the time reversal of the codimension-two entry problem, are discussed. Some simple extensions to the model are considered in Section 2.4.

In Chapter 3 we consider three types of problems in solid mechanics. We discuss some of the concepts and methods to be used in the chapter including dynamic stress intensity factors, cohesive zones, slip, Airy stress functions and Muskhelishvili potentials. The first problem is that of a dynamic type-III crack. We begin by solving the basic problem in which the crack faces are assumed to be stress free and using a dynamic stress intensity factor determine a formula for the crack propagation speed. We then discuss the effect of using the model of Barenblatt [2, 3] and including a cohesive zone near the tip of the crack. In the next section the problem of two-dimensional contact of two identical elastic bodies is reviewed as an example of a problem whose field equation is the biharmonic equation. The problem is solved using both a superposition approach and the more elegant Muskhelishvili potential method. The results of several different loading histories are considered. The first problem solved is that of purely normal loading. The problem of a subsequent tangential loading after the initial normal loading is then considered. The effect of friction and the possibility of either no slip or some slip occurring on the contact region are discussed. The problem of simultaneous variations of the normal and tangential forces is considered in the form of incremental loadings giving rise to a sequence of static problems. The third problem of the chapter is a static type-I crack problem and shows how the Muskhelishvili potential method of the previous section is easily

modified to handle such a problem. The solution to the elliptic crack problem is then used to generate solutions to a problem in which we require the crack to close under an increasing load.

Chapter 4 concerns a problem related to the manufacture of car windscreens. The resulting codimension-two problem does not arise as a leading-order problem after exploiting a small parameter, as do all the other problems we consider in this thesis, but instead occurs naturally. The real industrial process involves placing a sheet of plate glass on a frame and heating it from above causing it to sag under its own weight. By controlling the precise heating the shape of the final windscreen is controlled. In the real problem the frame is not planar nor rectangular and the plate is sagging due to gravity and both viscous and elastic effects. We formulate a simplified version of the full problem in which we only consider a planar rectangular plate and the glass is taken to be an elastic plate. We show how the thin plate problem can be formulated as a variational inequality. In Section 4.2 the problem of a single simply-supported corner is analysed in detail to show how the edge reaction depends on the corner angle and in particular how a point force may occur at a right-angle corner. The analysis also demonstrates the possibility of the corner of the glass plate lifting off the frame. An analytical solution for a simply supported rectangle is reviewed in Section 4.3. A numerical solution of the simplified problem for different types of boundary conditions is presented. The simplified problem turned out to be one that had been considered in part already in the literature [79] and as such much of the results derived here are a review.

In Chapter 5 we move to problems in Stokes flow. The first two problems are concerned with sintering. We are mainly interested in the problem of sintering under the action of surface tension. Such a problem is hoped to give insight into the much more complicated problems that really occur when making high quality glass. Some details of the process used to make the high quality glass are discussed along with a discussion of some of the research that has already been done. The solution is complicated because unlike most of the other problems in this thesis the information is flowing out of an inner region into the codimension-two region rather than from an outer region. The matching for the problem is found to be complicated and for that reason we build up to the problem by first considering the case of zero surface tension where the flow is being driven in the outer region by sources. The use of the Riemann problem formulation is invaluable in this problem. In Section 5.2 the problem of Stokes flow with non-zero surface tension is considered. This was previously considered by Morgan [58]. In Section 5.2.7 we show how the necessary

matching information from the inner region can in this case be obtained by solving a far field problem. The analysis is then extended in the next section for more general initially local free boundary shapes. The third problem of the chapter is a model for the closure of a thin channel lying at an ice-till interface. We first solve the problem for the case of a rigid impermeable bed and then consider the coupled problem when the till is also modelled by the slow flow equations.

In Chapter 6 we consider some Hele–Shaw problems. The chapter begins with a quick review of the problem of two point injection in a Hele–Shaw cell. This is followed by the three discs problem. The problem involves a half-space of fluid moving at a constant velocity in a Hele–Shaw cell and meeting three stationary touching discs of fluid aligned along the direction of motion of the half space. This problem has been solved exactly by Richardson [76] by means of a complex variable method. We will present a codimension-two solution valid for small times after the initial impact. This problem has three codimension-two regions and the solution shows how we apply our procedure of following the flow of information when we have several codimension-two regions which are related by outer problems. In Section 6.2 this problem is generalised to the case of n discs. The following section deals with the Muskat problem [60] which is concerned with the removal of one fluid from a porous medium by injecting a second fluid to force the first out. This problem is also analogous to a two fluid Hele–Shaw problem. The problem demonstrates the extra analysis needed when the field equations in the thin region are non-trivial.

Finally conclusions are drawn in Chapter 7 and problems that remain open are listed.

1.7 Statement of originality

Originality is claimed for the particular way in which the water entry problem is solved in Section 2.1.1.1. The results of the stability analysis of Section 2.3.1 are also original work. The initial value problem of Section 2.3.2 is all new material. The numerical solution of Section 2.4.1 and the application of the non-constant velocity results to a dropped body in Section 2.4.2, for the water entry problem, are new results.

The majority of the material in Chapter 3 is review. The presentation of how contact and crack problems are codimension-two problems, however, gives them a new novel setting. The analysis of Section 3.3.1.4 is new material.

Most of Chapter 4 is a review of a problem previously looked at in 1969 [79]. It mainly serves to update the results and check their accuracy, as well as to add the correction that point forces do not occur at the lift off points and to explain when point forces may occur. However, the corner problem analysis of Section 4.2 is new work.

The Stokes flow sintering problems of Chapter 5 are original work although as discussed in Section 5.2 a previous analysis of the surface tension problem had been carried out by Morgan [58] and the inner problem solution is by Hopper [34]. The particular method used to solve the ice closure problem is new work.

The problem of sections 6.2 and an outline of it's solution were originally derived by Cummings [14]. However, the formulation as a succession of Riemann problems and the generalisation of Section 6.2.7 is all new work. The solution of the two Muskat problems of Section 6.3 is original work.

Chapter 2

The water entry problem

The water entry problem is the study of the normal impact of a nearly flat rigid convex body on an idealised fluid surface as shown below. Alternatively, the problem can be thought of as the impact of a body which has zero gradient at the initial point of contact, with the codimension-two model only being valid in a small region around the impacting body and only for small times after the initial contact. This problem was first considered by Wagner [100] in an attempt to determine the forces on a landing seaplane. It has since been considered by many others including [11, 20, 37, 46, 58, 94]. The body is assumed to move with a constant velocity and the fluid is taken to be inviscid and incompressible (since the Reynolds number $Re \sim 10^8$ and the Mach number in water $M_w \sim 10^{-2}$). For typical values of surface tension and large impact velocities of the body the Froude number and Weber number for a ship are found to be large ($Fr^2 \sim 10$, $We \sim 10^4$) which suggests that neglecting the effects of gravity and surface tension is realistic. Also the effects of air between the body and the water will be neglected and the body is assumed to be moving through a vacuum. Some of these effects are considered in [19, 27, 46, 102]. The angle that the body makes with the fluid surface is known as the deadrise angle. In the case of large

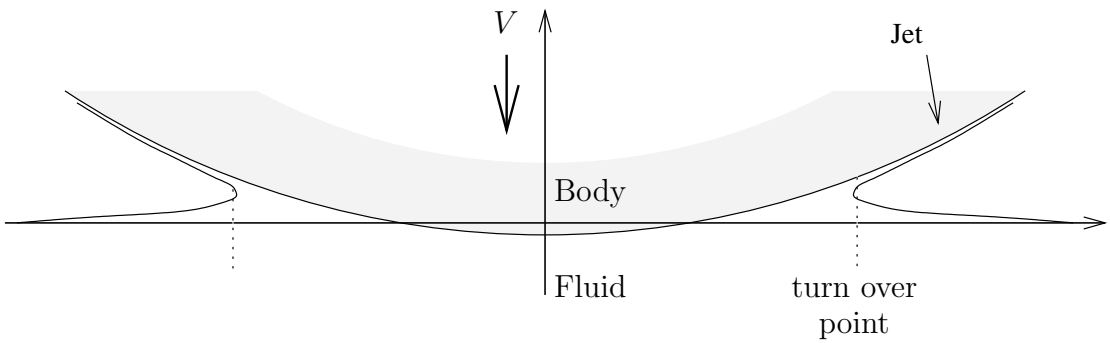

Figure 2.1: The geometry of the water entry problem.

impact velocities and small deadrise angles which we are considering the fluid surface undergoes a violent motion and there exist small regions of the flow in which large changes occur. The rapid motion of the surface and regions of large change are very important in practice and also severely hamper a numerical analysis of the problem. However both these circumstances favour an asymptotic approach.

2.1 The two dimensional water entry model

We take L to be the typical length scale over which we are interested. In dimensional variables we define the body profile by $y^* = Lf^*(\epsilon x^*/L)$, where $f^*(0) = 0$ and ϵ is a small number, and denote the velocity with which the body travels by V. Then the position of the body at a time t^* is

$$y^* \;=\; Lf\left(\frac{\epsilon x^*}{L}\right) - Vt^* \;\;.$$

We nondimensionalise by defining

$$x^* = Lx \quad , \quad y^* = Ly \quad , \quad t^* = \frac{L}{V}t$$

to obtain the nondimensional position of the body

$$y \;=\; f(\epsilon x) - t \;\;.$$

As shown in [37], for $\epsilon \ll 1$, the codimension-one formulation of the model is as shown in Figure 2.2.

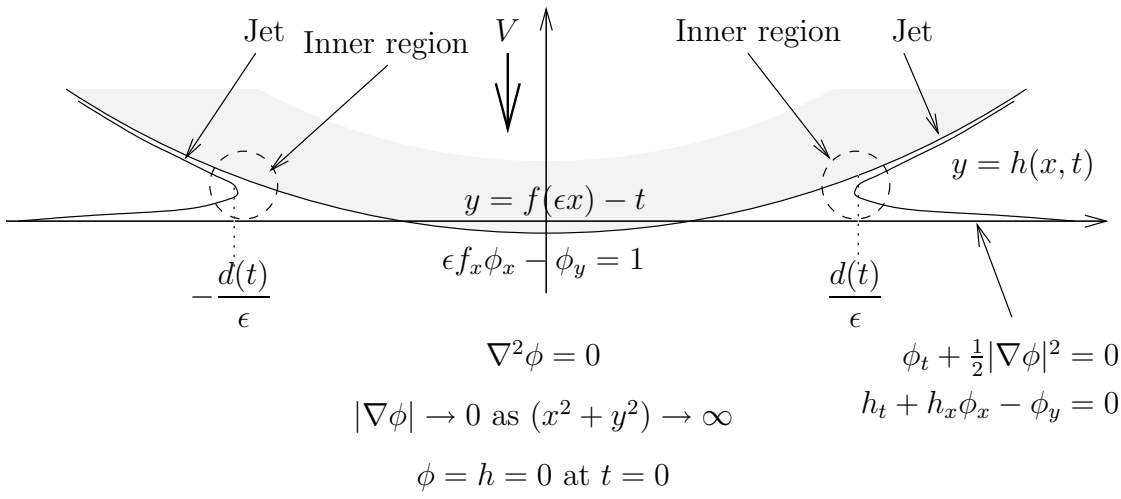

Figure 2.2: The codimension-one water entry problem.

For simplicity we have taken the free surface to be initially flat. However, the theory is easily applied to solid/liquid or liquid/solid impacts when one or both are not initially flat provided the deadrise angle is small and the initial body shape and free surface are convex or flat. The flow is initially at rest and thus initially irrotational, by Kelvin's theorem the flow is therefore always irrotational. Furthermore, as mentioned earlier we assume the flow is incompressible and hence we have a velocity potential $\phi(x, y, t)$ which satisfies Laplace's equation. On the free surface $y = h(x, t)$ we have Bernoulli and kinematic conditions. The free surface 'turns over' and forms two jets running along the body. Howison et al. [37] show that these turn-over points lie within $O(\epsilon)$ of $(\pm d(t)/\epsilon,\ f(\pm d(t)) - t)$. Furthermore they show that the jets only exert a second-order influence on the codimension-two model.

A natural approach now is to look for a perturbation solution by introducing certain scalings.

2.1.1 The outer problem

Relative to an $O(1)$ length scale for f the separation of the turn-over points is of $O(1/\epsilon)$. We, therefore, take the length scale of the outer problem to be $O(1/\epsilon)$. The velocity in the outer region will be $O(1)$ and thus we introduce the scaled outer variables $\hat{x}$, $\hat{y}$ and $\hat{\phi}$ defined by

$$\hat{x} = \epsilon x \quad , \quad \hat{y} = \epsilon y \quad , \quad \hat{\phi} = \epsilon \phi \ .$$

In outer coordinates the body position becomes

$$\hat{y} \ = \ \epsilon(f(\hat{x}) - t) \ .$$

and we write the free surface $y = h(x, t)$ as

$$\hat{y} \ = \ \epsilon \hat{h}(\hat{x}, t) \ .$$

With these scalings the free points lie at $\hat{x} = \pm d(t)$ and the jet roots lie at $(\pm d(t) + O(\epsilon^2), \epsilon(f(\pm d(t)) - t) + O(\epsilon^2))$. It is now reasonable to linearise the boundary conditions onto the x axis and to ignore the jets (this assumption is shown to be valid by Howison et al. [37]) so that

$$\hat{h}(d(t), t) \ = \ f(d(t)) - t$$

to leading order.

We note for clarity that in our framework it is the body shape that explicitly defines the small parameter ϵ. If we were to work in the small-time framework (which would be more suited to considering the initial stages of the impact of a raindrop on a solid surface) we could define the time scale to be ϵ^2 in which case the order of the length of the contact region would be ϵ.

We can now seek a regular perturbation solution for ϕ and h in powers of ϵ in the form

$$\hat{\phi} = \phi_0 + \epsilon\phi_1 + \dots \tag{2.1}$$

$$\hat{h} = h_0 + \epsilon h_1 + \dots \ . \tag{2.2}$$

The leading order outer problem we obtain (on dropping any remaining hats) is

$$\phi_{0xx} + \phi_{0yy} = 0 \quad \text{in} \quad y < 0 \tag{2.3}$$

$$\phi_{0y} = -1 \quad \text{on} \quad y = 0 \ , \ |x| < d(t) \tag{2.4}$$

$$\phi_{0y} = h_{0t} \quad \text{on} \quad y = 0 \ , \ |x| > d(t) \tag{2.5}$$

$$\phi_{0t} = 0 \quad \text{on} \quad y = 0 \ , \ |x| > d(t) \tag{2.6}$$

$$h_0 = f - t \quad \text{at} \quad x = \pm d(t) \tag{2.7}$$

$$|\nabla\phi_0| \to 0 \quad \text{as} \quad (x^2 + y^2) \to \infty \tag{2.8}$$

$$h_0 \to 0 \quad \text{as} \quad |x| \to \infty \tag{2.9}$$

$$\phi_0 = 0 \quad \text{at} \quad t = 0 \tag{2.10}$$

$$h_0 = 0 \quad \text{at} \quad t = 0 \ . \tag{2.11}$$

Integrating (2.6) and applying the initial condition (2.10) we obtain

$$\phi_0 = 0 \quad \text{on} \quad y = 0 \ , \ |x| > d(t) \ . \tag{2.12}$$

Hence we have a mixed boundary value problem for ϕ_0.

2.1.1.1 The codimension-two free boundary problem

Since the free boundary must lie below the convex impacting body we have the inequality

$$h_0(x,t) < f(x) - t \quad \text{on} \quad y = 0 \ , \ |x| > d(t) \ , \tag{2.13}$$

and we assume that no cavitation occurs in the flow which means the fluid remains in contact with the body for $x \in (-d(t), d(t))$. Therefore, in the absence of surface tension, the pressure is positive in this region which implies

$$\phi_{0t} < 0 \quad \text{on} \quad y = 0 \ , \ |x| < d(t) \ . \tag{2.14}$$

Thus the complete codimension-two free boundary problem is equations (2.3)–(2.5), (2.7)–(2.14) which are summarised in Figure 2.3. Since the data on the boundary changes from Neumann to Dirichlet at the free points ϕ_0 will probably have a singularity there. Note that we can make the boundary data homogeneous by making the change of variable $\phi_0 = \bar{\phi} - y$.

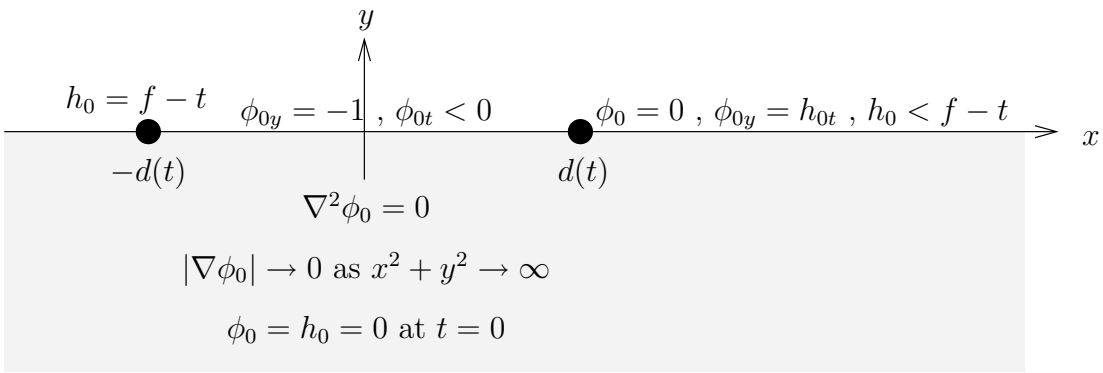

Figure 2.3: The codimension-two free boundary problem.

Local analysis near a free point

We change to local cylindrical polar coordinates moving with the free point, that is $x - d(t) = \delta r\cos\theta$, $y = \delta r\sin\theta$ where $\epsilon \ll \delta \ll 1$. The leading order problem for $\bar{\phi}$ is then

$$\begin{aligned}
\nabla^2\bar{\phi} &= 0 \qquad \text{for} \quad \theta \in (-\pi, 0) \\
\bar{\phi}_\theta &= 0 \qquad \text{on} \quad \theta = -\pi && (2.15)\\
\dot{d}(t)\bar{\phi}_r &< 0 \qquad \text{on} \quad \theta = -\pi && (2.16)\\
\bar{\phi} &= 0 \qquad \text{on} \quad \theta = 0 && (2.17)\\
\bar{\phi}_\theta &= -\dot{d}(t) r h_{0r} \qquad \text{on} \quad \theta = 0 && (2.18)\\
h_{0r} &< 0 \qquad \text{on} \quad \theta = 0 \ . && (2.19)
\end{aligned}$$

We assume near $r = 0$ the solution to this problem will be dominated by a single power of r (i.e. $\Re\{Cr^n e^{in\theta}\}$). Therefore we try a solution of the form

$$\bar{\phi} = r^n(A(t)\cos n\theta + B(t)\sin n\theta) \qquad \text{where} \quad n \in \mathbb{R} \ .$$

Applying the boundary conditions (2.15) and (2.17) we find $\bar{\phi}$ is of the form

$$\bar{\phi} = A(t) r^{n+\frac{1}{2}} \sin\left(n + \frac{1}{2}\right)\theta \qquad \text{for} \quad n \in \mathbb{N} \ .$$

Substituting this into the inequality (2.16), and using the fact that $\dot{d}(t) > 0$, gives

$$A(t)\left(n+\frac{1}{2}\right)\sin\left(n+\frac{1}{2}\right)\pi \;\; > \;\; 0 \;\; .$$

Combining (2.18) and (2.19) and substituting in for $\bar{\phi}$ we obtain

$$A(t)\left(n+\frac{1}{2}\right) \;\; > \;\; 0 \;\; .$$

Hence these two inequalities together imply that $n = 0, \pm 2, \ldots$.

We would now like to determine what the worse case singularity is for our problem. One way to do this is to use the trace theorem for Sobolev spaces (for a definition of a Sobolev space see Appendix A) which for our problem states that if we assume the solution lies in $\mathcal{H}^1(\mathbb{R}^2)$ then the solution evaluated on the boundary must be in $\mathcal{H}^{\frac{1}{2}}(\mathbb{R})$, and thus it cannot have any singularities of negative power. Thus we expect $\bar{\phi}$ to have at worst a square root singularity. As discussed in Chapter 1 we must make some assumption as to the power of the singularity at the free point that our solution will have. Using the maxim of Van Dyke we take the minimum singularity, that is $n = 0$. We can only confirm our assumption is correct when we have solved both the codimension-two problem using this assumption and also solved the inner problems and shown that they match. Such confirmation using matched asymptotic expansions is given by Howison et al. [37].

Solution of the mixed boundary value problem

Recall the mixed boundary value problem for $\bar{\phi}$ (Figure 2.3 with ϕ_0 replaced with $\bar{\phi} - y$) is

$$\begin{aligned}
\nabla^2\bar{\phi} &= 0 \qquad && \text{in} \quad y < 0 \\
\bar{\phi}_y &= 0 \qquad && \text{on} \quad y = 0 \quad , \quad |x| < d(t) \\
\bar{\phi} &= 0 \qquad && \text{on} \quad y = 0 \quad , \quad |x| > d(t) \\
|\nabla(\bar{\phi} - y)| &\to 0 \qquad && \text{as} \quad x^2 + y^2 \to \infty \;\; .
\end{aligned}$$

Using the result and assumption above we can simply spot the solution to this problem with a square root singularity at the free points is going to be of the form $const.\Re\{\sqrt{d^2 - z^2}\}$, where $z = x + iy$.

We can also solve the problem, where $\bar{\phi}$ has no negative power singularities, by a more systematic approach as follows. Since $\bar{\phi}$ is harmonic, let

$$\bar{\phi} \;\; = \;\; \Re\{g(z)\} \tag{2.20}$$

then

$$\bar{\phi}_x \;=\; \Re\left\{\frac{dg}{dz}\right\} \qquad \bar{\phi}_y \;=\; \Re\left\{i\frac{dg}{dz}\right\} \;=\; \Im\left\{\frac{dg}{dz}\right\} \;.$$

Thus if we define

$$G(z) \;=\; \begin{cases} -\overline{\dfrac{dg}{dz}}(\overline{z}) = -u(x,-y) + iv(x,-y) & \text{in} \quad y > 0 \\ \dfrac{dg}{dz}(z) = u(x,y) + iv(x,y) & \text{in} \quad y < 0 \end{cases}$$

where we have analytically continued $g(z)$ into the upper half plane, then u and v represent the horizontal and vertical velocities in the lower half plane, respectively.

On the contact region $\bar{\phi}_y = 0$ implies $v = 0$ and hence

$$G(x,0) \;=\; \begin{cases} -u(x,0) & \text{on} \quad y = 0^+ \quad , \quad |x| < d \\ u(x,0) & \text{on} \quad y = 0^- \quad , \quad |x| < d \end{cases}$$

whereas on the non-contact region $\bar{\phi} = 0$ implies $\bar{\phi}_x = 0$ which in turn implies $u = 0$ from which we see G is continuous. Introducing the notation

$$\lim_{y \to 0^+} G(z) = G^+(x) \quad , \quad \lim_{y \to 0^-} G(z) = G^-(x) \;,$$

then

$$G^+(x) \;=\; -G^-(x) \qquad \text{for} \quad x \in (-d(t), d(t)) \;. \tag{2.21}$$

Thus the problem for $G(z)$ is a Riemann problem: a function must be found which is analytic on the whole of the complex plane apart from the jump condition in (2.21). The theory of the Riemann problem is discussed in Appendix B. This particular problem is one with an open contour for which the details of the solution procedure are given in Section B.3. From the example in Section B.3 we can deduce that the only solution to our problem is unbounded at both ends with index one and thus has a solution of the form

$$G(z) \;=\; \frac{Az + B}{\sqrt{z^2 - d(t)^2}} \;,$$

where A and B are constants (nothing to do with A and B from the previous section). At infinity we require $\bar{\phi} \sim y$ and hence we take $B = 0$. Integrating we find

$$g(z) \;=\; A\sqrt{z^2 - d(t)^2} \;.$$

As expected $\bar{\phi}$ has square root singularities at the free points. Recalling our definition of $\bar{\phi}$, (2.20), we see that in $y < 0$

$$\bar{\phi} \;=\; -\Re\left\{\sqrt{d(t)^2-(x+iy)^2}\right\} \quad ,$$

where the constant has been chosen to give the correct behaviour at infinity. Finally we see that the leading-order outer solution for ϕ is

$$\phi_0 \;=\; -y-\Re\left\{\sqrt{d(t)^2-(x+iy)^2}\right\} \quad . \tag{2.22}$$

2.1.1.2 Determination of the surface elevation

Recalling the kinematic condition (2.5), $\phi_{0y} = h_{0t}$ on $y = 0$, $|x| > d(t)$, we substitute in from above for ϕ_0 giving

$$h_{0t} \;=\; -1+\frac{x}{\sqrt{x^2-d(t)^2}} \quad . \tag{2.23}$$

Integrating this and applying the initial condition (2.10) we obtain

$$h_0(x,t) \;=\; -t+\int_0^t \frac{x}{\sqrt{x^2-d(\tau)^2}}d\tau \quad . \tag{2.24}$$

2.1.1.3 The law of motion of the free point

At the free point we have the condition (2.7) which implies

$$f(d(t)) \;=\; \int_0^t \frac{d(t)}{\sqrt{d(t)^2-d(\tau)^2}}d\tau \quad .$$

This is an Abel integral problem which in general we can solve by writing as a convolution integral, taking the Laplace transform, rearranging and applying an inverse Laplace transform. Inverting yields

$$d^{-1}(x) \;=\; \frac{2}{\pi}\int_0^x \frac{f(\zeta)}{\sqrt{(x^2-\zeta^2)}}d\zeta \quad . \tag{2.25}$$

For a wedge shaped body, $f(x) = |x|$, this gives

$$d(t) \;=\; \frac{\pi t}{2}$$

as shown by Howison et al. [37] (this result has been confirmed by more rigorous analysis by Fraenkel and McLeod [20]). Further substituting this back into (2.24) we find the free surface shape is given by

$$h(x,t) \;=\; -t+\frac{2x}{\pi}\sin^{-1}\left(\frac{\pi t}{2x}\right) \quad .$$

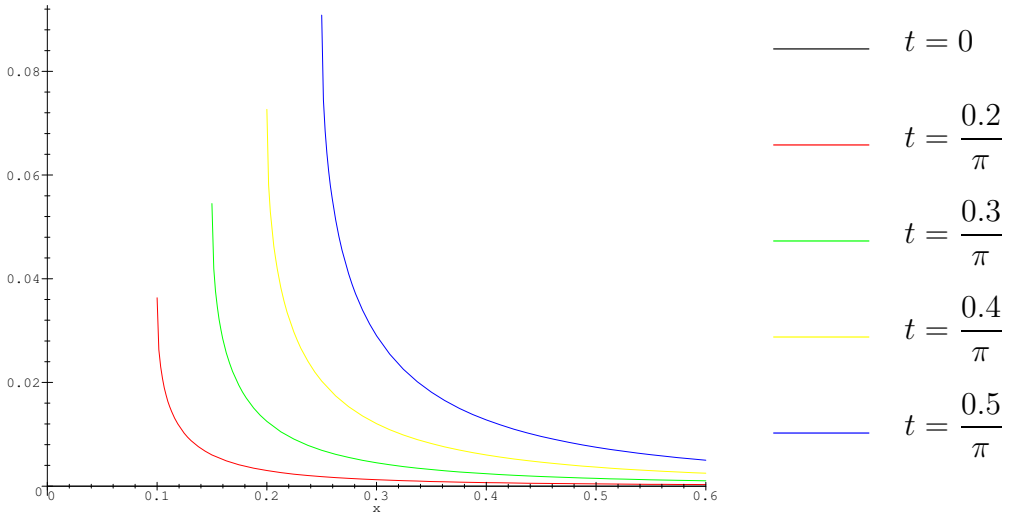

Figure 2.4: The free surface shape for a wedge.

Figure 2.4 shows this free surface shape at increasing times.

For a parabolic body, $f(x) = x^2$, we find

$$d(t) \quad = \quad \sqrt{2t}$$

(also shown by Howison et al. [37]) and the corresponding free surface shape is

$$h(x,t) \quad = \quad -t - |x| \left(x^2 - 2t\right)^{\frac{1}{2}} + x^2 \quad .$$

Figure 2.5 shows this free surface shape at increasing times.

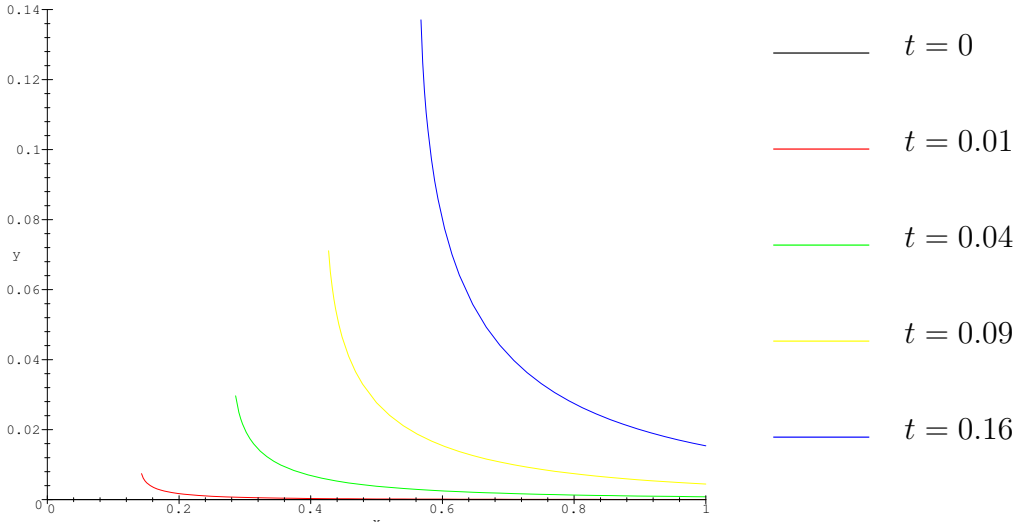

Figure 2.5: The free surface shape for a parabola.

Thus we have solved the codimension-two problem having found the velocity potential

ϕ, the free surface shape h and the free boundary position d. Reviewing the method, a key point is that we are solving the problem by following the flow of information. That is we have solved the outer problem, which is driving the flow, by formulating it as a Riemann problem and using the conditions at infinity. Following the flow of information in the problem we could now proceed to solve the problems in the inner and then jet regions. However as discussed in Chapter 1 when solving the codimension-two problem we have had to make certain assumptions which can only be verified once the inner problem is solved and the matching shown to work. Thus in a sense although the information is generally flowing from the codimension-two solution into the inner region there is a certain amount of information flowing back in the other direction which is necessary to confirm any assumption previously made.

This idea of following the flow of information will be seen more clearly in the Stokes flow and Hele–Shaw problems of Chapter 5 and 6 when the flow in the codimension-two region is being driven by another region. In those cases we shall see how the solution in the region driving the flow is needed first before the solution in the codimension-two region can be obtained systematically.

2.1.2 The inner and jet regions

The solutions in the inner and jet regions will not be discussed in any detail here as they will not be necessary for any of the further results. The details of the solution in these regions can be found in [102]. The inner region is found to be of size $O(\epsilon)$ in terms of the original variables. The inner solution is found using conformal maps and complex potentials. The width of the jet, $h(t)$, as it leaves the inner region is shown to be

$$h(t) \;=\; \frac{\pi d(t)}{8\dot{d}(t)^2} \;\;.$$

Thus the flow entering the jet has a speed $\dot{d}(t)/\epsilon$ and a thickness $\epsilon h(t)$ which implies the volume of fluid in the jet is $O(1)$, which is small compared with the volume displaced by the body which is $O(\epsilon^{-1})$. We have therefore justified the assumption we made earlier in order to neglect the jets. We should note finally that the jet region has a thickness of $O(\epsilon)$ but a length of $O(\epsilon^{-1})$.

2.1.3 The leading order pressure and force on the body

The pressure in each of the three regions is evaluated using Bernoulli's equation. Howison et al. [37] show that the leading order pressure in the codimension-two

region is $O(\epsilon^{-1})$, the leading order pressure in the inner region is found to be $O(\epsilon^{-2})$ and the leading order pressure in the jet is found to be $O(\epsilon)$. In the codimension-two region writing the pressure p as $p \sim \epsilon^{-1}p_0 + \ldots$ Howison et al. showed

$$p_0(x,0,t) = \begin{cases} \dfrac{d(t)\dot{d}(t)}{\sqrt{d(t)^2 - x^2}} & \text{for } |x| < d(t) \\ 0 & \text{for } |x| > d(t) \end{cases} .$$

In the outer region the pressure is $O(\epsilon^{-1})$ and acts over a length of $O(\epsilon^{-1})$ and thus produces a force of $O(\epsilon^{-2})$, whilst in the inner region the pressure is of $O(\epsilon^{-2})$ but only acts over a length of $O(\epsilon)$ producing a force of $O(\epsilon^{-1})$, and in the jet region the pressure is $O(\epsilon)$ and acts over a length of $O(\epsilon^{-1})$ and produces an even smaller force of $O(1)$. Hence they showed that the leading order force on the body comes from the outer region. Writing the expansion of the force as $F \sim \epsilon^{-2}F_0 + \ldots$ then

$$\begin{aligned} F_0(t) &= \int_{-d(t)}^{d(t)} P_0(x,t)dx \\ &= \pi d(t)\dot{d}(t) . \end{aligned}$$

For the particular case of the wedge these results have been confirmed by more rigorous analysis by Fraenkel and McLeod [20].

Before we go into more details of this solution we will show how the problem can be posed as a variation formulation from which the issues of existence, uniqueness and well-posedness can be efficiently addressed.

2.2 Variational formulation of the outer problem

A variational inequality can be constructed for the two- or three-dimensional codimension-two entry problem [37, 45]. Generalising to three dimensions we keep y as the vertical coordinate and describe the free curve by $t = w(x,z)$, assuming it only passes any given point once. Note the extra terms that arise in the full model due to the third dimension do not appear in the leading order codimension-two boundary conditions. Thus the only difference to the equations given in Figure 2.3 is that the Laplacian in the field equation is over z as well and $f = f(x,z)$ and $h = h(x,z,t)$.

As with the example of the obstacle problem in Chapter 1, to produce the variational formulation we will require the field equation to be the Euler-Lagrange equation of a minimisation problem and the boundary conditions to be natural on either the contact or non-contact regions. Furthermore the function we work with must lie in

$\mathcal{H}^1$, without this sufficient regularity at the boundary we would not be able to make the necessary estimates required to give the variational formulation. Then because ϕ_0 has infinite first derivatives on the free curve we make the transformation

$$\tilde{\phi} \;=\; -\int_0^t \phi_0(x,y,z,\tau)d\tau$$

in an attempt to produce a function to work with which has continuous first derivatives. Wilson [102] was first motivated to make this transformation by the Baiocchi transformation and the fact that the same transformation had previously been used by Korobkin [45] in his Lagrangian formulation of the impact of a blunt body.

As was shown in the introduction for the obstacle problem it is useful to first derive a complementarity formulation of the problem. From (2.3), the displacement potential satisfies Laplace's equation. The x and z derivatives are clearly continuous on $y=0$ so it only remains to show that the y derivatives are also continuous there. For $t < w(x,z)$, that is times before the codimension-two free boundary reaches the point (x,z), (2.5) and (2.12) give

$$\begin{aligned} \tilde{\phi}_y(x,0,z,t) &= -h_0(x,z,t) \\ \tilde{\phi}(x,0,z,t) &= 0 \;, \end{aligned} \tag{2.26}$$

and for $t > w(x,z)$

$$\begin{aligned} \tilde{\phi}_y(x,0,z,t) &= -\left(\int_0^w + \int_w^t\right)\phi_{0y}(x,0,z,\tau)d\tau \\ &= -h_0(x,z,w) + (t-w) \\ &= t - f(x,z) \end{aligned} \tag{2.27}$$

having used the fact that $f = h_0 - w$ on the free curve. Hence, as $t \to w \pm 0$, $\tilde{\phi}_y|_{y=0} \to w - f(x,z)$ and therefore $\tilde{\phi}$ has continuous first spatial derivatives everywhere. Hence

$$\nabla^2\tilde{\phi} \;=\; 0 \qquad \text{in} \quad y<0 \tag{2.28}$$

$$\tilde{\phi}\left(\tilde{\phi}_y - t + f\right) \;=\; 0 \qquad \text{on} \quad y=0 \;. \tag{2.29}$$

Next we must derive two inequalities. For $t < w(x,z)$ on $y=0$

$$\tilde{\phi}_y - t + f \;=\; f - t - h_0 \;\geq\; 0 \;.$$

which when combined with (2.27) gives

$$\tilde{\phi}_y - t + f \geq 0 \qquad \text{on} \quad y=0 \quad , \quad \forall t \;. \tag{2.30}$$

From (2.26), $\tilde{\phi} = 0$ on the surface of the fluid for all times before the body touches a particular point on $y = 0$. From the pressure condition $\phi_{0t} < 0$ on the contact region, it can be seen that ϕ_0 is a decreasing function in time on $y = 0$ and so

$$\tilde{\phi} \;\geq\; 0 \qquad \text{on} \quad y = 0 \quad , \quad \forall t \quad . \tag{2.31}$$

Thus (2.28) and (2.29) together with (2.30) and (2.31) constitute a complementarity problem for the leading order outer codimension-two water entry model. The existence of a variational inequality can be proved from this complementarity problem as we shall now demonstrate.

Let $\mathcal{V} \subseteq \mathcal{H}^1$ be a convex set whose elements satisfy (2.31). Define, for u, $v \in \mathcal{V}$ a bilinear form

$$a(u, v) \;=\; \iiint_{y<0} \nabla u . \nabla v dD$$

and a linear mapping

$$l(u) \;=\; \iint_{y=0} u(x, 0, z)(t - f(x, z)) dS \quad .$$

Then for any $v \in \mathcal{V}$

$$\begin{aligned}
a(\tilde{\phi}, v - \tilde{\phi}) \;&=\; \iiint_{y<0} \nabla\tilde{\phi} . \nabla(v - \tilde{\phi}) dD \\
&=\; \iint_{y=0} (v - \tilde{\phi})\tilde{\phi}_n dS - \iiint_{y<0} (v - \tilde{\phi})\nabla^2\tilde{\phi} dD \qquad \text{by Green's Thm} \\
&=\; \iint_{y=0} (v - \tilde{\phi})\tilde{\phi}_y dS \qquad \text{using (2.28)} \\
&\geq\; \iint_{y=0} (v - \tilde{\phi})(t - f) dS \qquad \text{using (2.30) and (2.31)} \quad .
\end{aligned}$$

Hence $a(\tilde{\phi}, v - \tilde{\phi}) \geq l(v - \tilde{\phi})$ for all $v \in \mathcal{V}$, which is a variational inequality for this problem.

To apply the uniqueness and existence theorem stated in Appendix A we require the further condition that $a(.,.)$ be coercive. Unfortunately $a(.,.)$ is only coercive (that is there exists an $\alpha > 0$ such that $a(v, v) \geq \alpha||v||^2$ for all $v \in \mathcal{V}$) if the fluid region is finite since $|\tilde{\phi}|^2$ is not integrable over $\mathbb{R}^3$. This can be overcome by imposing an artificial boundary condition at a large distance from the body which then allows us to apply the uniqueness and existence theorem stated in Appendix A.

As noted in the introduction the numerical solution of the variational problem is an efficient means of obtaining a numerical solution. In particular the variational

formulation lends itself ideally to a solution using finite elements and hence an irregular grid can be easily used allowing for specific refinements around certain areas of the flow. Furthermore, the position of the free boundary is built into the solution procedure by means of using a projected SOR method. Hence the location of the free boundary is easily found as part of the solution without the need to track its position and the actual numerical scheme can be applied over a fixed domain rather than a domain which varies as the free boundary moves. Such a numerical solution using finite elements, restricted to a regular grid, was carried out by Wilson [102]. His numerical results show good agreement with the asymptotic results.

2.3 Stability and water exit

In this section we shall discuss the difficulty in formulating the problem of water exit. We shall illustrate both the ill-posedness of one model for the exit problem and the stability of the entry problem by means of two different approaches, firstly as a stability analysis of a local model and secondly as a perturbation to a linearised initial value problem.

2.3.1 A local stability analysis of the water entry problem

In order to conduct a linear stability analysis of the codimension-two water entry problem we shall consider the local behaviour of the free surface h and the codimension-two free boundary, in space and time, when the free surface is subjected to a small perturbation. This problem was previously considered in [37] but did not yield a dispersion relation. The following analysis will initially follow along the lines of their paper. The results of our analysis will produce the previously unobtained dispersion relation which will show clearly the nature of the stability of the water entry problem.

Firstly we recall from Section 2.2 the three-dimensional codimension-two free boundary model is

$$\begin{aligned}
\nabla^2\phi &= 0 \qquad \text{in} \quad y<0 \\
\phi_y &= -1 \qquad \text{on} \quad y=0 \quad , \quad t>w(x,z) \\
\phi &= 0 \qquad \text{on} \quad y=0 \quad , \quad t<w(x,z) \\
\phi_y &= h_t \qquad \text{on} \quad y=0 \quad , \quad t<w(x,z) \\
h &= f-t \qquad \text{at} \quad t=w(x,z) \\
|\nabla\phi| &\to 0 \qquad \text{as} \quad x^2+y^2+z^2\to\infty
\end{aligned}$$

$$
\begin{aligned}
h &\to 0 \qquad \text{as} \quad x^2+z^2 \to \infty \\
\phi &= 0 \qquad \text{at} \quad t=0 \\
h &= 0 \qquad \text{at} \quad t=0
\end{aligned}
$$

where $\phi = \phi(x,y,z,t)$, $f = f(x,z)$ and $h = h(x,z,t)$.

This still possess the purely two-dimensional solution for ϕ and h (when the body is $f = f(x)$), namely

$$
\begin{aligned}
\phi &= -y - \Re\left\{\sqrt{d(t)^2-(x+iy)^2}\right\} \\
h &= -t + \int_0^t \frac{x}{\sqrt{x^2-d(\tau)^2}} d\tau \quad ,
\end{aligned}
$$

the position of the free boundary being $x = d(t)$.

2.3.1.1 The local space and time model

We wish to consider small perturbations to the free boundary and surface of the purely two-dimensional solution to the local in space and time three-dimensional problem.

To look locally in both time and space about $t = t_0$ and $x = d(t_0)$, $y = 0$ we define the local length scale to be $O(\epsilon')$ where $\epsilon \ll \epsilon' \ll 1$. Expanding the full solution and balancing terms in the kinematic condition we find the local variables are given by

$$
x = d(t_0) + \epsilon' x' \quad , \quad y = \epsilon' y' \quad , \quad z = z' \quad , \quad t = t_0 + \epsilon' t'
$$

$$
\phi = \epsilon'^{\frac{1}{2}} \phi' \quad , \quad h = f(d(t_0)) - t_0 + \epsilon'^{\frac{1}{2}} h' \quad .
$$

Then the position of the unperturbed free boundary becomes

$$
x' = \dot{d}(t_0) t' + O(\epsilon') \quad .
$$

Writing $\dot{d}(t_0) = V$, the leading order position of the unperturbed free boundary is $x' = Vt'$. Also expanding the unperturbed solution for ϕ in local variables gives

$$
\phi' \sim -\sqrt{2d(t_0)}\,\Re\left\{\sqrt{Vt'-x'-iy'}\right\} \qquad \text{as} \quad x'^2+y'^2 \to \infty \quad , \quad t' \to \infty \quad .
$$

Thus to leading order in ϵ', the unperturbed two-dimensional ϕ' satisfies (on dropping the primes)

$$
\begin{aligned}
\nabla^2\phi &= 0 \qquad \text{in} \quad y<0 && (2.32)\\
\phi_y &= 0 \qquad \text{on} \quad y=0 \quad , \quad x<Vt && (2.33)\\
\phi &= 0 \qquad \text{on} \quad y=0 \quad , \quad x>Vt && (2.34)\\
\phi_y &= h_t \qquad \text{on} \quad y=0 \quad , \quad x>Vt && (2.35)\\
h &= 0 \qquad \text{at} \quad x=Vt \quad , \quad y=0 && (2.36)\\
\phi &\sim A\Re\left\{\sqrt{Vt-x-iy}\right\} \qquad \text{as} \quad x^2+y^2 \to \infty \quad , \quad t \to \infty \quad , && (2.37)
\end{aligned}
$$

where $\phi = \phi(x, y, z, t)$, $f = f(x)$ and $h = h(x, z, t)$, for which we know the solution is

$$\phi \;=\; A\Re\left\{\sqrt{Vt - x - iy}\right\}$$

where $A = -\sqrt{2d(t_0)}$ is a constant. Substituting this into (2.35), integrating with respect to t and applying condition (2.36) we find

$$h \;=\; \frac{A}{V}\sqrt{x - Vt} \;\; .$$

Therefore, we see that the unperturbed two-dimensional local solution, about which we will perturb, is in the form of a travelling wave as we would expect.

Stability analysis of the local model

To analyse the stability of this solution we will introduce a small perturbation to the free surface h. We define a new coordinate ξ to be $\xi = x - Vt$ and perturb the free surface such that it now has position

$$h \;=\; \frac{A}{V}\sqrt{\xi} + \delta H_1(\xi)e^{\sigma t}\sin nz \;\; ,$$

where δ is a prescribed small number, σ is the growth rate we wish to find and $n > 0$. This will cause the codimension-two free boundary, that was at $\xi = 0$, to now have position $\xi = \delta e^{\sigma t}\sin nz$. The perturbed problem for ϕ and h is

$$\begin{aligned}
\nabla^2\phi &= 0 \qquad \text{in} \quad y < 0 \\
\phi_y &= 0 \qquad \text{on} \quad y = 0 \;\; , \;\; \xi < \delta e^{\sigma t}\sin nz \\
\phi &= 0 \qquad \text{on} \quad y = 0 \;\; , \;\; \xi > \delta e^{\sigma t}\sin nz \\
\phi_y &= h_t - Vh_\xi \qquad \text{on} \quad y = 0 \;\; , \;\; \xi > \delta e^{\sigma t}\sin nz \\
h &= 0 \qquad \text{at} \quad \xi = \delta e^{\sigma t}\sin nz \;\; , \;\; y = 0 \;\; .
\end{aligned}$$

From the form of the problem we expect to be able to construct a solution using matched asymptotic expansions. The outer problem will be when ξ and y are order one and the inner problem will be when they are $O(\delta)$.

We look for an outer solution of the form

$$\phi \;=\; A\Re\left\{\sqrt{-\xi - iy}\right\} + \delta\phi_1$$

where the appropriate model is

$$\nabla^2\phi = 0 \qquad \text{in} \quad y < 0 \tag{2.38}$$

$$\phi_y = 0 \qquad \text{on} \quad y = 0 \;\; , \;\; \xi < 0 \tag{2.39}$$

$$\phi = 0 \qquad \text{on} \quad y = 0 \;\; , \;\; \xi > 0 \tag{2.40}$$

$$\phi_y = h_t - Vh_\xi \qquad \text{on} \quad y = 0 \;\; , \;\; \xi > 0 \;\; . \tag{2.41}$$

The inner problem is obtained from the following scalings

$$\xi = \delta\hat{\xi} \quad , \quad y = \delta\hat{y} \quad , \quad z = \hat{z} \quad , \quad \phi = \delta^{\frac{1}{2}}\hat{\phi} \quad , \quad h = \delta^{\frac{1}{2}}\hat{h}$$

which result in the model

$$\begin{aligned}
\hat{\phi}_{\hat{\xi}\hat{\xi}} + \hat{\phi}_{\hat{y}\hat{y}} + \delta^2\hat{\phi}_{\hat{z}\hat{z}} &= 0 \qquad \text{in} \quad \hat{y} < 0 && (2.42)\\
\hat{\phi}_{\hat{y}} &= 0 \qquad \text{on} \quad \hat{y} = 0 \quad , \quad \hat{\xi} < e^{\sigma t}\sin nz && (2.43)\\
\hat{\phi} &= 0 \qquad \text{on} \quad \hat{y} = 0 \quad , \quad \hat{\xi} > e^{\sigma t}\sin nz && (2.44)\\
\hat{\phi}_{\hat{y}} &= \hat{h}_t - \delta V\hat{h}_{\hat{\xi}} \qquad \text{on} \quad \hat{y} = 0 \quad , \quad \hat{\xi} > e^{\sigma t}\sin nz && (2.45)\\
\hat{h} &= 0 \qquad \text{at} \quad \hat{\xi} = e^{\sigma t}\sin nz \quad , \quad \hat{y} = 0 && (2.46)
\end{aligned}$$

which has the leading order solution

$$\begin{aligned}
\hat{\phi}_0 &= A\Re\left\{\sqrt{e^{\sigma t}\sin nz - \hat{\xi} - i\hat{y}}\right\}\\
\hat{h}_0 &= \frac{A}{V}\sqrt{\hat{\xi} - e^{\sigma t}\sin nz}
\end{aligned}$$

which matches with the one-term outer solution already determined.

We now expand the one-term inner expansion for $\hat{\phi}$ in outer variables in order to determine how the second term in the outer solution should behave for small ξ and y. Using cylindrical polar coordinates defined by $\xi = r\cos\theta$ and $y = r\sin\theta$, we find

$$2to(1ti) = -Ar^{\frac{1}{2}}\sin\frac{\theta}{2} - \frac{\delta A}{2r^{\frac{1}{2}}}\sin\frac{\theta}{2}\,e^{\sigma t}\sin nz \quad .$$

Thus the outer expansion of ϕ will be of the form

$$\phi_{out} \sim \phi_0 + \delta\phi_1 + \ldots \quad ,$$

where ϕ_1 should satisfy

$$\begin{aligned}
\nabla^2\phi_1 &= 0 \qquad \text{in} \quad y < 0\\
\phi_{1y} &= 0 \qquad \text{on} \quad y = 0 \quad , \quad \xi < 0\\
\phi_1 &= 0 \qquad \text{on} \quad y = 0 \quad , \quad \xi > 0\\
\phi_1 &\sim -\frac{A}{2r^{\frac{1}{2}}}\sin\frac{\theta}{2}\,e^{\sigma t}\sin nz \qquad \text{as} \quad r \to 0\\
\phi_1 &\to 0 \qquad \text{as} \quad r \to \infty \quad .
\end{aligned}$$

A solution of the form

$$\phi_1 = -\frac{A}{2r^{\frac{1}{2}}}\sin\frac{\theta}{2}\,e^{\sigma t}\sin nzF(r)$$

clearly satisfies the boundary conditions and the local behaviour provided $F(r) \sim 1$ as $r \to 0$. Substituting this into the remaining field equation we see that F satisfies

$$F'' - n^2 F = 0 \ .$$

The solution to this is

$$F(r) = Ce^{-nr} + De^{nr}$$

where C and D are constants. In order for this solution to match out to the full solution we require $D = 0$ and thus $C = 1$ (since $n > 0$).

If we now expand the two-term outer expansion of ϕ in inner variables we can determine the appropriate behaviour for the second term of the inner expansion $\hat{\phi}$. We find that

$$\phi_{in} \sim \delta^{\frac{1}{2}} \left(\hat{\phi}_0 + \delta \hat{\phi}_1 + \ldots \right)$$

where $\hat{\phi}_1$ satisfies

$$\begin{aligned}
\nabla^2 \hat{\phi}_1 &= 0 \qquad \text{in} \quad \hat{y} < 0 \\
\hat{\phi}_{1\hat{y}} &= 0 \qquad \text{on} \quad \hat{y} = 0 \quad , \quad \hat{\xi} < e^{\sigma t} \sin nz \\
\hat{\phi}_1 &= 0 \qquad \text{on} \quad \hat{y} = 0 \quad , \quad \hat{\xi} > e^{\sigma t} \sin nz \\
\hat{\phi}_1 &\sim -\frac{nA}{2} \hat{r}^{\frac{1}{2}} \sin \frac{\theta}{2} \, e^{\sigma t} \sin nz \qquad \text{as} \quad \hat{r} \to \infty \ .
\end{aligned}$$

The appropriate solution is

$$\hat{\phi}_1 = -\frac{nA}{2} \Re \{ \sqrt{e^{\sigma t} \sin nz - \hat{\xi} - i\hat{y}} \} e^{\sigma t} \sin nz \ .$$

Thus so far we have a two term expansion for both the inner and outer ϕ, namely

$$\begin{aligned}
\phi_{out} &\sim -Ar^{\frac{1}{2}} \sin \frac{\theta}{2} - \frac{\delta A e^{-nr}}{2r^{\frac{1}{2}}} \sin \frac{\theta}{2} \, e^{\sigma t} \sin nz \\
\phi_{in} &\sim \delta^{\frac{1}{2}} A \Re \{ \sqrt{e^{\sigma t} \sin nz - \hat{\xi} - i\hat{y}} \} - \frac{\delta^{\frac{3}{2}} nA}{2} \Re \{ \sqrt{e^{\sigma t} \sin nz - \hat{\xi} - i\hat{y}} \} e^{\sigma t} \sin nz \ .
\end{aligned}$$

The outer solution fails to be an asymptotic expansion when $r = O(\delta)$ as we would expect since this is the inner length scale.

We now apply (2.41) and (2.45) to determine the second terms in the expansions for h. Firstly considering the outer solution we look for a second term of the form $H_1(\xi) e^{\sigma t} \sin nz$. Substituting into (2.41) for ϕ_{out} produces

$$\sigma H_1 - V H_1' = -\frac{A e^{-n\xi}}{4\xi^{\frac{3}{2}}} \ . \tag{2.47}$$

Up to this point the analysis has been approximately the same as that of Howison et al. [37]. It is from here onwards that the analysis most differs from that in [37]. The general solution to (2.47) is

$$H_1 \;=\; -\frac{A}{4V}e^{\frac{\sigma\xi}{V}}\int_{\xi}^{X}\frac{e^{-\left(\frac{\sigma}{V}+n\right)\xi'}}{{\xi'}^{\frac{3}{2}}}d\xi' \tag{2.48}$$

where $X > 0$ is the constant of integration. X will be determined by matching the inner and outer expansion. Now applying (2.45) we shall find the second term in the inner expansion of $\hat{h}$. We see

$$\hat{h}_{0t} - V\hat{h}_{1\xi} \;=\; \hat{\phi}_{1y} \;\;.$$

Substituting in for $\hat{h}_{0t}$ and $\hat{\phi}_{1y}$ gives

$$\hat{h}_{1\xi} \;=\; -\frac{A}{4V}\left(\frac{2\sigma}{V}+n\right)\frac{e^{\sigma t}\sin nz}{\sqrt{\hat{\xi}-e^{\sigma t}\sin nz}} \;\;.$$

Integrating and applying condition (2.46) yields

$$\hat{h}_1 \;=\; -\frac{A}{2V}\left(\frac{2\sigma}{V}+n\right)\sqrt{\hat{\xi}-e^{\sigma t}\sin nz}e^{\sigma t}\sin nz \;\;.$$

Thus we have the two term inner and outer expansions for the free surface

$$\begin{aligned} h_{out} &\sim \frac{A}{V}\sqrt{\xi} - \delta\frac{A}{4V}e^{\frac{\sigma\xi}{V}}\int_{\xi}^{X}\frac{e^{-\left(\frac{\sigma}{V}+n\right)\xi'}}{{\xi'}^{\frac{3}{2}}}d\xi' e^{\sigma t}\sin nz \\ h_{in} &\sim \delta^{\frac{1}{2}}\frac{A}{V}\sqrt{\hat{\xi}-e^{\sigma t}\sin nz} - \delta^{\frac{3}{2}}\frac{A}{2V}\left(\frac{2\sigma}{V}+n\right)\sqrt{\hat{\xi}-e^{\sigma t}\sin nz}e^{\sigma t}\sin nz \;\;. \end{aligned}$$

We are now in a position to perform all the matches up to and including $2ti(2to) = 2to(2ti)$ (this being the Van Dyke matching notation [99] as discussed in Chapter 1). To do so we must write the inner expansion in outer variables and the outer expansion in inner variables and expand. We shall begin by expanding H_1 in inner variables since it the most complicated term.

$$\begin{aligned} H_1 &= -\frac{A}{4V}e^{\frac{\sigma\delta\hat{\xi}}{V}}\int_{\delta\hat{\xi}}^{X}\frac{e^{-\left(\frac{\sigma}{V}+n\right)\xi'}}{{\xi'}^{\frac{3}{2}}}d\xi' \\ &\sim -\frac{A}{4V}\left[1+\frac{\sigma}{V}\delta\hat{\xi}\right]\left[\int_{\delta\hat{\xi}}^{X}\frac{e^{-\left(\frac{\sigma}{V}+n\right)\xi'}-1}{{\xi'}^{\frac{3}{2}}}d\xi' + \int_{\delta\hat{\xi}}^{X}\frac{1}{{\xi'}^{\frac{3}{2}}}d\xi'\right] \\ &= -\frac{A}{4V}\left[1+\frac{\sigma}{V}\delta\hat{\xi}\right]\left[\int_{0}^{X}\frac{e^{-\left(\frac{\sigma}{V}+n\right)\xi'}-1}{{\xi'}^{\frac{3}{2}}}d\xi' - \int_{0}^{\delta\hat{\xi}}\frac{e^{-\left(\frac{\sigma}{V}+n\right)\xi'}-1}{{\xi'}^{\frac{3}{2}}}d\xi' - \frac{2}{\sqrt{X}} + \frac{2}{\sqrt{\delta\hat{\xi}}}\right] \end{aligned}$$

$$\sim \quad -\frac{A}{4V}\left[1+\frac{\sigma}{V}\delta\hat{\xi}\right]\left[\frac{2}{\sqrt{\delta\hat{\xi}}}-\frac{2}{\sqrt{X}}+\int_0^X \frac{e^{-\left(\frac{\sigma}{V}+n\right)\xi'}-1}{\xi'^{\frac{3}{2}}}d\xi'+2\delta^{\frac{1}{2}}\left(\frac{\sigma}{V}+n\right)\sqrt{\hat{\xi}}\right]$$

$$\sim \quad -\frac{A}{2V}\left[\frac{1}{\sqrt{\delta\hat{\xi}}}-\frac{1}{\sqrt{X}}+\frac{1}{2}\int_0^X \frac{e^{-\left(\frac{\sigma}{V}+n\right)\xi'}-1}{\xi'^{\frac{3}{2}}}d\xi'+\delta^{\frac{1}{2}}\left(\frac{2\sigma}{V}+n\right)\sqrt{\hat{\xi}}\right]+\ldots \quad .$$

Putting this together with the expansions for the other terms we obtain

$$\begin{aligned} h_{out} \quad &\sim \quad \delta^{\frac{1}{2}}\frac{A}{V}\sqrt{\hat{\xi}}-\delta\frac{A}{2V}e^{\sigma t}\sin nz\left[\frac{1}{\sqrt{\delta\hat{\xi}}}-\frac{1}{\sqrt{X}}+\frac{1}{2}\int_0^X \frac{e^{-\left(\frac{\sigma}{V}+n\right)\xi'}-1}{\xi'^{\frac{3}{2}}}d\xi'\right. \\ &\qquad\qquad \left.+\delta^{\frac{1}{2}}\left(\frac{2\sigma}{V}+n\right)\sqrt{\hat{\xi}}\right]+\ldots \\ h_{in} \quad &\sim \quad \left[\frac{A}{V}\sqrt{\xi}-\delta\frac{A}{2V}e^{\sigma t}\sin nz\frac{1}{\sqrt{\xi}}\right]-\delta\frac{A}{2V}\left(\frac{2\sigma}{V}+n\right)\sqrt{\xi}e^{\sigma t}\sin nz+\ldots \quad . \end{aligned}$$

If we now perform all the matches up to and including $2ti(2to) = 2to(2ti)$ we find everything matches as required provided

$$\int_0^X \frac{e^{-\left(\frac{\sigma}{V}+n\right)\xi'}-1}{\xi'^{\frac{3}{2}}}d\xi' \quad = \quad \frac{2}{\sqrt{X}} \quad . \tag{2.49}$$

This is an implicit dispersion relation relating the growth rate σ of the perturbation to the two parameters n and X which define the mode of the perturbation in the z and ξ directions respectively. Noting that $X > 0$ implies the right-hand side of this relation is strictly positive or zero, means that we have the necessary condition

$$\frac{\sigma}{V}+n \quad \leq \quad 0$$

for the above relation to hold. That is

$$\sigma \quad \leq \quad -nV \quad . \tag{2.50}$$

This result is the same as that given in [37] however their analysis would appear to be closely related to the specific case of $X = 0$ which presents a problem with the term $2/\sqrt{X}$.

Since in the case of water entry $V > 0$ (2.50) shows that the codimension-two free boundary and free surface are both stable to small perturbations. For a particular mode in the z direction, i.e. a fixed n, the least stable mode is when $\sigma = -nV$ for which $X = \infty$.

2.3.1.2 Comparison with other types of stability analysis

It is interesting to compare this analysis with the linear stability analyses of (a) conventional 'codimension-one' free boundary problems, for example the motion of a free surface in a Hele-Shaw cell and (b) the motion of a free singular curve such as a line vortex in inviscid hydrodynamics. The evolution of a vortex filament in the absence of boundaries has been extensively studied. For the particular case of a filament with a small core radius moving in an inviscid, incompressible fluid an asymptotic representation of the self-induced motion can be obtained. This is known as the Localised Induction Approximation equation [6] or the filament equation. A review of the history of the filament equation is given by Ricca [73] and a review of the equation is given by Saffman [80]. Some of the history and a derivation of the filament equation using matched asymptotic expansions is also given by Hunton [39].

In the case (a) there is no singular behaviour near the free boundary (the solution is uniformly analytic except at the free boundary), and the analysis is straightforward without the need for matched asymptotic expansions. Thus we could say in this case that the singular behaviour and the 'law of motion' are both *globally* determined. In case (b) the behaviour is singular and matched asymptotic expansions are necessary. In this case both the singular behaviour and the 'law of motion' are, to leading order, *locally* determined. In our case, the singular behaviour is still *locally* determined (and is thought of as matching with the local form of the full, codimension-one, problem), but the 'law of motion' is *globally* determined because it is not enough to simply consider an inner region as is the case with the vortex motion.

Closely related to this stability analysis is the study of a linearised initial value problem which is discussed in the next section.

2.3.2 A linearised initial value problem

As in the previous section we introduce a small perturbation onto the free boundary in the third dimension. To perform the analysis we shall assume that the two free boundaries are far enough apart that we can simply consider them independently and thus we shall only consider a one free boundary problem where the unperturbed free boundary lies along the line $x = d(t)$ in three dimensions.

From our earlier analysis the solution to the unperturbed problem for ϕ with only one free boundary at $x = d(t)$ is

$$\phi \;=\; -y + A(t)\left\{\sqrt{d(t) - x - iy}\right\}$$

where $A(t)$ will be a known function given by the full codimension-two solution. The corresponding free surface elevation is

$$h \;=\; -t - \frac{1}{2}\int_0^t \frac{A(\tau)}{\sqrt{x - d(\tau)}} d\tau \tag{2.51}$$

where the fixed coordinates have been centred such that $d(0) = 0$. Applying the matching condition $h(d) = f(d) - t$ then yields the result

$$\frac{A(t)}{\dot{d}(t)} \;=\; -\frac{2}{\pi}\frac{d}{d\eta}\int_0^\eta \frac{f(w)}{\sqrt{\eta - w}} dw \tag{2.52}$$

which defines $d(t)$.

The above is the unperturbed solution about which we shall perturb. The functions $A(t)$ and $d(t)$ are thus prescribed functions in the following analysis. We now suppose that at a time $t = t_0 > 0$ the free surface is perturbed such that at time $t = t_0$ the perturbed free surface is

$$h(x, z, t_0) \;=\; -t_0 - \frac{1}{2}\int_0^{t_0} \frac{A(\tau)}{\sqrt{x - d(\tau)}} d\tau + \frac{\delta}{2}\left[x - d(t_0)\right]^\alpha e^{-nx} \sin nz \;\;, \tag{2.53}$$

where δ is a prescribed small number and α and $n > 0$ define the mode of the perturbation applied. The perturbed codimension-two free boundary is still constrained to lie in the plane $y = 0$ and thus the new perturbed position of the free boundary will take the form

$$x \;=\; g(z,t) \;=\; d(t) + \delta T(t) \sin nz$$

where $T(t)$ is to be determined. Hence the perturbed problem for the velocity potential ϕ is as shown in Figure 2.6.

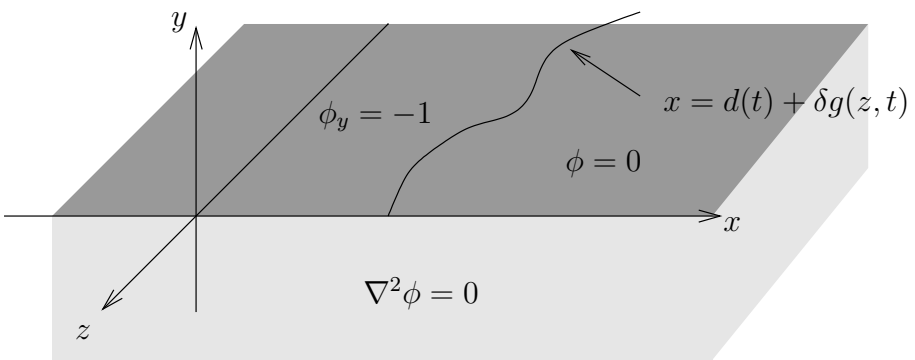

Figure 2.6: The perturbed problem for the velocity potential ϕ.

Thus the strategy for the problem is given a perturbation to the free surface elevation find the corresponding perturbation to the codimension-two free boundary position. We can solve this by determining inner and outer asymptotic expansion solutions for the velocity potential ϕ and the free surface elevation h which satisfy the Van Dyke matching principle [99].

2.3.2.1 Determination of the velocity potential

Firstly we shall centre the problem on the position of the unperturbed boundary by defining $\tilde{x} = x - d(t)$. Hence the problem may be written as

$$\begin{aligned} \nabla^2\phi &= 0 \qquad \text{in} \quad y < 0 && (2.54)\\ \phi_y &= -1 \qquad \text{on} \quad \tilde{x} < \delta g(z,t) \quad , \quad y = 0 && (2.55)\\ \phi &= 0 \qquad \text{on} \quad \tilde{x} > \delta g(z,t) \quad , \quad y = 0 \ , && (2.56) \end{aligned}$$

where the kinematic condition has been omitted since it is currently not required.

The leading-order outer problem for ϕ

The leading order outer problem is simply the unperturbed problem and has solution

$$\phi_0 = -y + A(t)\Re\left\{\sqrt{-\tilde{x} - iy}\right\} \ .$$

The inner problem for ϕ

Now for the inner problem we define inner variables $\tilde{x} = \delta\hat{x}$, $y = \delta\hat{y}$ and $\phi = \delta^{\frac{1}{2}}\hat{\phi}$. Equations (2.54)–(2.56) therefore become

$$\begin{aligned} \hat{\phi}_{\hat{x}\hat{x}} + \hat{\phi}_{\hat{y}\hat{y}} + \delta^2\hat{\phi}_{zz} &= 0 \qquad \text{in} \quad \hat{y} < 0\\ \hat{\phi}_{\hat{y}} &= -\delta^{\frac{1}{2}} \qquad \text{on} \quad \hat{x} < g(z,t) \quad , \quad \hat{y} = 0\\ \hat{\phi} &= 0 \qquad \text{on} \quad \hat{x} > g(z,t) \quad , \quad \hat{y} = 0 \ . \end{aligned}$$

The first two terms of the inner solution are

$$\phi_{in} \sim \delta^{\frac{1}{2}} A(t)\Re\left\{\sqrt{g(z,t) - \hat{x} - i\hat{y}}\right\} - \delta\hat{y} \ .$$

Matching the inner and outer expansions of ϕ

In order to apply the Van Dyke matching principle we must expand the inner and outer solutions in outer and inner variables respectively. Firstly expanding the one term outer expansion in inner variables gives

$$i(1to) \;=\; \delta^{\frac{1}{2}} A(t) \Re\left\{\sqrt{-\hat{x}-i\hat{y}}\right\} - \delta\hat{y} + \ldots \quad .$$

Next expanding the two term inner expansion in outer variables gives

$$o(2ti) \;=\; A(t)\Re\left\{\sqrt{-\tilde{x}-iy} + \frac{\delta g(z,t)}{2\sqrt{-\tilde{x}-iy}} + \ldots\right\} - y \quad .$$

By placing the two expansions in common variables (either inner or outer) we see that the $1ti(1to) = 1to(1ti)$ and that the $2ti(1to) = 1to(2ti)$. However, to proceed further we need the next term in ϕ_{out}.

Calculation of the second term in the outer expansion of ϕ

From the analysis above, we see that the next term in ϕ_{out} should be of order δ, that is the expansion takes the form

$$\phi_{out} \;\sim\; \phi_0 + \delta\phi_1 + \ldots \quad .$$

In particular the expansion above of ϕ_{in} shows that

$$2to(1ti) \;=\; A(t)\Re\left\{\sqrt{-\tilde{x}-iy} + \frac{\delta g(z,t)}{2\sqrt{-\tilde{x}-iy}}\right\} \quad , \tag{2.57}$$

and this must match with the $1ti(2to)$. That is, the next term ϕ_1 in the outer expansion must when expanded in inner variables give to leading order the second term above. Hence ϕ_1 must satisfy

$$\begin{aligned}
\nabla^2\phi_1 &= 0 \qquad \text{in} \quad y<0 \\
\phi_{1y} &= 0 \qquad \text{on} \quad \tilde{x}<0 \quad , \quad y=0 \\
\phi_1 &= 0 \qquad \text{on} \quad \tilde{x}>0 \quad , \quad y=0 \\
\phi_1 &\sim \Re\left\{\frac{A(t)g(z,t)}{2\sqrt{-\tilde{x}-iy}}\right\} \qquad \text{near} \quad (0,0,z) \\
\phi_1 &\to 0 \qquad \text{as} \quad r\to\infty \quad ,
\end{aligned}$$

where we have again omitted the kinematic condition. Changing to cylindrical polar coordinates, $\tilde{x} = r\cos\theta$, $y = r\sin\theta$, ϕ_1 must satisfy

$$\nabla^2\phi_1 \;=\; 0 \qquad \text{in} \quad r>0 \quad , \quad \theta\in(-\pi,0) \tag{2.58}$$

$$\phi_{1\theta} = 0 \qquad \text{on} \quad \theta = -\pi \tag{2.59}$$

$$\phi_1 = 0 \qquad \text{on} \quad \theta = 0 \tag{2.60}$$

$$\phi_1 \sim -\frac{A(t)g(z,t)}{2r^{\frac{1}{2}}} \sin\frac{\theta}{2} \qquad \text{near} \quad r = 0 \ . \tag{2.61}$$

We can solve this in the same way as we solved the similar problem in the previous section for the local stability analysis problem. The solution is

$$\phi_1 = -\frac{A(t)T(t)}{2r^{\frac{1}{2}}} e^{-nr} \sin nz \sin\frac{\theta}{2} \ .$$

All the matches up to $2ti(2to) = 2to(2ti)$ hold as necessary.

Changing back into Cartesian coordinates we have established the inner and outer expansions for ϕ to two terms. Namely

$$\phi_{in} = \delta^{\frac{1}{2}} A(t) \Re\left\{\sqrt{g(z,t) - \hat{x} - i\hat{y}}\right\} - \delta\hat{y} \tag{2.62}$$

$$\phi_{out} = -y + A(t)\Re\left\{\sqrt{d(t) - x - iy}\right\} + \frac{\delta A(t) g(z,t)}{2} \Re\left\{\sqrt{d(t) - x - iy}\right\} \frac{e^{-n[(x-d(t))^2 + y^2]^{\frac{1}{2}}}}{[(x-d(t))^2 + y^2]^{\frac{1}{2}}} \ , \tag{2.63}$$

where $\delta\hat{x} = x - d(t)$, $\delta\hat{y} = y$ and $g(z,t) = T(t)\sin nz$.

2.3.2.2 Derivation of the free surface elevation

Having calculated the outer expansion for ϕ we can use the relationship

$$h_t = \phi_y \qquad \text{on} \quad y = 0 \ , \ x > d(t) \ , \tag{2.64}$$

with the initial condition (2.53) to calculate the outer expansion for the surface elevation h. Similarly in inner variables we have the relationship

$$\delta\hat{h}_t - \dot{d}\hat{h}_{\hat{x}} = \hat{\phi}_{\hat{y}} \qquad \text{on} \quad y = 0 \ , \ \hat{x} > g(z,t) \ ,$$

from which we can determine the inner expansion for $\hat{h}$.

The outer surface elevation

Substituting for ϕ_{out} from (2.63) into (2.64) gives

$$h_t = -1 - \frac{A(t)}{2\sqrt{x - d(t)}} - \frac{\delta A(t) T(t)}{4[x - d(t)]^{\frac{3}{2}}} e^{-n[x-d(t)]} \sin nz \ .$$

Writing h in the form $h \sim h_0 + \delta h_1 + \ldots$, then h_0 is simply the unperturbed solution (2.51). Equating terms of $O(\delta)$ gives

$$h_{1t} \;=\; -\frac{\delta A(t)T(t)}{4[x-d(t)]^{\frac{3}{2}}} e^{-n[x-d(t)]} \sin nz \quad .$$

Integrating this also from t_0 to t using condition (2.53) we have

$$h_1 \;=\; -\int_{t_0}^{t} \frac{A(\tau)T(\tau)}{4(x-d(\tau))^{\frac{3}{2}}} e^{-n[x-d(\tau)]} d\tau \sin nz + \frac{1}{2}\left[x-d(t_0)\right]^{\alpha} e^{-nx} \sin nz \quad . \quad (2.65)$$

The inner surface elevation

Substituting for ϕ_{in} from (2.62) into (2.65) gives

$$\delta h_t - \dot{d} h_{\hat{x}} \;=\; -\frac{\delta^{\frac{1}{2}} A(t)}{2\sqrt{\hat{x}-g(z,t)}} - \delta \qquad \text{on} \quad \hat{y}=0 \quad , \quad \hat{x} > g(z,t) \quad .$$

Expanding h as $h_{in} = \hat{h}_0 + \delta^{\frac{1}{2}}\hat{h}_1 + \delta\hat{h}_2 + \ldots$ and equating terms of equal order we find

$$\begin{aligned} O(1) \qquad \hat{h}_{0\hat{x}} &= 0 \\ \Rightarrow \;\; \hat{h}_0 &= B(t) \quad , \end{aligned} \quad (2.66)$$

$$\begin{aligned} O(\delta^{\frac{1}{2}}) \qquad \dot{d}\hat{h}_{1\hat{x}} &= \frac{\delta^{\frac{1}{2}} A(t)}{2\sqrt{\hat{x}-g(z,t)}} \\ \Rightarrow \;\; \hat{h}_1 &= \frac{A(t)}{\dot{d}(t)}\sqrt{\hat{x}-g(z,t)} + C(z,t) \quad , \end{aligned} \quad (2.67)$$

$$\begin{aligned} O(\delta) \qquad \dot{d}\hat{h}_{2\hat{x}} &= 1 + \dot{B}(t) \\ \Rightarrow \;\; \hat{h}_2 &= \frac{1+\dot{B}(t)}{\dot{d}(t)}\hat{x} + D(z,t) \quad . \end{aligned} \quad (2.68)$$

In order to determine the functions B, C and D we must again employ the matching principle.

Matching the inner and outer expansions for h

Firstly we expand the inner solution in outer variables giving

$$\begin{aligned} \hat{h}_0 &= B(t) \\ \hat{h}_1 &= \frac{A(t)\sqrt{x-d(t)}}{\delta^{\frac{1}{2}}\dot{d}(t)} + C(t) - \frac{\delta^{\frac{1}{2}} A(t) g(z,t)}{2\dot{d}(t)\sqrt{x-d(t)}} + O(\delta^{\frac{3}{2}}) \\ \hat{h}_2 &= \frac{(1+\dot{B}(t))(x-d(t))}{\delta\dot{d}(t)} + D(z,t) \quad . \end{aligned}$$

Next we expand the outer solution in inner variables. Writing h_0 in inner variables we see that the integrand becomes large near the upper limit $\tau = t$ and so we split the range of integration such that

$$h_0 \;=\; -t - \frac{1}{2}\int_0^{t-\delta^{\frac{1}{2}}} \frac{A(\tau)}{\sqrt{\delta\hat{x} + d(t) - d(\tau)}}d\tau - \frac{1}{2}\int_{t-\delta^{\frac{1}{2}}}^{t} \frac{A(\tau)}{\sqrt{\delta\hat{x} + d(t) - d(\tau)}}d\tau \;\; .$$

In order to write this as an asymptotic expansion we must now expand the integrals. For ease of notation we shall denote the integrals by I_1 and I_2. Considering I_2 first we make the substitution $\tau = t - \delta s$ giving

$$I_2 \;=\; \int_0^{\delta^{-\frac{1}{2}}} \frac{\delta A(t-\delta s)}{(\delta\hat{x} + d(t) - d(t-\delta s))^{\frac{1}{2}}}ds \;\; .$$

If we now expand both $A(t-\delta s)$ and $d(t-\delta s)$ about t and then further expand binomially the denominator of the integrand we find

$$I_2 \;=\; \int_0^{\delta^{-\frac{1}{2}}} \frac{\delta^{\frac{1}{2}}A(t)}{(\hat{x} + s\dot{d}(t))^{\frac{1}{2}}}ds - \int_0^{\delta^{-\frac{1}{2}}} \frac{\delta^{\frac{3}{2}}s\dot{A}(t)}{(\hat{x} + s\dot{d}(t))^{\frac{1}{2}}}ds + \int_0^{\delta^{-\frac{1}{2}}} \frac{\delta^{\frac{3}{2}}s^2\ddot{d}(t)A(t)}{4(\hat{x} + s\dot{d}(t))^{\frac{3}{2}}}ds + \ldots \;\; .$$

Calculating these integrals and simplifying the resulting expression leads us to

$$I_2 \;=\; \frac{2\delta^{\frac{1}{4}}A(t)}{\dot{d}(t)^{\frac{1}{2}}} - \frac{2\delta^{\frac{1}{2}}A(t)\hat{x}^{\frac{1}{2}}}{\dot{d}(t)} + \frac{\delta^{\frac{3}{4}}A(t)\hat{x}}{\dot{d}(t)^{\frac{3}{2}}} + O(\delta^{\frac{5}{4}}) \;\; . \tag{2.69}$$

Secondly we consider I_1. Over the range of the integral $\delta\hat{x} \ll d(t) - d(\tau)$ and so we can expand the denominator of the integrand directly to give

$$I_1 \;=\; \int_0^{t-\delta^{-\frac{1}{2}}} \frac{A(\tau)}{(d(t) - d(\tau))^{\frac{1}{2}}}d\tau - \int_0^{t-\delta^{-\frac{1}{2}}} \frac{\delta A(\tau)\hat{x}}{2(d(t) - d(\tau))^{\frac{3}{2}}}d\tau + \ldots \;\; . \tag{2.70}$$

The range of the first of the two integrals above can be restored to $(0,t)$ provided we subtract off what we have added in. That is

$$\int_0^{t-\delta^{-\frac{1}{2}}} \frac{A(\tau)}{(d(t) - d(\tau))^{\frac{1}{2}}}d\tau \;=\; \int_0^{t} \frac{A(\tau)}{(d(t) - d(\tau))^{\frac{1}{2}}}d\tau - \int_0^{\delta^{-\frac{1}{2}}} \frac{\delta A(t-\delta s)}{(d(t) - d(t-\delta s))^{\frac{1}{2}}}ds \;, \tag{2.71}$$

where the second integral has already been transformed as above. The second of these integrals can now be handled in the same manner as above and is found to be

$$-\frac{2\delta^{\frac{1}{4}}A(t)}{\dot{d}(t)^{\frac{1}{2}}} + O(\delta^{\frac{5}{4}}) \;\; .$$

Thus combining (2.69), (2.70) and (2.71) we have

$$\begin{aligned} h_0 &= -t - \frac{1}{2}\int_0^t \frac{A(\tau)}{d(t)-d(\tau)^{\frac{1}{2}}}d\tau + \frac{\delta^{\frac{1}{2}}A(t)\hat{x}^{\frac{1}{2}}}{\dot{d}(t)} \\ &\quad -\frac{\delta^{\frac{3}{4}}A(t)\hat{x}}{2\dot{d}(t)^{\frac{3}{2}}} + \frac{\delta\hat{x}}{4}\int_0^{t-\delta^{-\frac{1}{2}}} \frac{A(\tau)}{(d(t)-d(\tau))^{\frac{3}{2}}}d\tau + O(\delta^{\frac{5}{4}}) \ . \end{aligned}$$

The last two terms of this expression can be combined to give

$$-\frac{\delta\hat{x}}{\dot{d}(t)}\frac{d}{dt}\left[\frac{1}{2}\int_0^{t-\delta^{\frac{1}{2}}} \frac{A(\tau)}{(d(t)-d(\tau))^{\frac{1}{2}}}d\tau\right] \ .$$

Using the result of (2.71) this further simplifies to give

$$\begin{aligned} h_0 &= -t - \frac{1}{2}\int_0^t \frac{A(\tau)}{(d(t)-d(\tau))^{\frac{1}{2}}}d\tau + \frac{\delta^{\frac{1}{2}}A(t)\hat{x}^{\frac{1}{2}}}{\dot{d}(t)} + \\ &\quad -\frac{\delta\hat{x}}{\dot{d}(t)}\frac{d}{dt}\left[\frac{1}{2}\int_0^t \frac{A(\tau)}{(d(t)-d(\tau))^{\frac{1}{2}}}d\tau\right] + O(\delta^{\frac{5}{4}}) \ . \end{aligned}$$

Having expanded h_0 in inner variables we must now expand h_1. Writing (2.65) in inner variables we again split the range of integration and consider the two parts separately using techniques similar to those already employed. After some work we obtain

$$\begin{aligned} h_1 &= -\frac{A(t)T(t)\sin nz}{2(\delta\hat{x})^{\frac{1}{2}}\dot{d}(t)} + \frac{e^{-nd(t)}}{2\dot{d}(t)}\frac{d}{dt}\left[\int_{t_0}^t \frac{A(\tau)T(\tau)e^{nd(\tau)}}{(d(t)-d(\tau))^{\frac{1}{2}}}d\tau\right]\sin nz \\ &\quad +\frac{1}{2}\left[d(t)-d(t_0)\right]^{\alpha} e^{-nd(t)}\sin nz + O(\delta^{\frac{1}{4}}). \end{aligned}$$

Performing the seven matchings of the $nti(mto) = mto(nti)$ for $n = 1, 2, 3$ and $m = 1, 2$ we see the inner and outer solutions do indeed match and the unknown functions B, C and D are found to be

$$B(t) = -t - \frac{1}{2}\int_0^t \frac{A(\tau)}{(d(t)-d(\tau))^{\frac{1}{2}}}d\tau \ , \tag{2.72}$$

$$C(z,t) = 0 \ ,$$

$$D(z,t) = \frac{e^{-nd(t)}}{2\dot{d}(t)}\frac{d}{dt}\left[\int_0^t \frac{A(\tau)T(\tau)e^{nd(\tau)}}{(d(t)-d(\tau))^{\frac{1}{2}}}d\tau\right]\sin nz \tag{2.73}$$

$$+\frac{1}{2}\left[d(t)-d(t_0)\right]^{\alpha} e^{-nd(t)}\sin nz \ . \tag{2.74}$$

2.3.2.3 The law of motion of the free boundary

Using the inner expansion for h we can now produce a law of motion for the free boundary. At the free boundary we have the condition

$$h(x,z,t) \;=\; f(x)-t \qquad \text{at} \quad x=d(t)+\delta g(z,t) \;\;,$$

which implies

$$h_{in}(g(z,t),z,t) \;=\; f(d(t)+\delta g(z,t))-t \;\;.$$

Expanding $f(d(t)+\delta g(z,t))$ as a Taylor expansion about $d(t)$ we have

$$\hat{h}_0+\delta^{\frac{1}{2}}\hat{h}_1+\delta\hat{h}_2+\ldots \;=\; f(d(t))-t+\delta g(z,t)f'(d(t))+\ldots \quad \text{at} \quad \hat{x}=g(z,t) \;\;.$$

Substituting in for $\hat{h}_0$, $\hat{h}_1$ and $\hat{h}_2$ from (2.66), (2.67) and (2.68) we have

$$B(t)+\delta\left[\frac{1+\dot{B}(t)}{\dot{d}(t)}g(z,t)+D(z,t)\right] \;=\; f(d(t))-t+\delta g(z,t)f'(d(t)) \;\;.$$

Substituting for B and D from(2.72) and (2.74) and equating powers of δ we see

$$O(1) \qquad f(d(t)) \;=\; -\frac{1}{2}\int_0^t \frac{A(\tau)}{(d(t)-d(\tau))^{\frac{1}{2}}}d\tau \tag{2.75}$$

$$O(\delta) \qquad T(t)f'(d(t))\sin nz \;=\; \frac{T(t)}{\dot{d}(t)}\frac{d}{dt}\left[-\frac{1}{2}\int_0^t \frac{A(\tau)}{(d(t)-d(\tau))^{\frac{1}{2}}}d\tau\right]\sin nz+$$
$$\frac{e^{-nd(t)}}{2\dot{d}(t)}\frac{d}{dt}\left[\int_{t_0}^t \frac{A(\tau)T(\tau)e^{nd(\tau)}}{(d(t)-d(\tau))^{\frac{1}{2}}}d\tau\right]\sin nz+\frac{1}{2}\left[d(t)-d(t_0)\right]^{\alpha}e^{-nd(t)}\sin nz \;\;.$$

The first of these is the result from the unperturbed problem and has solution (2.52). Substituting from the first equation into the second and simplifying gives

$$-[d(t)-d(t_0)]^{\alpha}\dot{d}(t) \;=\; \frac{d}{dt}\left[\int_{t_0}^t \frac{A(\tau)T(\tau)e^{nd(\tau)}}{(d(t)-d(\tau))^{\frac{1}{2}}}d\tau\right]$$

which when integrated implies

$$-\frac{[d(t)-d(t_0)]^{\alpha+1}}{\alpha+1} \;=\; \int_{t_0}^t \frac{A(\tau)T(\tau)e^{nd(\tau)}}{(d(t)-d(\tau))^{\frac{1}{2}}}d\tau \;\;.$$

This is an Abel type problem and we invert to obtain

$$T(t) \;=\; B_{\alpha}\frac{\dot{d}(t)}{A(t)}[d(t)-d(t_0)]^{\alpha+\frac{1}{2}}e^{-nd(t)} \qquad \text{for} \quad t>t_0>0 \quad , \quad \alpha\geq-\frac{1}{2} \tag{2.76}$$

where

$$B_\alpha = -\frac{(2\alpha+3)}{(\alpha+1)\pi}\int_0^{\frac{\pi}{2}}(\sin\theta)^{2\alpha+3}d\theta \quad .$$

The constraint on α is required to prevent the codimension-two free boundary perturbation from being initially infinite.

The leading order problem has given us a means of calculating $\dot{d}(t)/A(t)$ in terms of f and d. From (2.76) we see that in the case of water entry when $d(t)$ increases with increasing time then the perturbation $T(t)$ decays exponentially and thus the water entry free boundary is stable to initial perturbations of the form chosen.

A simple example

Let us consider a half wedge shaped body for which $f(x) = x$. Substituting this into (2.52) and integrating we find

$$\frac{A(t)}{\dot{d}(t)} \quad = \quad -\frac{4}{\pi}d(t)^{\frac{1}{2}} \quad ,$$

which on substitution into (2.76) gives

$$T(t) \quad = \quad -\frac{\pi B_\alpha}{4}\frac{[d(t)-d(t_0)]^{\alpha+\frac{1}{2}}}{d(t)^{\frac{1}{2}}}e^{-nd(t)} \quad .$$

which shows for the entry case the problem posed is stable.

As was noted earlier this local linearised initial value problem is closely related to the previous stability analysis. The two problems do, however, differ in that the local stability analysis problem no longer involves the impact velocity of the body, that is the condition $\phi_y = -1$ becomes $\phi_y = 0$ whereas in the linearised initial value problem we simply considered the problem for a single free boundary keeping the condition $\phi_y = -1$ unaltered. Obviously the two problems also differ in the approach, that is, in the stability analysis no initial conditions are required whereas with the initial value problem they are. Despite these differences comparisons between the two results can be drawn. Both give the same qualitative result that the entry problem is stable to small perturbations. In particular the case of $\alpha = -1/2$ for the initial value problem is very similar to the case $X = \infty$ for the stability analysis, when the dispersion relation is just $\sigma = -nV$ which corresponds to the case $d(t) = Vt$.

2.3.3 Water exit problems

Water exit problems present much more difficulty than entry problems. One might think that the exit problems should simply be the entry model but with t replaced by $-t$, which is formally permissible. Hence solutions can be generated for the exit of a partially submerged body by considering the entry of the same body into water which has some initial non-zero surface shape (or is initially in motion) which is chosen to give the correct final position of the water and body. The solution can then be reversed in time to give a solution to the exit problem. However, it is not clear how large is the set of initial conditions for which this procedure generates acceptable solutions. Another possible solution to the exit of a partially submerged body from (say) initially static water is that the body is simply removed, leaving the water motionless (in the absence of surface tension). Of course this solution demands that contact between the body and the water is immediately lost on all the wetted portion of the body, which is physically unrealistic.

Turning to the codimension-two model (Figure 2.3), the solution procedure demonstrated fails, simply because whereas in entry problems, for each x the time $d^{-1}(x)$ is a natural final condition (see Figure 2.7) for integration of the equation $\phi_y = h_t$, this relies on the fact that $d(t)$ is increasing. For exit problems, however, as can be seen below, there is no upper limit to which we can integrate in order to fix h, and thus the position of the codimension-two free boundary. It should also be noted that it is no longer possible to prove uniqueness from a variational formulation of the leading order outer problem, since the bilinear form $a(.,.)$ has to be multiplied by -1 which means it is no longer coercive (see Section 2.2 for the variational formulation).

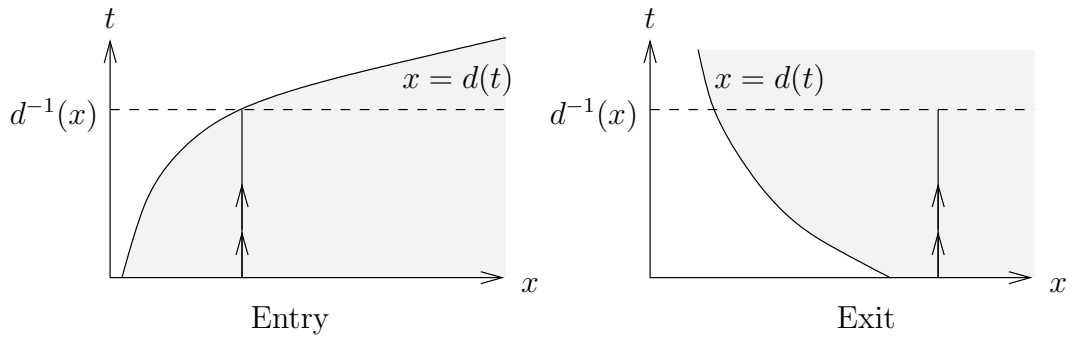

Figure 2.7: The domain of definition of the free surface elevation for the water entry and water exit problems.

A final pointer to the ill-posedness of one particular exit problem, namely the time reversal of the codimension-two entry problem, is the local linear stability analysis

of the codimension-two free boundary problem carried out in Section 2.3.1 and the linearised initial value problem consider above. For the case of $V < 0$ the same dispersion relation (2.49) still holds for the local stability analysis. This shows that an exit solution formulated as the time reversal of an entry solution is unstable and ill-posed since it shows the the most stable mode still only has $\sigma = -nV$, which for $V < 0$ is a growing mode. For the initial value problem reversing time shows $T(t)$ growing exponentially which again implies that the time reversal of the problem is unstable and ill-posed.

2.3.4 Conjectures on how to pose an exit problem

With regard to how to pose a water exit problem the need for some regularisation is apparent. On physical grounds, one might propose the incorporation of other effects into the model; for example, on small length scales surface tension may be a significant smoothing mechanism, while in other circumstances a coupled model involving air moving underneath the exiting body may be more appropriate. A second possibility is regularisation via a weak solution of the kind described by Rogers and Szymczak [77] whom allow a partially saturated region to form underneath the body. The latter idea is appealing both in the light of observed instabilities under exiting cylinders [27] and in view of the instability described in Sections 2.3.1 and 2.3.2. One might think of a partially saturated region as a model for the effect of a large number of thin fingers of air that have developed from an initially small perturbation; this idea has much in common with models of 'mushy regions' in Stefan problems with volumetric heating [52].

As a last remark we hypothesise that the solution to the exit problem should be the time-reversal of an entry problem for which the free surface should be uniformly smooth.

2.3.5 The Basilisk lizard

Finally we remark that in nature the Basilisk Lizard, *Basiliscus basiliscus* [25], can be seen to demonstrate an ingenious solution to the water exit problem. These reptiles can run on water, and support their weight by exploiting the large pressures generated when their feet hit the water surface approximately normally. Their feet subsequently penetrate some distance into the water, creating a cavity (and are hence well into the full nonlinear régime), and are then rotated so that they can be withdrawn more or

less vertically through the cavity before it collapses thus avoiding negative pressures which would act to suck the lizard down.

2.4 Extensions to the model

Various extensions to the problem are possible, Wilson [102] considered several such as the inclusion of gravity and surface tension, a non-planar initial free surface, bodies initially in contact with the fluid and given variable impact velocity. Morgan [58] further considered the effect of a non-symmetric body, an $O(1)$ forward velocity and an $O(\epsilon^{-1})$ forward velocity. In this section we shall review the extensions of bodies initially in contact with the fluid and non-symmetric bodies and extend the non-constant body velocity extension to the case when the body velocity is governed by it simply being dropped.

2.4.1 Bodies initially in contact with the fluid

The theory is easily modified for the case of a body initially partially submerged in the half-space of fluid. If we denote the initial point at which the body meets the fluid surface by $x = d(0)$ and we say that $y = f(x)$ is the initial position of the body (rather than just its shape as we said before) then the outer problem is completely unaltered except for the initial conditions and so we find

$$d^{-1}(x) \;=\; \frac{2}{\pi}\int_{d(0)}^{x} \frac{f(\zeta)}{\sqrt{x^2-\zeta^2}}d\zeta \quad .$$

For a wedge shaped body, $f(x) = |x| - d(0)$, this implies

$$d^{-1}(x) \;=\; \frac{2}{\pi}\left[(x^2-d(0)^2)^{\frac{1}{2}} + d(0)\sin^{-1}\left(\frac{d(0)}{x}\right) - \frac{\pi d(0)}{2}\right] \quad .$$

We cannot explicitly invert this relationship to get a formula for $d(t)$. As an example we have instead inverted it numerically for the case $d(0) = 0.5$ to obtain the graph shown in Figure 2.8. We can then numerically integrate the equation for the free boundary at increasing times to produce the graph in Figure 2.9.

2.4.2 Non-constant body velocity

We now define the impact speed of the body to be $v(t)$ where v has a magnitude of order V. Thus we nondimensionalise v by defining $v = V\hat{v}$. Then in dimensionless

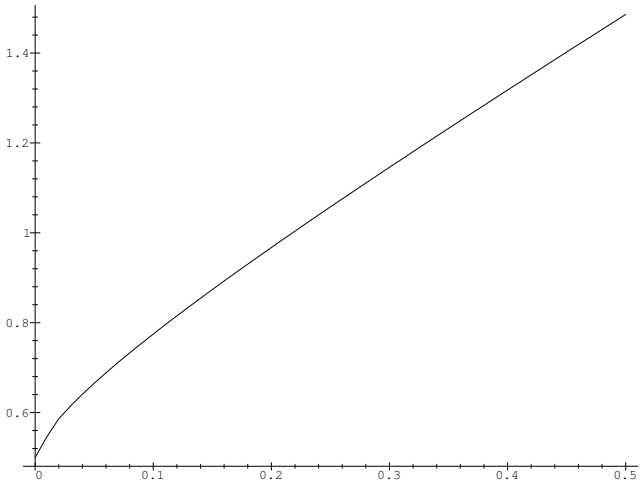

Figure 2.8: The position of the free point $d(t)$ in the case $d(0) = 0.5$.

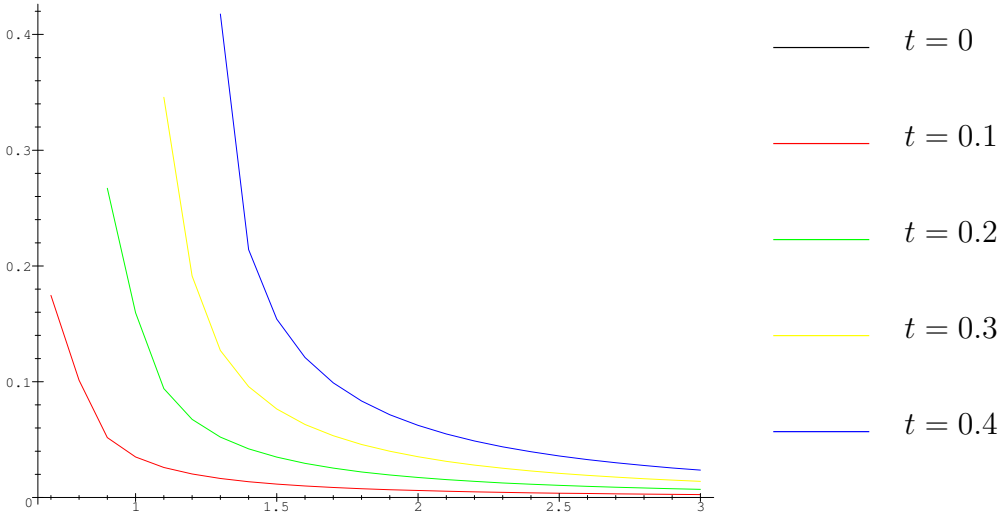

Figure 2.9: The free surface shape for a wedge initially in contact with the fluid.

variables the position of the body is

$$\hat{y} \;=\; \epsilon\left(\hat{f}(\hat{x}) - \int_0^t \hat{v}(\tau)d\tau\right) \quad .$$

This has the effect (on dropping the hats) of changing equations (2.4) and (2.7) to

$$\phi_{0y} \;=\; -v(t) \qquad \text{on} \quad y = 0 \quad , \quad |x| < d(t) \tag{2.77}$$

$$h_0(x,t) \;=\; f(x) - \int_0^t v(\tau)d\tau \qquad \text{at} \quad |x| = d(t) \quad , \quad \forall\, t \geq 0 \tag{2.78}$$

respectively. The solution of the leading order outer problem then becomes

$$\phi_0 \;=\; -v(t)\left[y + \Re\left\{\sqrt{d(t)^2 - (x+iy)^2}\right\}\right]$$

from which we determine

$$h_0(x,t) \;=\; -\int_0^t v(\tau)d\tau + \int_0^t \frac{xv(\tau)}{(x^2-d(\tau)^2)^{\frac{1}{2}}}d\tau \quad . \tag{2.79}$$

Substituting this into (2.78) we obtain

$$d(t)\int_0^t \frac{v(\tau)}{(d(t)^2-d(\tau)^2)^{\frac{1}{2}}}d\tau \;=\; f(d(t)) \quad .$$

This equation can be solved using the same technique as in Section 2.1.1.3 yielding

$$\int_0^t v(\tau)d\tau \;=\; \frac{2}{\pi}\int_0^d \frac{f(\zeta)}{(d^2-\zeta^2)^{\frac{1}{2}}}d\zeta \quad . \tag{2.80}$$

The leading order pressure on the body can still be found from the condition $P_0 = -\phi_{0t}$ giving

$$P_0(x,0,t) \;=\; \frac{v(t)d(t)\dot{d}(t)}{(d(t)^2-x^2)^{\frac{1}{2}}} + \dot{v}(t)(d(t)^2-x^2)^{\frac{1}{2}} \quad .$$

Integrating this pressure over the body we find the leading order force is

$$F_0(t) \;=\; \pi v(t)d(t)\dot{d}(t) + \frac{1}{2}\pi\dot{v}(t)d(t)^2 \quad .$$

If we wish to consider the problem where $v(t)$ is not simply given but is determined by the motion of the body then we require a further equation for the motion of the body. Taking the simple case that the body is dropped so that there are no external forces we have

$$F_0 \;=\; -k\dot{v}$$

where $k = m/\rho L^2$, m being the mass of the body per unit length. Substituting in for F_0 and integrating yields

$$\alpha + \frac{\pi}{2}vd^2 \;=\; -kv \tag{2.81}$$

where α is a constant of integration. Taking a particular example of a parabolic body $f(x) = x^2$, (2.80) implies

$$v(t) \;=\; d(t)\dot{d}(t) \quad .$$

Substituting this into (2.81) and integrating we find

$$\beta + \alpha t + \frac{\pi}{8}d^4 \;=\; -\frac{k}{2}d^2$$

where β is another constant of integration. Applying the initial conditions that $d(0) = 0$ and $v(0) = 1$ yields a quadratic in d^2

$$d^4 + \frac{4k}{\pi}d^2 - \frac{8k}{\pi}t \;=\; 0 \;\;.$$

Solving this and substituting back into (2.81) we obtain

$$\begin{aligned} d^2 &= \frac{-2k}{\pi} + \frac{2k}{\pi}\sqrt{1 + \frac{2\pi t}{k}} \\ v &= \left(1 + \frac{2\pi t}{k}\right)^{-\frac{1}{2}} \;\;. \end{aligned}$$

Further substituting back into (2.79) we find for a parabolic body which is simply dropped the free surface shape is

$$h(x,t) \;=\; \frac{k}{\pi}\left[1 - \left(1 + \frac{2\pi t}{k}\right)^{\frac{1}{2}}\right] - x\left[x^2 + \frac{2k}{\pi} - \frac{2k}{\pi}\left(1 + \frac{2\pi t}{k}\right)^{\frac{1}{2}}\right]^{\frac{1}{2}} + x^2 \;\;.$$

Plots of this surface shape for increasing times with $k = 1$ are shown in Figure 2.10.

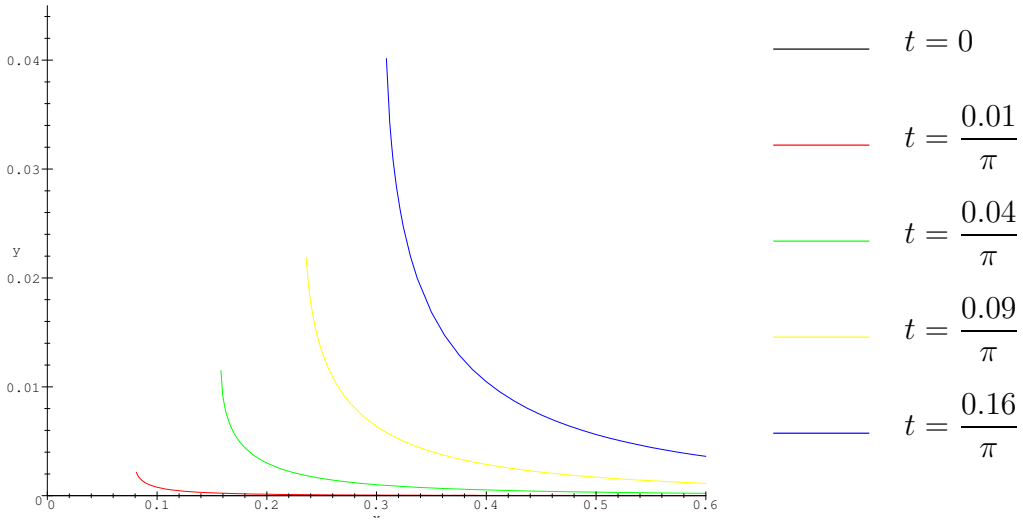

Figure 2.10: The free surface shape for a dropped parabolic body.

The three-dimensional axisymmetric version of this problem can also be solved.

2.4.2.1 Three-dimensional axisymmetric problem

For a three-dimensional axisymmetric body which has nondimensional form $y = \epsilon f(r)$, where (r, θ, y) are cylindrical polar coordinates, Wilson [102] showed the codi-

mension-two model is

$$\begin{aligned}
\frac{1}{r}\left(r\phi_r\right)_r + \phi_{yy} &= 0 \qquad \text{in} \quad y<0 \\
\phi_y &= -v(t) \qquad \text{on} \quad y=0 \quad , \quad r<d(t) \\
\phi &= 0 \qquad \text{on} \quad y=0 \quad , \quad r>d(t) \\
\phi_y &= h_t \qquad \text{on} \quad y=0 \quad , \quad r>d(t) \\
h &= f - \int_0^t v(\tau)d\tau \qquad \text{at} \quad r=d(t) \\
|\nabla\phi| &\to 0 \qquad \text{as} \quad r\to\infty \\
\phi = h &= 0 \qquad \text{at} \quad t=0
\end{aligned}$$

and has solution

$$\begin{aligned}
\phi &= -v(t)\left(\frac{2d^3}{\pi}\right)^{\frac{1}{2}} \int_0^\infty \frac{e^{-k|y|}}{k^{\frac{1}{2}}} J_{\frac{3}{2}}(kd)J_0(kr)dk \\
h &= \frac{2}{\pi}\int_0^t v(\tau)\left[\frac{d}{(d^2-r^2)^{\frac{1}{2}}} - \sin^{-1}\left(\frac{d(\tau)}{r}\right)\right]d\tau \quad ,
\end{aligned}$$

where J_i is a Bessel function of order i. Applying the matching condition at $r=d(t)$ gives

$$\int_0^t v(\tau)d\tau = \frac{1}{d}\int_0^\xi \frac{\xi f(\xi)}{(d^2-\xi^2)^{\frac{1}{2}}}d\xi \quad . \tag{2.82}$$

The leading order pressure on the body is given by $p=-\phi_t|_{y=0}$. Integrating this over a disc of radius d we obtain the leading order force on the body

$$F_0 = 4v\dot{d}d^2 + \frac{4}{3}\dot{v}d^3 \quad , \tag{2.83}$$

where the expansion for the force takes the form $F\sim\epsilon^{-2}F_0+\ldots$. As before if the body is dropped then $F=-k\dot{v}$ which implies

$$-k\dot{v} = 4v\dot{d}d^2 + \frac{4}{3}\dot{v}d^3 \quad .$$

Integrating this once and applying the conditions $v(0)=1$ and $d(0)=0$ we obtain

$$-kv = \frac{4}{3}vd^3 - k \quad . \tag{2.84}$$

For a parabolic body $f(x)=x^2$ (2.82) gives

$$v = \frac{4}{3}d\dot{d} \quad .$$

Substituting back into (2.84), integrating and applying the initial conditions we find d satisfies

$$\frac{16}{45k}d^5 + \frac{2}{3}d^2 - t \;=\; 0 \;. \tag{2.85}$$

Moghisi and Squire [57] present experimental results for a sphere dropped into water. For small time they state that their experimental results predict

$$F \;\sim\; \frac{a\pi}{2}t^{\frac{1}{2}}$$

in nondimensional form for a sphere of radius one, where $a = 5.22 \pm 0.1$. For small time (2.85) implies

$$d(t) \;\sim\; \left(\frac{3t}{2}\right)^{\frac{1}{2}}$$

and hence (2.83) implies

$$F \;\sim\; \frac{3d}{\epsilon^2} \;=\; \frac{3}{\epsilon^2}\left(\frac{3t}{2}\right)^{\frac{1}{2}} \;.$$

For a sphere of radius one the local form of the body for small time is parabolic with $\epsilon = 1/\sqrt{2}$. Comparing the theoretical and experimental results we see both predict a one half power dependence on t. Comparing the coefficients the experimental coefficient for $a = 5.22$ is 8.20 and the theoretical result predicts a coefficient of 7.35 which is in reasonable agreement.

2.4.2.2 The 'bouncing' bomb

The 'bouncing' bomb was used in the Second World War. The bomb was invented by Barnes Wallis although the idea had been used in Nelson's day when cannon balls were sometimes skipped across the water. The bomb was designed to make 12 bounces across the water to clear torpedo nets. The bomb was cylindrical in shape (approximately 1.5m long by 1.25m in diameter) and dropped from a height of about 20m from a plane travelling at about 150m/s. As the bomb was released it was spun backwards at about 500rpm giving it stability. Being dropped from 20m the bomb has a vertical velocity of about 20m/s when it hits the surface of the water. Thus on impact the horizontal velocity is an order of magnitude larger than the vertical velocity.

The above analysis clearly does not result in the body being able to 'bounce' off the water. What allows the bomb to 'bounce' is the difference in magnitudes between

the horizontal and vertical velocities. The particular case when the vertical velocity is $O(1)$ and the horizontal velocity is $O(\epsilon^{-1})$ has been considered by Morgan [58] when the vertical velocity is constant and the body is a wedge. To extend such a result to a non-constant vertical velocity is a simple matter and could represent the skimming of a flat stone across a lake. Unfortunately the asymmetry of the problem no longer permits the explicit inversion of the integral equation relating v to d and hence we can only obtain a pair of equations for v and d which must be solved numerically. Such an approach could then be further extended to the case of a cylindrical body.

2.4.3 Non-symmetric body shape

In this case the free points that previously lay at $x = \pm d(t)$ will now be denoted by $x = -d_1(t)$ and $x = d_2(t)$. By making the substitution

$$x = \frac{1}{2}(d_2(t) - d_1(t)) + \overline{x}$$

the codimension-two problem for ϕ is again symmetric and the free points lie at $\overline{x} = \pm\overline{d}(t)$ where

$$\overline{d}(t) = \frac{1}{2}(d_1(t) + d_2(t)) \ .$$

Thus the solution for ϕ is

$$\begin{aligned} \phi &= -y - \Re\left\{\sqrt{\overline{d}(t)^2 - (\overline{x} + iy)^2}\right\} \\ &= -y - \Re\left\{\sqrt{(d_2(t) - z)(d_1(t) + z)}\right\} \ . \end{aligned}$$

Note the form of the solution in the fixed frame could have easily been derived directly from the Riemann problem formulation. Applying the kinematic condition to the solution in the fixed frame we find the free boundary shape is given by

$$h(x,t) = -t + \frac{1}{2}\int_0^t \frac{(2x - d_2(\tau) + d_1(\tau))}{\sqrt{(x + d_1(\tau))(x - d_2(\tau))}} d\tau \ .$$

The conditions at the free points now become

$$\begin{aligned} h(-d_1(t)) &= f(-d_1(t)) - t \\ h(d_2(t)) &= f(d_2(t)) - t \end{aligned}$$

which when applied yields the two integral equations

$$\begin{aligned} f(-d_1(t)) &= -\frac{1}{2}\int_0^t \frac{(2d_1(t) - d_1(\tau) + d_2(\tau))}{\sqrt{(d_1(t) - d_1(\tau))(d_1(t) + d_2(\tau))}} d\tau \\ f(d_2(t)) &= \frac{1}{2}\int_0^t \frac{(2d_2(t) - d_2(\tau) + d_1(\tau))}{\sqrt{(d_2(t) + d_1(\tau))(d_2(t) - d_2(\tau))}} d\tau \ . \end{aligned}$$

For a body shape given by $f(x) = -\alpha x$ for $x < 0$ and $f(x) = \beta x$ for $x > 0$ it can be seen on dimensional grounds that the form of d_1 and d_2 will be $d_1(t) = At$ and $d_2(t) = Bt$ where A and B are positive constants. Substituting back in we can integrate to obtain two algebraic equations for A and B which can then be solved. As noted by Morgan a similar procedure can be applied for any body shape where the dependence on x is $(\pm x)^n$, where the above is the simple case $n = 1$.

Chapter 3

Solid contact and crack problems

In this chapter we shall look at three types of related problems in solid mechanics. A diagrammatic representation of the three types of problems we will consider is shown in Figure 3.1.

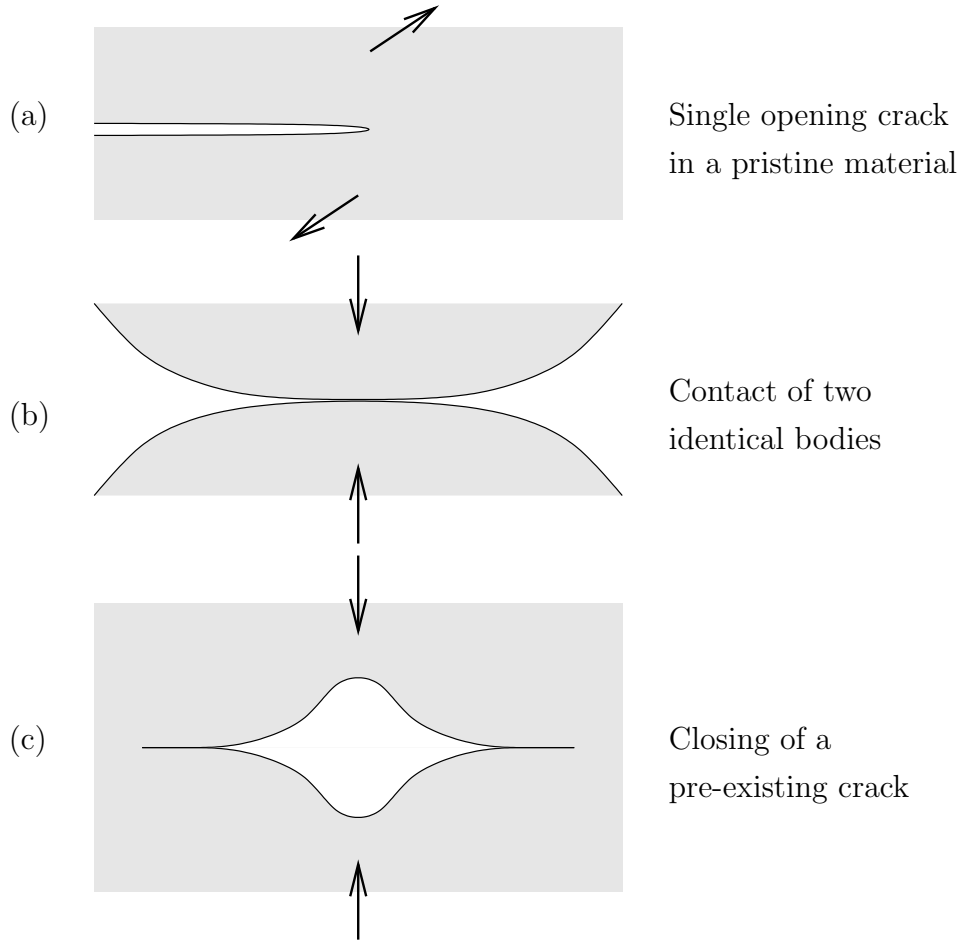

Figure 3.1: The three types of solid mechanics problems to be considered.

Both contact and crack problems have traditionally been considered in what could be termed a codimension-two framework. Because the displacements are small compared to the typical length scales it is quite natural to linearise what would be a free boundary problem to produce a mixed boundary value problem whose domain is quite often a half space. For the single crack problem we shall consider this means that the transverse displacements are small compared to the crack length whereas for the contact and closing crack problems it will be the in-plane displacements being small compared to the contact or crack width. Thus, when classically formulating solid contact and crack problems the linearisation of the boundary conditions onto a known curve is performed implicitly such that the model is already a codimension-two free boundary problem.

The first discussions of elastic phenomena can be found in the work of Hooke around 1680 but the first real attempts to construct a theory of elasticity using a continuum approach date from the early to mid 1700s. Every year countless papers are published on contact and crack problems in elasticity. There is now a vast body of literature on solid contact and crack problems of which a large proportion are codimension-two problems. Books on the subject include [22, 26, 43, 61, 82, 84, 85, 86, 87, 93] of which in particular [22, 86] deal specifically with crack problems and [43] deals with contact problems.

We will begin the chapter by looking at a two-dimensional dynamic crack propagation problem whose geometry is shown in Figure 3.1(a). The loads are applied as shown by the arrows perpendicular to the plane of the page. This is known as a type-III crack problem. If the loads had been applied in the plane of the page, the problem would be called type-I if the loads were in the vertical direction and type-II if they were in the horizontal direction. The problem will be modelled as one of brittle fracture, that is any plastic deformations are assumed to be restricted to a negligibly small region around the crack tip and thus the outermost problem can be modelled by linear elasticity.

In 1920 Griffith [28] first formulated an energy criterion to characterise the stress at a crack tip and predict the onset of crack growth. In 1957 Irwin [40] introduced the characterising parameter of the *elastic stress intensity factor* K which he defined to be $\sqrt{2\pi}$ times the coefficient of the singularity in the stress near the crack tip. Irwin then proposed that a crack would begin to grow in a cracked body with limited plastic deformation when K reached a critical value called the *fracture toughness*. Irwin showed that his stress intensity factor criterion and Griffith's energy criterion for the onset of crack growth were equivalent. Using the stress intensity factor we

will show how a formula for the crack tip speed can be obtained. However, the stress intensity factor approach inevitably has a square root singularity in the stress at the crack tip. Such a result cannot be literally accepted. Instead this result is interpreted on the basis that the size of the region over which the behaviour of the material deviates from linear elasticity is on a smaller length scale.

We will then consider the effect of including a *cohesive zone*. The cohesive zone idea provides a simple device for studying crack tip phenomena on a small length scale on which deviations from linear elasticity would occur. The essential idea of a cohesive zone is to simulate material response beyond the linear elastic range by introducing a *cohesive traction* or *cohesive stress* behind the crack tip which resists the crack opening. The cohesive zone is taken to terminate when the displacement reaches some critical value.

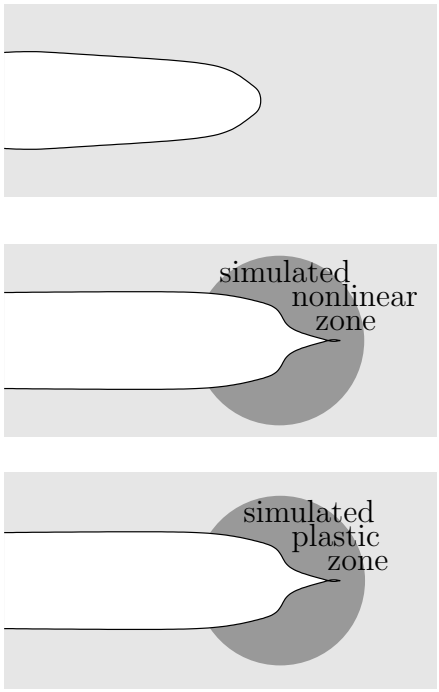

Brittle crack tip
- parabolic shape
- singular stress at tip

'Barenblatt' crack tip
- cusp shaped near tip
- constant width after some point behind tip
- zero stress at crack tip

'Dugdale' crack tip
- Same shape and stress characteristics as Barenblatt but modelling a plastic zone near the crack tip

Figure 3.2: Schematic of three types of crack.

A cohesive zone model for equilibrium conditions was first formulated by Barenblatt [2, 3] by considering the relationship between bonding forces between atoms and their separation distance. The same idea was subsequently applied to dynamic problems by Barenblatt [5]. The crack opening displacement is zero at the crack tip and increases with distance behind that point and reaches some final value at the end of the cohesive zone.

A cohesive zone model of crack tip plasticity was introduced by Dugdale [16]. The relevant physical phenomenon was the highly localised plastic deformation ahead of a crack tip in a ductile material. Such a model circumvents the path-dependent nature of plastic flow and so can be applied to growing as well as stationary cracks, that is by modelling the effects of a plastic region by a cohesive stress the model has no path dependency. The cohesive stress is taken as the tensile flow stress of an ideally plastic solid. Figure 3.2 shows schematically the differences between a brittle crack, a 'Barenblatt' crack and a 'Dugdale' crack.

The second type of problem we shall consider is a plane strain contact problem in the geometry shown in Figure 3.1(b). We shall restrict ourselves to the problem of two identical elastic bodies pressed together by various different loadings. Locally near the contact region the undeformed bodies will be parabolic in shape. We shall show how the codimension-two problem can be solved using both a superposition technique and the more elegant Muskhelishvili potential method.

We begin by considering the simplest problem of Hertzian contact, that is one in which the two elastic bodies are pressed together by a purely normal load (or one elastic body is pressed against a rigid body by a purely normal force) and the effects of friction are not included. As a particular example we shall consider the case of two identical two-dimensional bodies being pushed together normally. The first satisfactory analysis of the stresses at the contact of two elastic bodies was by Hertz [29] in 1880. His interest in the problem was related to his study of Newton's optical interference fringes in the gap between two glass lenses. He was concerned about the possible influence of elastic deformation of the surfaces of the lenses due to the contact pressure between them. Hertz developed his analysis for the case of an elliptical contact region and then considered the particular cases of two dimensional contact (i.e. a strip) by taking the limit as one of the principal axes of the ellipse became infinite. We will not follow Hertz's approach but shall instead start by exploiting the two-dimensionality of the problem from the beginning as is now traditional. This problem and related problems are discussed at length by Johnson [43]. Hertz [30] also attempted to use his theory to give a precise definition of hardness but it was to prove unsatisfactory (a satisfactory definition of hardness had to wait for the development of the theory of plasticity).

Including friction we will then consider the effect of a further shearing force after the initial loading. We will see how such a subsequent loading gives rise to regions of *slip*. Slip occurs when the tangential force between the two bodies reaches its limiting value, beyond which frictional forces can no longer keep the two bodies

'stuck' together, and hence they 'slip' past each other. If the slip region grows to be the entire contact region then the two bodies become completely 'unstuck' and begin to slide past one another. Lastly using an incremental technique we will consider the effects of simultaneously varying the normal and tangential loads after first applying a purely normal load.

Many more loading and unloading histories can be considered. Over a dozen different cases are considered by Mindlin and Deresiewicz [56] for the case of spheres rather than cylinders. In their paper they also calculate the energy dissipated in an oscillating motion. The non-uniqueness of the solution when unloading is discussed by Turner [95]. Such a three-dimensional symmetric problem requires a slightly more complicated solution procedure than for the two-dimensional problem to determine the displacements but has the benefit that the displacements decay like r^{-1} (rather than growing like $\log r$ as we will discover for the two-dimensional case) which makes matching out from the local problem near the contact region an easier task.

The third type of problem we will consider has the geometry shown in Figure 3.1(c). We will begin by considering the single problem of a finite length elliptical crack subjected to a normal load (this is a type-I problem). The solution to this static type-I crack problem will be produced using the Muskhelishvili potential method. The elliptic crack will have a minus one half power stress singularity at the stationary crack tips. If the load is then varied dependent upon the crack width we obtain a new solution for which the crack is cusp shaped at the ends and the stress at the crack tips is non-singular. The problem posed is connected with an ink delivery system. Ink is required to flow through the crack and the flow is to be regulated by closing the crack. The desired form of closing is for the crack to 'zip' shut from the edges inward. We shall consider three specific forms for varying the load with the crack width to see how they affect the shape and manner in which the crack shuts.

3.1 Equations of linear elasticity

In elasticity Lagrangian coordinates are natural. The points in the undeformed body are labelled (x, y, z) and on deformation move to (x', y', z') through a displacement $(u_1(x, y, z), u_2(x, y, z), u_3(x, y, z))$ such that

$$(x', y', z') \;=\; (x + u_x(x, y, z), y + u_y(x, y, z), z + u_z(x, y, z)) \quad .$$

The model is formulated in terms of (x, y, z) and is thus defined on the domain of the undeformed body. We will employ the theory of linear elasticity which means

the deformations are small compared to the typical length scale of the problem which leads to Lagrangian coordinates being approximately the same as Eulerian.

Defining the stress tensor

$$\sigma_{ij} = \lambda \frac{\partial u_k}{\partial x_k} \delta_{ij} + 2\mu \varepsilon_{ij} \qquad \text{for} \quad i,j,k = x,y,z \tag{3.1}$$

where ε_{ij} is the strain tensor defined as

$$\varepsilon_{ij} = \frac{1}{2}\left(\frac{\partial u_i}{\partial x_j} + \frac{\partial u_j}{\partial x_i}\right) \qquad \text{for} \quad i,j,k = x,y,z \tag{3.2}$$

then

$$\sigma = \begin{bmatrix} \lambda\left(\frac{\partial u_x}{\partial x} + \frac{\partial u_y}{\partial y} + \frac{\partial u_z}{\partial z}\right) + 2\mu\frac{\partial u_x}{\partial x} & \mu\left(\frac{\partial u_x}{\partial y} + \frac{\partial u_y}{\partial x}\right) & \mu\left(\frac{\partial u_x}{\partial z} + \frac{\partial u_z}{\partial x}\right) \\ \mu\left(\frac{\partial u_x}{\partial y} + \frac{\partial u_y}{\partial x}\right) & \lambda\left(\frac{\partial u_x}{\partial x} + \frac{\partial u_y}{\partial y} + \frac{\partial u_z}{\partial z}\right) + 2\mu\frac{\partial u_y}{\partial y} & \mu\left(\frac{\partial u_y}{\partial z} + \frac{\partial u_z}{\partial y}\right) \\ \mu\left(\frac{\partial u_x}{\partial z} + \frac{\partial u_z}{\partial x}\right) & \mu\left(\frac{\partial u_y}{\partial z} + \frac{\partial u_z}{\partial y}\right) & \lambda\left(\frac{\partial u_x}{\partial x} + \frac{\partial u_y}{\partial y} + \frac{\partial u_z}{\partial z}\right) + 2\mu\frac{\partial u_z}{\partial z} \end{bmatrix}. \tag{3.3}$$

The small displacement $\mathbf{u} = (u_x, u_y, u_z)$ of a point (x, y, z) in an elastic body which is in equilibrium satisfies Navier's equation

$$\begin{aligned} \nabla \cdot \sigma &= 0 \\ \Rightarrow \quad (\lambda + 2\mu)\nabla(\nabla \cdot \mathbf{u}) - \mu \nabla \times (\nabla \times \mathbf{u}) &= 0 \end{aligned} \tag{3.4}$$

and in a dynamic situation it becomes

$$\nabla \cdot \sigma = \rho \mathbf{u}_{tt} \tag{3.5}$$

where ρ is the density of the material.

For future reference we note that in two dimensions we can rearrange (3.1) and (3.2) to obtain

$$E\varepsilon_{xx} = (1-\nu^2)\sigma_{xx} - \nu(1+\nu)\sigma_{yy} \tag{3.6}$$

$$E\varepsilon_{yy} = (1-\nu^2)\sigma_{yy} - \nu(1+\nu)\sigma_{xx} \tag{3.7}$$

$$E\varepsilon_{xy} = 2(1+\nu)\sigma_{xy} \ , \tag{3.8}$$

where $E = \frac{\mu(2\mu+3\lambda)}{\lambda+\mu}$ is Young's modulus and $\nu = \frac{\lambda}{2(\lambda+\mu)}$ is Poisson's ratio, having used the fact that in two dimensions $\sigma_{zz} = \nu(\sigma_{xx} + \sigma_{yy})$.

3.1.1 Airy stress function

A fruitful method for solving two-dimensional plane strain problems was originated by Airy around 1860. If we define a stress function Υ by

$$\sigma_{xx} \;=\; \Upsilon_{yy} \quad , \quad \sigma_{yy} \;=\; \Upsilon_{xx} \quad , \quad \sigma_{xy} \;=\; -\,\Upsilon_{xy}$$

where the subscripts on the left denote the components of the stress tensor while the subscripts on the right denote partial derivatives then we see

$$\begin{aligned} \nabla^2\Upsilon &= \sigma_{xx} + \sigma_{yy} \\ &= 2(\lambda+\mu)\left(\frac{\partial u_x}{\partial x} + \frac{\partial u_y}{\partial y}\right) \\ &= 2(\lambda+\mu)\nabla\cdot\mathbf{u} \ . \end{aligned}$$

Taking the divergence of (3.4) implies

$$(\lambda+2\mu)\nabla^2(\nabla\cdot\mathbf{u}) \;=\; 0 \ .$$

Combining these two results yields the biharmonic equation

$$\nabla^4\Upsilon \;=\; 0 \ . \tag{3.9}$$

For future reference we note that in cylindrical polar coordinates, the stress and strain components can be written as

$$\sigma_{rr} \;=\; \frac{1}{r}\frac{\partial\Upsilon}{\partial r} + \frac{1}{r^2}\frac{\partial^2\Upsilon}{\partial\theta^2} \tag{3.10}$$

$$\sigma_{\theta\theta} \;=\; \frac{\partial^2\Upsilon}{\partial r^2} \tag{3.11}$$

$$\sigma_{r\theta} \;=\; \frac{\partial}{\partial r}\left(\frac{1}{r}\frac{\partial\Upsilon}{\partial\theta}\right) \tag{3.12}$$

and

$$\varepsilon_{rr} \;=\; \frac{\partial u_r}{\partial r} \tag{3.13}$$

$$\varepsilon_{\theta\theta} \;=\; \frac{u_r}{r} + \frac{1}{r}\frac{\partial u_\theta}{\partial\theta} \tag{3.14}$$

$$\varepsilon_{r\theta} \;=\; \frac{1}{r}\frac{\partial u_r}{\partial\theta} + \frac{\partial u_\theta}{\partial r} - \frac{u_\theta}{r} \tag{3.15}$$

respectively, where the subscripts on u denote components of displacement rather than partial derivatives.

3.1.2 The Muskhelishvili potential

Two-dimensional solutions using the Airy stress function formulation are considered the traditional approach to solving problems in plane elasticity. An alternative more elegant method using a complex variable formulation is possible. This technique was first used by Kolosov (around 1910) and brought to fruition by Muskhelishvili (around 1930) although it remained unknown outside Russia until about 1950. The method relies upon the fact that the equations of two-dimensional elasticity possess a general solution in terms of two arbitrary harmonic functions. This permits the problem to be reduced to a classical problem in complex analysis, the Riemann problem. The complete internal stress field corresponding to a particular potential can be found efficiently. The mathematics behind the Muskhelishvili method are more complicated than the Airy stress function approach but, once understood, they permit a simple and direct solution procedure to a wide variety of contact and crack problems.

In plane strain, the general solution to (3.4) is

$$2\mu(u_x + iu_y) \;=\; \kappa^*\phi(z) - z\overline{\phi}'(\overline{z}) - \overline{\psi}(\overline{z}) \tag{3.16}$$

where $z = x + iy$, ϕ and ψ are two arbitrary analytic functions and prime denotes differentiation with respect to z. κ^* is Kolosov's constant which in the case of plane strain is $3 - 4\nu$. The form of the above solution is easily derivable by noting that the solution to the field equation (3.9) is

$$\Upsilon \;=\; \Re\left\{\overline{z}\phi(z) + \chi(z)\right\} \tag{3.17}$$

$$\;=\; \frac{1}{2}\left[\overline{z}\phi(z) + z\overline{\phi(z)} + \chi(z) + \overline{\chi(z)}\right] \quad . \tag{3.18}$$

Then

$$\frac{\partial\Upsilon}{\partial x} + i\frac{\partial\Upsilon}{\partial y} \;=\; \phi(z) + z\overline{\phi'(z)} + \overline{\psi(z)} \tag{3.19}$$

where $\psi(z) = d\chi/dz$. Furthermore rearranging the equations for σ_{xx} and σ_{yy} we can write

$$2\mu\frac{\partial u_x}{\partial x} \;=\; \frac{\partial^2\Upsilon}{\partial y^2} - \frac{\lambda}{2(\lambda+\mu)}\nabla^2\Upsilon \tag{3.20}$$

$$2\mu\frac{\partial u_y}{\partial y} \;=\; \frac{\partial^2\Upsilon}{\partial x^2} - \frac{\lambda}{2(\lambda+\mu)}\nabla^2\Upsilon \quad . \tag{3.21}$$

Defining

$$P \;=\; \nabla^2\Upsilon \;=\; 4\Re\left\{\phi'(z)\right\} \tag{3.22}$$

then

$$\nabla^2 P \;=\; \nabla^4 \Upsilon \;=\; 0$$

and hence P is a harmonic function. Taking Q to be the harmonic function conjugate to P and defining

$$\begin{aligned} P + iQ &= 4\phi'(z) \\ \frac{\partial \tilde{p}}{\partial x} + i\frac{\partial \tilde{q}}{\partial x} &= \phi'(z) \end{aligned}$$

then by the Cauchy Riemann equations

$$P \;=\; 4\frac{\partial \tilde{p}}{\partial x} \;=\; 4\frac{\partial \tilde{q}}{\partial y} \;. \tag{3.23}$$

Substituting from (3.22) and (3.23) into (3.20) and (3.21) we obtain

$$\begin{aligned} 2\mu\frac{\partial u_x}{\partial x} &= -\frac{\partial^2 \Upsilon}{\partial x^2} + \frac{2(\lambda+2\mu)}{\lambda+\mu}\frac{\partial \tilde{p}}{\partial x} \\ 2\mu\frac{\partial u_y}{\partial y} &= -\frac{\partial^2 \Upsilon}{\partial y^2} + \frac{2(\lambda+2\mu)}{\lambda+\mu}\frac{\partial \tilde{q}}{\partial y} \end{aligned}$$

which we can integrate and add together to produce

$$2\mu(u_x + iu_y) \;=\; -\left(\frac{\partial \Upsilon}{\partial x} + i\frac{\partial \Upsilon}{\partial y}\right) + 2\frac{\lambda+2\mu}{\lambda+\mu}\phi(z)$$

where the functions of integration have been taken to be zero since they only represent rigid body motions. Further substituting in from (3.19) yields (3.16).

By substituting (3.16) into (3.3) we could deduce the stresses in terms of ϕ and ψ. However a more elegant result is

$$\sigma_{xx} + \sigma_{yy} \;=\; 2[\Phi(z) + \overline{\Phi}(\overline{z})] \tag{3.24}$$

$$(\sigma_{yy} - \sigma_{xx}) + 2i\sigma_{xy} \;=\; 2[\overline{z}\Phi'(z) + \Psi(z)] \tag{3.25}$$

where $\Phi(z) = \phi'(z)$ and $\Psi(z) = \psi'(z)$. From these two equations the internal stresses can be determined and they also implicitly give the displacement field at each point from (3.16). Eliminating σ_{xx} between (3.24) and (3.25) gives

$$\sigma_{yy} - i\sigma_{xy} \;=\; z\overline{\Phi'(z)} + \overline{\Phi(z)} + \Phi(z) + \overline{\Psi(z)} \;. \tag{3.26}$$

Case I: Problems posed on the upper half space

For a problem posed on the upper half space, on $y = 0$ either the components of stress $\sigma_{yy} = -p(x)$ and $\sigma_{xy} = q(x)$, or the surface displacements u_x and u_y, or a combination of both, will be given.

From (3.26), on the boundary $y = 0$ we have

$$\begin{aligned} \Phi^+(x) + \overline{\Phi^-}(x) + x\overline{\Phi^-}'(x) + \overline{\Psi^-}(x) &= -p(x) - iq(x) && (3.27) \\ \Phi^+(x) + \overline{\Phi^-}(x) + x\Phi^{+\prime}(x) + \Psi^+(x) &= -p(x) + iq(x) \ . && (3.28) \end{aligned}$$

If we define

$$\Omega(z) = -\Phi(z) - z\Phi'(z) - \Psi(z) \ , \tag{3.29}$$

then $\Omega(z)$ is holomorphic in the upper half-plane because $\Phi(z)$ and $\Psi(z)$ are. Consider $\overline{\Phi}(z)$ and $\overline{\Omega}(z) = -\overline{\Phi}(z) - z\overline{\Phi}'(z) - \overline{\Psi}(z)$ which are holomorphic in the lower half-plane. By (3.27) and (3.28) on any unloaded part of the axis

$$\begin{aligned} \Phi^+(x) &= \overline{\Omega^-}(x) \\ \overline{\Phi^-}(x) &= \Omega^+(x) \end{aligned}$$

where the $\pm$ notation is the same as was used in the water entry problem. From the first of these equations it follows that $\overline{\Omega}(z)$, which is holomorphic in the lower half plane, is the analytic continuation of $\Phi(z)$ from the upper to the lower half plane. Similarly the second of these equations implies $\Omega(z)$ is the analytic continuation into the upper half plane of $\overline{\Phi}(z)$. Hence by (3.29) $\Psi(z)$ may also be analytically continued such that

$$\Psi(z) = -\Phi(z) - \overline{\Phi}(z) - z\Phi'(z) \ . \tag{3.30}$$

Inserting this into (3.25) gives

$$(\sigma_{yy} - \sigma_{xx}) + 2i\sigma_{xy} = 2\left[(\overline{z} - z)\Phi'(z) - \Phi(z) - \overline{\Phi}(z)\right] \tag{3.31}$$

which together with (3.24) allows the stresses to be derived from Φ alone. Once Φ is determined for a particular problem, a complete solution can be obtained. Substituting (3.30) into (3.26) we obtain

$$\sigma_{yy} - i\sigma_{xy} = (z - \overline{z})\overline{\Phi}'(\overline{z}) + \Phi(z) - \Phi(\overline{z}) \tag{3.32}$$

from which the traction components of stress can be found, that is σ_{yy} and σ_{xy} on the line $y = 0$. Additionally by differentiating (3.16) with respect to x we see

$$2\mu\left(\frac{\partial u_x}{\partial x} + i\frac{\partial u_y}{\partial x}\right) = (\overline{z} - z)\overline{\Phi}'(\overline{z}) + \Phi(\overline{z}) + \kappa^*\Phi(z) \ . \tag{3.33}$$

In a typical contact problem contact takes place over a region of the x-axis. The remaining part of the x-axis is traction free. By letting $y \to 0$ in (3.32) and (3.33) we see immediately that Φ must be a function with the properties

$$\Phi^+(x) - \Phi^-(x) = -p(x) - iq(x) \tag{3.34}$$

$$\kappa^*\Phi^+(x) + \Phi^-(x) = 2\mu(u_x' + iu_y') \tag{3.35}$$

where the notation $\pm$ used is the same as that in the water entry problem and the general tractions σ_{yy} and σ_{xy} are denoted by $-p$ and q.

Case II: Problems posed on the whole plane with cuts along the x axis

In this case we introduce

$$\Omega(z) = \overline{\Phi}(z) + z\overline{\Phi}'(z) + \overline{\Psi}(z)$$

so

$$\Psi(z) = \overline{\Omega}(z) - \Phi(z) - z\Phi'(z) \ .$$

Then (3.26) becomes

$$\sigma_{yy} - i\sigma_{xy} = \Phi(z) + \Omega(\overline{z}) + (z - \overline{z})\overline{\Phi'(z)} \ . \tag{3.36}$$

Further defining

$$\omega(z) = \int \Omega(z)dz = z\overline{\Phi}(z) + \overline{\psi}(z) + const$$

then $\omega(z)$ is determined up to an additive constant by Φ and Ψ. (3.16) then becomes

$$2\mu(u_x + iu_y) = \kappa^*\phi(z) - \omega(\overline{z}) - (z - \overline{z})\overline{\Phi}(z) + const \ . \tag{3.37}$$

Differentiating with respect to x yields

$$2\mu\left(\frac{\partial u_x}{\partial x} + i\frac{\partial u_y}{\partial x}\right) = \kappa^*\Phi(z) - \Omega(\overline{z}) - (z - \overline{z})\overline{\Phi'(z)} \ . \tag{3.38}$$

Defining L to be the union of all the cuts along the x axis and letting $y \to 0$ from above and below we obtain from (3.36)

$$\begin{aligned} \sigma_{yy}^{+} - i\sigma_{xy}^{+} &= \Phi^{+}(x) + \Omega^{-}(x) \qquad \text{on} \quad L \\ \sigma_{yy}^{-} - i\sigma_{xy}^{-} &= \Phi^{-}(x) + \Omega^{+}(x) \qquad \text{on} \quad L \end{aligned}$$

which can be combined to give

$$[\Phi(x) + \Omega(x)]^{+} + [\Phi(x) + \Omega(x)]^{-} = 2p(x) \qquad \text{on} \quad L \tag{3.39}$$

$$[\Phi(x) - \Omega(x)]^{+} - [\Phi(x) - \Omega(x)]^{-} = 2q(x) \qquad \text{on} \quad L \tag{3.40}$$

where

$$p(x) = \frac{1}{2}\left[\sigma_{yy}^{+} + \sigma_{yy}^{-}\right] - \frac{i}{2}\left[\sigma_{xy}^{+} + \sigma_{xy}^{-}\right] \tag{3.41}$$

$$q(x) = \frac{1}{2}\left[\sigma_{yy}^{+} - \sigma_{yy}^{-}\right] - \frac{i}{2}\left[\sigma_{xy}^{+} - \sigma_{xy}^{-}\right] \quad . \tag{3.42}$$

Thus given the stress components σ_{yy} and σ_{xy} on the crack faces we can solve the Riemann problems to obtain $\Phi(z)$ and $\Omega(z)$.

If, however, we are given the displacements of the crack faces we can formulate two Riemann problems using (3.38). Letting $y \to 0$ from above and below and then combining the two resulting equations we obtain

$$\begin{aligned} [\kappa^{*}\Phi(x) - \Omega(x)]^{+} + [\kappa^{*}\Phi(x) - \Omega(x)]^{-} &= 2f(x) \qquad \text{on} \quad L \\ [\kappa^{*}\Phi(x) + \Omega(x)]^{+} - [\kappa^{*}\Phi(x) + \Omega(x)]^{-} &= 2g(x) \qquad \text{on} \quad L \end{aligned}$$

where

$$\begin{aligned} f(x) &= \mu\left[(u_x^{+\prime} + u_x^{-\prime}) + i(u_y^{+\prime} + u_y^{-\prime})\right] \\ g(x) &= \mu\left[(u_x^{+\prime} - u_x^{-\prime}) + i(u_y^{+\prime} - u_y^{-\prime})\right] \quad . \end{aligned}$$

If we are given a combination of types of boundary conditions, that is say we are given displacements on some parts of the cuts and stresses on others then in general we need to use both sets of Riemann problems to solve the model.

3.2 A dynamic type-III crack moving at a constant velocity

Nearly all earthquakes occur on pre-existing faults. A dynamic type-III crack moving at a constant speed has been studied both experimentally [7, 15, 48, 54, 69] and

theoretically [50, 59, 65, 83] in an attempt to predict what actually happens during an earthquake. One particular factor the model should predict is the crack tip speed. Furthermore, the stress near the crack tip is important. We will review just two particular models.

We will begin this section by first considering the propagation of a single crack which lies along the centre line of a strip in two dimensions without any cohesive zone near the crack tip; that is, the crack face will be stress free along its entire length (similar problems have been considered by Kuo [50], Nilsson [65] and Sih and Chen [83]). The codimension-two model domain is a strip with a semi-infinite cut along the centre line. By means of a conformal mapping we will show how this can be transformed to a problem on a half space and subsequently solved by formulation as a Riemann problem. Using a critical stress intensity factor as discussed at the beginning of the chapter a formula for the crack tip speed will be produced. However, as also mention earlier, the stress intensity factor approach inevitably has a square root singularity in the stress at the crack tip.

Having reviewed the basic result for the motion of a single crack in terms of a stress intensity factor we will then follow the analysis of Morgan et al. [59] and examine the effect of including a cohesive zone near the crack tip. This problem near the crack tip will also be solved by formulating it as a Riemann problem. The solution is then matched to an outer solution which is the previous solution for the problem with no cohesive zone. Morgan et al. then continue on to include a second mode of viscous resistance on the entire crack face but we shall not present that analysis here. We should note that a similar problem to that considered by Morgan et al. was considered by Nakanishi [62] using a Wiener–Hopf technique.

3.2.1 Solution when the crack face is stress free along its entire length

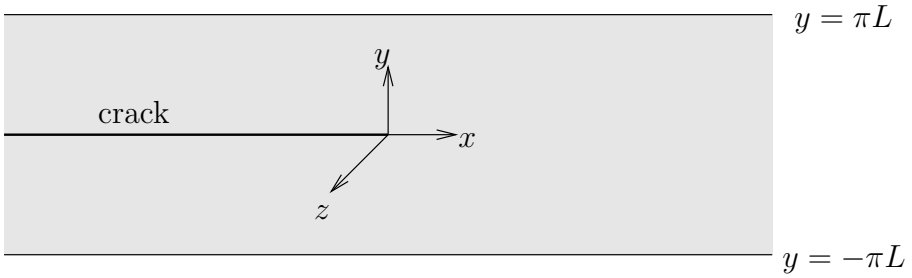

Figure 3.3: The initial configuration of the crack.

We shall begin by considering one of the simplest type-III problems, that of a single semi infinite crack (linearised to lie) along the centre line of a strip. The initial configuration is as shown in Figure 3.3. The upper and lower boundaries are displaced a distance ϵL in opposite directions parallel to the z-axis and the boundaries of the crack are taken to be stress free. The size of the region near the crack tip over which the assumption of linear elasticity fails will be related to the small parameter ϵ. The displacements will be of the form $\mathbf{u} = (0, 0, w(x, y))$ for which the dynamic field equation (3.5) becomes

$$c^2 \left(w_{xx} + w_{yy}\right) \quad = \quad w_{tt}$$

where $c^2 = \mu/\rho$. We shall assume that the crack tip moves at a constant velocity v.

Nondimensionalising the problem with

$$x = L\hat{x} \quad , \quad y = L\hat{y} \quad , \quad w = \epsilon L\hat{w} \quad , \quad t = \frac{L}{c}\hat{t} \quad , \quad v = c\hat{v}$$

and immediately dropping the hats we obtain the nondimensional codimension–two model shown in Figure 3.4.

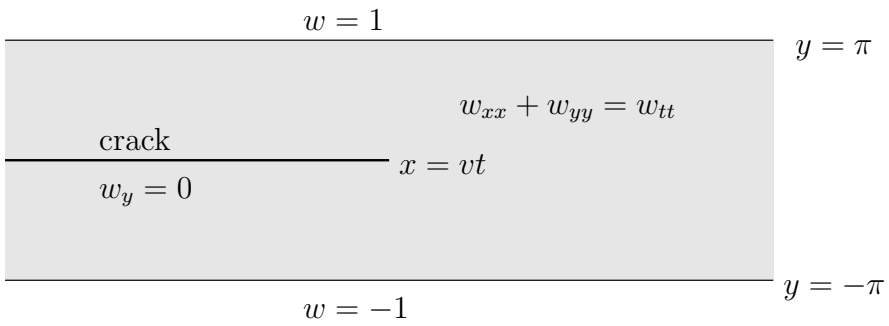

Figure 3.4: The codimension-two type-III dynamic crack problem.

We can further eliminate the time dependence by moving into a frame moving with the crack tip speed by making the substitution

$$\hat{x} = \frac{x - vt}{(1 - v^2)^{\frac{1}{2}}} \quad ,$$

and again immediately dropping the hat, to produce the problem shown in Figure 3.5.

By applying a sequence of conformal maps we can map this problem onto the upper half plane. Defining $z = x + iy$ as usual, we apply the map

$$\tilde{s} \quad = \quad ie^{\frac{z}{2}}$$

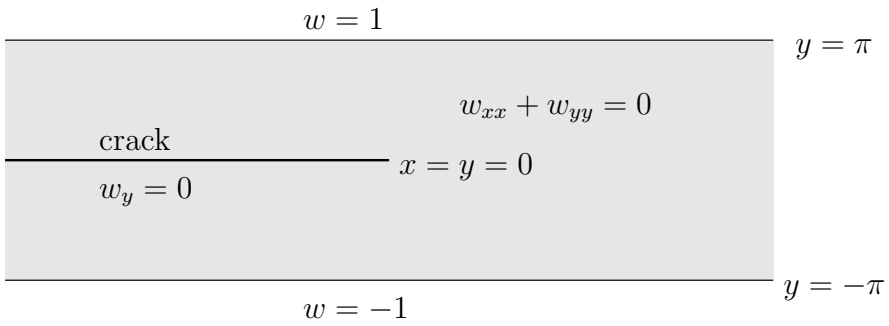

Figure 3.5: The codimension-two type-III dynamic crack problem in the moving frame.

which maps the domain in the z-plane into the domain shown in the $\tilde{s}$-plane (see Figure 3.6). We then apply the further map

$$\tilde{s} \;=\; (s^2-1)^{\frac{1}{2}}$$

to map the problem on to the upper half of the s-plane (Note since the boundary of the original domain was polygonal we could have used the Schwartz–Christoffel transformation to derive a suitable mapping).

Taking the solution to be of the form

$$w \;=\; \Im\{f(z)\}$$

then the mixed boundary value problem in the complex s plane is to find an f such that

$$\begin{aligned}
\Re\left\{\frac{df}{ds}\frac{e^z}{(1-e^z)^{\frac{1}{2}}}\right\} \;=\; \Re\left\{\frac{df}{ds}\frac{1-s^2}{s}\right\} \;&=\; 0 \qquad \text{for} \quad -1<\Re s<1 \quad , \quad \Im s=0 \\
\Im f \;&=\; 1 \qquad \text{for} \quad \Re s<-1 \quad , \quad \Im s=0 \\
\Im f \;&=\; -1 \qquad \text{for} \quad \Re s>1 \quad , \quad \Im s=0 \;\; .
\end{aligned}$$

We also note that since w is constant on the fixed boundaries $w_x = 0$ there which gives the condition

$$\Im\left\{\frac{df}{ds}\frac{1-s^2}{s}\right\} \;=\; 0 \qquad \text{for} \quad \Re s<-1 \quad \text{or} \quad \Re s>1 \quad , \quad \Im s=0 \;\; .$$

We can formulate this as a Riemann problem as was done by Sih et al. [83]. Defining $s = s_1 + is_2$ and

$$G(s) \;=\; \begin{cases} \dfrac{df}{ds}(s) \;=\; u(s_1,s_2)+iv(s_1,s_2) & \text{in} \quad s_2>0 \\[2ex] \overline{\dfrac{df}{ds}}(\overline{s}) \;=\; u(s_1,-s_2)-iv(s_1,-s_2) & \text{in} \quad s_2<0 \end{cases}$$

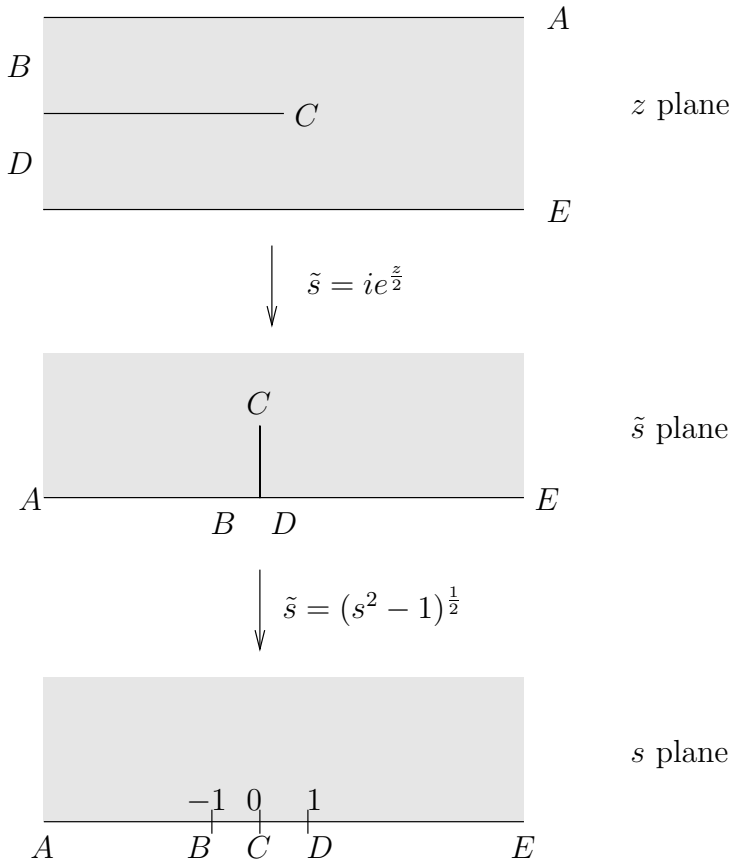

Figure 3.6: The domain of the crack problem in the z, $\tilde{s}$ and s planes.

then the boundary conditions result in the Riemann problem

$$\begin{aligned} G^+(s_1) + G^-(s_1) &= 0 \qquad \text{for} \quad s_1 \in (-1,1) \\ G^+(s_1) - G^-(s_1) &= 0 \qquad \text{for} \quad s_1 \notin (-1,1) \ . \end{aligned}$$

Using the results of Appendix B we see that this is a problem with index one where the solution will be unbounded at the free points. We require the stresses at infinity to be bounded and hence the solution is

$$G(z) = \frac{C}{\sqrt{s^2-1}} \ .$$

Integrating this and applying the conditions on the fixed boundaries yields

$$f(s) = \frac{2}{\pi} \log \left[-is - i\sqrt{s^2-1} \right]$$

which when written back in original variables gives

$$w = \Im f(z) = \frac{2}{\pi} \Im \left\{ \log \left[e^{\frac{z}{2}} + (e^z - 1)^{\frac{1}{2}} \right] \right\} \ .$$

For z small

$$w_y \;=\; \frac{1}{\pi}\Re\left\{\left(\frac{e^z}{e^z-1}\right)^{\frac{1}{2}}\right\} \;\sim\; \frac{1}{\pi}\Re\left\{\frac{1}{\sqrt{z}}\right\} \quad .$$

The nondimensional dynamic stress intensity factor K in the moving frame of reference is defined to be

$$K \;=\; \lim_{x\to 0}\left[\sqrt{\left(2\pi(1-v^2)^{\frac{1}{2}}x\right)}w_y|_{y=0}\right]$$

and hence from the above result we have

$$K = \sqrt{\frac{2(1-v^2)^{\frac{1}{2}}}{\pi}} \quad .$$

Taking K to be known for a specific material we can then solve this equation for the crack propagation speed v yielding

$$v = \sqrt{1-\frac{\pi^2}{4}K^4} \quad .$$

The critical value of the stress intensity factor for the onset of fracture is when $v = 0$ which implies

$$K_c \;=\; \sqrt{\frac{2}{\pi}} \quad .$$

Thus with this model locally near the crack tip the solution $w \sim O(\epsilon x^{\frac{1}{2}})$ and the stress is singular. As discussed at the beginning of the chapter such a result cannot be literally accepted but must instead be interpreted on the basis that the size of the region over which the behaviour of the material deviates from linear elasticity is on a smaller length scale. The cohesive zone idea provides a simple device for studying crack tip phenomena on a small length scale on which deviations from linear elasticity would occur.

3.2.2 Inclusion of a cohesive zone

The cohesive zone is introduced locally near the crack tip when the dimensional w_y becomes $O(1)$, that is the cohesion acts on a dimensionless length scale of $O(\epsilon^2)$. This assumption implies the cohesive stress is $O(\mu)$ so that it balances the elastic shear stress on the length scale $O(\epsilon^2)$. Hence we scale in by defining inner variables

$$x = \epsilon^2\hat{x} \quad , \quad y = \epsilon^2\hat{y} \quad , \quad w = \epsilon\hat{w} \quad .$$

We recall that the essential idea of a cohesive zone is to simulate material response beyond the linear elastic range by introducing a cohesive stress behind the crack tip which resists the crack opening. Furthermore the cohesive zone is taken to terminate when the displacement reaches some critical value. We will take the simplest model for when the cohesive zone is assumed to be modelling plastic deformation near the crack tip. The simplest model for a plastic cohesive zone is

$$\hat{w}_{\hat{y}} = g_0 \ ,$$

that is the boundary is no longer stress free but instead has some imposed constant stress g_0. We further assume this force only acts on an interval of length $\hat{d}$ in the inner region. The inner problem, therefore, takes the form shown in Figure 3.7.

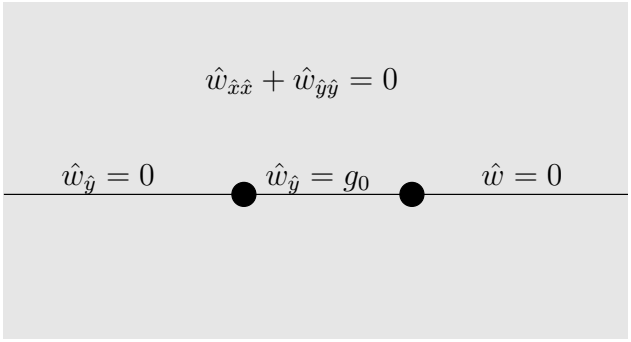

Figure 3.7: The inner crack problem with a cohesive zone.

We can now proceed to solve this problem by formulating it as a Riemann boundary value problem. We write the solution to this inner problem in the form

$$\hat{w} \ = \ \Re W(\hat{z}) \ .$$

Defining

$$G(\hat{z}) \ = \ \begin{cases} \dfrac{dW}{d\hat{z}}(\hat{z}) \ = \ u(\hat{x},\hat{y}) + iv(\hat{x},\hat{y}) & \text{in} \quad \hat{y} > 0 \\ -\overline{\dfrac{dW}{d\hat{z}}}(\overline{\hat{z}}) \ = \ -u(\hat{x},-\hat{y}) + iv(\hat{x},-\hat{y}) & \text{in} \quad \hat{y} < 0 \end{cases}$$

we can write the mixed boundary value problem as the Riemann problem

$$\begin{aligned} G^+(\hat{x}) &= G^-(\hat{x}) \qquad \text{for} \quad \hat{x} > 0 \\ G^+(\hat{x}) &= -G^-(\hat{x}) - 2ig_0 \qquad \text{for} \quad -\hat{d} < \hat{x} < 0 \\ G^+(\hat{x}) &= -G^-(\hat{x}) \qquad \text{for} \quad \hat{x} < -\hat{d} \ . \end{aligned}$$

Using the results from Appendix B the solution to this problem which is zero at infinity and bounded at the origin takes the form

$$\frac{dW}{d\hat{z}} = -\frac{\sqrt{\hat{z}}}{\pi}\int_{-\hat{d}}^{0}\frac{g_0}{(\tau-\hat{z})\sqrt{\tau}}d\tau \ . \tag{3.43}$$

In order for this to match to the outer solution we require

$$\frac{\partial\hat{w}}{\partial\hat{y}} \sim \frac{1}{\pi\sqrt{\hat{z}}} \qquad \text{as} \quad \hat{z}\to\infty$$

from which we deduce

$$\begin{aligned} -i &= g_0\int_{-\hat{d}}^{0}\frac{1}{\sqrt{\tau}}d\tau \\ &= -2g_0\sqrt{-\hat{d}} \ . \end{aligned}$$

Rearranging this we obtain

$$4{g_0}^2\hat{d} = 1 \ . \tag{3.44}$$

Integrating (3.43) we obtain

$$W = \frac{g_0}{\pi}\left[(\hat{z}+\hat{d})\log\left(\frac{\sqrt{\hat{z}}-\sqrt{-\hat{d}}}{\sqrt{\hat{z}}+\sqrt{-\hat{d}}}\right) - 2\sqrt{-\hat{d}\hat{z}} - i\pi\hat{d}\right]$$

having used the fact that $W(0)=0$. Expanding this for small z we find

$$W \sim z^{\frac{3}{2}}$$

and hence we have a three-halves power singularity in the tip displacement and only a one-half power singularity in the tip stress, compared with a one-half and a minus one-half power singularity, respectively, without the cohesive region. The region of cohesion will terminate when the displacement reaches some critical value $\hat{w}=\delta$ at $\hat{x}=-\hat{d}$. Applying the condition $\delta=\Re W(-\hat{d})$ yields the result

$$\delta = \frac{2\hat{d}g_0}{\pi} \ .$$

Substituting in from (3.44) for $\hat{d}$ produces

$$\delta = \frac{1}{2\pi g_0} \ .$$

Thus the addition of a cohesion zone rather than the use of a stress intensity factor has resulted in no prediction of the crack tip speed but has resulted in a finite crack

tip stress. Furthermore the inclusion of a cohesive zone has changed the singularity in the displacement at the crack tip from one-half to three-halves and hence has changed the singularity in the stress from minus one-half to plus one-half. This change in the nature of the singularity at the crack tip is related to the change in index of the Riemann problem. The Riemann problem without the cohesive zone had an index of one whereas the inclusion of the cohesive zone changes the index to minus one and hence gives rise to the bounded crack tip stress. As $\hat{d} \to 0$ the the solution without a cohesive zone is recovered.

It is possible to recover a result for the crack tip speed by introducing a viscous resistance force on the entire crack face, that is the nondimensional crack face boundary condition becomes

$$w_y \;=\; -\alpha w_x \qquad \text{on} \quad x < 0 \quad , \quad y = 0 \quad .$$

The analysis for this problem follows much along the lines of that already performed. The results can be found in Morgan et al. [59] where it is shown that this does produce a means of finding a crack tip velocity.

3.3 Two-dimensional contact of two identical elastic bodies

As discussed at the beginning of the chapter we will begin this section by considering the normal contact of two identical two-dimensional bodies. As was mentioned this is one of the oldest type of contact problems originally having been considered by Hertz [29] and can also be found in many of the books listed at the beginning of the chapter. The Hertz theory takes no account of any frictional forces. However, provided the two bodies are made of the same material (they need not be the same shape but we shall assume they are for mathematical convenience) then any two points which first meet at the edge of a growing contact region will subsequently move tangentially at the same rate, that is they will remain 'stuck' together and no frictional forces will arise. It is only if the two bodies are made of different materials that these two points which initially meet at the edge of the growing contact region would wish to move tangentially at differing rates. In this case a force due to friction would occur. Depending on the magnitude of the frictional force points may become unstuck producing a region of slip. Such a problem has been considered by Nowell et al. [66] among others. The normal loading of a single axisymmetric body pressed

against a rigid half space with the inclusion of friction has been considered by Spence [88, 89] and Turner [95].

In Section 3.3.2 we shall consider the effect of applying a shearing force after the initial normal force. Clearly unlike the simple case of normal loading the friction is crucial for this problem. Without the friction the shearing forces will simply cause the two bodies to slide over one another. The analysis will show how the two bodies do not remain completely 'stuck' but instead a region of slip occurs at the edge of the contact region. Lastly we will consider the effect of simultaneous variations to the normal and shearing forces after initially applying a normal load. In each of these problems for ease of analysis we will only consider the simplest case when it is assumed that the pressure distribution is independent of the shear. This is known as the Mindlin approximation. Coupled problems can also be solved as shown by Spence [90].

3.3.1 Normal contact force

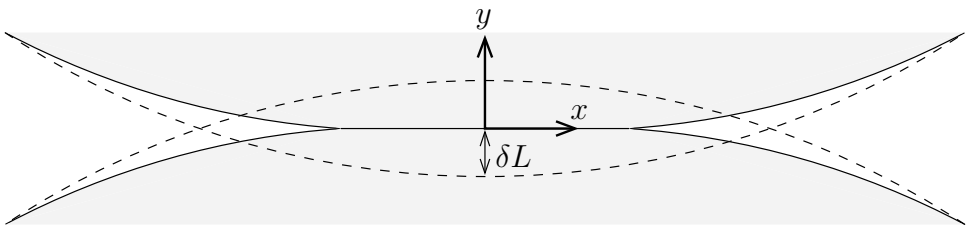

Figure 3.8: The positions of the deformed and undeformed bodies.

The two identical bodies are pushed together each by a force N which will be applied at a point a distance L from the surface of the body along a line normal to the contact surface. The bodies are assumed to only initially touch at one point and are taken to be convex. The shape of the bodies is denoted by $y = f(x)$ and the bodies each come together a small distance δL, where δ is to be determined. The boundary of the upper body in the absence of the other, shown in Figure 3.8, is $(x, f(x) - \delta L)$. Hence the codimension-one free boundary is

$$(x + u_x(x, y), f(x) - \delta L + u_y(x, y)) \qquad \text{for} \quad y = f(x) - \delta L \ .$$

We take axes such that the two bodies initially touch at a point at which they have zero gradient which implies $f(0) = f'(0) = 0$.

The small displacement $\mathbf{u} = (u_x, u_y)$ of a point (x, y) in the body satisfies Navier's equation (3.4) which in two dimensions implies

$$(\lambda + 2\mu)\nabla(\nabla.\mathbf{u}) - \mu\nabla \times (\nabla \times \mathbf{u}) \;=\; \mathbf{0} \qquad \text{in} \quad y(x) \geq f(x) - \delta L \;\; .$$

The non-contact part of the deformed boundary is stress free while the contact part experiences a stress due to the normal force from the opposing body which will take the form $(0, p(x))$, where $p(x)$ is to be determined as part of the solution. The two stress conditions can be expressed as

$$\sigma\mathbf{n} \;=\; \mathbf{0} \qquad \text{on the non-contact region} \tag{3.45}$$

$$\sigma\mathbf{n} \;=\; p(x)\mathbf{j} \qquad \text{on the contact region} \;\; , \tag{3.46}$$

where $\mathbf{n}$ is the outward normal to the surface. Also from the geometry of the problem we see that on the contact region $y' = 0$ whilst on the non-contact region $y' > 0$ which implies

$$f + u_y \;=\; \delta L \qquad \text{on} \quad y = f(x) - \delta L \quad , \quad |x| < d \tag{3.47}$$

$$f + u_y \;>\; \delta L \qquad \text{on} \quad y = f(x) - \delta L \quad , \quad |x| > d \tag{3.48}$$

where d is the point on the body $y = f(x) - \delta L$ which lies at the end of the contact region. Finally we require the force on the contact region to be positive and equal to the applied load N which gives us the two conditions

$$\int_{-d}^{d} p(x)dx \;=\; N \tag{3.49}$$

$$p(x) \;\geq\; 0 \qquad \text{on} \quad y = f(x) - \delta L \quad , \quad |x| < d \;\; . \tag{3.50}$$

In order to nondimensionalise this model we must consider what the typical values are for all the variables. Clearly u and v have typical values of the order of the maximum displacement δL. The contact set will be small in comparison to the body size and thus we take, as usual, the typical length to be $O(\epsilon L)$ where $\epsilon \ll 1$. The body therefore has the local form

$$\begin{aligned} \epsilon L\hat{y} \;&=\; f(0) + \epsilon L\hat{x}f'(0) + \frac{1}{2}(\epsilon L)^2\hat{x}^2 f''(0) + \ldots - \delta L \\ &=\; \frac{1}{2}\epsilon^2 L^2\hat{x}^2 f''(0) + \ldots - \delta L \end{aligned}$$

since $f(0) = f'(0) = 0$. The local body shape $\epsilon\hat{x}^2 f''(0)$ must be of the same order as the deformations so that f is a significant term in (3.47). Thus $\delta = \epsilon^2$ and the scaling

for f should be $\epsilon^2 L$. In order for the pressure term $p(x)$ to remain significant in (3.46) it must be scaled with ϵ times a suitable quantity of $O(\mu)$. Hence we scale p with ϵE. This in turn suggests from (3.49) that we scale the load N with $\epsilon^2 EL$. Thus N/EL is small as is necessary if the displacements are to be small and the problem is to be representable by linear elasticity. Finally from (3.1) and (3.2) we find the appropriate scalings for the stresses and strains are ϵE and ϵ respectively. The measurable small parameter in this problem is

$$\epsilon' \;=\; \frac{N}{EL} \;.$$

To relate this parameter to ϵ and hence δ requires the local codimension-two solution near the contact region to be matched to an outer solution for the whole body. This matching takes place in Section 3.3.1.4.

Summarising, the scalings to be made are

$$x = \epsilon L\hat{x} \quad , \quad y = \epsilon L\hat{y} \quad , \quad d = \epsilon L\hat{d} \quad , \quad u_x = \epsilon^2 L\hat{u}_x \quad , \quad u_y = \epsilon^2 L\hat{u}_y \quad ,$$

$$f = \epsilon^2 L\hat{f} \quad , \quad N = \epsilon^2 EL\hat{N} \quad , \quad p = \epsilon E\hat{p} \quad , \quad \sigma = \epsilon E\hat{\sigma} \quad , \quad \varepsilon = \epsilon\hat{\varepsilon} \;.$$

The scalings imply that to leading order the free boundary is just $\hat{y} = 0$ and hence the normal to both the free boundary and the contact part of the boundary is $\mathbf{n} = (0, -1)$. It is for this reason that such contact problems are naturally linearised onto half spaces.

Thus to leading order, on dropping the hats we obtain the codimension-two model shown in Figure 3.9. The problem has simplified to that of a normal force applied to a section of a half space.

3.3.1.1 Solution of the codimension-two model

We shall first solve the problem using the traditional approach using the Airy stress function defined in Section 3.1.1. To be consistent with the scalings already performed the stress function is non-dimensionalised with $\epsilon^3 EL^2$.

In terms of the stress function the model takes the form

$$\nabla^4 \Upsilon \;=\; 0 \qquad \text{in} \quad y \geq 0 \tag{3.51}$$

$$\Upsilon_{xy} \;=\; 0 \qquad \text{on} \quad y = 0 \quad , \quad |x| < d \tag{3.52}$$

$$\Upsilon_{xx} \;=\; -p(x) \quad \text{on} \quad y = 0 \quad , \quad |x| < d \tag{3.53}$$

$$\Upsilon_{xy} \;=\; 0 \qquad \text{on} \quad y = 0 \quad , \quad |x| > d \tag{3.54}$$

$$\Upsilon_{xx} \;=\; 0 \qquad \text{on} \quad y = 0 \quad , \quad |x| > d \;. \tag{3.55}$$

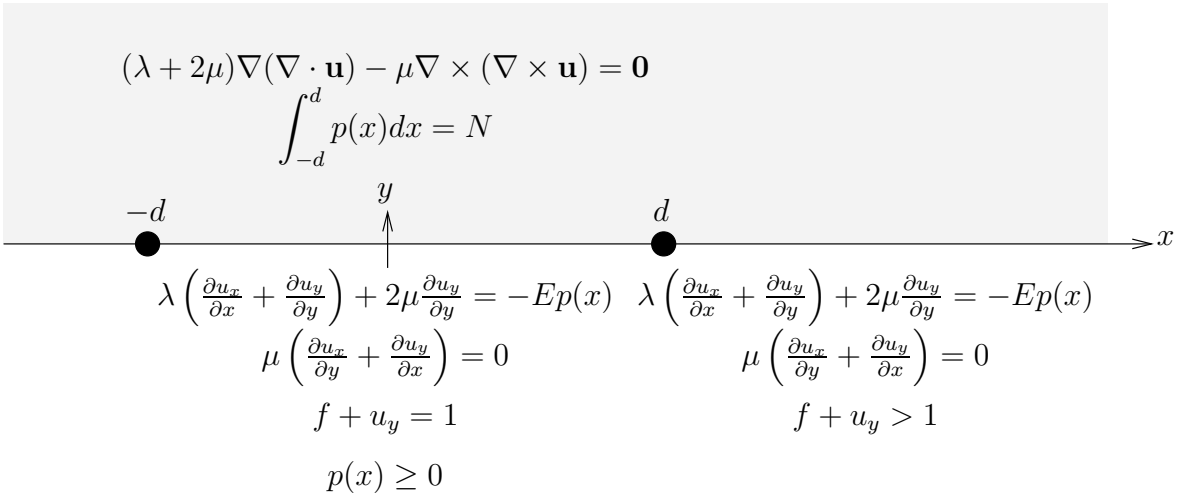

Figure 3.9: The codimension-two free boundary problem.

The remaining conditions need not be transformed as they will not be used at this point. We can build up the solution to this problem by firstly considering the simpler problem of a point force P applied at the origin on the boundary of an elastic half space and then employing the principle of superposition of solutions to construct the solution to the full problem above. This type of approach is similar to the method of solving inviscid flow past a slender body by considering a distribution of sources of varying strength along the body [53].

Changing to cylindrical polar coordinates the biharmonic equation becomes

$$\left(\frac{\partial^2}{\partial r^2} + \frac{1}{r}\frac{\partial}{\partial r} + \frac{1}{r^2}\frac{\partial^2}{\partial \theta^2}\right)\left(\frac{\partial^2 \Upsilon}{\partial r^2} + \frac{1}{r}\frac{\partial \Upsilon}{\partial r} + \frac{1}{r^2}\frac{\partial^2 \Upsilon}{\partial \theta^2}\right) = 0$$

which has general solutions dominated by a single power of r given by

$$\Upsilon = \begin{cases} A_0 \cos 2\theta + B_0 \sin 2\theta + C_0\theta + D_0 & \text{for } n = 0 \\ r(A_1 \cos\theta + B_1 \sin\theta + C_1\theta \sin\theta + D_1\theta\cos\theta) & \text{for } n = 1 \\ r^2(A_2 \cos 2\theta + B_2 \sin 2\theta + C_2\theta + D_2) & \text{for } n = 2 \\ r^n(A_n \cos n\theta + B_n \sin n\theta + C_n \sin(n-2)\theta + D_n \cos(n-2)\theta) & \text{otherwise .} \end{cases} \tag{3.56}$$

Any linear combination of these four types of solutions is in general a solution to the biharmonic equation. In order to determine the value of all possible coefficients we must apply several conditions. As well as applying the boundary conditions we require σ_{rr} to be symmetric about the y axis, all the stresses (equations (3.10)–(3.12)) to tend to zero as $r \to \infty$ and the force at the origin to be equal to P. In cylindrical polar coordinates (where θ is measured from the y axis making the problem symmetric

about $\theta = 0$) these conditions are

$$\begin{aligned}
\frac{\partial^2 \Upsilon}{\partial r^2} &= 0 \qquad \text{on} \quad \theta = \pm\frac{\pi}{2} \\
\frac{\partial}{\partial r}\left(\frac{1}{r}\frac{\partial \Upsilon}{\partial \theta}\right) &= 0 \qquad \text{on} \quad \theta = \pm\frac{\pi}{2} \\
\frac{1}{r}\frac{\partial \Upsilon}{\partial r} + \frac{1}{r^2}\frac{\partial^2 \Upsilon}{\partial \theta^2} &\to 0 \qquad \text{as} \quad r \to \infty \\
\frac{\partial^2 \Upsilon}{\partial r^2} &\to 0 \qquad \text{as} \quad r \to \infty \\
\frac{\partial}{\partial r}\left(\frac{1}{r}\frac{\partial \Upsilon}{\partial \theta}\right) &\to 0 \qquad \text{as} \quad r \to \infty \\
-\lim_{r\to 0}\int_{-\frac{\pi}{2}}^{\frac{\pi}{2}} \sigma_{rr} r\cos\theta d\theta &= P \ .
\end{aligned}$$

Applying these conditions we find the only permissible modes are

$$\Upsilon = \begin{cases} D_0 \\ r\left(A_1\cos\theta + B_1\sin\theta - \dfrac{P}{\pi}\theta\cos\theta\right) \end{cases} .$$

However if we calculate the three components of stress we find that the constants D_0, A_1 and B_1 do not appear. Thus they make no difference to the stresses and displacements in the body. We can therefore choose them to be zero giving us our final solution

$$\begin{aligned}
\Upsilon &= -\frac{P}{\pi} r\theta\sin\theta \\
\sigma_{rr} &= -\frac{2P}{\pi}\frac{\cos\theta}{r} \\
\sigma_{\theta\theta} &= 0 \\
\sigma_{r\theta} &= 0 \ .
\end{aligned}$$

In cartesian coordinates the components of stress are

$$\sigma_{xx} = \sigma_{rr}\sin^2\theta = -\frac{2P}{\pi}\frac{x^2 y}{(x^2+y^2)^2} \tag{3.57}$$

$$\sigma_{yy} = \sigma_{rr}\cos^2\theta = -\frac{2P}{\pi}\frac{y^3}{(x^2+y^2)^2} \tag{3.58}$$

$$\sigma_{xy} = \sigma_{rr}\cos\theta\sin\theta = -\frac{2P}{\pi}\frac{xy^2}{(x^2+y^2)^2} \ . \tag{3.59}$$

Further combining (3.6)–(3.8) with (3.13)–(3.15) and using the above results for the components of stress and strain we find

$$\frac{\partial u_r}{\partial r} = -\frac{2(1-\nu^2)P}{\pi}\frac{\cos\theta}{r}$$

$$\frac{u_r}{r} + \frac{1}{r}\frac{\partial u_\theta}{\partial \theta} = \frac{2\nu(1+\nu)P}{\pi}\frac{\cos\theta}{r}$$
$$\frac{1}{r}\frac{\partial u_r}{\partial \theta} + \frac{\partial u_\theta}{\partial r} - \frac{u_\theta}{r} = 0 \ .$$

We can integrate these equations in turn yielding

$$u_r = -\frac{2(1-\nu^2)P}{\pi}\cos\theta \ln r + \frac{(1+\nu)(1-2\nu)P}{\pi}\theta\sin\theta + C_1\sin\theta + C_2\cos\theta \quad (3.60)$$
$$u_\theta = \frac{2(1-\nu^2)P}{\pi}\sin\theta\ln r + \frac{(1+\nu)(1-2\nu)P}{\pi}\theta\cos\theta + \frac{(4\nu-1)(1+\nu)P}{\pi}\sin\theta$$
$$+C_1\cos\theta - C_2\sin\theta + C_3 r + C \ . \quad (3.61)$$

By symmetry points on the y axis only displace along the y axis which implies for $\theta = 0$, $u_\theta = 0$, which means $C_1 = C_3 = C = 0$.

Now that we have the solution for a point force P, by the method of superposition we can write down the solution due to the force distribution $p(x)$. If we place a force $p(s)ds$ at $x = s$ then we can add up the contributions due to all forces for which $|s| < d$ by integrating over this range of s. From (3.57), (3.58) and (3.59) the stresses are, therefore,

$$\sigma_{xx} = -\frac{2y}{\pi}\int_{-d}^{d}\frac{p(s)(x-s)^2}{[(x-s)^2+y^2]^2}ds \quad (3.62)$$
$$\sigma_{yy} = -\frac{2y^3}{\pi}\int_{-d}^{d}\frac{p(s)}{[(x-s)^2+y^2]^2}ds \quad (3.63)$$
$$\sigma_{xy} = -\frac{2y^2}{\pi}\int_{-d}^{d}\frac{p(s)(x-s)}{[(x-s)^2+y^2]^2}ds \quad (3.64)$$

and from (3.60) and (3.61) the displacements at the surface are

$$u_x = -\frac{(1+\nu)(1-2\nu)}{2}\left[\int_{-d}^{x} p(s)ds - \int_{x}^{d} p(s)ds\right]$$
$$u_y = -\frac{2(1-\nu^2)}{\pi}\int_{-d}^{d} p(s)\ln|x-s|ds + C_2 \ .$$

Another way of viewing this solution is as a Green's function solution where the Green's function is the solution of the point force problem. Differentiating these expressions with respect to x removes the need to determine C_2 at this stage and yields

$$\frac{\partial u_x}{\partial x} = -(1-2\nu)(1+\nu)p(x) \quad (3.65)$$
$$\frac{\partial u_y}{\partial x} = -\frac{2(1-\nu^2)}{\pi}\int_{-d}^{d}\frac{p(s)}{x-s}ds \ . \quad (3.66)$$

From (3.6), (3.65) and the fact that $\sigma_{yy} = -p(x)$ we see that at the surface $\sigma_{xx} = \sigma_{yy} = -p(x)$.

At this point we have still to determine $p(x)$. However before doing so we will show how equations for the stresses and displacements and (3.66) can be obtained using the Muskhelishvili potential method.

3.3.1.2 Alternative solution procedure using the Muskhelishvili potential

The construction of a solution from the point force solution or a Green's function presented above is considered as the traditional approach to solving a problem in plane elasticity. We will now show how the solution may be more elegantly obtained using the Muskhelishvili potential method outlined in Section 3.1.2. The equations relating the surface tractions to the surface displacements in the contact zone will be found to be the same as those already derived, as one would expect.

In nondimensional form (3.16) becomes

$$\frac{2\mu}{E}(u_x + iu_y) = \kappa^*\phi(z) - z\overline{\phi}'(\overline{z}) - \overline{\psi}(\overline{z}) \ , \tag{3.67}$$

where ϕ and ψ have been nondimensionalised with $\epsilon^2 EL$, (3.24), (3.31) and (3.33) become

$$\sigma_{xx} + \sigma_{yy} = 2[\Phi(z) + \overline{\Phi}(\overline{z})] \tag{3.68}$$

$$\sigma_{yy} - i\sigma_{xy} = (z - \overline{z})\overline{\Phi}'(\overline{z}) + \Phi(z) - \Phi(\overline{z}) \tag{3.69}$$

$$\frac{2\mu}{E}\left(\frac{\partial u_x}{\partial x} + i\frac{\partial u_y}{\partial x}\right) = (\overline{z} - z)\overline{\Phi}'(\overline{z}) + \Phi(\overline{z}) + \kappa^*\Phi(z) \tag{3.70}$$

and (3.34) and (3.35) become

$$\Phi^+(x) - \Phi^-(x) = -p(x) - iq(x) \tag{3.71}$$

$$\kappa^*\Phi^+(x) + \Phi^-(x) = \frac{2\mu}{E}(u_x' + iu_y') \ . \tag{3.72}$$

For the particular contact problem we are considering, Figure 3.9, we have $q = 0$ and $u_y' = f'$ on the contact region and $p = q = 0$ on the non-contact region. Thus we need to use both conditions (3.71) and (3.72) to obtain the solution. If we had been given both surface tractions p and q or both surface displacements u_x and u_y on the entire boundary then we could solve the problem using just one of (3.71) and (3.72).

Following the solution procedure and notation set out in Appendix B we have

$$\left.\begin{array}{rcl} G(t) & = & 1 \\ g(t) & = & -p(t) - iq(t) \end{array}\right\} \qquad \text{on} \quad L$$

where L is the interval $(-d, d)$ of the x-axis. To solve this problem we therefore use the results of Section B.3 for Riemann problems with open contours.

We complete the contour L with L' where L' is the remainder of the x axis. Then we define

$$\begin{aligned} G_1(t) &= 1 \qquad \text{on } L \text{ and } L' \\ g_1(t) &= \begin{cases} -p(t) - iq(t) & \text{on } L \\ 0 & \text{on } L' \end{cases} . \end{aligned}$$

If the end points of L are denoted by $a = -d$ and $b = d$ then

$$\begin{aligned} G_1(a-) &= 1 \quad , \quad G_1(a+) = 1 \\ G_1(b-) &= 1 \quad , \quad G_1(b+) = 1 \end{aligned}$$

and hence

$$\frac{G_1(a-)}{G_1(a+)} = 1 \quad , \quad \frac{G_1(b-)}{G_1(b+)} = 1 \ .$$

Thus $\theta = 0$ and $\Delta = 0$ which implies $\gamma = \gamma' = 0$ and hence the index $\kappa = 0$. The problem is therefore straightforward with $\Phi^{\pm}(z) = \Phi_1^{\pm}(z)$.

Now the solution for a problem with zero index satisfying $\Phi(\infty) = 0$ is

$$\Phi_1^{\pm}(z) = X_1^{\pm}(z)\Psi^{\pm}(z)$$

where

$$\begin{aligned} X_1^{\pm}(z) &= e^{\Gamma^{\pm}(z)} \\ \Gamma(z) &= \int_{-\infty}^{\infty} \frac{\log G_1(\tau)}{\tau - z} d\tau = 0 \\ \Psi(z) &= \frac{1}{2\pi i} \int_{-\infty}^{\infty} \frac{g_1(\tau)}{\tau - z} d\tau = \frac{1}{2\pi i} \int_{-d}^{d} \frac{p + iq}{z - \tau} d\tau \ . \end{aligned}$$

Thus we have

$$\Phi(z) = \frac{1}{2\pi i} \int_{-d}^{d} \frac{p(\tau)}{z - \tau} d\tau \tag{3.73}$$

where we have used the fact that $q = 0$. This however is not the finished solution since we have as yet not determined p.

Substituting (3.73) into (3.72) and then taking the imaginary part we find, on noting $E/\mu = 2(1 + \nu)$, that

$$\frac{\partial u_y}{\partial x} = -\frac{2(1 - \nu^2)}{\pi} \int_{-d}^{d} \frac{p(s)}{x - s} ds$$

which is the same as (3.66).

3.3.1.3 Determination of the normal traction

If we now recall the condition from Figure 3.9, $f+u_y = 1$ on $y = 0$, then differentiating it with respect to x and substituting into (3.66) yields the integral equation

$$\int_{-d}^{d} \frac{p(s)}{s-x} ds \;\; = \;\; -\frac{\pi}{2(1-\nu^2)} f_x \;\; .$$

We assume the local form of the body is $f(x) = Bx^2$. From Section B.4 we can see that the general form of the solution of such an integral equation which is bounded at both the end points is

$$p(x) \;\; = \;\; \frac{(d^2-x^2)^{\frac{1}{2}}}{2(1-\nu^2)\pi} \int_{-d}^{d} \frac{s}{(d^2-s^2)^{\frac{1}{2}}(s-x)} ds \;\; ,$$

where we have taken $B = 1/2$ which corresponds to a cylindrical body of radius 1. Rearranging this expression in the form

$$p(x) \;\; = \;\; \frac{(d^2-x^2)^{\frac{1}{2}} x}{2(1-\nu^2)\pi} \int_{-d}^{d} \frac{1}{(d^2-s^2)^{\frac{1}{2}}(s-x)} ds + \frac{(d^2-x^2)^{\frac{1}{2}}}{2(1-\nu^2)\pi} \int_{-d}^{d} \frac{1}{(d^2-s^2)^{\frac{1}{2}}} ds$$

it can be shown easily that the first integral is zero and the second integral is simply π yielding the result

$$p(x) \;\; = \;\; \frac{(d^2-x^2)^{\frac{1}{2}}}{2(1-\nu^2)} \;\; .$$

If we finally apply condition (3.49) we find

$$N \;\; = \;\; \frac{\pi d^2}{4(1-\nu^2)} \tag{3.74}$$

which determines the semi-contact width d , whereupon

$$p(x) \;\; = \;\; \frac{2N}{\pi d^2}(d^2-x^2)^{\frac{1}{2}} \;\; . \tag{3.75}$$

The maximum pressure is therefore

$$p_0 \;\; = \;\; \frac{2N}{\pi d} \;\; .$$

The stresses in the solid bodies can now be found by substituting $p(x)$ back into (3.62), (3.63) and (3.64). We already know that at the surface of the bodies, $\sigma_{xx} =$

$\sigma_{yy} = -p(x)$ on the contact region while $\sigma_{xx} = \sigma_{yy} = \sigma_{xy} = 0$ on the non contact region. Also along the y axis it is easy to show

$$\sigma_{xx} = -\frac{p_0}{d}\left[\frac{(d^2+2y^2)}{(d^2+y^2)^{\frac{1}{2}}} - 2y\right] \tag{3.76}$$

$$\sigma_{yy} = -\frac{p_0 d}{(d^2+2y^2)^{\frac{1}{2}}} \tag{3.77}$$

$$\sigma_{xy} = 0 \ . \tag{3.78}$$

To obtain the stresses at a more general point within the solid is difficult using direct integration of (3.62)–(3.64). Using the Muskhelishvili potential these internal stresses can be more efficiently computed. Recall for a purely normal force the Muskhelishvili potential (3.73) is

$$\Phi(z) = \frac{1}{2\pi i}\int_{-d}^{d}\frac{p(\tau)}{z-\tau}d\tau \ . \tag{3.79}$$

Substituting in (3.75) and integrating we obtain

$$\Phi(z) = \frac{p_0 i}{2d}\left[z - \sqrt{z^2-d^2}\right] \ .$$

From this we can evaluate $\Phi'(z)$, $\overline{\Phi}(z)$ and $\overline{\Phi(z)}$ from which we can find the internal stresses from (3.68) and (3.69).

3.3.1.4 Parameters determining the contact region

If we were to redimensionalise the results so far we would find that the small parameter ϵ only occurs in the equations for the displacements. However, as yet ϵ^2 has only been defined as the ratio between the maximum displacement and the distance from the boundary at which the force was applied. As mentioned initially the measurable small parameter of the problem is $\epsilon' = N/EL$, that is the Young's modulus E, the typical length scale L (the radius of the cylinder assuming the load is applied at the centre of the cylinder) and the applied load N are given values for the problem. In order to relate ϵ to ϵ' we must match the codimension-two solution to an outer problem.

For our two-dimensional problem the outer problem will simply be that of a point force N on a cylinder. The expansion of such a solution in inner variables will be dominated to leading order by the singularity at the origin. This singularity of the solution will be the same as that of a point force on a half space where the vertical displacement at the centre of the cylinder is zero. From the point force analysis

(equations (3.60) and (3.61)) we can see that the leading order solution expanded to one term in inner variables and then rewritten in outer variables should be, on $x = 0$,

$$u_y \;=\; -2C_\nu \epsilon' \log y + \ldots \quad ,$$

where

$$C_\nu \;=\; \frac{(1-\nu^2)}{\pi} \quad .$$

This must match to the inner solution expanded in outer variables.

Now from (3.7), (3.76) and (3.78) we know that on the y axis

$$\frac{\partial u_y}{\partial y} \;=\; -(1-\nu^2)\frac{2N}{\pi}\left[\frac{1}{(d^2+y^2)^{\frac{1}{2}}} + \frac{\nu}{1-\nu}\left(2y - \frac{(d^2+2y^2)}{(d^2+y^2)^{\frac{1}{2}}}\right)\right] \quad .$$

Integrating this from zero to y and then expanding it in outer variables we obtain

$$u_y \;=\; \epsilon^2 + \frac{C_\nu \epsilon' \nu}{1-\nu} + C_\nu \epsilon' \log(C_\nu \epsilon') - 2C_\nu \epsilon' \log y \ldots \quad .$$

Writing ϵ^2 as an expansion in ϵ' of the form $C_\nu \epsilon' \epsilon_0(\epsilon') + C_\nu \epsilon' \epsilon_1(\epsilon') + \ldots$, where $\epsilon_1 \ll \epsilon_0$, we obtain

$$u_y \;=\; C_\nu \epsilon' \left(\epsilon_0(\epsilon') + \log(C_\nu \epsilon')\right) + C_\nu \epsilon' \left(\epsilon_1(\epsilon') + \frac{\nu}{1-\nu} - 2\log y\right) + \ldots \quad .$$

For the matching to work we require

$$\begin{aligned} \epsilon_0(\epsilon') &= -\log(C_\nu \epsilon') \\ \epsilon_1(\epsilon') &= -\frac{\nu}{1-\nu} \end{aligned}$$

and hence

$$\epsilon^2 \;=\; -C_\nu \epsilon' \left[\log(C_\nu \epsilon') + \frac{\nu}{1-\nu} + \ldots\right] \quad .$$

It is noted by Johnson [43] that such a result (obtained in a more ad hoc manner by Johnson) when compared with experiment is found to be surprisingly accurate over reasonable parameter ranges.

3.3.2 Application of a shearing force after initially applying a normal force

In this section we consider the problem of applying an additional tangential force $Q < \alpha N$, where α is the coefficient of friction, assuming that the contact width and pressure distribution due to the normal force N remain unchanged.

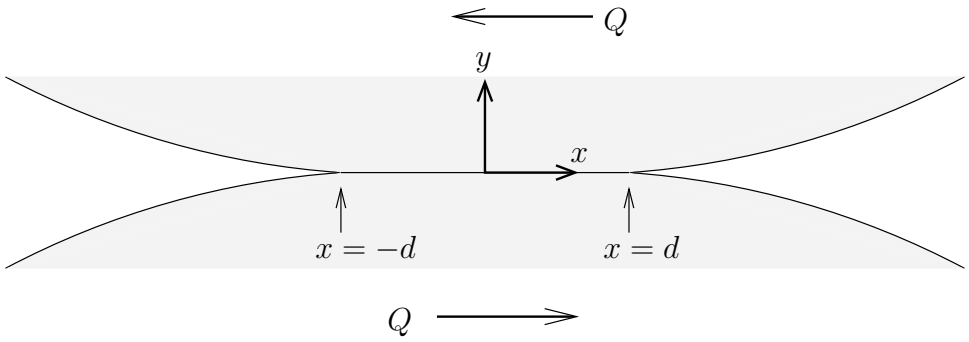

Figure 3.10: The geometry of the additional shearing force problem.

The centre of the contact region will deform with no relative motion between the bodies but this may not be true of all points in $|x| < d$. Small relative motions known as *slip* will be found to occur across some of the contact region. Since we do not know where the slip might occur we begin by considering the whole contact region to be a stuck region.

3.3.2.1 Determination of the traction with no slip

If distant points move horizontally a distance $\epsilon^2 H$ then the undeformed point x moves to $x' = x + \epsilon^2 H$, but we know that $x' = x + u$ and hence on the contact region we have $u = \epsilon^2 H$. If we denote the shearing traction by $q(x)$, which is to be determined, then as before we require the total force distribution to equal Q. Formulating a model in the same manner as before and then nondimensionalising with the same scaling leads to the model

$$\begin{aligned}
(\lambda + 2\mu)\nabla(\nabla.\mathbf{u}) - \mu\nabla \times (\nabla \times \mathbf{u}) &= 0 \qquad \text{in} \quad y \geq 0 \\
\mu\left(\frac{\partial u_x}{\partial y} + \frac{\partial u_y}{\partial x}\right) &= Eq(x) \quad \text{on} \quad y = 0 \quad , \quad |x| < d \\
\lambda\left(\frac{\partial u_x}{\partial x} + \frac{\partial u_y}{\partial y}\right) + 2\mu\frac{\partial u_y}{\partial y} &= 0 \qquad \text{on} \quad y = 0 \quad , \quad |x| < d \\
u_x &= \frac{H}{L} \qquad \text{on} \quad y = 0 \quad , \quad |x| < d \\
\mu\left(\frac{\partial u_x}{\partial y} + \frac{\partial u_y}{\partial x}\right) &= 0 \qquad \text{on} \quad y = 0 \quad , \quad |x| > d \\
\lambda\left(\frac{\partial u_x}{\partial x} + \frac{\partial u_y}{\partial y}\right) + 2\mu\frac{\partial u_y}{\partial y} &= 0 \qquad \text{on} \quad y = 0 \quad , \quad |x| > d \\
\int_{-d}^{d} q(x)dx &= Q \quad .
\end{aligned}$$

We can solve this in the same manner as before by either constructing a superposition solution or using a Muskhelishvili potential. We find

$$\begin{aligned}
\sigma_{xx} &= -\frac{2}{\pi}\int_{-d}^{d}\frac{q(s)(x-s)^3}{[(x-s)^2+y^2]^2}ds \\
\sigma_{yy} &= -\frac{2y^2}{\pi}\int_{-d}^{d}\frac{q(s)(x-s)}{[(x-s)^2+y^2]^2}ds \\
\sigma_{xy} &= -\frac{2y}{\pi}\int_{-d}^{d}\frac{q(s)(x-s)^2}{[(x-s)^2+y^2]^2}ds
\end{aligned}$$

and on the x axis

$$\begin{aligned}
\frac{\partial u_x}{\partial x} &= -\frac{2(1-\nu^2)}{\pi}\int_{-d}^{d}\frac{q(s)}{x-s}ds \\
\frac{\partial u_y}{\partial x} &= (1-2\nu)(1+\nu)q(x) \quad .
\end{aligned}$$

But this time we know $u_x = H/L$ and so we have the integral equation

$$\int_{-d}^{d}\frac{q(s)}{x-s}ds = 0$$

for which from Section B.4 we know the only relevant non-trivial solution can be

$$q(x) = \frac{Q}{\pi(d^2-x^2)^{\frac{1}{2}}} \quad .$$

However, this is singular at the edges of the contact region which is inconsistent with the fact that slip must occur if $q(x) > \alpha p(x)$. Thus we expect a region of slip near the edges of the contact region and a region of stick near the centre.

3.3.2.2 Determination of the traction with slip

If we consider a force Q of limiting value αN then the bodies are on the point of sliding and therefore the traction is

$$q'(x) = \alpha p_0\left(1-\frac{x^2}{d^2}\right)^{\frac{1}{2}}$$

for which we find the tangential displacement within the contact region is

$$u'_x = C' - (1-\nu^2)\alpha p_0\frac{x^2}{d} \quad .$$

However this can only satisfy the condition $u_x = H/L$ at one point rather than across the entire contact region. To satisfy this condition we introduce a further shear q''

such that

$$\begin{aligned} q(x) &= q'(x) + q''(x) \\ u_x(x) &= u'_x(x) + u''_x(x) \qquad \text{on} \quad y = 0 \ . \end{aligned}$$

The condition is then satisfied if

$$u''_x(x) = C'' + \frac{c}{d}(1-\nu^2)\alpha p_0 \frac{x^2}{c}$$

for which

$$q''(x) = -\frac{c}{d}\alpha p_0 \left(1 - \frac{x^2}{c^2}\right)^{\frac{1}{2}} \qquad \text{for} \quad |x| < c \ .$$

So on the stick region

$$q(x) = \frac{\alpha p_0}{d}\left[(d^2 - x^2)^{\frac{1}{2}} - (c^2 - x^2)^{\frac{1}{2}}\right] \ .$$

This is everywhere within $|x| < c$ less than the limiting traction and equal to $\alpha p(x)$ on the stick/slip boundary $|x| = c$. Outside the stick region we have limiting friction

$$q(x) = \frac{\alpha p_0}{d}(d^2 - x^2)^{\frac{1}{2}} \ .$$

This satisfies a necessary condition that the slip be of opposite sign to that of the traction. The size of the stick region $|x| < c$ is determined from the condition

$$\begin{aligned} Q &= \int_{-d}^{d} q(x)dx \\ &= \alpha N \left(1 - \frac{c^2}{d^2}\right) \end{aligned} \tag{3.80}$$

which implies

$$c = \left(1 - \frac{Q}{\alpha N}\right)^{\frac{1}{2}} d \ .$$

From this we can see that keeping N constant and increasing Q causes the slip region to develop inward until at limiting friction the stick region is only the line $x = 0$, beyond which sliding occurs.

3.3.3 Simultaneous variations of normal and shearing forces

If we now consider an oblique force F applied subsequently to an initial normal force N_0 then in our earlier analysis N and Q are going to increase incrementally. To avoid confusing notation we shall temporarily switch to denoting the position of the free point by a rather than d. We will proceed by following the method used by Johnson [43] when analysing the similar problem for spheres. During the application of the oblique force the contact width is taken as that of the Hertz theory. For an increment in the oblique force dF the tangential and normal forces increment by

$$\begin{aligned} dQ &= dF \sin\beta \\ dN &= dF \cos\beta \end{aligned}$$

where β is the angle at which the force is applied measured from the vertical. Thus from (3.74) the increment in the growth of the contact region is given by

$$2a\ da = K\ dN = K\frac{dQ}{\tan\beta}$$

where $K = 4(1-\nu^2)/\pi$. If we assume the incremental increase in the tangential force does not give rise to any slip then the increase in tangential traction is

$$dq(x) = \frac{dQ}{\pi(a^2-x^2)^{\frac{1}{2}}}$$

which on substituting in for dQ from above gives

$$dq = \frac{2d}{\pi K}\frac{\tan\beta}{(a^2-x^2)^{\frac{1}{2}}}da \ .$$

To find the traction at a point x we integrate this equation. If x lies inside the initial contact region then $a = d_0$ when $q = 0$ and we integrate to when $a = d_1$ and $q = q(x)$. If, however, x lies initially outside the contact region then $q = 0$ until $a = x$ which gives us a different lower limit of integration. We thus obtain

$$q(x) = \begin{cases} \dfrac{2\tan\beta}{\pi K}[(d_1^2-x^2)^{\frac{1}{2}} - (d_0^2-x^2)^{\frac{1}{2}}] & \text{for } \ 0 < x < d_0 \\ \dfrac{2\tan\beta}{\pi K}(d_1^2-x^2)^{\frac{1}{2}} & \text{for } \ d_0 < x < d_1 \end{cases}$$

and from the Hertz theory we find

$$p(x) = \frac{2(N_0 + F_1\cos\beta)}{\pi d_1^2}(d_1^2-x^2)^{\frac{1}{2}} \qquad \text{for } \ 0 < x < d_1 \ .$$

For the assumption of no slip to have been valid we require $q(x) \leq \alpha p(x)$ for $|x| < d_1$ which is true provided $\tan\beta \leq \alpha$. Thus an oblique force applied at an angle less than that of friction produces no slip.

If, however, the inclination of the force exceeds the angle of friction, some slip must occur and the above analysis fails. A strip of slip must occur at the edge of the contact region within which the traction will be $\alpha p(x)$ at all stages of the loading. The inner boundary of the slip region will lie within the original contact strip, its value being given by the usual condition of equilibrium with the tangential force (3.80), giving

$$1 - \frac{c^2}{d_1^2} \;=\; \frac{F\sin\beta}{\alpha(N_0 + F\cos\beta)} \quad .$$

Sliding begins when $c = 0$ for which

$$F \;=\; \frac{\alpha N_0}{\cos\beta(\tan\beta - \alpha)} \quad .$$

In the absence of an initial load we get the normal rule of dry friction that sliding occurs if $\tan\beta > \alpha$.

As was discussed at the beginning of the chapter we have only demonstrated a few possible two-dimensional loading problems but many more have been considered in the literature; in particular over a dozen different cases are considered by Mindlin and Deresiewicz [56] for the case of spheres rather than cylinders.

3.4 A static type-I crack problem

The Muskhelishvili potential method can also be used to consider the simple problem of a static type-I elliptic crack as shown in Figure 3.11 (where the crack has already been linearised onto the axis).

Using the results of Section 3.1.2 for the case when both σ_{yy} and σ_{xy} are given on the crack face, that is (3.39)–(3.42) in dimensionless form, we have the following two Riemann problems:

$$\begin{aligned} [\Phi(x) + \Omega(x)]^+ + [\Phi(x) + \Omega(x)]^- &= 0 \qquad \text{for} \quad |x| < d_0 \\ [\Phi(x) - \Omega(x)]^+ - [\Phi(x) - \Omega(x)]^- &= 0 \qquad \text{for} \quad |x| < d_0 \end{aligned}$$

Using the results from Appendix B for the case of an open contour we see that the solutions are

$$\Phi(z) - \Omega(z) \;=\; -\frac{p_\infty}{2}$$

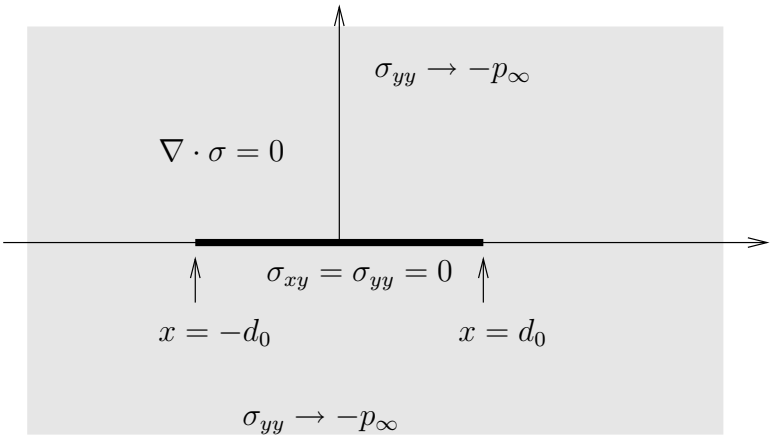

Figure 3.11: The type-I crack problem.

$$\Phi(z) + \Omega(z) \;=\; -\frac{p_\infty z}{\sqrt{z^2 - d^2}}$$

having also used the stress conditions at infinity.

We can substitute these back into the dimensionless forms of (3.36) and (3.38) to obtain the vertical displacement and stress

$$u_y \;=\; -2p_\infty(1-\nu^2)(d^2-x^2)^{\frac{1}{2}} \qquad \text{on} \quad y=0 \quad , \quad |x| < d \tag{3.81}$$

$$\sigma_{yy} \;=\; -\frac{p_\infty |x|}{(x^2-d^2)^{\frac{1}{2}}} \qquad \text{on} \quad y=0 \quad , \quad |x| > d \tag{3.82}$$

along the axis. Hence if the initial shape h of the crack were taken to be an ellipse

$$h \;=\; 2p_\infty(1-\nu^2)(d^2-x^2)^{\frac{1}{2}}$$

then the crack would close simultaneously along its whole length when the pressure was applied. We note also that the stress has a square root singularity at $x = \pm d$.

3.4.1 An ink delivery problem

The above result can be used to address one of the problems brought to the 1995 European Study Group with Industry, in Cambridge, by Domino Printing Sciences.

Domino wished to make a small valve by moulding an aperture in a sheet of rubber and then closing it by compression from above and below. The aperture shape is to be chosen such that it closes and opens at the centre. Schematically what they required was as shown in Figure 3.12.

The closing and opening of the aperture is used as a means of delivering ink in a printing process. The closing mechanism described is desired to prevent the

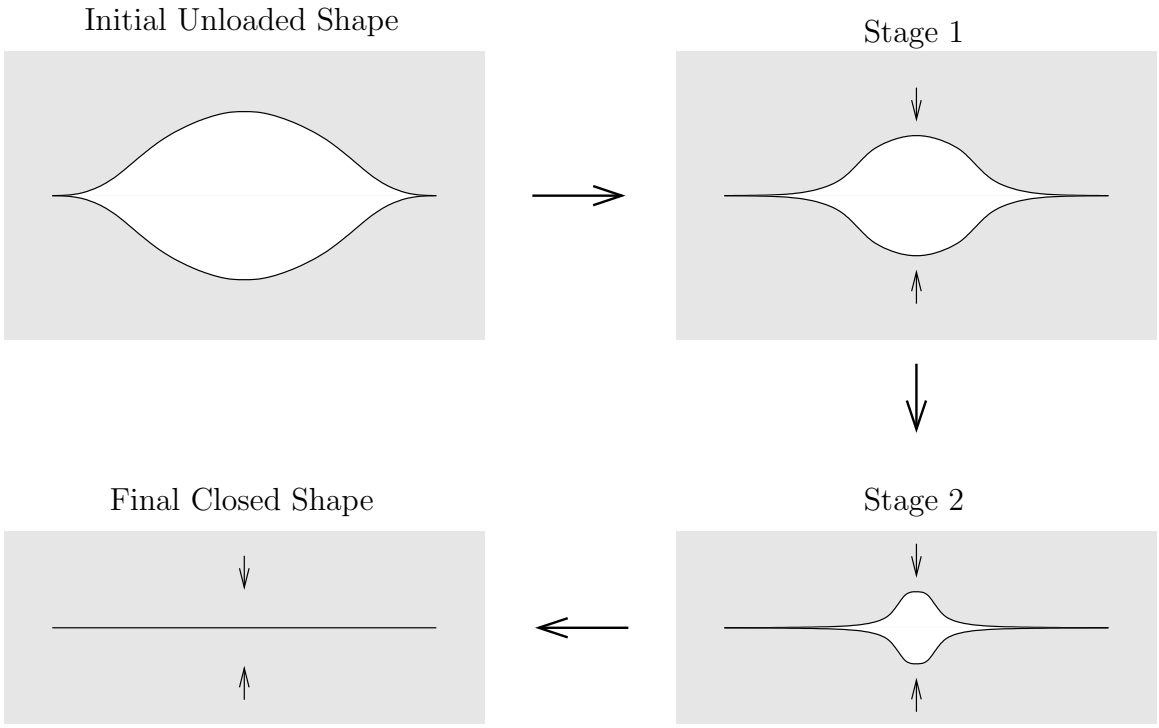

Figure 3.12: The industrial requirement.

production of satellite drops that would spoil the printed image. The diameter of the aperture can be taken to be small compared to its length and the problem can be considered as two-dimensional. Thus we have a long thin crack in an elastic material which under the assumptions of linear elasticity is linearised onto the axis. Noting that the pressure required to expel the fluid in the aperture is small ($O(100Pa)$) compared with the elastic stress required to close the aperture ($0(50kPa)$) we shall also neglect the pressure within the aperture. Thus we have a situation similar to that just considered above.

We could produce a solution with the required attributes simply by formulating another set of Riemann problems. However, for the closing crack the conditions to be applied along the cut $|x| < d_0$ are of mixed type. That is we have zero stress conditions on the part of the crack still open but we now have $\sigma_{xy} = 0$ and must give u_y on the closed part of the crack. Thus the problem is similar in type to the contact problems where we solved one Riemann problem with an unknown stress $\sigma_{yy} = -p(x)$ on part of the boundary and then applied a further condition to find p. However, for the case of a crack we must solve two Riemann problems containing the unknown stress and then apply further conditions using the known displacement. A much easier method of constructing a solution which satisfies the schematic requirements

is by considering the incremental loading of the static elliptic crack problem above in a similar manner as was done for the contact problem. The solution derived can be reassuringly shown to be the same as those obtained using the Muskhelishvili method.

We wish to produce a loading such that the crack 'zips' closed from the ends inwards. Thus we now take the position of the free point d to be a function of the applied pressure. At $p_\infty = 0$ the rubber is in the undeformed state and the crack semi-width is d_0. The aperture will be fully closed when the pressure reaches p_0. At any instant for a given p_∞ the aperture is thus closed for $|x| > d(p_\infty)$ and open for $|x| < d(p_\infty)$.

From (3.81) and (3.82) an increment in the pressure dp_∞ gives rise to increments in the normal displacement and stress of du_y and σ_{yy} given by

$$\begin{aligned} du_y &= -2dp_\infty(1-\nu^2)(d(p_\infty)^2 - x^2)^{\frac{1}{2}} \qquad \text{on} \quad y = 0 \quad , \quad |x| < d(p_\infty) \\ d\sigma_{yy} &= -dp_\infty \frac{|x|}{(x^2 - d(p_\infty)^2)^{\frac{1}{2}}} \qquad \text{on} \quad y = 0 \quad , \quad |x| > d(p_\infty) \quad . \end{aligned}$$

We will now integrate these equations for d initially d_0 up to d using the conditions $u_y(d_0) = 0$ and $\sigma_{yy}(d_0) = 0$. However for $d < |x| < d_0$ the stress remains zero until the point x lies outside of the open region of the crack and hence the lower limit of integration becomes x instead of d_0. Similarly for the displacement when $d < |x| < d_0$ the crack has closed and hence u_y changes no further changing the upper limit to x. Integrating yields

$$u_y(d) = \begin{cases} -2(1-\nu^2)\displaystyle\int_{d_0}^{d} (a^2 - x^2)^{\frac{1}{2}} p'_\infty(a)da & \text{for} \quad |x| < d \\ -2(1-\nu^2)\displaystyle\int_{d_0}^{x} (a^2 - x^2)^{\frac{1}{2}} p'_\infty(a)da & \text{for} \quad d < |x| < d_0 \end{cases} \tag{3.83}$$

$$\sigma_{yy}(d) = \begin{cases} -|x|\displaystyle\int_{d_0}^{d} \frac{1}{(x^2 - a^2)^{\frac{1}{2}}} p'_\infty(a)da & \text{for} \quad |x| > d_0 \\ -|x|\displaystyle\int_{x}^{d} \frac{1}{(x^2 - a^2)^{\frac{1}{2}}} p'_\infty(a)da & \text{for} \quad d < |x| < d_0 \end{cases} \quad . \tag{3.84}$$

The initial shape of the aperture h is given by the condition $h(x) = -u_y(x)$ and the actual shape of the aperture s at any moment for a given d is given by the condition $s(d) = h(x) + u_y(d)$.

We shall now consider three particular expressions for p_∞ in order to show how changing the way in which the pressure increases with the decreasing contact width changes the particular aperture shape and stress as it closes. Each of the three pressure variations considered will be seen to produce the type of closing mechanism

required where the aperture shape has a cusp at the end points rather than being elliptic like the original static problem from which the solution has been derived.

Linear pressure increase with decreasing aperture width

$$p_\infty \;=\; -\frac{p_0}{d_0}(d-d_0) \;\;\Rightarrow\;\; p'_\infty(d) \;=\; -\frac{p_0}{d_0}$$

Substituting into (3.83) and (3.84) we find the vertical displacement and stress on relevant parts of the axis are

$$\begin{aligned} u_y(d) \;&=\; \frac{(1-\nu^2)p_0}{d_0}\left[d(d^2-x^2)^{\frac{1}{2}}H(d-|x|) - x^2\cosh^{-1}\left(\frac{d}{x}\right)H(d-|x|)\right. \\ &\qquad \left. -d_0(d_0^2-x^2)^{\frac{1}{2}} + x^2\cosh^{-1}\left(\frac{d_0}{x}\right)\right] \qquad \text{on} \;\; y=0 \\ \sigma_{yy}(d) \;&=\; \frac{p_0}{d_0}|x|\left[\cos^{-1}\left(\frac{d_0}{|x|}\right)H(|x|-d_0) - \cos^{-1}\left(\frac{d}{|x|}\right)\right] \quad \text{on} \;\; y=0 \;\;,\;\; |x|>d(p) \end{aligned}$$

where $H(x)$ is the Heaviside function. We further find that the actual aperture shape is

$$s(d) \;=\; \frac{(1-\nu^2)p_0}{d_0}\left[d(d^2-x^2)^{\frac{1}{2}} - x^2\cosh^{-1}\left(\frac{d}{x}\right)\right] \;\;.$$

Figure 3.13 shows plots of the aperture shape for different values of d having taken the premultiplier to be 1.

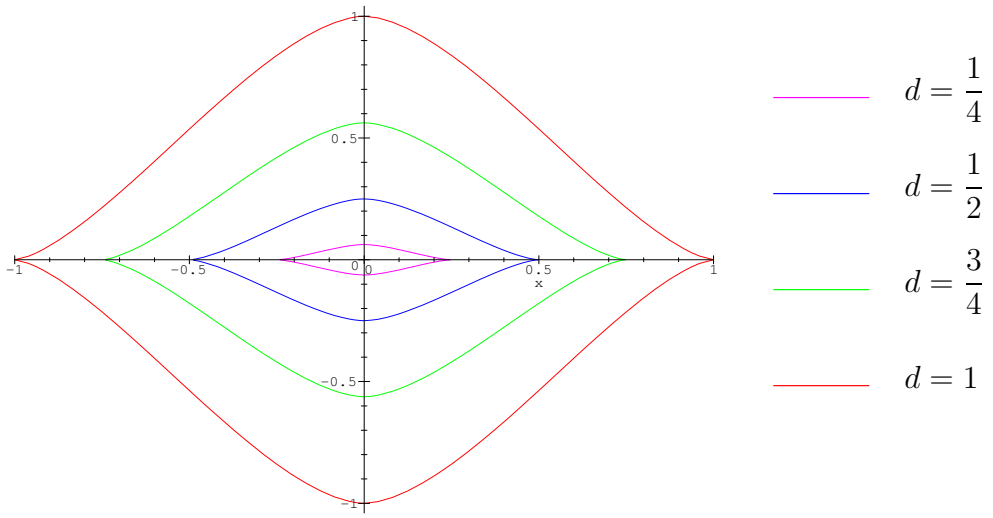

Figure 3.13: The first aperture shape.

Expanding the aperture shape s and the x derivative of the vertical stress near the free point $x = d$ yields

$$\begin{aligned} s &\sim \frac{(1-\nu^2)p_0}{d_0}\frac{4\sqrt{(}2d)}{3}(d-x)^{\frac{3}{2}} \qquad \text{as} \quad x \to d^- \\ \frac{d\sigma_{yy}|_{y=0}}{dx} &\sim -\frac{2p_0 d}{d_0}\frac{1}{\sqrt{2d(x-d)}} \qquad \text{as} \quad x \to d^+ \end{aligned}$$

from which we can see that near the free point the aperture shape has a three halves power singularity and the derivative of the stress has a minus one half power singularity.

Quadratic pressure increase with decreasing aperture width

$$p_\infty = -\frac{p_0}{d_0^2}(d^2 - d_0^2) \quad \Rightarrow \quad p'_\infty(d) = -\frac{2p_0}{d_0^2}d$$

The vertical displacement and stress on relevant parts of the axis are found to be

$$\begin{aligned} u_y(d) &= \frac{4(1-\nu^2)p_0}{3d_0^2}\left[(d^2-x^2)^{\frac{3}{2}}H(d-|x|) - (d_0^2-x^2)^{\frac{3}{2}}\right] \text{ on } \; y=0 \\ \sigma_{yy}(d) &= \frac{2p_0}{d_0^2}|x|\left[(x^2-d_0^2)^{\frac{1}{2}}H(|x|-d_0) - (x^2-d^2)^{\frac{1}{2}}\right] \qquad \text{on} \quad y=0 \quad , \quad |x| > d(p) \end{aligned}$$

and the aperture shape is found to be

$$s(d) = \frac{4(1-\nu^2)p_0}{3d_0^2}(d^2-x^2)^{\frac{3}{2}} \quad .$$

Figure 3.14 shows plots of the aperture shape for different values of d having taken the premultiplier to be 1.

Again expanding near the free point we find

$$\begin{aligned} s(d) &\sim \frac{4(1-\nu^2)p_0}{3d_0^2}(2d)^{\frac{3}{2}}(d-x)^{\frac{3}{2}} \qquad \text{as} \quad x \to d^- \\ \frac{d\sigma_{yy}|_{y=0}}{dx} &\sim -\frac{p_0 d}{d_0^2}\sqrt{\frac{2d}{x-d}} \qquad \text{as} \quad x \to d^+ \end{aligned}$$

from which we can see that near the free point this aperture shape also has a three halves power singularity and the derivative of the stress also has a minus one half power singularity.

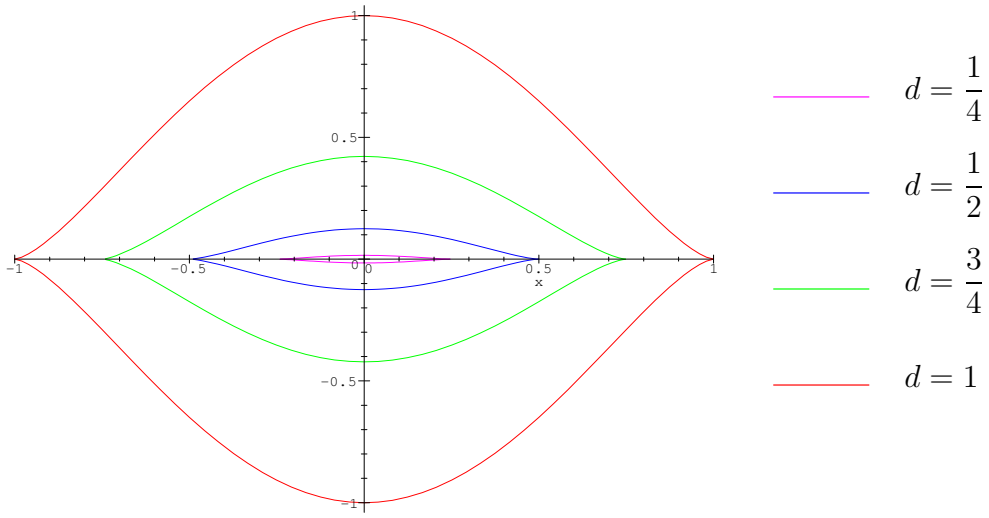

Figure 3.14: The second aperture shape.

Quadratic pressure increase with increasing aperture width closed

$$p_\infty \;=\; -\frac{p_0}{d_0^2}(d-d_0)^2 \quad\Rightarrow\quad p'_\infty(d) \;=\; -\frac{2p_0}{d_0^2}(d_0-d)$$

For this case the vertical displacement and stress on relevant parts of the axis are found to be

$$\begin{aligned} u_y(d) \;=\; & \frac{4(1-\nu^2)p_0}{d_0^2}\left[\frac{1}{3}(d_0^2-x^2)^{\frac{3}{2}} - \frac{1}{3}(d^2-x^2)^{\frac{3}{2}}H(d-|x|) - \frac{d_0^2}{2}(d_0^2-x^2)^{\frac{1}{2}}\right. \\ & + \frac{d_0 d}{2}(d^2-x^2)^{\frac{1}{2}}H(d-|x|) + \frac{d_0}{2}x^2\cosh^{-1}\left(\frac{d_0}{x}\right) \\ & \left. - \frac{d_0}{2}x^2\cosh^{-1}\left(\frac{d}{x}H(d-|x|)\right)\right] \qquad \text{on} \quad y=0 \\ \sigma_{yy}(d) \;=\; & \frac{2p_0}{d_0^2}|x|\left[d_0\cos^{-1}\left(\frac{d_0}{x}\right)H(|x|-d_0) - \cos^{-1}\left(\frac{d}{x}\right)\right. \\ & \left. - (x^2-d_0^2)^{\frac{1}{2}}H(|x|-d_0) + (x^2-d^2)^{\frac{1}{2}}\right] \qquad \text{on} \quad y=0 \quad , \quad |x|>d(p) \end{aligned}$$

and the aperture shape is

$$s(d) \;=\; \frac{4(1-\nu^2)p_0}{d_0^2}\left[\frac{d_0 d}{2}(d^2-x^2)^{\frac{1}{2}} - \frac{d_0}{2}x^2\cosh^{-1}\left(\frac{d}{x}\right) - \frac{1}{3}(d^2-x^2)^{\frac{3}{2}}\right] \quad .$$

Figure 3.15 shows plots of the aperture shape for different values of d having taken the premultiplier to be 1.

Near the free point we find

$$s(d) \;\sim\; \frac{4(1-\nu^2)p_0}{d_0^2}\left[\frac{2}{3}\sqrt{2d}(d_0-d)(d-x)^{\frac{3}{2}}\right.$$

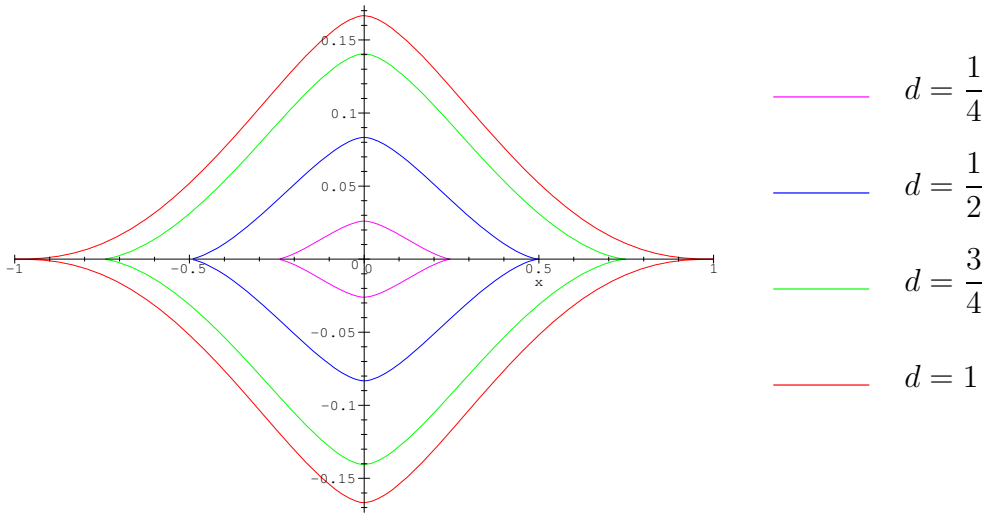

Figure 3.15: The third aperture shape.

$$+\frac{1}{30}\sqrt{\frac{2}{d}}(15d+7d_0)(d-x)^{\frac{5}{2}}\Bigg] \qquad \text{as} \quad x \to d^-$$

$$\frac{d\sigma_{yy}|_{y=0}}{dx} \sim -\frac{p_0(d_0-d)}{d_0^2}\sqrt{\frac{2d}{x-d}} \qquad \text{as} \quad x \to d^+$$

from which we can see that in general near the free point this aperture shape also has a three halves power singularity and the derivative of the stress also has a minus one half power singularity. However for the initial free boundary shape $d = d_0$ and the singularity is a five halves power.

As discussed initially each of these three solutions could have been found by directly solving the appropriate Riemann problem and can be verified as the solution to those Riemann problems simply by substituting them back in. The change in the displacement singularity near $x = d$ from a one half to a three halves power is related to a change in the index of the corresponding Riemann problems rather like the change brought about by the inclusion of the cohesive zone in the type-III crack problem.

The inverse problem

Having considered the problem of finding the aperture shape given a pressure it is reasonable to now ask what is the pressure for a particular desired aperture shape. To determine this we must invert the relationship

$$h = 2(1-\nu^2)\int_{d_0}^{x}(a^2-x^2)^{\frac{1}{2}}p'(a)da \ .$$

Differentiating with respect to x we obtain

$$\frac{dh}{dx} = -2(1-\nu^2)x\int_{d_0}^{x}\frac{1}{(a^2-x^2)^{\frac{1}{2}}}p'(a)da \ .$$

By making the usual sorts of substitutions we can transform this into the familiar Abel Integral problem which we can invert in the usual manner to obtain

$$p(d) = -\frac{1}{\pi(1-\nu^2)}\int_{d}^{d_0}\frac{dh}{dx}\frac{1}{(x^2-d^2)^{\frac{1}{2}}}dx \ ,$$

having used the fact that $p(d_0)=0$. Using this formula the required pressure for all sorts of different aperture shapes can be determined.

Chapter 4

Contact of an elastic plate supported by a frame

As part of the process of manufacturing a car windscreen a sheet of semi-molten glass is placed on a frame and allowed to settle under its own weight to the required shape. To control the shape of the glass plate as it sags the plate is heated from above in a controlled manner. The frame used is approximately rectangular although it is not completely planar and the corners are rounded off. A particular problem with this method is that as the glass sags under its own weight the corners can lift off from the frame. In order to understand this process and hence suggest means to overcome the problem we would first like to be able to predict the shape of the glass and the force on the frame and hence the points at which it lifts off from the frame.

A full model would have to take into account the fact that glass is a visco-elastic material, the heating from above, the precise shape of the frame used and possibly

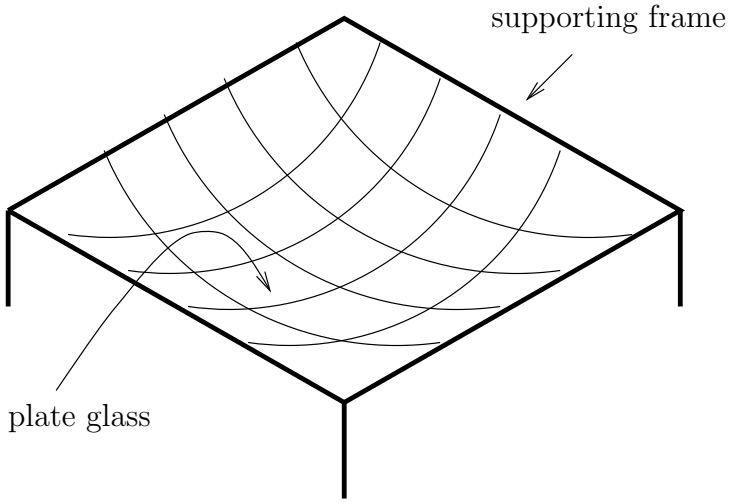

Figure 4.1: The geometry of a simplified plate glass problem.

many other factors. However as a first approximation we shall consider the glass to be an elastic plate (since over short time scales glass behaves like an elastic solid) and the frame to be a planar rectangle as shown in Figure 4.1. We will also neglect the effect of the heating.

4.1 Thin plate equations

The equations and boundary conditions that govern small deflections of laterally loaded plates can in principle be derived from the full equations of elasticity using asymptotic expansions; however, to do so is a lengthy and complicated procedure. The traditional means of deriving the equations for a thin plate is to consider the forces acting on a small element of the plate and derive the equations from there in the same manner as the equations for a string or beam might be derived.

We assume the Young's modulus of the plate is constant. The load acting on the plate is assumed to be normal to its surface and the deflections are assumed to be small in comparison with the thickness of the plate. At the boundary the edges of the plate are assumed to be free to move in the plane of the plate and thus the reaction forces at the edges are normal to the plate. With these assumptions we can neglect any strain in the middle plane of the plate during bending.

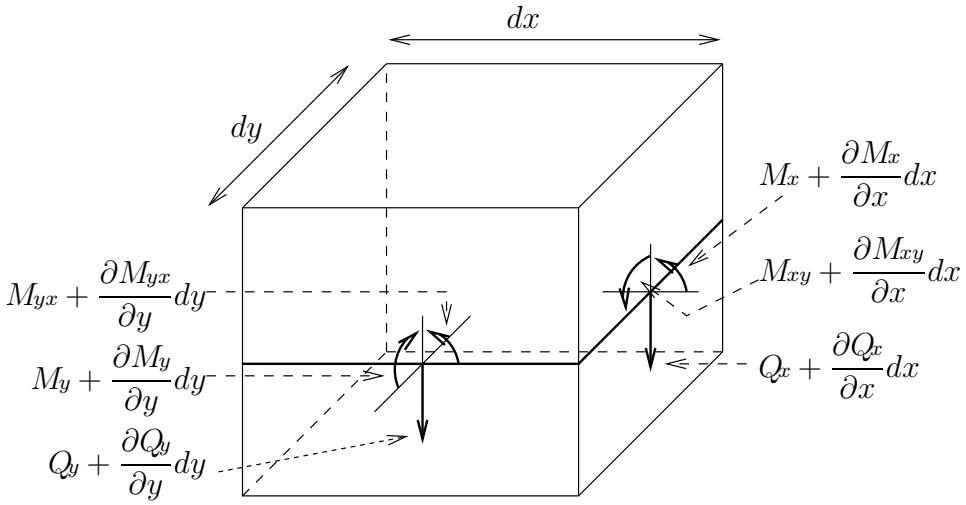

Figure 4.2: An element of an elastic plate.

We now consider a small element of the plate as shown in Figure 4.2, where M_x and M_y are the bending moments, M_{xy} and M_{yx} are the twisting moment and Q_x and Q_y are the shearing forces (all per unit length). Denoting the small vertical displacement

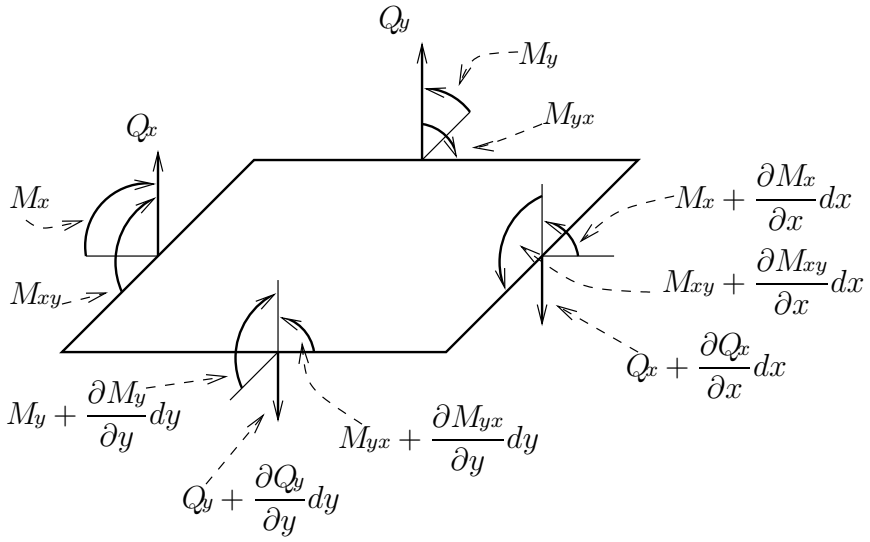

Figure 4.3: The moments and forces per unit length on the middle plane of an elastic plate.

of the plate by $w(x, y)$ the constitutive equations for the moments can be expressed (see Timoshenko [92](p37–41)) as

$$M_x = -D(w_{xx} + \nu w_{yy}) \tag{4.1}$$

$$M_y = -D(w_{yy} + \nu w_{xx}) \tag{4.2}$$

$$M_{xy} = -M_{xy} = D(1-\nu)w_{xy} \tag{4.3}$$

where ν is Poisson's ratio and D is the flexural rigidity. The middle plane of the element showing all the moments and forces is represented in Figure 4.3. As well as all the forces shown in Figure 4.3 there is also the load distributed over the upper surface of the plate. The intensity of the normal load is denoted by $q(x, y)$ and thus the load acting on the element is $qdxdy$. Note, since the stress component σ_{zz} is neglected, we are not able to apply the load on the upper or lower surface of the plate. Thus every transverse load considered in the thin-plate theory is merely a discontinuity[1] in the magnitude of the shearing forces, which vary parabolically through the thickness of the plate.

Thus balancing all the forces along the edges vertically we see

$$\frac{\partial Q_x}{\partial x}dxdy + \frac{\partial Q_y}{\partial y}dxdy + qdxdy = 0$$

which implies

$$\frac{\partial Q_x}{\partial x} + \frac{\partial Q_y}{\partial y} + q = 0 \ . \tag{4.4}$$

[1]Solving a three-dimensional problem locally near a load applied over a distance of the order of the thickness of the plate will look like a delta function on the length scale of the plate.

Taking moments of all the forces acting on the element with respect to the x axis, we obtain

$$\frac{\partial M_{xy}}{\partial x}dxdy - \frac{\partial M_y}{\partial y}dydx + Q_y dxdy = 0$$

where the moment of the load and the moment due to the change in Q_y have been neglected since they are small compared to the terms retained. This implies

$$\frac{\partial M_{xy}}{\partial x} - \frac{\partial M_y}{\partial y} + Q_y = 0 \tag{4.5}$$

and a similar consideration of the moments about the y axis gives

$$\frac{\partial M_{yx}}{\partial y} + \frac{\partial M_x}{\partial x} - Q_x = 0 \ . \tag{4.6}$$

There are no forces in the x and y direction and no moments with respect to the z axis and hence (4.4)–(4.6) completely define the equilibrium of the element. Substituting for Q_x and Q_y into (4.4) and using the fact that $M_{xy} = -M_{yx}$, the equation of equilibrium becomes

$$\frac{\partial^2 M_x}{\partial x^2} + \frac{\partial^2 M_y}{\partial y^2} - 2\frac{\partial^2 M_{xy}}{\partial x \partial y} = -q \ .$$

Finally substituting from (4.1)–(4.3) we obtain

$$D\nabla^4 w = q \ .$$

The usual three possible types of boundary condition, assuming the edge is $x = const$, are:

1. Clamped edges — the deflection along the edge is zero and the gradient is prescribed:

$$w = 0$$
$$w_x = 0$$

   having taken the edge to be clamped with zero gradient.

2. Simply supported edges — the deflection along the edge is zero and the edge can rotate freely with respect to the edge line (i.e. no bending moments M_x along the edge):

$$w = 0$$
$$M_x = 0 \ .$$

   Using the first condition the second may be simplified to

$$w_{xx} = 0 \ .$$

3. Free edges — no bending moments M_x and shearing forces balancing forces due to twisting moments:

$$\begin{aligned} M_x &= 0 \\ Q_x - \frac{\partial M_{xy}}{\partial y} &= 0 \ . \end{aligned}$$

Note, from (4.6), Q_x the vertical shearing force can be expressed as

$$Q_x = \frac{\partial M_{yx}}{\partial y} + \frac{\partial M_x}{\partial x} = -D\frac{\partial}{\partial x}\left(\nabla^2 w\right) \ .$$

These two conditions are known as the Kirchhoff edge conditions. The second of these two boundary condition can also be expressed as

$$M_x = D(1-\nu)w_{xyy}$$

where

$$M = -D\nabla^2 w \ .$$

Since the plate is in equilibrium the total load will exactly balance the total reaction along the edges. The reaction per unit length on an edge $x = const$ is

$$R_e = Q_x - \frac{\partial M_{xy}}{\partial y} \ . \tag{4.7}$$

For a plate with a smooth edge it is a simple matter to integrate the load q over the plate and the reaction around the edge of the plate to verify that they are equal. However, for cases when the edge is only piecewise smooth more care must be taken. To illustrate this we consider the case of a right-angle corner. Figure 4.4 shows two right-angle corners except that the first is rounded off. The first two plots then show schematically how the twisting moment M_{nt} varies as we move along the edge and round the corner, where s is a coordinate along the boundary and n and t refer to the normal and tangential directions to the boundary. The second two plots show the derivative of the twisting moment with respect to the position along the edge. Thus we see that for the smoothed off corner the twisting moment varies continuously as we go around the corner and hence no delta function occurs in its derivative. However for the sharp corner the twisting moment has a discontinuity which leads to a delta function in its derivative.

On one side of the sharp corner the twisting moment is given by $-M_{xy} = M_{yx}$ whilst on the other it is M_{xy}. Hence there is a jump discontinuity in the twisting

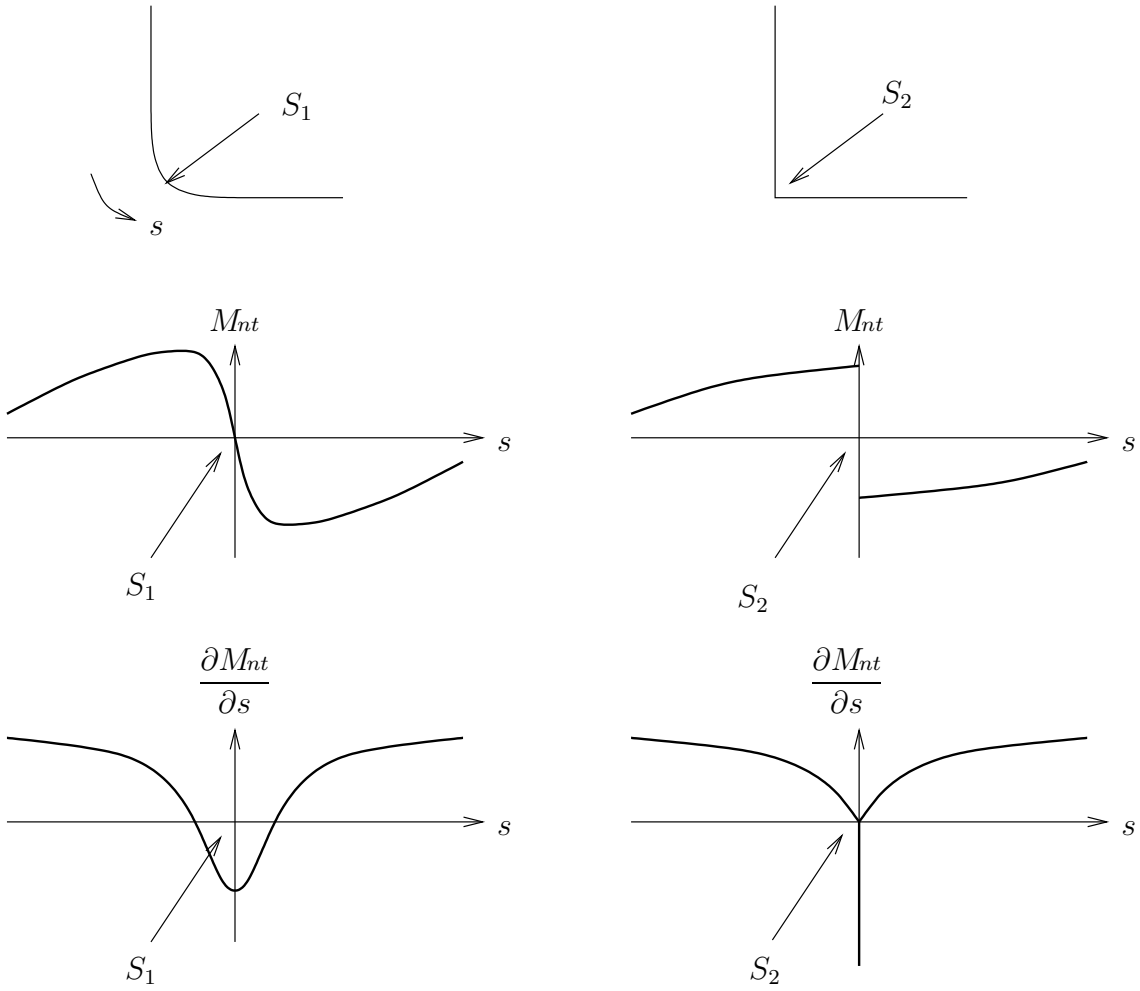

Figure 4.4: Representation of how a point force occurs at the corner.

moment located at the corner. The force per unit length due to a twisting moment is given by $-\frac{\partial}{\partial s}(M_{nt})$. Since M_{nt} has a jump discontinuity at the corner, $-\frac{\partial}{\partial s}(M_{nt})$ gives a delta function of the form $-2M_{xy}\delta(x)\delta(y)$. Thus when integrating the force per unit length around the boundary we pick up the integral of this delta function at each corner resulting in an additional point force of magnitude $-2M_{xy}$, that is an additional upward edge reaction (since M_{xy} will be negative). Thus if the plate is only simply supported from below an extra point load $2M_{xy}$ must be applied at each corner to balance this extra edge reaction. Thus in summary the magnitude of the reaction at a corner is

$$R \;=\; 2M_{nt} \;. \tag{4.8}$$

4.1.1 Variational formulation

As with all elasticity problems we would expect there to be a variational problem which is simply to minimise the energy. To show this is also the case for thin plate problems we shall consider the strain energy

$$V = \frac{D}{2}\iint \left[(w_{xx}+w_{yy})^2 - 2(1-\nu)\left(w_{xx}w_{yy}-w_{xy}^2\right)\right] dxdy \ .$$

A small variation in the energy δV caused by a small variation in w of δw must balance the work done by the external force due to the virtual displacement. The work done by the external forces must include not only the load q, but the bending moments M_n and transverse forces $Q_n - M_{nt_s}$ distributed along the edge of the plate. Thus the work done by the external forces is

$$\delta V = \iint q(\delta w)dxdy - \int M_n(\delta w)_n ds + \int \left(Q_n - M_{nt_s}\right)(\delta w)ds \ .$$

It is a simple task to show that the variation of the strain energy (see [92] p90 for some details) is

$$\begin{aligned}\delta V = D\Bigg(&\iint \nabla^4 w(\delta w)dxdy \\ &+\int \left[(1-\nu)\left(w_{xx}\cos^2\alpha + 2w_{xy}\sin\alpha\cos\alpha + w_{yy}\sin^2\alpha\right) + \nu\nabla^2 w\right](\delta w)_n ds \\ &+\int \Big[(1-\nu)\left[(w_{xx}-w_{yy})\sin\alpha\cos\alpha - w_{xy}\left(\cos^2\alpha-\sin^2\alpha\right)\right] \\ &-(w_{xxx}+w_{xyy})\cos\alpha - (w_{yyy}+w_{xxy})\sin\alpha\Big](\delta w)ds\Bigg) \ ,\end{aligned}$$

where α is the angle between the normal to the boundary and the x axis. These two expressions for δV must balance and thus the following three equations must hold for permissible δw:

$$\begin{aligned}\iint \left(D\nabla^4 w - q\right)(\delta w)dxdy &= 0 \\ \int \Big[D\Big[(1-\nu)\left(w_{xx}\cos^2\alpha + 2w_{xy}\sin\alpha\cos\alpha + w_{yy}\sin^2\alpha\right) & \\ +\nu\nabla^2 w\Big] + M_n\Big](\delta w)_n ds &= 0 \\ \int \Big(D\Big[(1-\nu)\left[(w_{xx}-w_{yy})\sin\alpha\cos\alpha - w_{xy}\left(\cos^2\alpha-\sin^2\alpha\right)\right] & \\ -(w_{xxx}+w_{xyy})\cos\alpha - (w_{yyy}+w_{xxy})\sin\alpha\Big] - \left(Q_n - M_{nt_s}\right)\Big)(\delta w)ds &= 0 \ .\end{aligned}$$

The first of these requires that

$$D\nabla^4 w = q$$

which is true since this is just the field equation for the problem. It can also be checked that for all three possible types of boundary conditions the second and third equations will be satisfied. We should note that none of the three types of boundary conditions are the natural boundary condition which would be $\nabla^2 w = 0$ and $(\nabla^2 w)_n = 0$. Thus we have shown that minimising

$$\frac{D}{2}\int\int \left[(w_{xx}+w_{yy})^2 - 2(1-\nu)\left[w_{xx}w_{yy} - w_{xy}^2\right]\right] dxdy$$
$$-\int\int qwdxdy + \int M_n w_n ds - \int (Q_n - M_{nt_s})\, wds$$

over all permissible w is the same as solving the mixed boundary value problem. In our particular case permissible w would be all w satisfying $w \geq 0$ on the boundary with $w \in \mathcal{H}^2$. The existence and uniqueness of a solution to the problem is now assured by the theorem presented in Appendix A.

Alternatively a constrained minimisation problem can be formulated [72](p178–181). The problem is to minimise

$$\frac{D}{2}\int\int \left\{\psi_{1x}^2 + \psi_{2y}^2 + 2\nu\psi_{1x}\psi_{2y} + \frac{1-\nu}{2}(\psi_{1y}+\psi_{2x})^2 - 2wq\right\} dxdy$$
$$-\int wQ_n ds + \int \psi_n M_n ds - \int \psi_s M_{nt} ds$$

subject to the constraints

$$G_1 \;=\; w_x + \psi_1 \;=\; 0 \qquad G_2 \;=\; w_y + \psi_2 \;=\; 0\ .$$

The benefit of this formulation is that although we now need to find three functions w, ψ_1 and ψ_2 they are only required to lie in $\mathcal{H}^1$. Thus for a finite element solution we only need to use linear elements which simplifies the finite element part of the solution considerably although now we have 3 functions and 2 lagrangian multipliers to find.

4.1.2 Nondimensional thin plate model

Since the plate is bending due to gravity, the load per unit area of the plate is $q = -\rho g$ where ρ is the density per unit area. We nondimensionalise the equations with

$$x = L\hat{x} \quad , \quad y = L\hat{y} \quad , \quad w = \frac{\rho g L^4}{D}\hat{w}$$

$$M = \rho g D L^2 \hat{M} \quad , \quad Q = \rho g D L^2 \hat{Q}\ ,$$

where L is the length of the shorter two sides of the rectangle, and immediately drop the hats. Thus the field equation is

$$\nabla^4 w = -1 \tag{4.9}$$

and on each part of the boundary one of the following pairs of types of boundary conditions will hold:

$$w = 0 \tag{4.10}$$
$$w_x = 0 \tag{4.11}$$

$$w = 0 \tag{4.12}$$
$$w_{xx} = 0 \tag{4.13}$$

$$w_{xx} + \nu w_{yy} = 0 \tag{4.14}$$
$$M_x - (1-\nu) w_{xyy} = 0 \ . \tag{4.15}$$

We would like to investigate the problem of a laterally loaded plate with simply supported boundary conditions along the whole boundary. Since we expect such a problem to exhibit interesting behaviour near the corners we shall begin by considering the problem for a single corner.

4.2 Behaviour near a corner

The general problem of a simply supported corner with angle α is shown in Figure 4.5.

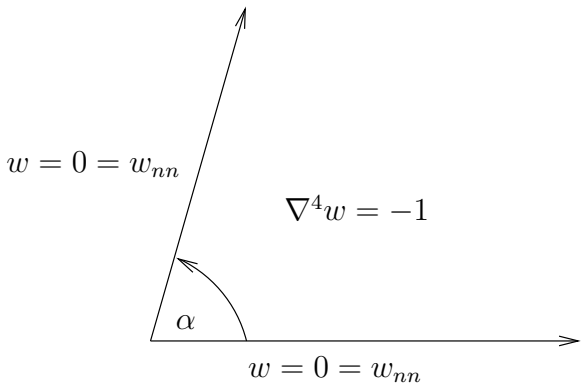

Figure 4.5: The simplified problem for a single corner.

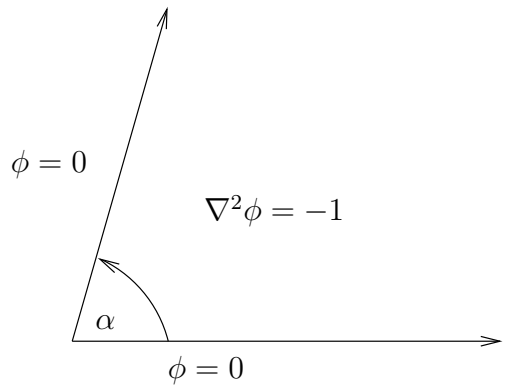

Figure 4.6: The further simplified problem for a single corner.

We can deduce the solution from that of a simpler one by making the substitution $\phi = \nabla^2 w$ yielding the new problem shown in Figure 4.6. This has the general solution

$$\phi = -\frac{r^2}{4}\left(1 - \tan\alpha \sin 2\theta - \cos 2\theta\right) + \sum_{n=1}^{\infty} A_n \sin\frac{n\pi\theta}{\alpha} r^{\frac{n\pi}{\alpha}} \quad .$$

We must now solve the problem

$$\begin{aligned} \nabla^2 w &= \phi \\ w &= 0 \qquad \text{on} \quad \theta = 0, \alpha \quad . \end{aligned}$$

Doing so we find

$$\begin{aligned} w = & -\frac{r^4}{64} + \frac{r^4}{48}\cos 2\theta + \frac{r^4}{48}\tan\alpha \sin 2\theta - \frac{r^4}{192}\cos 4\theta - \frac{r^4}{192}\tan 2\alpha \sin 4\theta \\ & + \sum_{\substack{n=1 \\ n\,\text{odd}}}^{\infty} C_n r^{\frac{n\pi}{\alpha}} \sin\frac{n\pi\theta}{\alpha} + \sum_{\substack{n=1 \\ n\,\text{odd}}}^{\infty} B_n r^{2+\frac{n\pi}{\alpha}} \sin\frac{n\pi\theta}{\alpha} \quad . \end{aligned} \tag{4.16}$$

Note only the odd numbered eigenfunctions are included so that the solution is symmetrical about $\theta = \alpha/2$. From the form of this solution we see that for $\alpha < \pi/4$ the solution for small r is dominated by the particular solution terms (in this case the problem is known as Type I similarity [4]) but for $\alpha > \pi/4$ the eigenfunctions dominate (in this case the problem is known as Type II similarity). It is also clear that for $\alpha = \pi/4,\ \pi/2,\ 3\pi/4$ the $\tan\alpha$ or $\tan 2\alpha$ terms become infinite. The solution above however is valid for all α not equal to these critical values. We can find the particular form of the solution when $\alpha = \pi/4$ by making the substitution $\alpha = \pi/4 + \epsilon$, expanding for ϵ small, then asserting that no terms of $O(\epsilon^{-1})$ may appear in the final solution, which will force one of the coefficients C_n or D_n to have a particular

form, and then finally letting $\epsilon \to 0$ whilst keeping r fixed. Making the substitution $\alpha = \pi/4 + \epsilon$ and then expanding for ϵ small gives

$$\begin{aligned} w &\sim -\frac{r^4}{64} + \frac{r^4}{48}\cos 2\theta + \frac{r^4}{48}\sin 2\theta - \frac{r^4}{192}\cos 4\theta + \frac{r^4}{384\epsilon}\sin 4\theta \\ &\quad + C_1 r^4 \left(1 - \frac{16\epsilon}{\pi}\log r\right)\left(\sin 4\theta - \frac{16\epsilon\theta}{\pi}\cos 4\theta\right) + o(r^4) \ . \end{aligned} \tag{4.17}$$

As we take the limit as $\epsilon \to 0$ we require the solution to remain bounded which forces $C_1 = -1/384\epsilon + \tilde{C}_1$, where $\tilde{C}_1 = O(1)$ as $\epsilon \to 0$, and yields

$$\begin{aligned} w &\sim -\frac{r^4}{64} + \frac{r^4}{48}\cos 2\theta + \frac{r^4}{48}\sin 2\theta - \frac{r^4}{192}\cos 4\theta + \frac{r^4}{24\pi}\log r \sin 4\theta + \frac{r^4}{24\pi}\theta\cos 4\theta \\ &\quad + \tilde{C}_1 r^4 \sin 4\theta + o(r^4) \ . \end{aligned}$$

At this point one may be concerned with the behaviour of (4.17) when $r = O\left(e^{-\frac{1}{|\epsilon|}}\right)$ since the above is a nonuniform limit. However, as remarked above the solution (4.16) is valid for all $\epsilon \neq 0$ with the restriction that for $\alpha = \pi/4 + \epsilon$ the coefficient C_1 should be $O(1/\epsilon)$ to balance the growing $\tan 2\alpha$ term and thus force the solution to remain $O(1)$. Similar restrictions are required near the other critical angles $\alpha = \pi/2,\ 3\pi/4$. We will consider the asymptotic problem near to a critical angle in more detail in Section 4.2.1.

Defining

$$\begin{aligned} w_1 &= -\frac{r^4}{64} + \frac{r^4}{48}\cos 2\theta - \frac{r^4}{192}\cos 4\theta \\ w_2 &= \frac{r^4}{48}\tan\alpha \sin 2\theta - \frac{r^4}{192}\tan 2\alpha \sin 4\theta \ , \end{aligned}$$

splitting the solution up into regions and neglecting terms of $o(r^4)$ we have

$$w \sim \begin{cases} w_1 + w_2 & \text{for } 0 < \alpha < \frac{\pi}{4} \\ \tilde{C_1} r^4 \sin 4\theta + w_1 + \frac{r^4}{48}\sin 2\theta + \frac{r^4}{24\pi}\log r \sin 4\theta + \frac{r^4}{24\pi}\theta\cos 4\theta & \text{for } \alpha = \frac{\pi}{4} \\ C_1 r^{\frac{\pi}{\alpha}} \sin\frac{\pi\theta}{\alpha} + w_1 + w_2 & \text{for } \frac{\pi}{4} < \alpha < \frac{\pi}{2} \\ C_1 r^2 \sin 2\theta + \tilde{B_1} r^4 \sin 2\theta + w_1 - \frac{r^4}{12\pi}\log r \sin 2\theta - \frac{r^4\theta}{12\pi}\cos 2\theta & \text{for } \alpha = \frac{\pi}{2} \\ C_1 r^{\frac{\pi}{\alpha}} \sin\frac{\pi\theta}{\alpha} + B_1 r^{2+\frac{\pi}{\alpha}} \sin\frac{\pi\theta}{\alpha} + w_1 + w_2 & \text{for } \frac{\pi}{2} < \alpha < \frac{3\pi}{4} \\ C_1 r^{\frac{4}{3}} \sin\frac{4\theta}{3} + B_1 r^{\frac{10}{3}} \sin\frac{4\theta}{3} + \tilde{C_3} r^4 \sin 4\theta + w_1 - \frac{r^4}{48}\sin 2\theta & \\ + \frac{r^4}{72\pi}\log r \sin 4\theta + \frac{r^4}{72\pi}\theta\cos 4\theta & \text{for } \alpha = \frac{3\pi}{4} \\ C_1 r^{\frac{\pi}{\alpha}} \sin\frac{\pi\theta}{\alpha} + B_1 r^{2+\frac{\pi}{\alpha}} \sin\frac{\pi\theta}{\alpha} + C_3 r^{3\frac{\pi}{\alpha}} \sin\frac{3\pi\theta}{\alpha} + w_1 + w_2 & \text{for } \frac{3\pi}{4} < \alpha < \pi \\ C_1 r \sin\theta + C_3 r^3 \sin 3\theta + B_1 r^3 \sin\theta + w_1 & \text{for } \alpha = \pi \end{cases}$$

The reaction on the edge $\theta = 0$ is given by

$$\begin{aligned} R_e &= -(w_{yyy} + (2-\nu)w_{xxy}) \\ &= \frac{1}{r^3}\left[2w_\theta - w_{\theta\theta\theta} - 3rw_{r\theta} + (2-\nu)(-r^2 w_{rr\theta} + 2rw_{r\theta} - 2w_\theta)\right] \end{aligned} \tag{4.18}$$

and any point force which might occur at the corner is given by

$$\begin{aligned} R &= 2M_{xy} \\ &= \frac{1}{r^2}\left(rw_{r\theta} - w_\theta\right) \quad . \end{aligned} \tag{4.19}$$

Substituting w into (4.18) and defining

$$\begin{aligned} R_{e1} &= -\frac{r}{4}(3-\nu)\tan\alpha + \frac{r}{8}(1-\nu)\tan 2\alpha \\ R_{e2} &= -\frac{C_1\pi}{\alpha^3}(1-\nu)(\pi-2\alpha)(\pi-\alpha)r^{\frac{\pi}{\alpha}-3} \\ R_{e3} &= -\frac{B_1\pi}{\alpha^3}(\alpha+\pi)(4\alpha+\pi-\nu\pi)r^{\frac{\pi}{\alpha}-1} \\ R_{e4} &= -\frac{3C_3\pi}{\alpha^3}(1-\nu)(3\pi-2\alpha)(3\pi-\alpha)r^{\frac{3\pi}{\alpha}-3} \end{aligned}$$

we find the reaction along the edge is given by

$$R_e \sim \begin{cases} R_{e1} & \text{for} \quad 0 < \alpha < \dfrac{\pi}{4} \\ -(1-\nu)\dfrac{r}{\pi}\log r - (3-\nu)\dfrac{r}{4} - (1-\nu)\dfrac{13r}{12\pi} - 24\tilde{C_1}(1-\nu)r & \text{for} \quad \alpha = \dfrac{\pi}{4} \\ R_{e2} + R_{e1} & \text{for} \quad \dfrac{\pi}{4} < \alpha < \dfrac{\pi}{2} \\ (3-\nu)\dfrac{r}{\pi}\log r + (9-4\nu)\dfrac{r}{3\pi} - 12B_1 r(3-\nu) & \text{for} \quad \alpha = \dfrac{\pi}{2} \\ R_{e2} + R_{e3} + R_{e1} & \text{for} \quad \dfrac{\pi}{2} < \alpha < \dfrac{3\pi}{4} \\ (1-\nu)\left[\dfrac{8C_1}{27}r^{-\frac{5}{3}} - \dfrac{280B_1}{27}r^{\frac{1}{3}} - 24C_3 r + \dfrac{3}{4}r - \dfrac{1}{3\pi}r\log r - \dfrac{13}{36\pi}r\right] & \text{for} \quad \alpha = \dfrac{3\pi}{4} \\ R_{e2} + R_{e3} + R_{e4} + R_{e1} & \text{for} \quad \dfrac{3\pi}{4} < \alpha < \pi \\ -6C_3(1-\nu) - 2B_1(5-\nu) & \text{for} \quad \alpha = \pi \end{cases}$$

Further substituting w into (4.19) we find the point force at the corner is

$$R \sim \begin{cases} 0 & \text{for} \quad \alpha < \dfrac{\pi}{2} \\ 4(1-\nu)C_1 & \text{for} \quad \alpha = \dfrac{\pi}{2} \\ \lim\limits_{\delta \to 0} \dfrac{2C_1(1-\nu)\pi(\alpha-\pi)}{\alpha^2}\delta^{-\left(2-\frac{\pi}{\alpha}\right)} & \text{for} \quad \dfrac{\pi}{2} < \alpha < \pi \\ 0 & \text{for} \quad \alpha = \pi \end{cases}$$

Note if $C_1 < 0$ this represents either the necessary extra point force at the corner or the point reaction upward on the support above. For $C_1 > 0$ this is simply an extra downward reaction. For $\alpha > \pi/2$ this is giving an infinite corner reaction which is not physically possible. We therefore expect that conditions at infinity will force C_1 to be zero to give a solution with physical meaning.

A plot of possible resulting edge reactions in this case is shown in Figure 4.7. For the particular values of C_1, B_1 and C_3 taken the edge reaction is one-signed. However for different values it is possible to get a positive (upward) reaction near the corner for $\alpha \in (\pi/4, \pi/2)$.

Considering the problem of a single corner has illustrated how an extra point force may occur at the corner only in the case $\alpha = \pi/2$ (and that the edge reaction may exhibit a sign change for $\alpha \in (\pi/4, \pi/2)$). However since for this angle the local

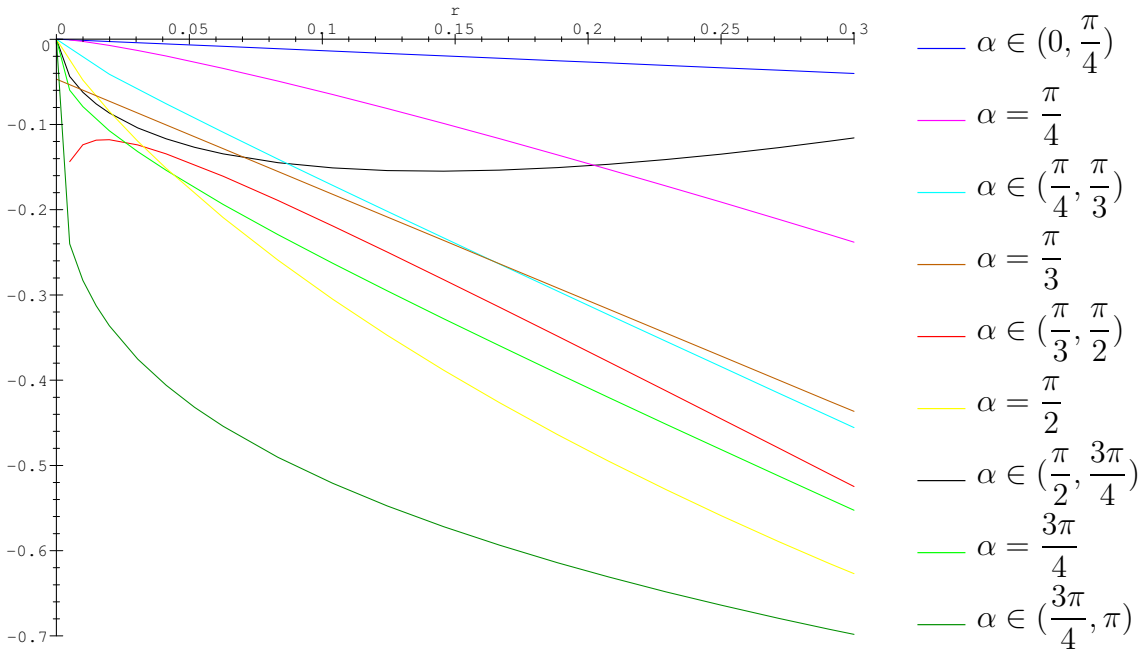

Figure 4.7: The edge reaction for different values of α.

solution is dominated by the first eigensolution the details of this force are not revealed simply by a local analysis. To make further progress in the case of a rectangular plate we will consider the full problem in Section 4.3. However, before doing so we will first return to the interesting question of the asymptotics of the solution near to a critical angle.

4.2.1 Asymptotics of the solution near a critical angle

In the section above we constructed the specific form of the solution at a critical angle from the general solution. However, for some problems an exact solution may only be known at some critical angle (see for example King et al. [44]). In this section we will show how from the particular solution for the case $\alpha = \pi/4$ we can construct an asymptotic solution valid for angles close to $\pi/4$. The solution produced will be seen to have an interesting asymptotic structure which we can explain since we have the general solution valid for all non-critical angles.

Suppose we only know that for $\alpha = \pi/4$ the solution is

$$w_0 \sim -\frac{r^4}{64} + \frac{r^4}{48}\cos 2\theta + \frac{r^4}{48}\sin 2\theta - \frac{r^4}{192}\cos 4\theta + \frac{r^4}{24\pi}\log r \sin 4\theta + \frac{r^4}{24\pi}\theta\cos 4\theta + \tilde{C}_1 r^4 \sin 4\theta \ .$$

Then for $\alpha = \pi/4 + \epsilon$, where $\epsilon \ll 1$ we can construct an asymptotic solution of the

form $w = w_0 + \epsilon w_1 + \ldots$. In this case the problem for w_1 is

$$\begin{aligned}
\nabla^4 w_1 &= 0 \qquad && \text{for} \quad \theta \in \left(0, \frac{\pi}{4}\right) \\
w_1 &= 0 \qquad && \text{on} \quad \theta = 0 \\
w_1 + w_{0\theta} &= 0 \qquad && \text{on} \quad \theta = \frac{\pi}{4} \\
r w_{1r} + w_{1\theta\theta} &= 0 \qquad && \text{on} \quad \theta = 0 \\
r w_{1r} + w_{1\theta\theta} + r w_{0r\theta} + w_{0\theta\theta\theta} &= 0 \qquad && \text{on} \quad \theta = \frac{\pi}{4}
\end{aligned}$$

for which we find the solution is

$$\begin{aligned}
w_1 &= \frac{r^4}{24}\sin 2\theta - \frac{r^4}{288}\sin 4\theta - \frac{16\tilde{C}_1 r^4}{\pi}\theta\cos 4\theta - \frac{16\tilde{C}_1 r^4}{\pi}\log r \sin 4\theta + \frac{r^4}{3\pi^2}\theta^2 \sin 4\theta \\
&\quad - \frac{r^4}{6\pi^2}\theta\cos 4\theta - \frac{r^4}{6\pi^2}\log r \sin 4\theta - \frac{r^4}{3\pi^2}(\log r)^2 \sin 4\theta - \frac{2r^4}{3\pi^2}\log r \theta \cos 4\theta
\end{aligned}$$

At this point we see that the expansion is no longer valid for $r = O\left(e^{-\frac{1}{|\epsilon|}}\right)$. We therefore rescale and solve an inner problem. We define an inner variable s by $r = e^{-\frac{s}{|\epsilon|}}$, where $s = O(1)$. Doing so we find that the inner solution will be of the form

$$w = e^{-\frac{4s}{|\epsilon|}}\left(\frac{u_0(s,\theta)}{|\epsilon|} + u_1(s,\theta)\right) \quad .$$

The problems for u_0 and u_1 are

$$\begin{aligned}
u_{0\theta\theta\theta\theta} + 20u_{0\theta\theta} + 64u_0 &= 0 \qquad && \text{for} \quad \theta \in \left(0, \frac{\pi}{4}\right) \\
u_0 &= 0 \qquad && \text{on} \quad \theta = 0, \frac{\pi}{4} \\
u_{0\theta\theta} + 4u_{0\theta} &= 0 \qquad && \text{on} \quad \theta = 0, \frac{\pi}{4}
\end{aligned}$$

$$\begin{aligned}
u_{1\theta\theta\theta\theta} + 20u_{1\theta\theta} + 64u_1 - 12u_{0s\theta\theta} - 96u_{0s} &= -1 \qquad && \text{for} \quad \theta \in \left(0, \frac{\pi}{4}\right) \\
u_1 &= 0 \qquad && \text{on} \quad \theta = 0 \\
u_1 \pm u_{0\theta} &= 0 \qquad && \text{on} \quad \theta = \frac{\pi}{4} \\
u_{1\theta\theta} + 4u_1 + u_{0s} &= 0 \qquad && \text{on} \quad \theta = 0 \\
u_{1\theta\theta} + 4u_1 + u_{0s} \pm u_{0\theta\theta\theta} \pm 4u_{0\theta} &= 0 \qquad && \text{on} \quad \theta = \frac{\pi}{4}
\end{aligned}$$

where the $\pm$ sign corresponds to the cases $\epsilon > 0$ and $\epsilon < 0$ respectively. Solving for u_0 and u_1 and matching to the outer solution we obtain

$$\begin{aligned}
u_0 &= \pm\frac{1}{384}\sin 4\theta\left(1 - e^{\pm\frac{16s}{\pi}}\right) \\
u_1 &= -\frac{1}{64} + \frac{1}{48}\cos 2\theta + \frac{1}{48}\sin 2\theta - \frac{1}{192}\cos 4\theta + \tilde{C}_1 e^{\pm\frac{16s}{\pi}}\sin 4\theta + \\
&\quad + \frac{1}{24\pi}e^{\pm\frac{16s}{\pi}}\theta\cos 4\theta \pm \frac{1}{6\pi^2}s e^{\pm\frac{16s}{\pi}}\sin 4\theta \quad .
\end{aligned}$$

At this point we see that this inner expansion now fails for $s = O(\epsilon^{-1})$, that is when $r = O\left(e^{-\frac{1}{\epsilon^2}}\right)$. If we continue on and solve another inner problem we will find that that fails when $r = O\left(e^{-\frac{1}{|\epsilon^3|}}\right)$. We can deduce this behaviour from the exact solution (4.16). This sequence of nested inner regions comes about as the asymptotic expansion solution tries to approximate the term

$$\begin{aligned}
r^{\frac{\pi}{\alpha}} &= r^{4\left(1+\frac{4\epsilon}{\pi}\right)^{-1}} \\
&\sim r^4 r^{-\frac{16\epsilon}{\pi}} r^{\frac{64\epsilon^2}{\pi^2}} \dots \\
&\sim r^4 \left(1 - \frac{16\epsilon}{\pi}\log r\right)\left(1 + \frac{64\epsilon^2}{\pi^2}\log r\right)\dots \qquad \text{for} \quad r \gg O(e^{-\frac{1}{|\epsilon|}}) \\
&\sim r^4 e^{\pm\frac{16s}{\pi}} \left(1 - \frac{64s|\epsilon|}{\pi^2}\log r\right)\dots \qquad \text{for} \quad r = O(e^{-\frac{1}{|\epsilon|}}) \\
&\vdots \qquad\qquad \vdots
\end{aligned}$$

where on the outermost scale the powers can be naively expanded in terms of logs but on each inner length scale one more power is exactly represented.

As indicated earlier we will now consider the full problem of a simply supported rectangular plate.

4.3 Consideration of the problem for a rectangular plate

We begin by considering the problem of a simply supported rectangular plate with sides of nondimensional length 1 and a. The method for obtaining an explicit solution to such a problem is presented in Chapter 5 of [92] and yields the formula

$$w = -\frac{16}{\pi^6} \sum_{\substack{m=1 \\ m\text{odd}}}^{\infty} \sum_{\substack{n=1 \\ n\text{odd}}}^{\infty} \frac{\sin m\pi x \sin \frac{n\pi y}{a}}{mn\left(m^2 + \frac{n^2}{a^2}\right)^2} \quad .$$

The reaction on the edges of the plate is given by formulae of the form (4.7) and any point force reaction at the corners is given by (4.8). The point force reactions at the corners for this problem are found to be non-zero and act upward. Hence if the plate were not simply supported from above and below it would lift at the corners since there would be a net upward force.

This solution, therefore, shows clearly that point forces at the corners of the plate would be needed in order for it to remain in contact everywhere with the frame. However, for the problem we initially posed the only load present is the weight of

the plate and hence in the absence of point forces at the corners the plate will lift. Thus the problem that must be solved has mixed boundary conditions of the simply supported and free types.

4.3.1 The codimension-two free boundary problem

The full problem with mixed boundary conditions is shown in Figure 4.8.

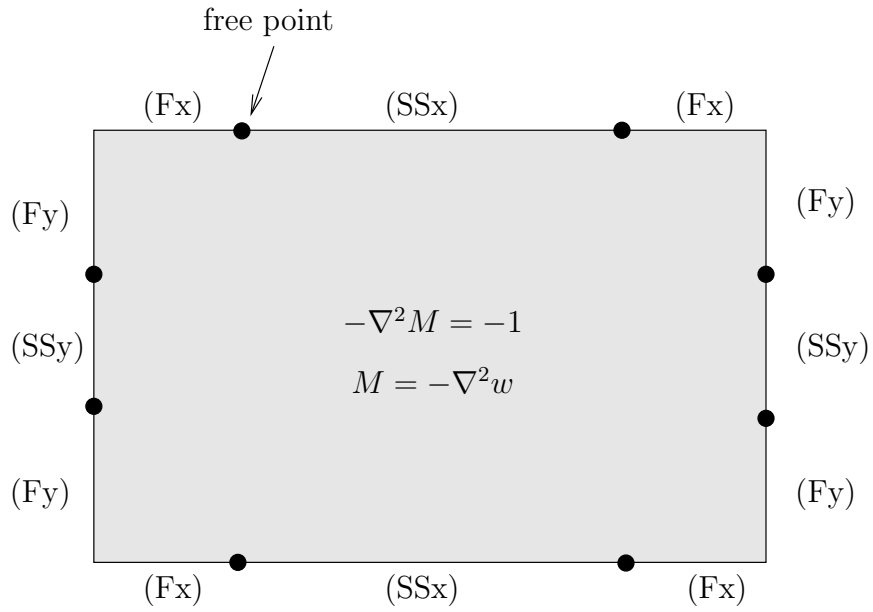

$$
\begin{aligned}
&(\text{SSy}) : \ w = 0 = w_{xx} \\
&(\text{Fy}) : \quad w_{xx} + \nu w_{yy} = 0 \qquad\qquad M_x - (1-\nu) w_{xyy} = 0 \\
&(\text{SSx}) : \ w = 0 = w_{yy} \\
&(\text{Fx}) : \quad \nu w_{xx} + w_{yy} = 0 \qquad\qquad M_y - (1-\nu) w_{xxy} = 0
\end{aligned}
$$

Figure 4.8: The codimension-two laterally loaded plate problem.

There are two codimension-two free boundaries on each edge. This problem is slightly different to those we have considered so far in the sense that it occurs naturally rather than as a limit of a codimension-one problem. Equally, however, it could be said that it is the limit of a codimension-one obstacle problem where the obstacle thickness tends to the line forming the frame as some small parameter tends to zero.

We shall first consider the local problem near a free point.

4.3.1.1 Local analysis near a free point

Locally near a free point the problem we must consider is as shown in Figure 4.9.

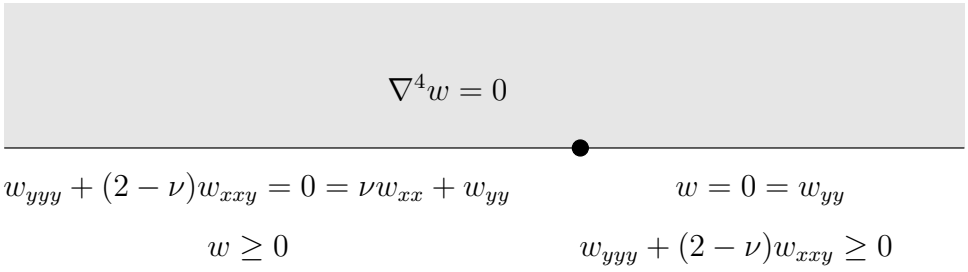

Figure 4.9: The local problem near a free point.

Changing to local polar coordinates the problem becomes

$$\begin{aligned}
\nabla^4 w &= 0 \quad \text{in} \quad r > 0 \ , \ \theta \in (0, \pi) \\
w &= 0 \qquad \text{on} \quad \theta = 0 \\
r w_r + w_{\theta\theta} &= 0 \qquad \text{on} \quad \theta = 0 \\
2w_\theta - w_{\theta\theta\theta} - 3r w_{r\theta} + (2-\nu)(-r^2 w_{rr\theta} + 2r w_{r\theta} - 2w_\theta) &\leq 0 \qquad \text{on} \quad \theta = 0 \\
2w_\theta - w_{\theta\theta\theta} - 3r w_{r\theta} + (2-\nu)(-r^2 w_{rr\theta} + 2r w_{r\theta} - 2w_\theta) &= 0 \qquad \text{on} \quad \theta = \pi \\
r w_r + w_{\theta\theta} + \nu r^2 w_{rr} &= 0 \qquad \text{on} \quad \theta = \pi \\
w &\geq 0 \qquad \text{on} \quad \theta = \pi \ .
\end{aligned}$$

The general solutions to the biharmonic equation of the form $r^n f(\theta)$ are given in equation (3.56). We require continuity of the third derivatives in order that the reaction along the boundary remains finite and hence the lowest permissible value of n is 3. Substituting the general solution into the boundary conditions results in the following matrix problem for the coefficients

$$\begin{bmatrix} 1 & 0 & 0 & 1 \\ n & 0 & 0 & n-4 \\ (\nu-1)n\sin n\pi & (\nu-1)n\cos n\pi & \alpha_1 & \alpha_2 \\ (\nu-1)n\cos n\pi & (\nu-1)n\sin n\pi & \alpha_3 & \alpha_4 \end{bmatrix} \begin{bmatrix} A_n \\ B_n \\ C_n \\ D_n \end{bmatrix} = \mathbf{0}$$

where

$$\begin{aligned}
\alpha_1 &= [n(\nu-1) - 2(1+\nu)]\cos n\pi \\
\alpha_2 &= [n(\nu-1) - 2(1+\nu)]\sin n\pi \\
\alpha_3 &= (\nu n - n + 4)\sin n\pi \\
\alpha_4 &= (\nu n - n + 4)\cos n\pi \ .
\end{aligned}$$

This can only have a non-trivial solution if the determinant of the matrix is zero which gives

$$\sin n\pi \cos n\pi(3 - 2\nu - \nu^2) \;=\; 0 \;\;.$$

The first acceptable solution is $n = 3$ for which

$$w \;\sim\; B_n r^3 \left(\sin 3\theta + \frac{3(1-\nu)}{5-\nu}\sin\theta\right)$$

and the inequalities imply $B_n < 0$.

Proceeding with the problem analytically seems far from simple. We shall, therefore, divert our attention to a numerical solution.

4.3.1.2 Numerical solution

Simply discretising the problem in Figure 4.8 (taking the point of the free boundary as fixed) would lead to a large set of implicit equations which would be time-consuming to solve on a computer. Instead, we shall apply a dynamic relaxation scheme as described in [78, 79]. The idea is to include in the field equation the extra terms that would occur if the problem were time dependent but with damping. Thus the field equations become

$$\begin{aligned} -\nabla^2 M + kw_t + w_{tt} &= -1 \\ M &= -\nabla^2 w \end{aligned}$$

where t is time. The damping coefficient is then chosen in such a way as to give near critical damping for the fundamental mode of the plate. With this damping the oscillations of the resulting solution die away, rapidly converging to the steady state we require. Once a steady state solution has been found for a given position of the free points the resulting reactions on the simply supported edge are considered. If the reaction is positive near the ends of the region the position of the free point node is moved one further from the corner but if it is negative it is moved one nearer. The iterative procedure then continues until the solution again converges to some required accuracy. This procedure is continued until two successive nodes are found at which the reaction on the free boundary changes from being both positive and negative to purely negative. We then consider this node to be the correct position for the free point.

For a regular finite difference mesh indexed by i in the x direction and j in the y direction, and with time indexed by n, the finite difference approximation used is

$$\begin{aligned}
\dot{w}_{i,j,n} &= \frac{1}{1+0.5k\Delta t}\Bigg[(1-0.5k\Delta t)\dot{w}_{i,j,n-1} \\
&\qquad + \frac{\Delta t}{\Delta x^2}\left(M_{i+1,j,n-\frac{1}{2}} - 2M_{i,j,n-\frac{1}{2}} + M_{i-1,j,n-\frac{1}{2}}\right) \\
&\qquad + \frac{\Delta t}{\Delta y^2}\left(M_{i,j+1,n-\frac{1}{2}} - 2M_{i,j,n-\frac{1}{2}} + M_{i,j-1,n-\frac{1}{2}}\right) - \Delta t\Bigg] && (4.20)\\
M_{i,j,n+\frac{1}{2}} &= -\frac{1}{\Delta x^2}\left(w_{i+1,j,n+\frac{1}{2}} - 2w_{i,j,n+\frac{1}{2}} + w_{i-1,j,n+\frac{1}{2}}\right) \\
&\qquad - \frac{1}{\Delta y^2}\left(w_{i,j+1,n+\frac{1}{2}} - 2w_{i,j,n+\frac{1}{2}} + w_{i,j-1,n+\frac{1}{2}}\right) && (4.21)\\
w_{i,j,n+\frac{1}{2}} &= w_{i,j,n-\frac{1}{2}} + \Delta t\dot{w}_{i,j,n} && (4.22)\\
w_{i,j,n} &= 0 && (4.23)\\
w_{i,j,n} &= 2w_{i+1,j,n} - w_{i+2,j,n} - \nu\frac{\Delta x^2}{\Delta y^2}\left(w_{i+1,j-1,n} - 2w_{i+1,j,n} + w_{i+1,j+1,n}\right) && (4.24)\\
w_{i,j,n} &= 2w_{i-1,j,n} - w_{i-2,j,n} - \nu\frac{\Delta x^2}{\Delta y^2}\left(w_{i-1,j-1,n} - 2w_{i-1,j,n} + w_{i-1,j+1,n}\right) && (4.25)\\
w_{i,j,n} &= 2w_{i,j+1,n} - w_{i,j+2,n} - \nu\frac{\Delta y^2}{\Delta x^2}\left(w_{i-1,j+1,n} - 2w_{i,j+1,n} + w_{i+1,j+1,n}\right) && (4.26)\\
w_{i,j,n} &= 2w_{i,j-1,n} - w_{i,j-2,n} - \nu\frac{\Delta y^2}{\Delta x^2}\left(w_{i-1,j-1,n} - 2w_{i,j-1,n} + w_{i+1,j-1,n}\right) && (4.27)\\
M_{i,j,n} &= M_{i+2,j,n} + (1-\nu)\left(w_{i,j-1,n} - 2w_{i,j,n} + w_{i,j+1,n} - w_{i+2,j-1,n}\right. \\
&\qquad \left. + 2w_{i+2,j,n} - w_{i+2,j+1,n}\right) && (4.28)\\
M_{i,j,n} &= M_{i-2,j,n} + (1-\nu)\left(w_{i,j-1,n} - 2w_{i,j,n} + w_{i,j+1,n} - w_{i-2,j-1,n}\right. \\
&\qquad \left. + 2w_{i-2,j,n} - w_{i-2,j+1,n}\right) && (4.29)\\
M_{i,j,n} &= M_{i,j+2,n} + (1-\nu)\left(w_{i-1,j,n} - 2w_{i,j,n} + w_{i+1,j,n} - w_{i-1,j+2,n}\right. \\
&\qquad \left. + 2w_{i,j+2,n} - w_{i+1,j+2,n}\right) && (4.30)\\
M_{i,j,n} &= M_{i,j-2,n} + (1-\nu)\left(w_{i-1,j,n} - 2w_{i,j,n} + w_{i+1,j,n} - w_{i-1,j-2,n}\right. \\
&\qquad \left. + 2w_{i,j-2,n} - w_{i+1,j-2,n}\right) && (4.31)\\
w_{i,j} &= 2w_{i+1,j,n} - w_{i+2,j,n} && (4.32)\\
w_{i,j} &= 2w_{i-1,j,n} - w_{i-2,j,n} && (4.33)\\
w_{i,j} &= 2w_{i,j+1,n} - w_{i,j+2,n} && (4.34)\\
w_{i,j} &= 2w_{i,j-1,n} - w_{i,j-2,n} && (4.35)\\
w_{i,j,n} &= w_{i+2,j,n} - w_{i+2,j+2,n} + w_{i,j+2,n} && (4.36)\\
w_{i,j,n} &= w_{i-2,j,n} - w_{i-2,j+2,n} + w_{i,j+2,n} && (4.37)
\end{aligned}$$

$$w_{i,j,n} = w_{i-2,j,n} - w_{i-2,j-2,n} + w_{i,j-2,n} \tag{4.38}$$

$$w_{i,j,n} = w_{i+2,j,n} - w_{i+2,j-2,n} + w_{i,j-2,n} \tag{4.39}$$

$$M_{i,j,n} = 0 \ . \tag{4.40}$$

An outline of how these difference equations are applied is shown in Figure 4.10. When the displacements and moments have been calculated for all points on the plate then the forces acting on the edges of the plate (marked by the solid line) are calculated by applying

$$\begin{aligned} \text{Reaction}_{i,1} &= \frac{1}{\Delta y}\left[M_{i,2,n} - M_{i,1,n} + (1-\nu)\left(w_{i-1,1,n} - 2w_{i,1,n} + w_{i+1,1,n}\right.\right. \\ &\qquad \left.\left. -w_{i-1,2,n} + 2w_{i,2,n} - w_{i+1,2,n}\right)\right] \\ \text{Reaction}_{1,j} &= \frac{1}{\Delta x}\left[M_{2,j,n} - M_{1,j,n} + (1-\nu)\left(w_{1,j-1,n} - 2w_{1,j,n} + w_{1,j+1,n}\right.\right. \\ &\qquad \left.\left. -w_{2,j-1,n} + 2w_{2,j,n} - w_{2,j+1,n}\right)\right] \end{aligned}$$

along the bottom and left hand edges. Finally any point forces occurring at the corners are calculated by applying

$$R = \frac{2}{\Delta x \Delta y}(1-\nu)\left(w_{2,2} - w_{1,2} - w_{2,1} + w_{1,1}\right) \ .$$

The numerical procedure is easily adjusted to consider the simpler problems of clamped and simply supported boundary conditions. This allows us to compare and contrast the three different sets of boundary conditions as well as validate the common core of the code by comparing the numerical results for simply supported boundary conditions with the series solution previously mentioned. The program has been used to consider three different sizes of plate with the three different types of boundary conditions. The value of ν has been taken to be 0.25 in accordance with the typical value for glass quoted in [92] p97. The plate sizes used are 1×1, 1×2 and 1×4 all with a mesh size of 0.025. Over the next several pages plots of the displacements and reactions for each case will be shown. To make the plots of displacements clearer further plots of particular cross sections through the plate are shown. For ease of reference in defining these cross-sections etc. we will label points on the plate as shown in Figure 4.11.

From these plots we see that in general the maximum displacement in the clamped case is always much less than in the other two. Comparing the results for the simply supported and free corners cases the increase in maximum displacement from the first to the second can be seen to be only slight. In the simply supported cases extra point forces are required at the corners, as well as the lateral load, to balance the reactions

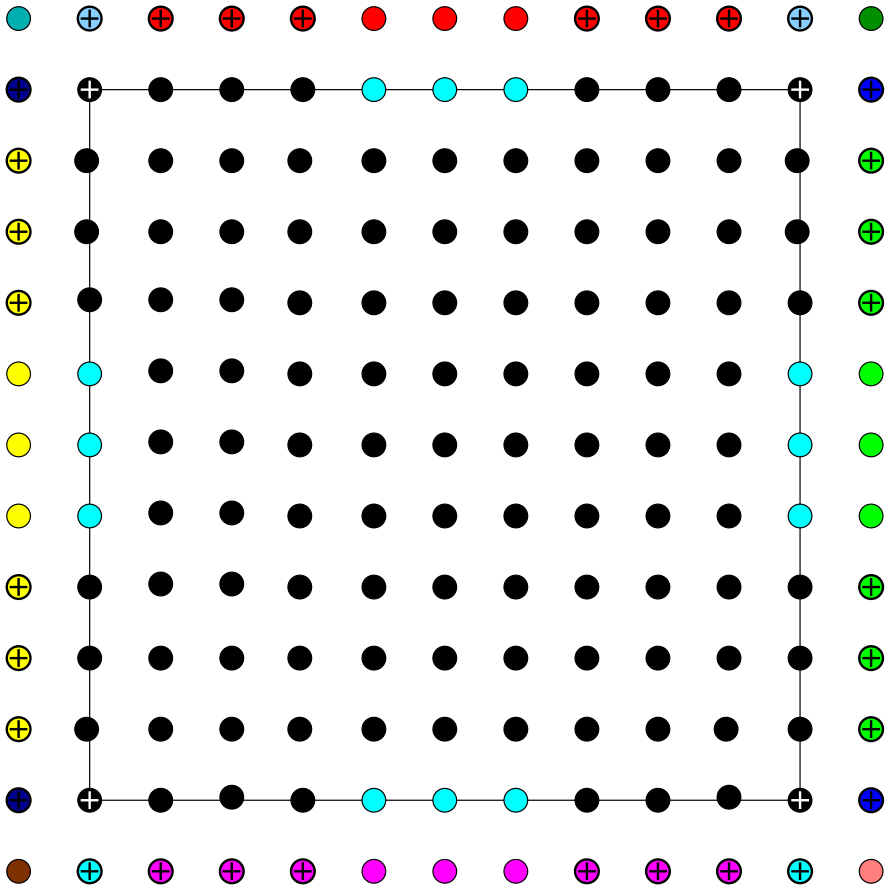

(A) Set initial values to zero

(B) Update displacements

1) At ● evaluate $\dot{w}$ using (4.20)
then update w using (4.22)

2) At ● update w using (4.23)

3) At ● & ⊕ using (4.24)
● & ⊕ update w using (4.25)
● & ⊕ using (4.26)
● & ⊕ using (4.27)

4) At ⊕ update w using (4.32)
⊕ using (4.33)
⊕ using (4.34)
⊕ using (4.35)

5) At ● update w using (4.36)
● using (4.37)
● using (4.38)
● using (4.39)

(C) Update moments

1) At ● & ● update M using (4.21)

2) At ⊕ update M using (4.40)

3) At ⊕ update w using (4.28)
⊕ using (4.29)
⊕ using (4.30)
⊕ using (4.31)

(D) Repeat steps (B) and (C) until required accuracy attained

Figure 4.10: The application of (4.20)–(4.40).

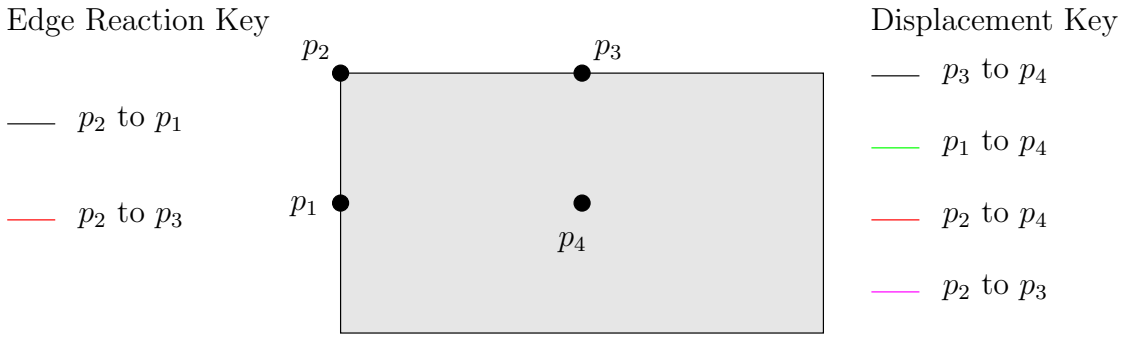

Figure 4.11: The points of reference and keys for Figures 4.12–4.14.

shown and thus keep the plate in contact along the entire edge. For the free corners cases it can be seen that the distance from the corner to the lift-off point is always around 0.25. It should also be noted that the lift-off point is approximately the same distance along the short side and long side, that is the lift-off length would appear to be determined mainly by the length of the shorter side. However, it would be wrong to say that the lift-off points are determined by a local problem near the corner since they are situated a reasonable distance along the side, that is we could not consider the free points to be a distance $\epsilon \ll 1$ away from the corners and then apply an asymptotic approach. In [79] it is implied that point forces will occur at the lift-off points. This is clearly false since point forces only occur where the twisting moment M_{nt} is discontinuous, as was seen from the explanation in Section 4.1, whereas in this case it is continuous all along the edge including at the lift-off points and corners.

The numerical technique applied above was taken from a paper [79] written in 1969. The technique has the benefit that it is easy to formulate and apply. However several years earlier (1965) saw the birth of variational formulations from which numerical solutions could be produced. The benefit of using the variational formulation of Section 4.1.1 as a starting point for a numerical solution is that a free boundary can be determined as part of the solution by using a projected SOR method rather than by trial and error as is the case above. The trial and error case above is only possible because the free boundary is only a collection of points, which are constrained to lie on the edge of the plate, and hence the number of different places they can lie is limited. The drawback of the variational formulation is that the actual application of the technique is more technically difficult to apply requiring the use of finite elements lying in $\mathcal{H}^2$. Such elements are needed to ensure enough continuity between elements. One major benefit of a finite element approach would be that the grid need not be

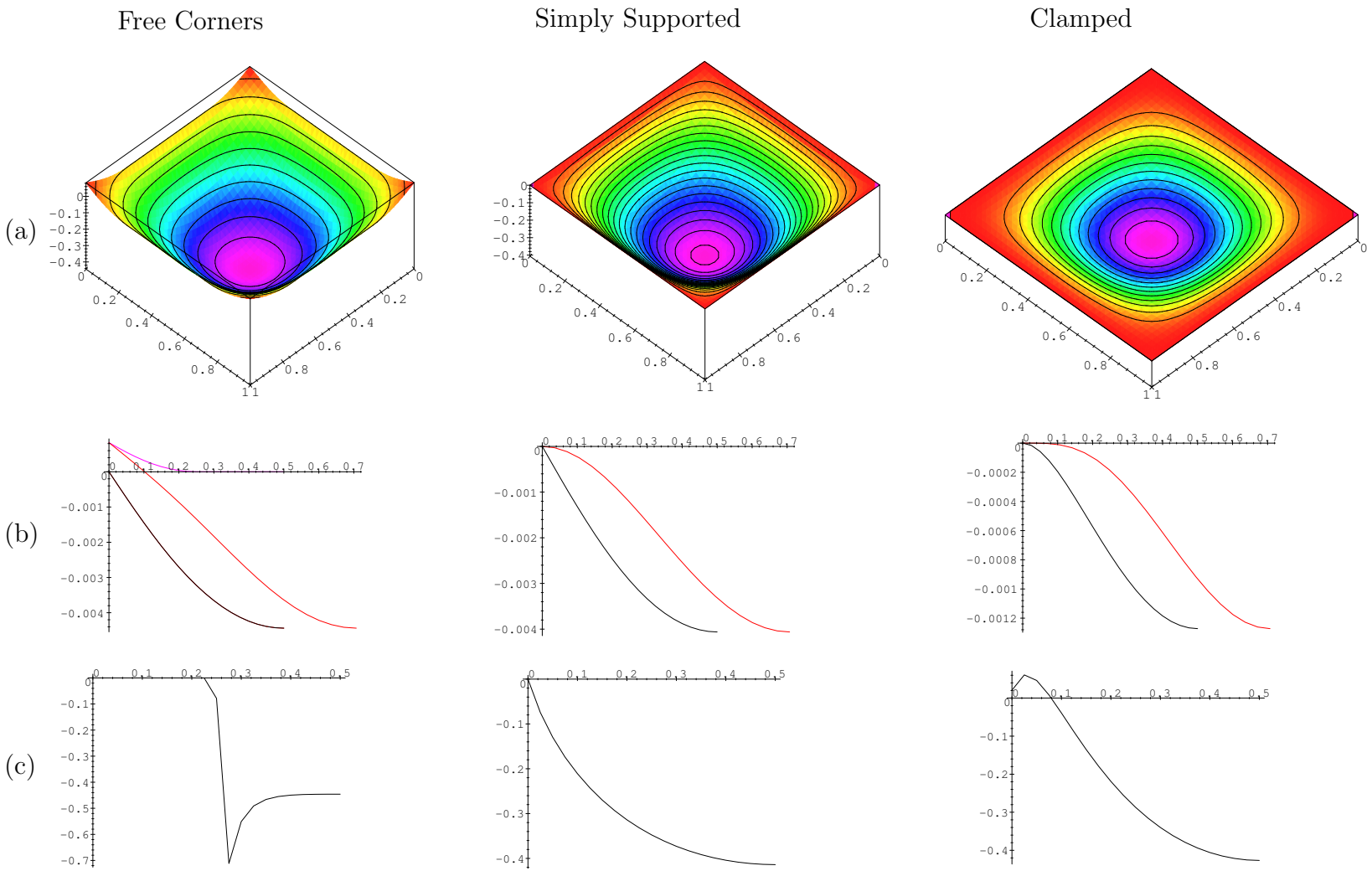

Figure 4.12: 1×1 plate : (a) Displacement w, (b) Cross sections of the displacement w, (c) Reactions along the edge. See Figure 4.11 for keys.

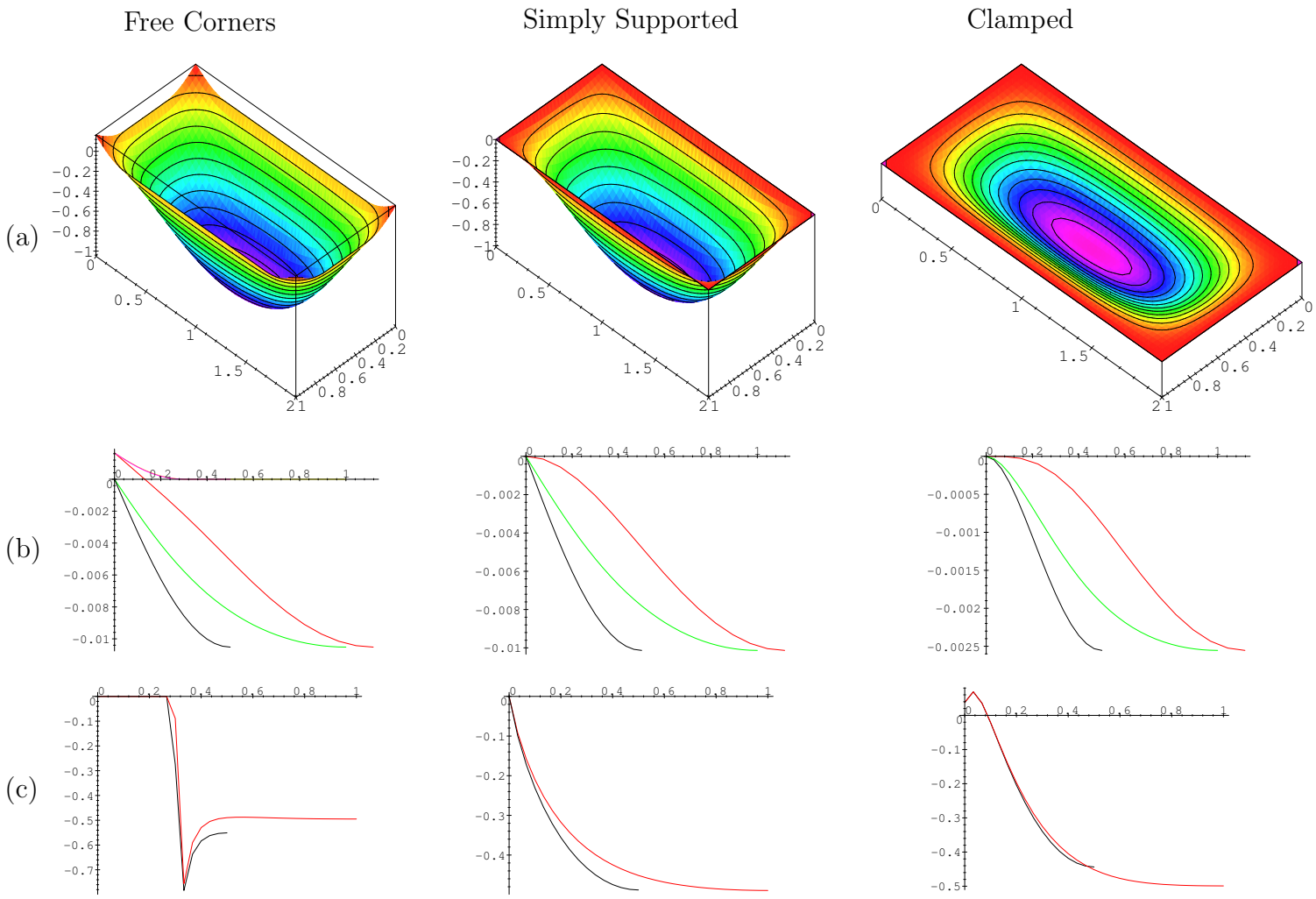

Figure 4.13: 1×2 plate : (a) Displacement w, (b) Cross sections of the displacement w, (c) Reactions along the edge. See Figure 4.11 for keys.

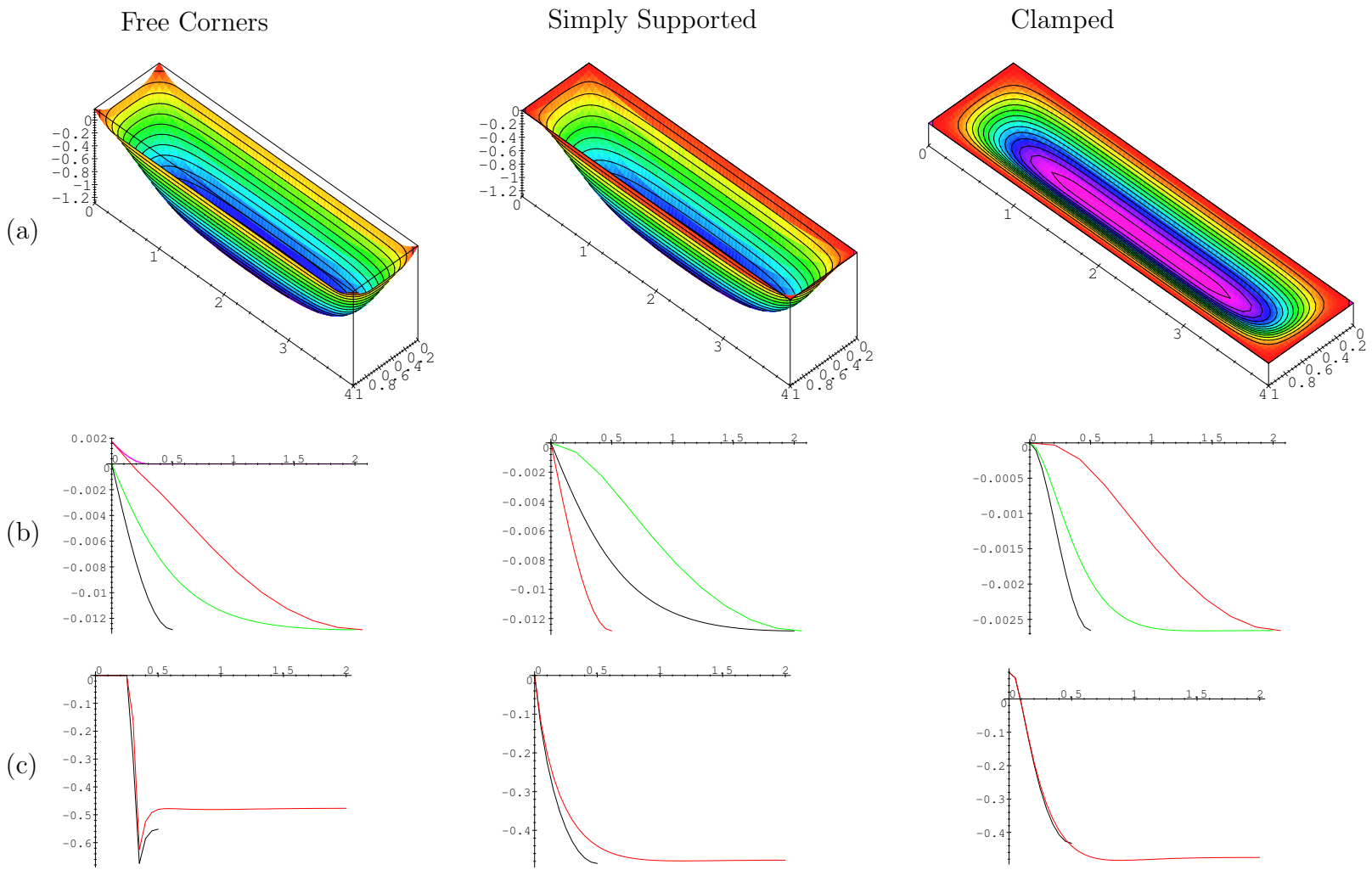

Figure 4.14: 1×4 plate : (a) Displacement w, (b) Cross sections of the displacement w, (c) Reactions along the edge. See Figure 4.11 for keys.

regular and can be refined near the lift-off points to produce more accurate estimates of its position.

Chapter 5

Stokes flow problems

In this chapter we shall discuss three problems that occur in Stokes flow. The first two problems of sintering due to injection and sintering under the action of surface tension are closely related. The problem of most interest is that of sintering under the action of surface tension which we will consider in Section 5.2. The analysis for the sintering problem, as we shall see later, is made more difficult by the need to use the inner problem near the free point $x = d(t)$ since it is the inner region which

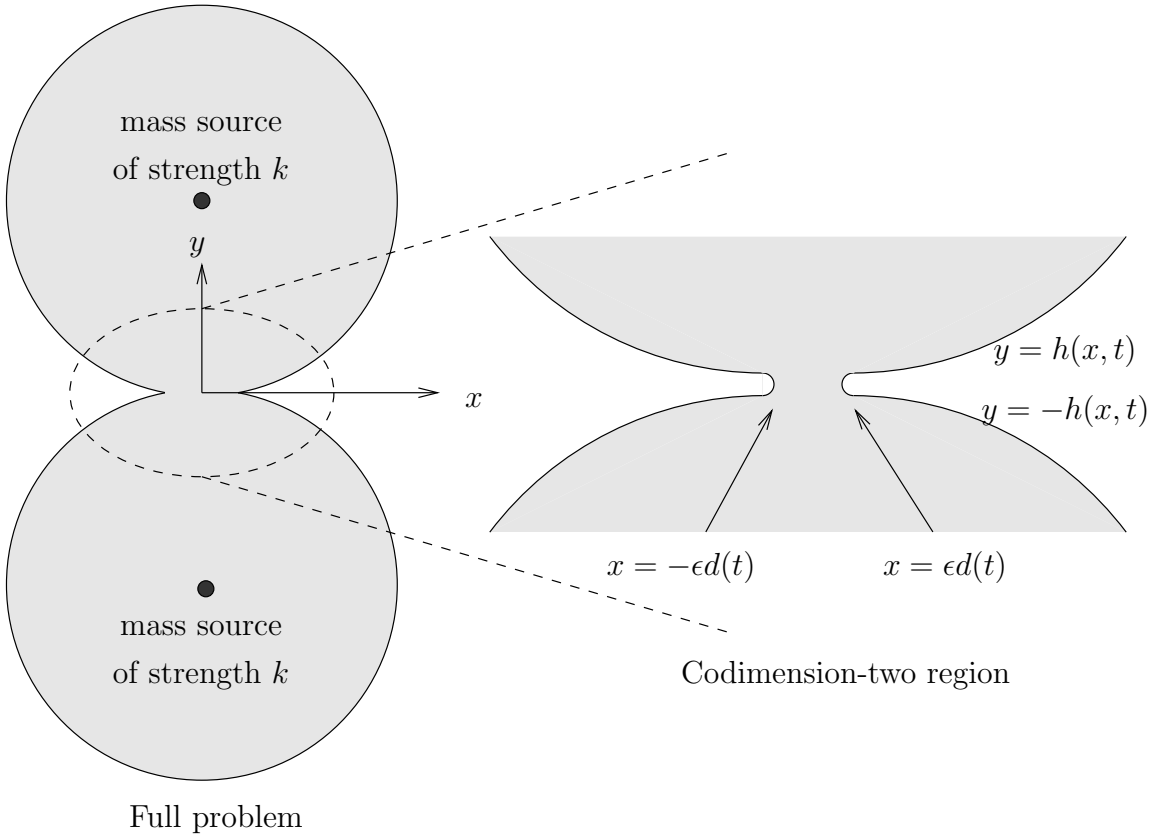

Figure 5.1: The geometry of the two-point Stokes flow injection problem.

drives the flow and the information in the problem flows mainly out of this region into the codimension-two region; however, as discussed in Chapter 1, as is the case in any of these problems certain assumptions are made which can only be verified by using information flowing in the other direction. Since the problem of sintering due to surface tension is complicated we shall instead build up to it by considering the problem of two point injection in the absence of surface tension. Because the driving mechanism for this flow is in the outer region, where a simple solution is easily obtained, it is much easier to solve the codimension-two problem and see what is happening. The geometry of the injection problem is shown in Figure 5.1. The sintering problem has the same geometry as the injection problem shown except that the sources are removed and it is the surface tension forces combined with the high curvature near the contact points $x = \pm d(t)$ that drive the flow.

The third problem models the closure of a long thin channel of water running between a glacier and the till bed below the glacier. We will first assume the till bed is rigid and impermeable such that we only have the single problem to solve in the ice. We will then consider the coupled problem when both the ice and till are modelled by slow flow.

The sintering process due to surface tension

Stokes flow with constant surface tension is one model used to represent certain types of industrial sintering processes. Sintering in general occurs when powders of ionic crystals, metals, or glass are placed under high pressure or raised to high enough temperatures that the mobility of the material is high enough that the particles coalesce. Such processes occur in nature, for example, the formation of rock strata from sand sediments under the influence of high pressure exerted by later decomposition. One of the earliest applications of this process in industry was for brick manufacture.

The many different phenomena that result in sintering cannot all be described by a single model. Things that may influence the model used include the type of material concerned, volume diffusion, evaporation followed by condensation and volume flow (viscous, plastic etc.) driven by surface tension. It is the last of these cases with which we will concern ourselves.

A modern application of viscous sintering is the production of high quality glass using what is known as a 'sol-gel' technique. This technique involves growing from a suspension a gel consisting of a maze of interconnected glassy strands. The gel is then heated and the surface tension forces cause it to collapse into a dense homogeneous

material. The final product should be free of voids making it a high quality glass that can be used in the production of glass fibres for the telecommunications industry.

Producing a solvable model for such a complicated structure is not a realistic goal. Instead much work has been done, particularly numerically (see for example [42, 49, 55, 96, 97, 98]), on so-called 'unit problems' such as the sintering of two cylinders or spheres. In particular we note that the three-dimensional numerical solution of Van de Vorst [97] relies upon initial conditions produced from a two-dimensional analytic solution. The justification for using initial conditions from a two-dimensional solution to start the three-dimensional computations is that, for small times, the neck curvature in the rz–plane will be dominant ($O(r_0^{-3})$, where r_0 is the radius of the contact circle) compared to the curvature in the θ–direction ($O(r_0^{-1})$), and thus the two-dimensional solution will be a good approximation when the contact region is small. The relative magnitudes of the curvatures can only be seen clearly once we solve the problem. We will find that the high curvature of the neck is situated in the innermost region which is on a length scale of $O(r_0^3)$ and hence the curvature is of $O(r_0^{-3})$.

It is not expected that the study of such problems will enable us to carry out a direct analysis of more complicated macroscopic systems, rather that constitutive laws can be extracted from them which can then be used to create a phenomenological theory for macroscopic systems.

The unit problem we wish to consider is the same as that in Figure 5.1 except that the sources are not present and instead it is the surface tension effects at the free boundary that drive the flow. A codimension-two analysis will be valid for small times after the initial contact. As remarked by Jagota and Dawson [42] "the initial stage of sintering is perhaps the least understood, mainly because of the geometrical complexities involved". They remark further that it is during these initial stages that many important phenomena occur. This problem has been previously considered by Morgan [58] in a codimension-two framework. Morgan also presents some of the details of the exact solution [32] for comparison. In the case of a flow with surface tension but without injection the flow is driven by the surface tension effects and high curvature near the point where the two cylinders meet. This is the innermost region and so a systematic solution procedure must involve matching the innermost region to the codimension-two solution to eliminate any unknown functions. The innermost region is essentially a travelling wave solution and has been considered by Hopper [34]. The solution procedure is somewhat complex and thus solving in the opposite direction to the flow of information may appear to be desirable. This is

what Morgan has attempted to do. In Appendix C we review the solution to the two cusp problem as posed by Morgan as a means of producing a matching condition. We will show how the codimension-two problem can be systematically solved by following the flow of information and matching to the inner Hopper [34] region rather than by trying to infer a match to an outer region as was done by Morgan. Having derived the codimension-two solution by matching to the solution of the inner problem we will then show how we can obtain all the necessary matching information by considering only the far field problem to the full inner problem. The solution to the far field problem is considerably easier to obtain than the Hopper solution and as such represents a major simplification of the whole solution procedure.

As mentioned above, however, we will begin by solving the injection problem since the analysis is easier than that for the surface tension model.

5.1 Point sources in Stokes flow

An exact solution for this problem can be derived using the method outlined in [38, 75]. The codimension-two problem will only be valid for small times when the order of the length of the contact width is also small. Thus as in the case of other small time problems with small contact sets, we denote the order of the length of the contact set by $\epsilon \ll 1$. The geometry of the problem is shown in Figure 5.1.

The Stokes flow field equations governing a slow flow are

$$-\nabla p + \nabla^2 \mathbf{u} = 0 \tag{5.1}$$

$$\nabla \cdot \mathbf{u} = 0 \ . \tag{5.2}$$

A new variable ψ, the stream function, is defined by

$$\mathbf{u} = (\psi_y, -\psi_x) \ . \tag{5.3}$$

Using this representation of the velocity, (5.2) is automatically satisfied. Substituting (5.3) into (5.1) and taking the curl of the resulting equation yields

$$\nabla^4 \psi = 0 \tag{5.4}$$

$$p_x = \psi_{xxy} + \psi_{yyy} \tag{5.5}$$

$$p_y = -\psi_{xxx} - \psi_{xyy} \ . \tag{5.6}$$

On a free boundary, $y = h(x,t)$, we have the kinematic condition

$$\psi_x + h_t + h_x \psi_y = 0 \qquad \text{on} \quad y = h(x,t) \tag{5.7}$$

and the stress conditions

$$(\sigma\mathbf{n})\cdot\mathbf{n} = 0 \qquad \text{on} \quad y = h(x,t) \tag{5.8}$$

$$(\sigma\mathbf{n})\cdot\mathbf{t} = 0 \qquad \text{on} \quad y = h(x,t) \tag{5.9}$$

where σ is the stress tensor, and $\mathbf{t}$ and $\mathbf{n}$ are the tangent and normal to the free surface, respectively. Eliminating between the two stress conditions it can be shown that

$$\begin{aligned} -\sigma_{22} + \sigma_{12}h_x &= 0 \qquad \text{on} \quad y = h(x,t) \\ \sigma_{11}h_x - \sigma_{12} &= 0 \qquad \text{on} \quad y = h(x,t) \ . \end{aligned}$$

Substituting in for the components of the stress tensor, written in terms of ψ and p, we obtain

$$\begin{aligned} -p - 2\psi_{xy} &= h_x(\psi_{yy} - \psi_{xx}) \qquad \text{on} \quad y = h(x,t) \\ (-p + 2\psi_{xy})\, h_x &= \psi_{yy} - \psi_{xx} \qquad \text{on} \quad y = h(x,t) \ . \end{aligned}$$

If we differentiate these two equations along the free boundary then we can eliminate the terms involving the pressure using (5.5) and (5.6) to obtain

$$\begin{aligned} 3\psi_{xxy} + \psi_{yyy} &= 2h_x(\psi_{xxx} - \psi_{xyy}) - h_{xx}(\psi_{yy} - \psi_{xx}) \\ &\qquad + h_x^2(\psi_{xxy} - \psi_{yyy}) \qquad \text{on} \quad y = h(x,t) \qquad (5.10) \\ (\psi_{yy} - \psi_{xx})h_{xx} &= h_x(\psi_{xyy} - \psi_{xxx}) - 2h_x^2(\psi_{xxy} - \psi_{yyy}) \\ &\qquad - h_x^3(\psi_{xxx} + 3\psi_{xyy}) \qquad \text{on} \quad y = h(x,t) \ . \qquad (5.11) \end{aligned}$$

Hence we can formulate a free boundary problem in slow flow in terms of the stream function, ψ, and the surface shape, h, only.

Since the field equation for this problem is the biharmonic equation we might expect that a general solution procedure for slow flow exists which is closely related to the general solution procedure demonstrated in Section 3.3.1.2. This is the case and we shall now derive the relevant formulae.

We begin by noting

$$\begin{aligned} \nabla^2\psi &= u_y - v_x \\ &= -\xi \end{aligned}$$

where ξ is the vorticity of the flow. Now since $\nabla^4\psi = 0$, ξ is harmonic. Secondly we note

$$\begin{aligned}\nabla^2 p &= \nabla\cdot(\nabla^2\mathbf{u}) \qquad \text{by (5.1)}\\ &= \nabla\cdot(\nabla(\nabla\cdot\mathbf{u}) - \nabla\times(\nabla\times\mathbf{u}))\\ &= 0 \qquad \text{by (5.2)}\end{aligned}$$

which implies p is harmonic also. If we observe further that

$$\begin{aligned}\xi_x &= v_{xx} - u_{xy} &(5.12)\\ &= \nabla^2 v \qquad \text{by (5.2)} &(5.13)\end{aligned}$$

and similarly

$$\xi_y = -\nabla^2 u \tag{5.14}$$

then combining (5.13) and (5.14) with (5.1) we obtain the Cauchy–Riemann equations

$$\begin{aligned}p_x &= -\xi_y\\ p_y &= \xi_x\ .\end{aligned}$$

Thus ξ and p are conjugate harmonic functions and therefore represent the real and imaginary parts of an analytic function of $z = x + iy$.

If we define

$$i\phi(z) = g(x,y) + i\tilde{g}(x,y) \tag{5.15}$$

to be one such function such that

$$-4i\phi'(z) = \xi + ip \tag{5.16}$$

and further define

$$G(x,y) = -\left[xg(x,y) + y\tilde{g}(x,y)\right] + \psi(x,y) \tag{5.17}$$

then

$$\begin{aligned}\nabla^2 G &= -\left[x\nabla^2 g + y\nabla^2\tilde{g} + 2(g_x + \tilde{g}_y)\right] + \nabla^2\psi\\ &= -4g_x + \nabla^2\psi\\ &= -4\Re\left\{i\phi'(z)\right\} + \nabla^2\psi\\ &= \xi + \nabla^2\psi\\ &= 0\end{aligned}$$

so G is harmonic as well. Letting $i\chi$ be the analytic function whose real part is $G(x,y)$ then (5.15) and (5.17) imply

$$\begin{aligned} \psi(x,y) &= -\Im\left\{\overline{z}\phi(z) + \chi(z)\right\} && (5.18)\\ &= \frac{1}{2}i\left[\overline{z}\phi(z) - z\overline{\phi(z)} + \chi(z) - \overline{\chi(z)}\right] \ . && (5.19)\end{aligned}$$

ϕ and χ have a certain degree of arbitrariness which can be seen by replacing ϕ by $\phi + az + c$ and χ by $\chi - k + \overline{c}z$, where $c, k \in \mathbb{C}$ and $a \in \mathbb{R}$. Doing so the value of ψ is only changed by the additive constant $\Im k$ (since $\{az\overline{z} + c\overline{z} + \overline{c}z\}$ is real), which does not affect any physical quantities. Furthermore we should also note that the Stokes flow equations are invariant under rigid body motions. Rigid body motions can be expressed as terms of the form $iaz\overline{z}$ and $i(c\overline{z} + \overline{c}z)$ which represent rotations and translations, respectively. In the case of the injection problem we will take the injection points to be fixed which fixes the rigid body motions.

The velocity potential, pressure and components of stress can all be written in terms of ϕ and χ making this representation of the solution very useful. The velocity potential $u + iv$ satisfies

$$\begin{aligned} (u+iv) &= -i(\psi_x + i\psi_y) \\ &= -2i\psi_{\overline{z}} \\ &= \phi(z) - z\overline{\phi'(z)} - \overline{\chi'(z)} \ . && (5.20)\end{aligned}$$

From (5.16) we see

$$p = -4\Re\{\phi'(z)\}$$

and hence the components of stress are

$$\begin{aligned} \sigma_{11} &= 2\Re\left\{2\phi'(z) - \overline{z}\phi''(z) - \chi''(z)\right\} \\ \sigma_{22} &= 2\Re\left\{2\phi'(z) + \overline{z}\phi''(z) + \chi''(z)\right\} \\ \sigma_{12} &= 2\Im\left\{\overline{z}\phi''(z) + \chi''(z)\right\} \ . \end{aligned}$$

Then

$$\begin{aligned} \sigma_{11} + \sigma_{22} &= 8\Re\left\{\phi'(z)\right\} && (5.21)\\ i(\sigma_{22} - \sigma_{11}) - 2\sigma_{12} &= 4i(\overline{z}\phi''(z) + \chi''(z)) \ . && (5.22)\end{aligned}$$

As with the contact problem we define $\Phi(z) = \phi'(z)$ and $\Psi(z) = \chi''(z)$. Furthermore, like the contact problem, the codimension-two problem will be on a half space. We thus analytically continue Φ into the lower half plane by defining

$$\Psi(z) = -\Phi(z) - \overline{\Phi}(z) - z\Phi'(z) \ . \quad (5.23)$$

With these substitutions (5.21) and (5.22) become

$$\sigma_{11} + \sigma_{22} = 4\left(\Phi(z) + \overline{\Phi(z)}\right) \tag{5.24}$$

$$(\sigma_{22} - \sigma_{11}) + 2i\sigma_{12} = 4\left[(\overline{z} - z)\Phi'(z) - \Phi(z) - \overline{\Phi}(z)\right] \quad . \tag{5.25}$$

Further substituting from (5.24) into (5.25) for σ_{11} gives

$$\sigma_{22} - i\sigma_{12} = 2\left[(z - \overline{z})\overline{\Phi'(z)} + \Phi(z) - \Phi(\overline{z})\right] \quad . \tag{5.26}$$

Differentiating (5.20) with respect to x gives

$$u_x + iv_x = (\overline{z} - z)\overline{\Phi'(z)} + \Phi(z) + \Phi(\overline{z}) \quad . \tag{5.27}$$

Taking the limit as $y \to 0$ in (5.26) and (5.27) yields two conditions which must be satisfied on the boundary

$$\Phi^+(x) - \Phi^-(x) = -\frac{1}{2}(\tilde{p} + i\tilde{q}) \tag{5.28}$$

$$\Phi^+(x) + \Phi^-(x) = u_x + iv_x \tag{5.29}$$

where on the boundary the tractions are $\sigma_{22} = -\tilde{p}(x)$ and $\sigma_{12} = \tilde{q}$. By symmetry $\tilde{q} = 0$ but $\tilde{p}$ is to be determined as part of the solution.

The fact that $\nabla \cdot \sigma = 0$ implies there exists an Airy stress function, Υ, defined in the usual way. Since the pressure is harmonic it follows from (5.21) and (5.22) that Υ is a biharmonic function and thus admits a representation similar to (3.17). Comparison of (5.21) and (5.22) with (3.24) and (3.25) shows this representation can be taken to be

$$\Upsilon = 2\Re\left\{\overline{z}\phi(z) + \chi(z)\right\} \quad .$$

The flow of information in this problem is from the outer region (which is driven by the source) into the codimension-two region and so we should begin by considering the solution of a point source in Stokes flow but with some kind of singularity at the origin which depends on the codimension-two region.

5.1.1 The outer problem

For a point source we know the form of the singularity in the velocity is

$$\mathbf{u} = \frac{k}{2\pi r}\mathbf{e}_r$$

where k is the flux out of the source. To write this as a singularity in ψ we use the definition (5.3) which, in cylindrical polar coordinates, shows

$$\frac{k}{2\pi r}\mathbf{e}_r \;=\; \frac{1}{r}\psi_\theta \mathbf{e}_r - \psi_r \mathbf{e}_\theta \;\;,$$

from which we deduce

$$\psi \;\sim\; \frac{k}{2\pi}\theta + \text{const} \;\;.$$

Centering the source at $(0,1)$ gives

$$\psi \;\sim\; \text{const} - \frac{k}{2\pi}\tan^{-1}\left(\frac{1-y}{x}\right) \qquad \text{as} \quad x \to 0 \;\;,\;\; y \to 1 \;\;. \tag{5.30}$$

Hence the outer problem is simply equations (5.4), (5.7)–(5.9) and (5.30) where the free boundary is $r^2 = x^2 + (y-1)^2 = s(t)^2$. This has the solution

$$\begin{aligned} \psi &= \text{const} - \frac{k}{2\pi}\tan^{-1}\left(\frac{1-y}{x}\right) \\ s &= \left(\frac{kt}{\pi}\right)^{\frac{1}{2}} \;\;. \end{aligned}$$

Thus the cylinders first touch at $(0,0)$ when the radius is 1 for which $t = \pi/k$.

5.1.2 The codimension-two problem

As mentioned earlier we define the contact set to be of length $O(\epsilon)$ and therefore the codimension-two length scalings are $x = \epsilon\hat{x}$ and $y = \epsilon\hat{y}$. We expect the codimension-two solution only to be valid for small times after the initial contact and so scale $t = \pi/k + \delta\hat{t}$. Expanding the outer solution for ψ in inner variables gives

$$\psi \;=\; \text{const} - \frac{k}{4} + \frac{k\epsilon}{2\pi}\hat{x} + O(\epsilon^2) \tag{5.31}$$

suggesting that the appropriate scaling for ψ is $\psi = \epsilon\hat{\psi}$ (so σ, the stress tensor, scales with ϵ^{-1}), and that it would be most convenient to take the constant to be $k/4$. This local expansion of the outer flow represents a uniform flow in the $-y$ direction. The same local form of the outer flow would trivially be produced if instead of injection the two cylinders were simply moved towards each other at a uniform speed of $k/2\pi$. As usual the scaling for h is $h = \epsilon^2\hat{h}$. Finally we note to obtain a dominant balance of terms from (5.7) we require $\delta = \epsilon^2$.

Substituting these scalings into (5.4), (5.7), (5.10) and (5.11) and expanding $\hat{\psi}$ as a regular asymptotic expansion

$$\hat{\psi} \sim \psi_0 + \epsilon\psi_1 + \ldots$$

produces the leading order model

$$\begin{aligned}
\nabla^4\psi_0 &= 0 \qquad \text{in} \quad y > 0 && (5.32)\\
h_t + \psi_{0x} &= 0 \qquad \text{on} \quad y = 0 \ , \ |x| > d(t) && (5.33)\\
3\psi_{0xxy} + \psi_{0yyy} &= 0 \qquad \text{on} \quad y = 0 \ , \ |x| > d(t) && (5.34)\\
\psi_{0yy} - \psi_{0xx} &= 0 \qquad \text{on} \quad y = 0 \ , \ |x| > d(t) && (5.35)\\
h &> 0 \qquad \text{on} \quad y = 0 \ , \ |x| > d(t) && (5.36)\\
\psi_{0yy} &= 0 \qquad \text{on} \quad y = 0 \ , \ |x| < d(t) && (5.37)\\
\psi_{0x} &= 0 \qquad \text{on} \quad y = 0 \ , \ |x| < d(t) && (5.38)\\
\sigma_{22_0} &\leq 0 \qquad \text{on} \quad y = 0 \ , \ |x| < d(t) && (5.39)
\end{aligned}$$

whose solution must match with (5.31). We note that this codimension-two model is the same as that formulated by Morgan [58] for the case of the sintering problem (i.e. non-zero surface tension but no sources). The inequality on the contact region expresses the fact that the stress σ_{22} will be negative there and the other two boundary conditions on the contact region express symmetry of the horizontal and vertical velocities, respectively. The stress inequality is not, however, expressible independently of the pressure. Condition (5.38) can be simplified further by integrating along the boundary to yield

$$\psi_0 = 0 \qquad \text{on} \quad y = 0 \ , \ |x| < d(t) \ . \qquad (5.40)$$

Note the constant of integration is chosen to be zero which is consistent with the choice made in (5.31).

We begin to solve this problem by examining the local behaviour at the free point $x = d(t)$.

5.1.2.1 A local analysis at a free point

We shall perform the usual analysis to determine the order of the singularity at the free point. We centre the coordinates on the free point $(d(t), 0)$ by making the change of variable $\xi = x - d(t)$. This affects the derivatives in time replacing them with

$\partial/\partial t - \dot{d}\partial/\partial\xi$. We then look locally in cylindrical polar coordinates $\xi = \delta r\cos\theta$ and $y = \delta r\sin\theta$, where $\delta \ll 1$. Fortunately locally the inequality on the stress σ_{22_0} can be interpreted in terms of ψ only. Since $\sigma_{22_0} < 0$ on $\theta = \pi$ and $\sigma_{22_0} = 0$ on $\theta = 0$ locally $\sigma_{22_{0x}} \geq 0$, that is $-3\psi_{0xxy} - \psi_{0yyy} \geq 0$. This leads to the local leading order model

$$\begin{aligned}
\nabla^4\psi_0 &= 0 \qquad \text{for} \quad \theta \in (0,\pi) \\
\frac{1}{r^3}\psi_{\theta\theta\theta} - \frac{3}{r^2}\psi_{0r\theta} + \frac{4}{r^3}\psi_{0\theta} + \frac{3}{r}\psi_{0rr\theta} &= 0 \qquad \text{on} \quad \theta = 0 \\
-\psi_{0rr} + \frac{1}{r}\psi_{0r} + \frac{1}{r^2}\psi_{0\theta\theta} &= 0 \qquad \text{on} \quad \theta = 0 \\
\psi_0 &> 0 \qquad \text{on} \quad \theta = 0 \\
\frac{1}{r^3}\psi_{\theta\theta\theta} - \frac{3}{r^2}\psi_{0r\theta} + \frac{4}{r^3}\psi_{0\theta} + \frac{3}{r}\psi_{0rr\theta} &\geq 0 \qquad \text{on} \quad \theta = \pi \\
\frac{1}{r^2}\psi_{0\theta\theta} + \frac{1}{r}\psi_{0r} &= 0 \qquad \text{on} \quad \theta = \pi \\
\psi_0 &= 0 \qquad \text{on} \quad \theta = \pi \ .
\end{aligned}$$

The general solution to the biharmonic equation, in cylindrical polar coordinates, dominated by a single power of r, r^n, is given in (3.56). To determine which values n may take we must apply the four boundary conditions and two inequalities above. As was the case with the water entry problem we appeal to the trace theorem for Sobolev spaces (see Appendix A) to assert that the solution cannot have any negative power singularities. Further by the maxim of Van Dyke we look for the lowest possible singularity. Taking the lowest possible singularity has been verified as correct by further matching to a solution in an inner region about the free point in the same manner as is possible for the water entry problem.

Applying the boundary conditions to the first non-negative mode, $n = 0$, we find $\psi_0 = B_0\sin 2\theta$. However, locally h_0 satisfies

$$\begin{aligned}
-\dot{d}h_{0\xi} + \psi_{0\xi} &= 0 \qquad \text{on} \quad y = 0 \\
h_0 &= 0 \qquad \text{at} \quad \xi = 0
\end{aligned}$$

which implies $h_0 = 0$ locally. This contradicts the fact that $d(t)$ is a free point and so we discard this possibility.

The next non-negative modes are from the general solution when $n \in (0,1)$. Applying the boundary conditions yields the matrix problem, for the coefficients A_n, B_n, C_n and D_n,

$$\begin{bmatrix}
0 & 1 & 1 & 0 \\
n & 0 & 0 & (n-2) \\
n\cos n\pi & n\sin n\pi & (n-4)\sin n\pi & (n-4)\cos n\pi \\
\cos n\pi & \sin n\pi & \sin n\pi & \cos n\pi
\end{bmatrix}
\begin{bmatrix} A_n \\ B_n \\ C_n \\ D_n \end{bmatrix} = 0$$

which only has a non-trivial solution provided

$$\sin 2n\pi \quad = \quad 0 \quad .$$

The first solution to this is $n = 1/2$ giving

$$\psi_0 \quad \sim \quad Dr^{\frac{1}{2}} \left(3\cos\frac{\theta}{2} + \cos\frac{3\theta}{2} \right) \qquad \text{near} \quad x = d(t) \quad , \quad y = 0$$

where $D > 0$ to satisfy the inequalities. For future reference we note this can be written as

$$\psi_0 \quad \sim \quad D\Im\left\{ i\frac{3\hat{z} + \overline{\hat{z}}}{\sqrt{\hat{z}}} \right\} \tag{5.41}$$

where $z = d + \delta\hat{z}$.

5.1.2.2 Solution of the codimension-two problem

The leading-order model defined by (5.32)–(5.39) can be stated in terms of the stress and velocity components as (on dropping the subscript 0)

$$\begin{aligned}
\nabla^4\psi &= 0 \qquad \text{in} \quad y > 0 \\
h_t + \psi_x &= 0 \qquad \text{on} \quad |x| > d(t) \quad , \quad y = 0 \\
\sigma_{22} &= 0 \qquad \text{on} \quad |x| > d(t) \quad , \quad y = 0 \\
\sigma_{12} &= 0 \qquad \text{on} \quad |x| > d(t) \quad , \quad y = 0 \\
h &> 0 \qquad \text{for} \quad |x| > d(t) \\
v &= 0 \qquad \text{on} \quad |x| < d(t) \quad , \quad y = 0 \\
\sigma_{12} &= 0 \qquad \text{on} \quad |x| < d(t) \quad , \quad y = 0 \\
\sigma_{22} &\leq 0 \qquad \text{on} \quad |x| < d(t) \quad , \quad y = 0 \quad .
\end{aligned}$$

The earlier analysis reduces this to the problem of satisfying equations (5.28) and (5.29). This is yet again a statement of the classic Riemann problem as discussed in Appendix B, and is almost identical to the problem in Section 3.3.1.2 except for an extra factor of 1/2. Thus from (3.79) the solution is

$$\Phi(z) \quad = \quad \frac{1}{4\pi i}\int_d^d \frac{\tilde{p}(t)}{z - t}dt \quad , \tag{5.42}$$

since $\tilde{q} = 0$, where $\tilde{p}$ is still to be determined. This solution assumes that $\tilde{p}(t)$ satisfies the condition

$$\tilde{p}(x) \quad \sim \quad \frac{p^*(x)}{(x \pm d)^\gamma} \qquad \text{for} \quad \Re\gamma < 1 \quad , \tag{5.43}$$

where $p^*(x)$ satisfies a Hölder condition. Substituting (5.42) into (5.29) and taking the imaginary part we find

$$0 \;=\; \int_{-d}^{d} \frac{\tilde{p}(t)}{t-x} dt \quad .$$

Using the results of Section B.4 a solution to this which is unbounded at the ends (the only bounded solution is zero) is seen to be

$$\tilde{p}(x) \;=\; \frac{A}{(d^2-x^2)^{\frac{1}{2}}}$$

where A is a real constant. Substituting for $\tilde{p}$ back into (5.42) and integrating we can find Φ. Further substituting Φ into (5.23) we can obtain Ψ. Lastly integrating Φ once and Ψ twice we obtain ϕ and χ and hence the stream function defined by (5.18) is

$$\psi \;=\; -\Im\left\{ \frac{A}{4}(z+\overline{z}) \sin^{-1}\left(\frac{z}{d}\right) + \frac{A}{2}(d^2-z^2)^{\frac{1}{2}} \right\} \quad .$$

If we expand this locally near the free point $x = d(t)$ by making the change of variables $z = d + \delta\hat{z}$ then we obtain the leading order expansion

$$\psi \;\sim\; -\Im\left\{ iA\sqrt{\frac{\delta d\hat{z}}{2}} \right\}$$

which does not match with the behaviour required by (5.41) which forces A to be zero which in turn means the stream function we have found is identically zero.

One method of generating other solutions to the problem is to assume that the free term, that is the right-hand side of (5.28), has a different property at the end points $x = \pm d$ to that we have so far assumed. The previous solution was naively produced by assuming $\tilde{p}$ had the same properties as it had for the contact problem of Chapter 3, namely (5.43). We could instead consider various other possibilities where $\tilde{p}$ has singularities at the end points of the form

$$\frac{g(t)}{(t \pm d)^{\gamma}}$$

for different values of γ. When $\Re\gamma > 1$ the solution procedure is adapted as described in Section B.5. Various different possibilities were tried until the solution with the correct local behaviour near $x = d$ was found for the case $1 < \Re\gamma < 2$. In this case we integrate the Riemann problem twice to obtain the new problem

$$\Phi^{+^{(-2)}}(x) - \Phi^{-^{(-2)}}(x) \;=\; -\frac{1}{2}\tilde{p}^{(-2)}(x) \qquad \text{for} \quad |x| < d \tag{5.44}$$

$$\Im\left\{ \Phi^{+^{(-2)}}(x) + \Phi^{-^{(-2)}}(x) \right\} \;=\; Ax \qquad \text{for} \quad |x| < d \tag{5.45}$$

where A is a constant (or function of t). The notation $\tilde{p}^{(-2)}(x)$ means the function $\tilde{p}(x)$ integrated twice with respect to x. The term Ax arises because we have integrated twice but excluded the possibility of a constant term as well because we require symmetry about $x = 0$. Note having integrated twice $\tilde{p}^{(-2)}(x)$ is no longer unbounded at the end points. The solution to (5.44) is

$$\Phi^{(-2)}(z) = \frac{1}{4\pi i}\int_{-d}^{d}\frac{\tilde{p}^{(-2)}(t)}{(z-t)}dt \ . \tag{5.46}$$

Substituting this into (5.45) we can invert the resulting equation by applying the result of Section B.4. The problem to invert is of the same form as that which was inverted in the contact problem of Section 3.3.1.3 and has solution

$$\tilde{p}^{(-2)}(x) = \tilde{A}(d^2 - x^2)^{\frac{1}{2}}$$

where $\tilde{A}$ is a constant. Substituting this back into (5.46) and integrating gives $\Phi^{(-2)}(z)$. Differentiating this twice and substituting into (5.23) produces Ψ. Integrating Ψ twice and differentiating $\Phi^{(-2)}(z)$ once we obtain

$$\begin{aligned}\chi(z) &= \frac{B(z^2 - 2d^2)}{(d^2 - z^2)^{\frac{1}{2}}} \\ \phi(z) &= \frac{Bz}{(d^2 - z^2)^{\frac{1}{2}}}\end{aligned}$$

from which (5.18) implies

$$\psi = -B\Im\left\{\frac{z^2 + z\overline{z} - 2d^2}{(d^2 - z^2)^{\frac{1}{2}}}\right\} \ , \tag{5.47}$$

where B is a constant. Expanding locally near $x = d$ the solution does indeed have the required behaviour (5.41). Further expanding (5.47) for large z gives to leading order

$$\begin{aligned}\psi &\sim -B\Im\left\{-i(z + \overline{z})\right\} \\ &\sim 2Bx\end{aligned}$$

which matches with the required far field behaviour (5.31) with $B = k/4\pi$ meaning the solution to the codimension-two problem is

$$\psi = -\frac{k}{4\pi}\Im\left\{\frac{z^2 + z\overline{z} - 2d^2}{(d^2 - z^2)^{\frac{1}{2}}}\right\} \ . \tag{5.48}$$

5.1.2.3 Determination of the free surface

Substituting (5.48) into (5.33) we obtain

$$h_t \;=\; -\frac{2k}{\pi}\frac{x}{(x^2-d^2)^{\frac{1}{2}}} \quad .$$

Integrating this and applying the initial condition $h = x^2/2$ produces

$$h(x,t) \;=\; \frac{1}{2}x^2 - \frac{2kx}{\pi}\int_0^t \frac{1}{(x^2-d(\tau)^2)^{\frac{1}{2}}}d\tau \quad .$$

5.1.2.4 The law of motion of the free point

The inner region near $x = d(t)$ is of size $O(\epsilon^2)$ compared to the codimension-two length scale. The free point lies in the inner region and thus to leading order we have the further matching condition $h(d) = 0$ which implies

$$\frac{\pi d(t)}{4k} \;=\; \int_0^t \frac{1}{(d(t)^2-d(\tau)^2)^{\frac{1}{2}}}d\tau \quad .$$

This equation is of the same form as that for the water entry problem when the body shape is $f(x) = \pi x^2/4k$. Thus from (2.25) the solution is

$$d(t) \;=\; 2\sqrt{\frac{2kt}{\pi}} \quad .$$

Substituting this back into the equation for h we find

$$h(x,t) \;=\; \frac{x}{2}\left(x^2 - \frac{8kt}{\pi}\right)^{\frac{1}{2}} \quad .$$

Figure 5.2 shows plots of this free surface shape at increasing times for $k = 1/8$.

As with the water entry problem we again note that although we can formally reverse the direction of time in all the results as a means of producing a solution to the suction problem it is an ill-posed process for the same reasons as given in Section 2.3.3. That is the solution relies upon the fact that $d(t)$ is an increasing function in order to apply the matching condition $h(d(t)) = 0$. For the suction problem $d(t)$ is a decreasing function and as shown diagrammatically in Section 2.3.3 we can no longer apply the final condition $h(d(t)) = 0$.

For completeness we note that we could have continued on to solve an inner problem in which the free boundary would be a parabola.

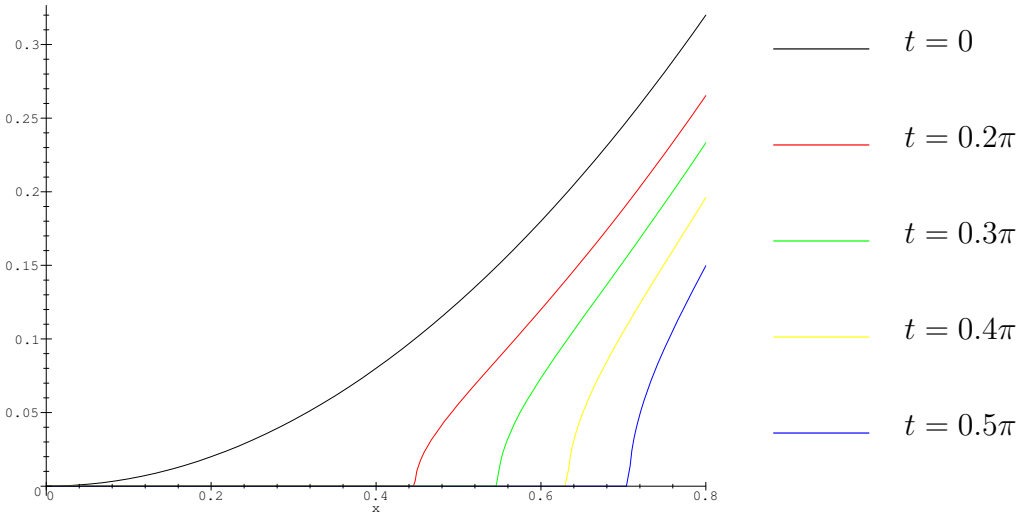

Figure 5.2: The free surface shape for the injection problem.

5.2 Stokes flow with non-zero surface tension

We now turn our attention to the problem of sintering due to surface tension which, as we mentioned at the beginning of the chapter, was really the problem we were most interested in.

5.2.1 The full problem

The equations for the full problem are almost the same as those of the injection problem. The main difference is the inclusion of a surface tension/curvature term in the free boundary stress conditions to drive the flow instead of a singularity at the centre of each disc. Thus the field equation is the same as (5.4), namely

$$\nabla^4 \psi \;=\; 0 \;.$$

The free boundary stress conditions (5.8) and (5.9) become

$$\begin{aligned} (\sigma \mathbf{n}) \cdot \mathbf{n} &= -\kappa \\ (\sigma \mathbf{n}) \cdot \mathbf{t} &= 0 \end{aligned}$$

where κ is the curvature of the free boundary. Note the equations have been non-dimensionalised to remove the explicit appearance of the magnitude of the surface tension. As before we can eliminate between these two conditions and differentiate along the boundary to obtain equations similar to (5.10) and (5.11)

$$3\psi_{xxy} + \psi_{yyy} \;=\; 2h_x(\psi_{xxx} - \psi_{xyy}) - h_{xx}(\psi_{yy} - \psi_{xx}) + h_x^2(\psi_{xxy} - \psi_{yyy}) \qquad (5.49)$$

$$
\begin{aligned}
& & & + \frac{h_{xxx}}{(1+h_x^2)^{\frac{3}{2}}} - \frac{3h_{xx}^2 h_x}{(1+h_x^2)^{\frac{5}{2}}} && \text{on} \quad y = h(x,t) \\
(\psi_{yy} - \psi_{xx})h_{xx} &=& h_x(\psi_{xyy} - \psi_{xxx}) - 2h_x^2(\psi_{xxy} - \psi_{yyy}) - h_x^3(\psi_{xxx} + 3\psi_{xyy}) & \qquad (5.50) \\
& & & - \frac{h_{xxx}h_x^2}{(1+h_x^2)^{\frac{3}{2}}} + \frac{3h_{xx}^2 h_x^3}{(1+h_x^2)^{\frac{5}{2}}} && \text{on} \quad y = h(x,t) \quad .
\end{aligned}
$$

Along the contact region we again have conditions of symmetry

$$
\begin{aligned}
\psi_{yy} &= 0 \\
\psi &= 0 \quad .
\end{aligned}
$$

The final boundary condition is the kinematic condition

$$
h_t + \psi_x + h_x\psi_y = 0 \qquad \text{on} \quad y = h(x,t) \quad .
$$

5.2.2 The codimension-two problem

Unlike the case of injection we do not solve an outer problem from which we can determine the appropriate scalings for the codimension-two variables. This is because it is the inner region that is driving the flow and hence information flows out of the inner region into the codimension-two region. Thus the precise scalings and necessary matching conditions will come from the inner region problem to be considered next.

As with the previous problem the codimension-two solution will only be valid for small times over which the order of the length of the contact set will be $\epsilon \ll 1$. Thus we scale x and y to be $O(\epsilon)$. The free boundary initially has the local form $y = \alpha x^2$ and thus we scale the free boundary shape h to be $O(\epsilon^2)$. Since we do not know the size of the stream function ψ in the codimension-two region we shall try a scaling of the order ϵ^{3-p}, where p is to be determined. The kinematic condition then requires that we scale time to be $O(\epsilon^p)$. Summarising, the scaling will be

$$
x = \epsilon\hat{x} \quad , \quad y = \epsilon\hat{y} \quad , \quad h = \epsilon^2\hat{h}
$$

$$
\psi = \epsilon^{3-p}\hat{\psi} \quad , \quad t = \epsilon^p\hat{t} \quad .
$$

and the position of the free points in the scaled variables will be $\hat{x} = \pm d(t)$.

Substituting these scalings into the full problem above and expanding $\hat{\psi}$ as a regular asymptotic expansion in powers of ϵ we obtain, on dropping the hats, the same leading order model as for the previous injection problem, that is equations

(5.32)–(5.37), (5.39) and (5.40). We know the appropriate solution to this which exhibits the minimum singularity behaviour (5.41) is of the form (5.47), namely

$$\psi \;=\; B(t)\Re\left\{\frac{z^2+z\overline{z}-2d^2}{(z^2-d^2)^{\frac{1}{2}}}\right\} \quad . \tag{5.51}$$

However, unlike in the injection case we do not yet have a matching condition from which to determine $B(t)$. Despite this we can still apply the kinematic boundary condition to yield

$$h \;=\; \alpha x^2 - 2\int_0^t \frac{xB(\tau)}{(x^2-d(\tau)^2)^{\frac{1}{2}}}d\tau \quad . \tag{5.52}$$

Furthermore we require that $h=0$ at $x=d$ from which we obtain the relationship

$$\alpha d(t) \;=\; 2\int_0^t \frac{B(\tau)}{(d(t)^2-d(\tau)^2)^{\frac{1}{2}}}d\tau \tag{5.53}$$

between B and d. Thus if we know either B or d we can invert the integral equation to obtain the other. To invert to find $B(t)$ we make the usual substitutions $\eta = d(t)^2$ and $w = d(\tau)^2$ to transform the integral into a convolution form. We can then apply a Laplace transform, rearrange and invert to obtain

$$B(t) \;=\; \frac{\alpha}{2}\dot{d}(t)d(t) \quad . \tag{5.54}$$

5.2.3 The inner region

Near to the turnover point the curvature of the free boundary will be large. The large curvature will mean the surface tension term in the surface stress boundary conditions can no longer be neglected. The resulting problem should consist of the full equations with the only simplification being the shape of the free boundary. To preserve the full problem on some local length scale about $x=\epsilon d(t)$ we take the following scalings

$$x = \epsilon d(t) + \epsilon^q \tilde{x} \quad , \quad y = \epsilon^q \tilde{y} \quad , \quad h = \epsilon^q \tilde{h}$$

$$\psi = \epsilon^{1-p}\dot{d}\epsilon^q\tilde{y} + \epsilon^q\tilde{\psi} \quad , \quad t = \epsilon^p t_1 + \epsilon^q \tilde{t}$$

where q is to be determined. Also we require $q>1$ and $q>p$ so that this inner problem is local in space and time compared to the codimension-two problem and not just local in space and time compared to the full problem. We expect the inner free surface shape to be a parabola since the local form of h from (5.52) is parabolic.

Fortunately the problem of Stokes Flow exterior to a parabola driven purely by surface tension effects has been considered by Hopper [34]. The Hopper solution for

the components of the velocity ([34] equation (4.6)) when written for a parabolic free boundary given by

$$\tilde{y} = \sqrt{2R(t)\tilde{x}}$$

is

$$\begin{aligned}\tilde{v} - i\tilde{u} &= \frac{i}{2\pi}(\zeta^2+1)^{-\frac{1}{2}}(\zeta+i)\left(\sinh^{-1}\zeta - \frac{i\pi}{2}\right) \\ &\quad + \frac{i}{2\pi}\left\{(\zeta^2+1)^{-\frac{1}{2}}\left[(\zeta-i) + \frac{2\eta(\xi-i)}{\zeta^2+1}\right]\left(\sinh^{-1}\zeta - \frac{i\pi}{2}\right)\right\}^* \\ &\quad + \frac{1}{\pi}\frac{\eta(\xi+i)}{(\zeta^2+1)^*} + \frac{\dot{R}}{2}\left[\xi + \frac{i\eta(\xi+i)}{\zeta^* - i}\right] \end{aligned} \tag{5.55}$$

where

$$\zeta = \left(\frac{2\tilde{z}}{R} - 1\right)^{\frac{1}{2}} - i \tag{5.56}$$

$$\tilde{z} = \tilde{x} + i\tilde{y} \tag{5.57}$$

and * denotes complex conjugation. We should note that because we have obtained the problem considered by Hopper as a local in space and time model we require $\dot{R} = 0$. In order to match this solution to the codimension-two solution we must expand it for large $\tilde{z}$. To do this we first write $\tilde{z}$ as $\tilde{r}e^{i\theta}$, substitute $\tilde{z}$ into the equation for ζ, then substitute ζ into (5.55) and then finally expand asymptotically for large $\tilde{r}$. Doing this we find

$$\begin{aligned}\tilde{v} - i\tilde{u} &\sim \frac{1}{4\pi}\left[\sin 2\theta - i\left(\cos 2\theta - 1 - 2\log\left(\frac{8\tilde{r}}{R}\right)\right)\right] \\ &\quad + \frac{1}{8\pi}\left[-\left(5\cos\frac{\theta}{2} - \cos\frac{5\theta}{2}\right) - i\left(\sin\frac{\theta}{2} - \sin\frac{5\theta}{2}\right)\right]\sqrt{\frac{R}{2\tilde{r}}}\log\left(\frac{8\tilde{r}}{R}\right) + \dots \end{aligned} \tag{5.58}$$

5.2.4 Matching difficulties

In order to match (5.58) to the solution in the codimension-two region we must write it in codimension-two variables. If we denote the radial distance from the free point $d(t)$ in the codimension-two region by r then it is related to $\tilde{r}$ by the formula $r = \epsilon^{q-1}\tilde{r}$. Equations (5.58) becomes

$$\begin{aligned}\tilde{v} - i\tilde{u} &\sim \frac{1}{4\pi}\left[\sin 2\theta - i\left(\cos 2\theta - 1 + 2(q-1)\log\epsilon - 2\log\left(\frac{8r}{R}\right)\right)\right] \\ &\quad - \frac{1}{8\pi}\left[-\left(5\cos\frac{\theta}{2} - \cos\frac{5\theta}{2}\right) - i\left(\sin\frac{\theta}{2} - \sin\frac{5\theta}{2}\right)\right]\sqrt{\frac{\epsilon^{q-1}R}{2r}}(q-1)\log\epsilon \\ &\quad + \dots \ . \end{aligned}$$

We now take the curl of our one term codimension-two solution (5.51), expand it in terms of the inner radial distance $\tilde{r}$ to one term and then rewrite it in terms of the codimension-two radial distance r giving

$$v - iu \;\sim\; \frac{B(t)}{2}\sqrt{\frac{d(t)}{2}}\left[-\left(5\cos\frac{\theta}{2} - \cos\frac{5\theta}{2}\right) - i\left(\sin\frac{\theta}{2} - \sin\frac{5\theta}{2}\right)\right]\frac{1}{\sqrt{r}}\epsilon^{2-p} \quad .$$

One final thing we should note is that the velocity in the Hopper region is measured relative to the moving frame. Thus to match we must consider the relationship

$$v - iu \;=\; -i\epsilon^{1-p}\dot{d} + \tilde{v} - i\tilde{u} \quad . \tag{5.59}$$

Comparing the two sides of this formula we see they cannot yet match. However it is clear to see that the solution we have so far in the codimension-two region will match with the second term from the Hopper solution provided we adjust our codimension-two scalings to allow for the log term. The additional term due to the moving frame should also match with the term $\log\epsilon$.

Since we have not matched the leading order term from the Hopper solution we deduce that we have an incorrect leading-order solution of the codimension-two problem and have instead found the next order solution. However, observing

$$\left(-\frac{\partial}{\partial x} - i\frac{\partial}{\partial y}\right)(-y\log r^2) \;=\; \sin 2\theta - i\left(\cos 2\theta - 1 - 2\log r\right) \quad ,$$

we can deduce that the leading order solution for ψ in the codimension-two region should for small r be of the form

$$-\frac{1}{4\pi}\epsilon y \log\left[\left(\frac{8}{R}\right)^2\left((x-d)^2 + y^2\right)\right] \quad . \tag{5.60}$$

5.2.5 Reassessment of the codimension-two region

Firstly we see that the term $-\epsilon^{1-p}\dot{d}$, due to the moving frame, must match with the term $\log\epsilon$ from the Hopper solution. For this to happen we require $p = 1$ and an additional factor of $-1/\log\epsilon$ in the codimension-two time scaling. Having adjusted the time scaling in order to preserve the codimension two problem that we have so far solved we must include the factor $-\log\epsilon$ in the codimension-two scaling of the stream function. Lastly if the solution we have so far is to match to the second term from the Hopper solution we will require $\epsilon\log\epsilon = \epsilon^{(q-1)/2}\log\epsilon$ which implies $q = 3$. Summarising the new codimension-two scalings will be

$$x = \epsilon\hat{x} \quad , \quad y = \epsilon\hat{y} \quad , \quad h = \epsilon^2\hat{h} \quad , \quad t = -\frac{\epsilon}{\log\epsilon}\hat{t}$$

and we shall seek a two term expansion for ψ of the form

$$\psi \;=\; \epsilon\psi_0 - \epsilon^2 \log\epsilon\psi_1 + O(\epsilon^2)$$

where we expect the solution for ψ_0 and ψ_1 to be related to (5.60) and (5.51), respectively.

Substituting these new scalings into the full problem we obtain the following two models for ψ_0 and ψ_1

$$\begin{aligned}
\nabla^4\psi_0 &= 0 \qquad \text{in} \quad y>0 \\
\psi_{0yy} &= 0 \qquad \text{on} \quad y=0 \\
3\psi_{0xxy}+\psi_{0yyy} &= 0 \qquad \text{on} \quad |x|>d \quad , \quad y=0 \\
\psi_0 &= 0 \qquad \text{on} \quad |x|<d \quad , \quad y=0
\end{aligned}$$

$$\begin{aligned}
\nabla^4\psi_1 &= 0 \qquad \text{in} \quad y>0 \\
h_t+\psi_{1x} &= 0 \qquad \text{on} \quad |x|>d \quad , \quad y=0 \\
3\psi_{1xxy}+\psi_{1yyy} &= 0 \qquad \text{on} \quad |x|>d \quad , \quad y=0 \\
\psi_{1yy}-\psi_{1xx} &= 0 \qquad \text{on} \quad |x|>d \quad , \quad y=0 \\
\psi_{1yy} &= 0 \qquad \text{on} \quad |x|<d \quad , \quad y=0 \\
\psi_1 &= 0 \qquad \text{on} \quad |x|<d \quad , \quad y=0 \quad .
\end{aligned}$$

The leading-order model shows that ψ_0 does not affect the free surface shape. It should also be noted that non-homogeneous terms and the surface tension/curvature term only begin to feed back into the second order problem for ψ_2 which we shall not be concerning ourselves with. The first-order problem is the same as our previous model and so can have the same solution. The expression (5.60) satisfies the leading order model and should match to the required behaviour near $x=d(t)$. However, the solution for ψ_0 needs to exhibit a similar behaviour near $x=-d(t)$. Hence the appropriate solutions to the leading and first order models are

$$\begin{aligned}
\psi_0 &= -\frac{1}{4\pi}y\log\left[\left(\frac{8}{R}\right)^2\left((x-d)^2+y^2\right)\right]+\frac{1}{4\pi}y\log\left[\left(\frac{8}{R}\right)^2\left((x+d)^2+y^2\right)\right] \\
&= -\frac{1}{4\pi}y\log\left[\frac{(x-d)^2+y^2}{(x+d)^2+y^2}\right] \qquad (5.61) \\
\psi_1 &= B(t)\Re\left\{\frac{z^2+z\overline{z}-2d^2}{(z^2-d^2)^{\frac{1}{2}}}\right\} \quad . \qquad (5.62)
\end{aligned}$$

Taking the curl of this expression for ψ yields the components of velocity which we can expand in inner variables and then rewrite in codimension-two variables to obtain

$$\begin{aligned} v - iu &\sim \frac{1}{4\pi}\left[\sin 2\theta - i\left(\cos 2\theta - 1 - 2\log\left(\frac{8r}{R}\right) + 2\log\left(\frac{16d}{R}\right)\right)\right] \\ &\quad - \frac{B(t)}{2}\sqrt{\frac{d(t)}{2}}\left[-\left(5\cos\frac{\theta}{2} - \cos\frac{5\theta}{2}\right) - i\left(\sin\frac{\theta}{2} - \sin\frac{5\theta}{2}\right)\right]\frac{1}{\sqrt{r}}\epsilon\log\epsilon \quad . \end{aligned} \tag{5.63}$$

5.2.6 Matching revisited

With the new scalings the matching equation (5.59) becomes

$$v - iu = i(\log\epsilon)\dot{d}(t) + \tilde{v} - i\tilde{u} \quad .$$

Substituting (5.58) and (5.63) in to the above relationship and matching to one term (using the modified matching rule for logs discussed in Chapter 1) we find d must satisfy

$$\dot{d}(t) = \frac{1}{\pi} + \frac{1}{\pi\log\epsilon}\log\left(\sqrt{\frac{R}{16d}}\right) \quad .$$

Expanding d in the form

$$d \sim d_0 + \frac{1}{\log\epsilon}d_1 + \ldots \quad .$$

Then to leading order the solution to the above equation is

$$d_0(t) = \frac{t}{\pi} \quad .$$

Having obtained an expression for d we can now substitute it into (5.54) yielding

$$B(t) = \frac{\alpha}{2}\dot{d}d = \frac{\alpha t}{2\pi^2} \quad .$$

Finally matching the second terms we find

$$R(t) = 4\pi^2 B(t)^2 d(t) = \alpha^2 d(t)^3 \quad .$$

Substituting $B(t)$ and $d(t)$ back into (5.52) we find

$$h(x,t) = \alpha x\left(x^2 - d(t)^2\right)^{\frac{1}{2}} \quad .$$

As a check on the matching we can now show that the free boundaries also match, as they must. Figure 5.3 shows plots of h at increasing times (for $\alpha = 1$).

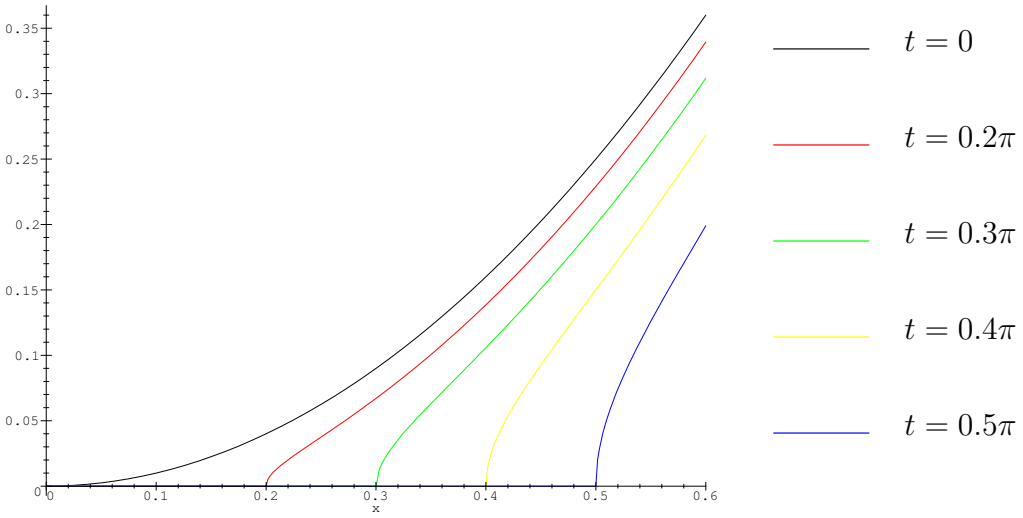

Figure 5.3: The free surface shape for the sintering problem.

5.2.7 Minimising the effort and maximising the results

Requiring to know the solution to the inner problem is undesirable since the inner problem is somewhat complex (and thus we were fortunate Hopper had already done it). For some other problems we may not even be able to solve the inner problem exactly. Thus we would like to be able to obtain as much information as is needed from the inner problem without actually solving it. One way to do this is to consider the far field behaviour of the inner problem and use that to match with.

Now the single cusp problem in Appendix C is essentially what we need give or take a few small changes to the reasoning. In Appendix C we are trying to model the force due to surface tension at a cusp by inserting a delta function behaviour at the origin where the reasoning for such a term comes from considering the force over the tip in the limit as we approach the tip. In this case we wish to determine the appropriate singularity to put in the far field problem (at the origin) to model the force from the inner parabolic boundary. The force in the x direction due to surface tension on a surface $x = g(y)$ is given by

$$\begin{aligned} F_x &= \int_{\text{tip}} -\kappa dy \\ &= \left[\frac{g_y}{\sqrt{1+g_y^2}} \right]_{\text{tip}} . \end{aligned}$$

In our case the equation of the tip boundary is $g(y) = 1/R(t)y^2$ and thus

$$\frac{g_y}{\sqrt{1+g_y^2}} = \frac{2y}{\sqrt{R^2+4y^2}} .$$

In the far field as $y \to \infty$ this gives $+1$ for $y > 0$ and -1 for $y < 0$ where the negative square root was correctly chosen in the $y < 0$ case. Thus the integral over the tip as seen in the far field is simply a point force of magnitude 2 in the x direction, that is it is the same as the result for the cusp problem in Appendix C. Thus our far field problem is the same as the problem generated in Appendix C when we looked locally near the cusp.

The cusp problem was obtained by scaling $\mathbf{x}$ and ψ to be $O(\hat{\epsilon})$. If this is to be a far field problem for the inner region then $\epsilon^3 \ll \hat{\epsilon} \ll \epsilon$. We can deduce the inner problem is on a length scale $O(\epsilon^3)$ by several means. One is that the asymptotic expansion for ψ from the codimension-two solution appears to break down when the codimension-two $\mathbf{x}$ is $O(\epsilon^2)$. Another approach is to consider the asymptotic behaviour of the codimension-two free boundary near $x = d$. Putting $x = d + \delta\hat{x}$ and $y = \delta\hat{y}$, where $\delta \ll 1$, into the codimension-two kinematic condition gives

$$\delta h_t - \dot{d} h_{\hat{x}} + \psi_{\hat{x}} \;=\; 0 \;\; .$$

Thus to leading order locally

$$\begin{aligned} h \;&\sim\; \frac{1}{\dot{d}} \psi|_{\hat{y}=0} \\ &=\; \frac{2B(t)}{\dot{d}(t)} \sqrt{2d(t)\hat{x}} \;\; . \end{aligned}$$

Since the codimension-two boundary is $y = \epsilon h(x)$ the inner problem must be on a length scale $O(\epsilon^2)$ relative to the codimension-two region so that the free boundary is non-trivial to leading order, i.e. need both sides of $O(\delta\hat{y}) = O(\epsilon\sqrt{\delta\hat{x}})$ to balance which implies $\delta = \epsilon^2$.

The cusp solution (C.8) is

$$\psi \;=\; -\frac{1}{4\pi} \hat{y} \log(\hat{x}^2 + \hat{y}^2) \;\; .$$

However it is also possible to add to this a term of the form $C(t)\hat{y}$ giving a general solution of the form

$$\psi \;=\; -\frac{1}{4\pi} \hat{y} \log \hat{A}(t)(\hat{x}^2 + \hat{y}^2) \;\; .$$

Since the inner problem is independent of any small parameters its far field solution when written in inner coordinates should also be independent of any small parameters. Hence the order of $\hat{A}$ should be such that when written in inner coordinates the far field solution is

$$\psi \;=\; -\frac{1}{4\pi} \tilde{y} \log A(t)(\tilde{x}^2 + \tilde{y}^2) \;\; .$$

Evaluating the horizontal velocity component due to this flow and expanding in codimension-two variables we obtain

$$u \sim \frac{1}{\pi}\log\epsilon \ .$$

As previously discussed when matching in Section 5.2.4 this leading-order behaviour from the inner region must balance the $\dot{d}$ term which occurs because the cusp solution is in a moving frame. In this way we again deduce that the time scaling for the problem should have been $-\epsilon/\log\epsilon$ and that $\dot{d} = 1/\pi$. From this point all the remaining codimension-two scalings can be deduced as in Section 5.2.4. With all this information the complete codimension-two solution can be obtained. The unknown $A(t)$ does not occur explicitly in the codimension-two solution for ψ_0 as might be expected since ψ_0 takes the form

$$\begin{aligned}\psi_0 &= -\frac{1}{4\pi}y\log A(t)\left((x-d)^2+y^2\right)+\frac{1}{4\pi}y\log A(t)\left((x+d)^2+y^2\right)\\ &= -\frac{1}{4\pi}y\log\left[\frac{(x-d)^2+y^2}{(x+d)^2+y^2}\right] \ .\end{aligned}$$

Comparing this with (5.61) we see A should be related to R (which in turn is related to d). Hence it is not surprising that we cannot deduce this without considering the full inner problem in which R is defined. However as noted not knowing $A(t)$ has not affected the codimension-two solution. Being able to obtain so much of the solution without solving the full inner problem is an important result.

5.2.8 Extension to different initial free boundary shapes

In the above analysis the initial free boundary shape was of the form $y = \alpha x^2$. If we now consider the general case of $y = \alpha|x|^n$, $n \in \mathbb{N}$, can we still formulate a codimension-two problem which we can solve by matching in to an inner region of a Hopper type? With this general initial free boundary shape we find the new scalings for the codimension-two region become

$$x = \epsilon\hat{x} \quad , \quad y = \epsilon\hat{y} \quad , \quad h = \epsilon^n\hat{h} \quad , \quad t = -\frac{\epsilon}{\log\epsilon}\hat{t}$$

and we shall seek a two term expansion for ψ of the form

$$\psi = \epsilon\psi_0 - \epsilon^n\log\epsilon\psi_1 + \ldots \ .$$

The actual codimension-two problem remains the same.

The scalings for the inner Hopper region take the same form as before, namely

$$x = \epsilon d(t) + \epsilon^q \tilde{x} \quad , \quad y = \epsilon^q \tilde{y} \quad , \quad h = \epsilon^q \tilde{h}$$
$$\psi = -\log \epsilon \dot{d} \epsilon^q \tilde{y} + \epsilon^q \tilde{\psi} \quad , \quad t = -\frac{\epsilon}{\log \epsilon} t_1 + \epsilon^q \tilde{t}$$

but now $q = 2n - 1$.

Matching the velocities as before the leading order match again determines $d(t)$ giving

$$\dot{d}(t) \;=\; \frac{q-1}{2\pi}$$

and hence

$$d(t) \;=\; \frac{q-1}{2\pi} t \ .$$

From this we see that the effect on the velocity of the free point is only to multiply it by a scalar rather than to change its dependence on t.

Having obtained $d(t)$ we can again invert (5.52) to determine

$$B(t) \;=\; \frac{\alpha}{2} \left(\frac{q-1}{2\pi} \right)^n \frac{t^{(n-1)}}{I}$$

where

$$I \;=\; \begin{cases} \dfrac{(n-2)!!}{(n-1)!!} & n \text{ even} \\ \dfrac{\pi}{2} \dfrac{(n-2)!!}{(n-1)!!} & n \text{ odd} \end{cases}$$

(!! is defined as $k!! = k(k-2)(k-4)...2$ for k even and $k!! = k(k-2)(k-4)...1$ for k odd).

We then complete the matching for the second terms to obtain

$$R(t) \;=\; \frac{16}{(q-1)^2} B(t)^2 d(t) \ .$$

As an example, when $n = 3$ the formulae become

$$d(t) \;=\; \frac{2t}{\pi}$$
$$B(t) \;=\; \frac{16\alpha t^2}{\pi^4} \;=\; \frac{4\alpha}{\pi^2} d(t)^2$$
$$R(t) \;=\; \frac{512\alpha^2 t^5}{\pi^7} \;=\; \frac{16\alpha^2}{\pi^2} d(t)^5$$

and the free boundary shape is

$$h(x,t) \;=\; \alpha |x|^3 - \frac{2\alpha}{\pi} x^3 \sin^{-1}\left(\frac{2t}{\pi x} \right) + \frac{2\alpha}{\pi^3} |x| t \left(\pi^2 x^2 - 4t^2 \right)^{\frac{1}{2}} \ .$$

Figure 5.4 shows plots of h at increasing times (for $\alpha = 1$).

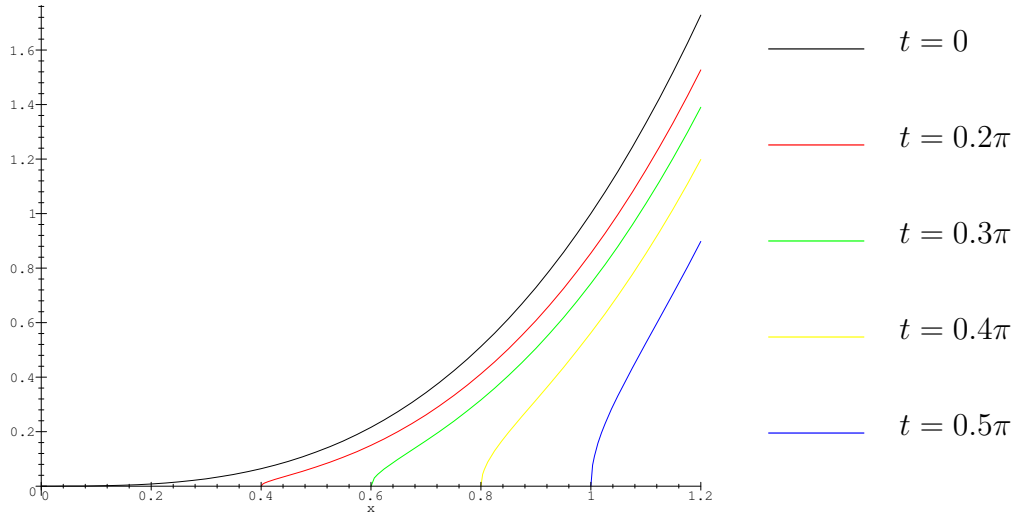

Figure 5.4: The free surface shape for the sintering problem with initial shape $|x|^3$.

5.3 Ice Closure

We shall consider the problem of the closure of a thin channel lying at an ice-till interface as shown in Figure 5.5.

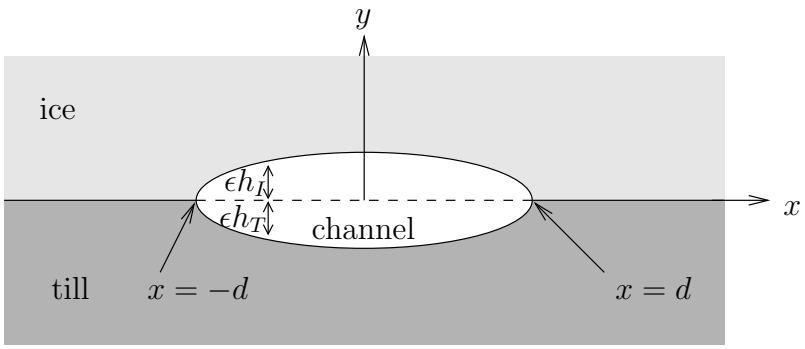

Figure 5.5: The geometry of the ice closure problem.

Water flows through the channel at a pressure different to the ice overburden pressure and far field till pressure. The difference between the pressure at infinity and the pressure in the channel is positive and thus the channel will close as the ice deforms. The wet till may also creep changing the shape of the channel floor. A model of this problem has been solved by Ng [63] using a complex variable method. In this section we will consider the same model but present a much more concise solution by exploiting the fact that the domain of the model is a half-space or two half-spaces.

5.3.1 Rigid impermeable bed

We begin by assuming the bed is rigid and impermeable with boundary $y = 0$. The ice is assumed to have a constant density ρ_I, to be incompressible and to satisfy the Stokes flow equations. The body force per unit area is due to gravity and hence the slow flow equations take the form

$$\begin{aligned} \nabla \cdot \mathbf{u} &= 0 \\ -\nabla(p + \rho_I g y) + \mu_I \nabla^2 \mathbf{u} &= 0 \end{aligned}$$

in the ice, where μ_I is the ice viscosity. For convenience the channel is assumed to be symmetrical about $x = 0$. Inside the channel the water exerts a pressure on the ice but no significant shear stress. For convenience we will consider the simplest case when this pressure is a constant. Where the ice is in contact with the till bed we will assume a no slip condition. A more complicated sliding law boundary condition could be considered. We nondimensionalise x and y with L the typical length scale of the channel width, the velocities with a typical velocity scale U and the pressure with $\mu_i U/L$. Such a nondimensionalisation gives rise to the parameter $S_t = \rho_I g L^2/\mu_I U$ which is known as the Stokes number. The pressure from the channel will be denoted by p_c, the pressure at infinity by p_∞ and the difference by $N = p_\infty - p_c$. Since the channel is much wider than it is high we have the typical codimension-two geometry which on linearising gives the problem shown in Figure 5.6.

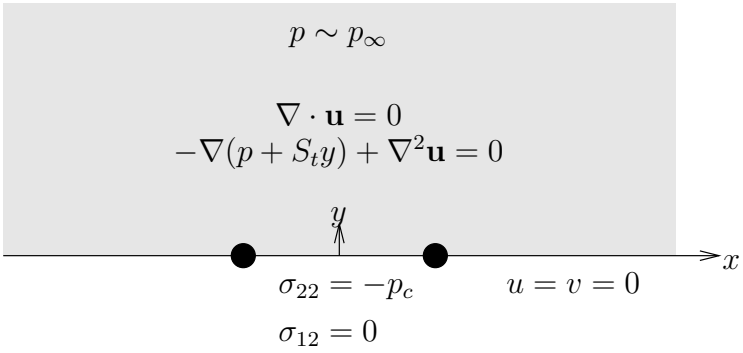

Figure 5.6: The codimension-two ice closure problem.

By defining $p^* = p + S_t y$ we can absorb the body force term into a modified pressure. The analysis at the beginning of the chapter then holds for formulating the problem in terms of complex potentials. The equations then become

$$\begin{aligned} u + iv &= \phi(z) - z\overline{\phi'(z)} - \overline{\chi'(z)} \\ \sigma_{11} + \sigma_{22} &= 4\left(\Phi(z) + \overline{\Phi(z)}\right) - S_t i(z - \overline{z}) \end{aligned}$$

$$i(\sigma_{22}-\sigma_{11})-2\sigma_{12} \;=\; 4i\left[(\overline{z}-z)\overline{\Phi'(z)}+\Phi(z)-\overline{\Phi}(z)\right]$$

from which we obtain

$$\begin{aligned} u_x+iv_x &= (\overline{z}-z)\Phi'(z)+\Phi(z)+\Phi(\overline{z}) \\ \sigma_{22}-i\sigma_{12} &= 2\left[(\overline{z}-z)\overline{\Phi'(z)}+\Phi(z)-\Phi(\overline{z})\right]+S_t i(z-\overline{z}) \ . \end{aligned}$$

On the boundary $y=0$ for $x\in(-d,d)$ we have $\sigma_{22}=-p_c$ and $\sigma_{12}=0$ and for $x\notin(-d,d)$ $u=v=0$. Hence the Riemann problem is

$$\begin{aligned} \Phi^+(x)-\Phi^-(x) &= -\frac{p_c}{2} \qquad \text{for} \quad |x|<d \\ \Phi^+(x)+\Phi^-(x) &= 0 \qquad \text{for} \quad |x|>d \ . \end{aligned}$$

Since the channel width is fixed for the no slip case we expect the solution to be unbounded at the end points. The solution which is unbounded at the end points is

$$\Phi \;=\; -\frac{1}{(z^2-d^2)^{\frac{1}{2}}}\left[\frac{p_c}{4\pi i}\int_{-d}^{d}\frac{(\tau^2-d^2)^{\frac{1}{2}}}{\tau-z}d\tau+\frac{p_\infty z}{4}\right]$$

and has index 1. On $y=0$ for $x\in(-d,d)$ this gives

$$u_x+iv_x \;=\; -\frac{Nx}{4(x^2-d^2)^{\frac{1}{2}}}$$

which implies

$$\begin{aligned} u &= 0 \\ v &= -\frac{N}{2}(d^2-x^2)^{\frac{1}{2}} \ . \end{aligned}$$

On $y=0$ for $x\notin(-d,d)$ this gives

$$\sigma_{22}-i\sigma_{12} \;=\; p_c-\frac{N|x|}{(x^2-d^2)^{\frac{1}{2}}}$$

which implies

$$\begin{aligned} \sigma_{12} &= 0 \\ \sigma_{22} &= p_c-\frac{N|x|}{(x^2-d^2)^{\frac{1}{2}}} \ . \end{aligned}$$

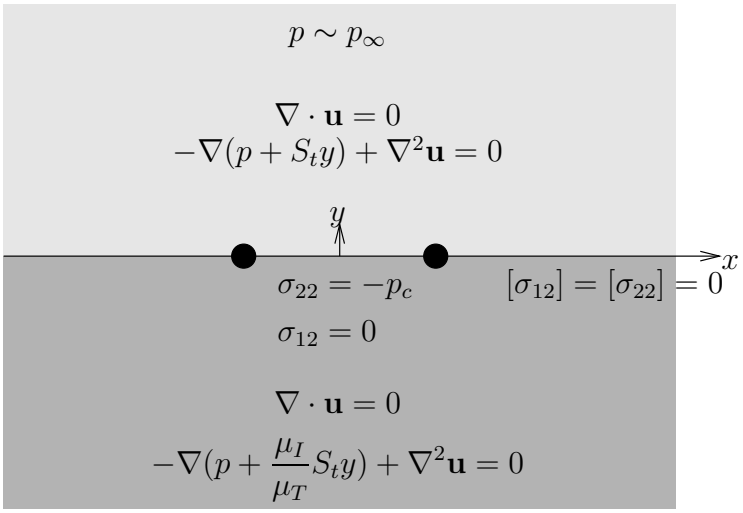

Figure 5.7: The codimension-two ice and till closure problem.

5.3.2 Inclusion of sediment creep

We will now consider the problem when the till bed is no longer rigid but also undergoes a slow flow. We will only consider the case when the till depth is large compared to the channel width and hence can be considered as infinite. On linearising the codimension-two problem is as shown in Figure 5.7.

If we denote the unknown velocities on $y = 0$, $x \notin (-d, d)$ by u_b and v_b then we can formulate two Riemann problems, one for the solution in the ice and one in the till. For the ice the Riemann problem is

$$\begin{aligned} \Phi_I^+(x) - \Phi_I^-(x) &= -\frac{p_c}{2} \qquad \text{for} \quad |x| < d \\ \Phi_I^+(x) + \Phi_I^-(x) &= {u_b}' + i{v_b}' \qquad \text{for} \quad |x| > d \end{aligned}$$

which has solution

$$\begin{aligned} \Phi_I &= -\frac{1}{(z^2 - d^2)^{\frac{1}{2}}} \left[\frac{p_c}{4\pi i} \int_{-d}^{d} \frac{(\tau^2 - d^2)^{\frac{1}{2}}}{\tau - z} d\tau + \frac{p_\infty z}{4} \right. \\ &\quad \left. -\frac{1}{2\pi i} \left(\int_{-\infty}^{-d} + \int_{d}^{\infty} \right) \frac{({u_b}' + i{v_b}')(\tau^2 - d^2)^{\frac{1}{2}}}{\tau - z} d\tau \right] . \end{aligned}$$

Similarly solving the problem for the till we find

$$\begin{aligned} \Phi_T &= -\frac{1}{(\overline{z}^2 - d^2)^{\frac{1}{2}}} \left[\frac{p_c}{4\pi i} \int_{-d}^{d} \frac{(\tau^2 - d^2)^{\frac{1}{2}}}{\tau - \overline{z}} d\tau + \frac{p_\infty \overline{z}}{4} \right. \\ &\quad \left. -\frac{\mu_T}{2\pi \mu_I i} \left(\int_{-\infty}^{-d} + \int_{d}^{\infty} \right) \frac{({u_b}' + i{v_b}')(\tau^2 - d^2)^{\frac{1}{2}}}{\tau - \overline{z}} d\tau \right] . \end{aligned}$$

Asserting that the stress components σ_{12} and σ_{22} are continuous on $y = 0$, $x \notin (-d, d)$ gives the condition

$$\left(\int_{-\infty}^{-d} + \int_{d}^{\infty}\right) \frac{(u_b{}' + iv_b{}')(\tau^2 - d^2)^{\frac{1}{2}}}{\tau - x} d\tau \;=\; 0 \qquad \forall\, x \notin (-d, d) \;\; .$$

For this to hold we require $u_b{}' = v_b{}' = 0$.

We can now evaluate the velocity and stress components on the relevant part of the boundary as before. We obtain

$$\begin{aligned} u_I &= u_T = 0 \qquad \text{for } x \in (-d, d) \\ v_I &= -\frac{N}{2}(d^2 - x^2)^{\frac{1}{2}} \qquad \text{for } x \in (-d, d) \\ v_T &= \frac{N\mu_I}{2\mu_T}(d^2 - x^2)^{\frac{1}{2}} \qquad \text{for } x \in (-d, d) \end{aligned}$$

and

$$\begin{aligned} \sigma_{12} &= 0 \qquad \text{for } x \notin (-d, d) \\ \sigma_{22} &= p_c - \frac{N|x|}{(x^2 - d^2)^{\frac{1}{2}}} \qquad \text{for } x \notin (-d, d) \;\; . \end{aligned}$$

We note both the closure velocities and normal stresses in these two problems are of the same form as the type-I crack problem of Section 3.4. In essence the ice closure problems are Stokes flow analogies of type-I crack problems in solid mechanics.

In this chapter by following the flow of information we were able to solve not only the injection problem, in which the main flow of information was from a simple outer problem into the codimension-two region, but also a more difficult problem when the main flow of information was out of an inner region near the codimension-two free point and into the codimension-two region. We further showed how the necessary information from the inner problem could be obtain by considering only the far field of the inner problem which drastically simplified the solution procedure. We were also able to apply the Muskhelishvili solution procedure to an ice flow problem.

In the next chapter we shall pursue the idea of following the flow of information further. We will consider a problem with a sequence of codimension-two regions in which the main information flow is from one outer problem into a codimension-two region and on into the next outer problem. We will then consider a problem in which the field equations in the thin region are non-trivial and see how this affects the solution procedure.

Chapter 6

Hele–Shaw problems

In this chapter we shall discuss several problems that can be modelled as Hele–Shaw flows. We will begin by reviewing the problem of two point injection. The codimension-two solution models the initial behaviour after two discs of fluid which are being injected (or brought together at a constant velocity) in a Hele–Shaw cell first touch. We will show that this problem is really nothing more than the water entry problem.

The second problem we will discuss is the three discs problem. In this problem a half space of fluid, moving at a constant velocity, meets a series of touching stationary discs of fluid lying in a straight line along the direction of motion of the half space. The codimension-two solution models the initial stages after the half space impacts with the first disc. This problem shows clearly how we follow the flow of information through a sequence of codimension-two problems. An exact solution to this type of problem is given by Richardson [76]. It was after initial discussions with Richardson about this problem that Cummings [14] outlined how the solution in the initial stages could be easily derived from a codimension-two formulation. We will go on to show how the codimension-two solution can be generalised to the case of n discs.

The third problem we will consider is the Muskat problem. The Muskat problem is a model for a two-fluid porous medium flow. The problem is equivalent to a two fluid Hele–Shaw problem. This is a notoriously difficult free boundary problem about which almost nothing is known. We shall consider a particular type of Muskat problem in which one of the fluids occupies a long thin region and hence we can apply a codimension-two type analysis. This codimension-two problem will show how we must modify the solution procedure when the solution in the thin region is non-trivial. We shall consider two specific problems, one in which the long thin region of fluid is being forced out by injecting the other fluid from all directions at infinity and the second in which the geometry is similar to that of the first Hele–Shaw cell problem

and the thin region is being forced out due to a uniform flow down from $y = \infty$ and a uniform flow up at $y = -\infty$.

6.1 Point sources in a Hele-Shaw cell

An exact solution to this problem has been done by Richardson [74]. This problem has been considered by Morgan [58](p54–62) in a codimension-two framework and the solution procedure is systematic and straightforward with the main information flow in the problem being from an outer region into the codimension-two region. The geometry of the problem is as shown in Figure 6.1. As with many of these problems the small parameter ϵ is being taken as the order of the length of the contact set relative to a characteristic outer length scale. However, as is often the case ϵ can also be identified with a small time scale.

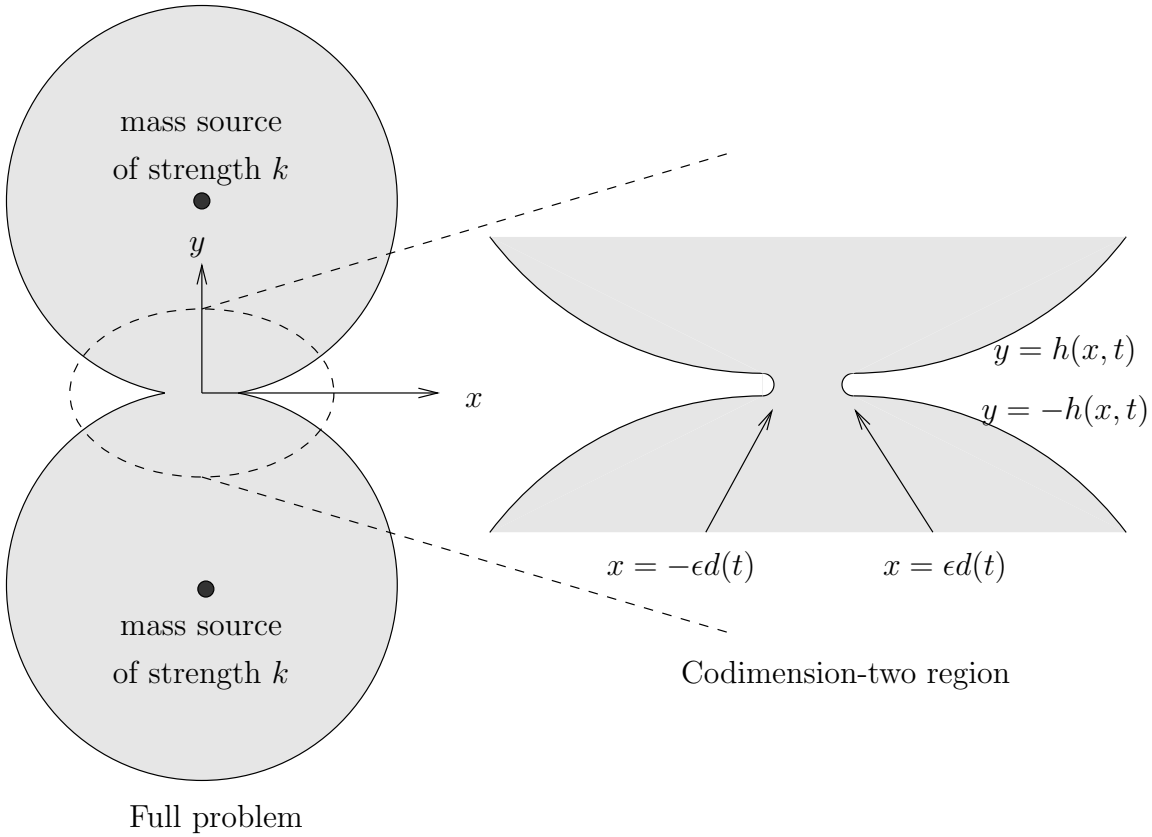

Figure 6.1: The geometry of the two point Hele-Shaw injection problem.

Hele–Shaw flow is governed by the field equations

$$\begin{aligned} \mathbf{u} &= -\nabla p \\ \nabla \cdot \mathbf{u} &= 0 \end{aligned} \tag{6.1}$$

where $\mathbf{u}$ represents the velocity averaged over the cell thickness and p represents the pressure. We can combine these to obtain

$$\nabla^2 p \;=\; 0 \;\;.$$

On a free boundary $y = h(x,t)$ the kinematic condition is

$$h_t \;=\; -p_y + p_x h_x \;\;. \tag{6.2}$$

In the absence of surface tension the stress condition to leading order gives that the pressure is continuous, that is

$$p \;=\; 0 \qquad \text{on} \quad y = h(x,t) \;\;,$$

since in a Hele-Shaw cell if the thickness is $O(\overline{\epsilon})$ then the pressure is $O(\overline{\epsilon}^{-2})$ which is larger than any of the velocity gradients.

The outer problem is that of a point source in a Hele–Shaw cell, that is

$$\begin{aligned}
\nabla^2 p &= 0 \qquad \text{in} \quad x^2 + (y-1)^2 < s(t)^2 \\
p &= 0 \qquad \text{on} \quad x^2 + (y-1)^2 = s(t)^2 \\
p &\sim -\frac{k}{4\pi}\log\left(x^2 + (y-1)^2\right) \qquad \text{as} \quad x^2 + (y-1)^2 \to 0 \\
s\dot{s} &= x p_x + (y-1) p_y \qquad \text{on} \quad x^2 + (y-1)^2 = s(t)^2 \;\;,
\end{aligned}$$

where $s(t)$ is the radius of the disc of fluid at time t. The solution to this is

$$\begin{aligned}
p &= \frac{-k}{4\pi}\log\left(\frac{x^2 + (y-1)^2}{s(t)^2}\right) \\
s(t) &= \left(\frac{kt}{\pi}\right)^{\frac{1}{2}} \;\;.
\end{aligned}$$

Since the contact region is of $O(\epsilon)$ in length, the codimension-two length scalings are $x = \epsilon\hat{x}$ and $y = \epsilon\hat{y}$. The free boundary scaling is $h = \epsilon^2\hat{h}$ because the free boundary will be approximately parabolic for small times after initial contact. The cylinders first touch at $t = \pi/k$ and we expect the codimension-two model to only be valid for small times after this. We therefore scale t as $t = \pi/k + \delta\hat{t}$ where $\delta \ll 1$ Expanding the outer pressure in inner variables gives

$$p \;=\; \frac{k}{2\pi}\epsilon\hat{y}$$

to leading order, which implies the appropriate pressure scaling is $p = \epsilon\hat{p}$. The kinematic condition (6.2) implies that $\delta = \epsilon^2$. Summarising the scalings we have

$$x = \epsilon\hat{x} \quad , \quad y = \epsilon\hat{y} \quad , \quad h = \epsilon^2\hat{h}$$

$$p = \epsilon\hat{p} \quad , \quad t = \frac{\pi}{k} + \epsilon^2\hat{t} \ .$$

Substituting these scalings into the model, expanding $\hat{p}$ and $\hat{h}$ as regular asymptotic expansions and then dropping the hats results in the following leading order model,

$$\begin{aligned}
\nabla^2 p &= 0 && \text{in} \quad y > 0 \\
p_y &= 0 && \text{on} \quad y = 0 \ , \quad |x| < d(t) \\
p &> 0 && \text{on} \quad y = 0 \ , \quad |x| < d(t) \\
p_y &= -h_t && \text{on} \quad y = 0 \ , \quad |x| > d(t) \\
p &= 0 && \text{on} \quad y = 0 \ , \quad |x| > d(t) \\
h &> 0 && \text{on} \quad y = 0 \ , \quad |x| > d(t) \\
h &= 0 && \text{at} \quad x = \pm d(t) \\
h &= \frac{x^2}{2} && \text{at} \quad t = 0 \\
p &\to \frac{ky}{2\pi} && \text{as} \quad x^2 + y^2 \to \infty \\
h &\to \frac{x^2}{2} - \frac{kt}{2\pi} && \text{as} \quad x^2 + y^2 \to \infty \ ,
\end{aligned}$$

in the upper half plane, where a symmetry condition has been put on the contact region. A local analysis near a free point shows that the pressure will have at worst a square root singularity at the free points. An inner region will exist around the free point for which a solution can be found which must match with the codimension-two solution. The inner problem is simply that of an Ivantsov parabola [41]. The Ivantsov parabola solution is reviewed in Appendix D for the particular case of Hele-Shaw flow since Ivantsov's original paper was for the heat equation. Expanding the inner solution out it can indeed be shown that taking the codimension-two solution to have a square root singularity at the free point is the correct thing to do. Using the substitutions

$$\begin{aligned}
\phi &= -p + \frac{ky}{2\pi} \\
H &= -h + \frac{x^2}{2} - \frac{kt}{2\pi} \\
\xi &= x \\
\eta &= -y
\end{aligned}$$

the problem can be shown to be equivalent to the codimension-two water entry model, for the case $f(x) = x^2/2$, considered in Chapter 2, as formulated in Figure 2.3 except

that the velocity of the body is now $k/2\pi$ rather than 1. The water entry solution (2.22), (2.23) and (2.25) tells us

$$\begin{aligned} p &= \frac{k}{2\pi}\Re\left\{\sqrt{d(t)^2-(x-iy)^2}\right\} \qquad \text{in} \quad y>0 \\ p &= \frac{k}{2\pi}\Re\left\{\sqrt{d(t)^2-(x+iy)^2}\right\} \qquad \text{in} \quad y<0 \\ h &= \frac{x}{2}\left(x^2-d(t)^2\right)^{\frac{1}{2}} \\ d(t) &= \sqrt{\frac{2kt}{\pi}} \ . \end{aligned}$$

Figure 6.2 shows the free boundary shape at increasing times for the case $k=\pi$.

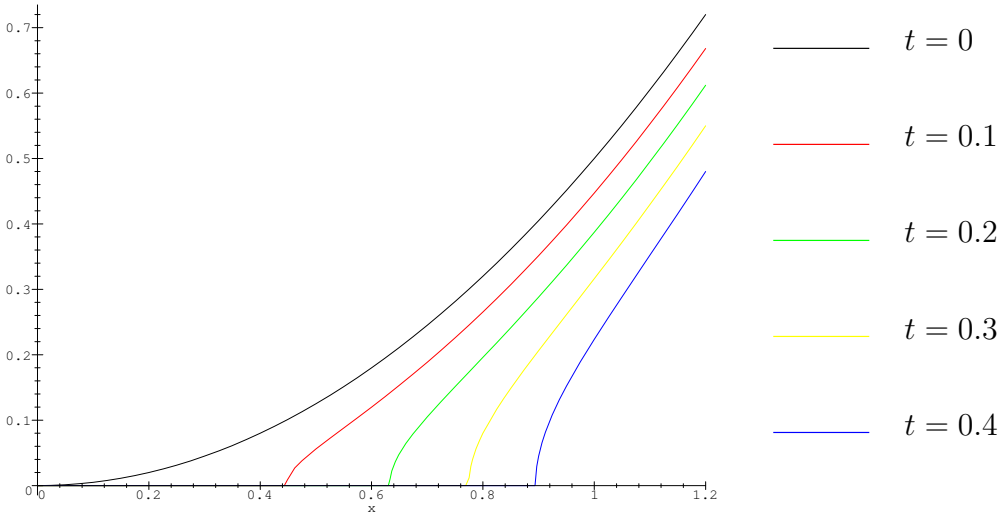

Figure 6.2: The free surface shape for the injection problem.

Yet again we note that although the solution of the time reversed problem can be formally given it is ill-posed as explained in Section 2.3.3. The ill-posedness of Hele–Shaw suction problems compared to injection problems is well known [51, 67]. As discussed by Ockendon [67] the close relationship between the water entry and the Hele–Shaw problems means that the codimension-two Hele-Shaw problem can also be expressed as a variational inequality from which existence and uniqueness of a solution can be proved for the case of injection along with the well-posedness of the problem.

If we consider the flow of information in the problem then it is clear that it is the outer flow, that is the point source, which is driving the flow. Thus we adopted the solution procedure of solving the outer region first followed by the codimension-two region. We could have then solved further for the inner region which is simply an

Ivantsov parabola [41]. The inner region solution then confirms the assumption that the codimension-two pressure has a square root singularity near the free points.

We again stress that this methodology of solving the problem along the main flow of information is a trivial concept but one which should be adhered to in order to produce a systematic solution. Breaking this rule and trying to infer a matching condition from an inappropriate region was seen to be dangerous when we considered the previous work done on the Stokes flow sintering problem with surface tension.

At this point it is not unreasonable to ask what happens if the driving mechanism of the sinks is replaced with a driving mechanism due to surface tension as was done in the similar problem for Stokes flow. A discussion of such a problem is given in Chapter 7.

The following problem is a good example of following the flow of information between not just two or three regions but through a sequence of coupled codimension-two problems.

6.2 The three discs problem

In this section we shall discuss the problem shown in Figure 6.3.

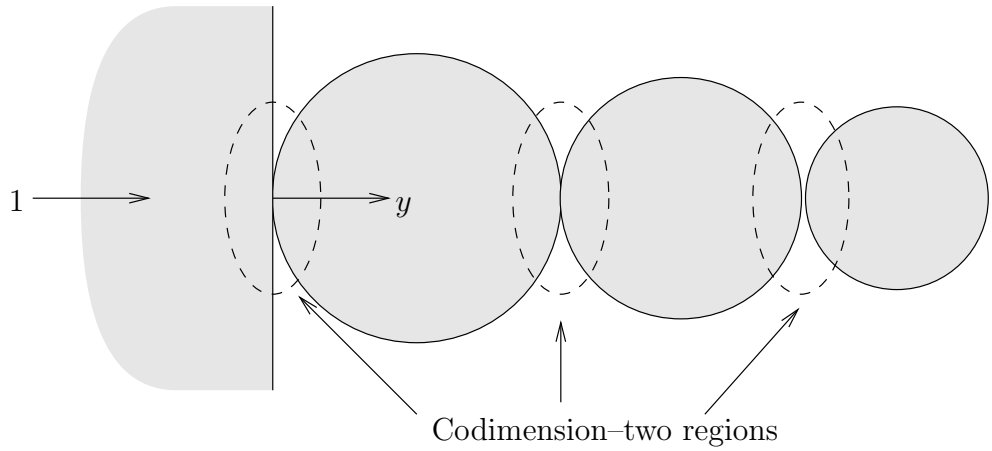

Figure 6.3: The geometry of the three discs problem.

In this problem a half space of fluid is driven by a constant pressure gradient at $y = -\infty$ and impacts with a stationary disc of fluid which is touching two further stationary discs as shown. This problem shows clearly how the information flows from the first outer problem through into the first codimension-two problem and then on into the second outer problem and so on. It is because it is such a good problem

for illustrating how we follow the flow of information in the problem that we present it here. This problem has been solved exactly by Richardson [76]. An outline of an asymptotic solution has also been considered in a codimension-two framework by Cummings [14], however it is only in a rough form and has not been published in the general literature. We will present the problem as a series of outer and codimension-two problem where the codimension-two problems will be shown to be in the form of two Riemann problems. By solving these outer and codimension-two problems in order we shall show how the information is flowing through the system. As with the previous Hele–Shaw problem inner regions will exist around the free points, in each of the codimension-two problems, which will be of the Ivantsov parabola [41] type. We will not need to use the solutions in these inner regions beyond the fact that they can confirm through matching that taking a square root at the codimension-two free points is again correct. Finally we will generalise the problem to having n discs.

To solve the problem we follow the flow of information (from left to right in Figure 6.3). The problem exhibits three regions (shown in Figure 6.3) where the problem may be expressed in a codimension-two formulation. For each such problem the far field behaviour to the left and right will be needed.

6.2.1 The first outer problem

We begin by considering the first outer problem for the moving half space. The outer problem is purely governed by the flow at $y = -\infty$ which is driven by a pressure gradient there. The outer problem is, therefore, simply

$$\begin{aligned} \nabla^2 p &= 0 \qquad \text{in} \quad y < s(t) \\ p &= 0 \qquad \text{on} \quad y = s(t) \\ \dot{s} &= p_y \qquad \text{on} \quad y = s(t) \\ p_y &\to -1 \qquad \text{as} \quad y \to -\infty \\ s &= 0 \qquad \text{at} \quad t = 0 \end{aligned}$$

to which the solution is

$$\begin{aligned} p &= t - y \\ s &= t \ . \end{aligned}$$

6.2.2 The first codimension-two problem

An enlargement of the region of interest with the relevant full equation is shown below.

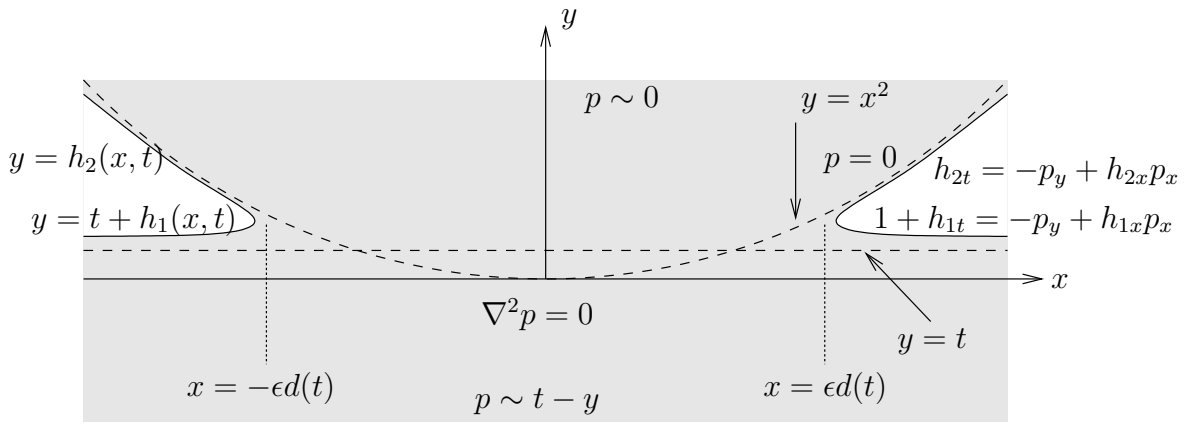

Figure 6.4: The full problem near the first codimension-two region.

We shall consider the problem in two halves and hence the free boundary has been split into two pieces, one above the turnover point and one below. By doing this we shall formulate the problem as two related problems each on a half space.

As before the measurable small parameter will be the elapsed time but we define it in such a way that the order of the contact width is ϵ. Thus we scale

$$t = \delta\hat{t} \quad , \quad x = \epsilon\hat{x} \quad , \quad y = \epsilon\hat{y} \ .$$

Inevitably this makes the free boundary scaling $h = \epsilon^2\hat{h}$ and then from the kinematic condition we determine $\delta = \epsilon^2$. The far field condition $p \sim t - y$ implies that p be scaled as $p = \epsilon\hat{p}$. Substituting these scalings into the model shown in Figure 6.4 and expanding p as a regular asymptotic expansion we obtain the leading order codimension-two models, on dropping the hats, shown in Figure 6.5. The behaviour at $y = \infty$ is because initially $p = 0$ in the disc and for short times thereafter the leading order outer behaviour in the disc will be unchanged.

To solve these two half space problems we can formulate them as Riemann boundary value problems in the same manner as was done for the water entry problem. On comparison with the water entry codimension-two model we see that the problem as defined above is missing one equation. Clearly we are missing an appropriate condition on the contact region. The required condition is that the pressure is continuous, that is

$$p_1 \ = \ p_2 \qquad \text{on} \quad |x| < d_1(t) \quad , \quad y = 0 \ . \tag{6.3}$$

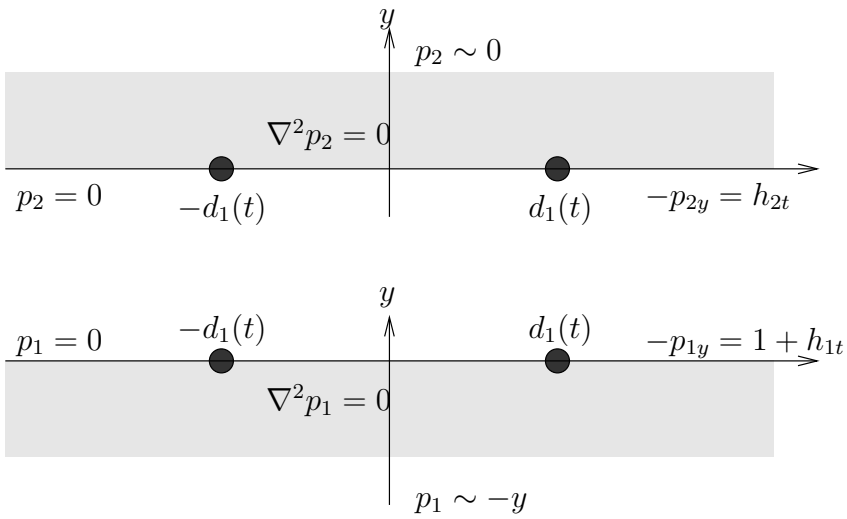

Figure 6.5: The first codimension-two problem.

However in order to formulate the problem in a similar manner to that done in Section 2.1.1.1 we take

$$p_y = -a \qquad \text{on} \quad |x| < d_1(t) \quad , \quad y = 0$$

as the boundary condition we use and then apply (6.3) to determine a. Using this condition in both the upper and lower half plane problems is possible because the vertical velocity $-p_y$ should be continuous there.

If we substitute $p = \psi - ay$ the lower half plane problem becomes

$$\begin{aligned} \nabla^2\psi &= 0 \qquad \text{in} \quad y < 0 \\ \psi_y &= 0 \qquad \text{on} \quad |x| < d_1(t) \quad , \quad y = 0 \\ \psi &= 0 \qquad \text{on} \quad |x| > d_1(t) \quad , \quad y = 0 \\ \psi &\sim (a-1)y \qquad \text{as} \quad y \sim -\infty \ . \end{aligned}$$

This only differs from the problem considered in Section 2.1.1.1 by the change in the far field condition. From the results of Section 2.1.1.1 we can immediately see

$$\psi = (1-a)\Re\left\{(d_1^2 - z^2)^{\frac{1}{2}}\right\}$$

and hence

$$p_1 = -ay + (1-a)\Re\left\{(d_1^2 - z^2)^{\frac{1}{2}}\right\} \ .$$

Substituting $y = -\eta$ into the upper half space problem we transform it to one in the lower half space which is again similar to the water entry problem. Thus by analogy

with that solution we find

$$p_2 = -ay + a\Re\left\{(d_1^2 - \overline{z}^2)^{\frac{1}{2}}\right\} \quad . \tag{6.4}$$

We can now apply condition (6.3) which shows $a = 1/2$.

6.2.2.1 Determination of the free surface position

To determine the free surface shape we apply the kinematic conditions shown in Figure 6.5. For the lower and upper parts of the boundary we find

$$\begin{aligned} h_{1t} + 1 &= \frac{1}{2} + \frac{1}{2}\frac{x}{(x^2 - d_1^2)^{\frac{1}{2}}} \\ h_{2t} &= \frac{1}{2} - \frac{1}{2}\frac{x}{(x^2 - d_1^2)^{\frac{1}{2}}} \end{aligned}$$

respectively. Integrating these and applying the appropriate initial conditions we obtain

$$h_1 = -\frac{t}{2} + \frac{1}{2}\int_0^t \frac{x}{(x^2 - d_1(\tau)^2)^{\frac{1}{2}}} d\tau \tag{6.5}$$

$$h_2 = x^2 + \frac{t}{2} - \frac{1}{2}\int_0^t \frac{x}{(x^2 - d_1(\tau)^2)^{\frac{1}{2}}} d\tau \quad . \tag{6.6}$$

6.2.2.2 The law of motion of the free point

At the turnover point $x = d_1(t)$ the two free boundaries must intersect which gives us the necessary condition

$$h_2 = h_1 + t \qquad \text{at} \quad x = d_1(t)$$

from which we can determine the law of motion of the free point. Applying this condition produces the integral problem

$$d_1(t) = \int_0^t \frac{1}{(d_1(t)^2 - d_1(\tau)^2)^{\frac{1}{2}}} d\tau \quad .$$

We invert this in the usual way to obtain

$$\begin{aligned} d_1^{-1}(x) &= \frac{2}{\pi}\int_0^x \frac{\xi^2}{(x^2 - \xi^2)^{\frac{1}{2}}} d\xi \\ &= \frac{x^2}{2} \end{aligned}$$

which is easily further inverted to give

$$d_1(t) \;=\; \sqrt{2t} \quad .$$

Further substituting this back into (6.5) and (6.6) we find

$$\begin{aligned} h_1 &= -\frac{t}{2} - \frac{x}{2}\left(x^2 - 2t\right)^{\frac{1}{2}} + \frac{x^2}{2} \\ h_2 &= \frac{x^2}{2} + \frac{t}{2} + \frac{x}{2}\left(x^2 - 2t\right)^{\frac{1}{2}} \quad . \end{aligned}$$

A plot of the two free boundary shapes (note the shapes are given by $h_1 + t$ and h_2) at increasing times is shown in Figure 6.6.

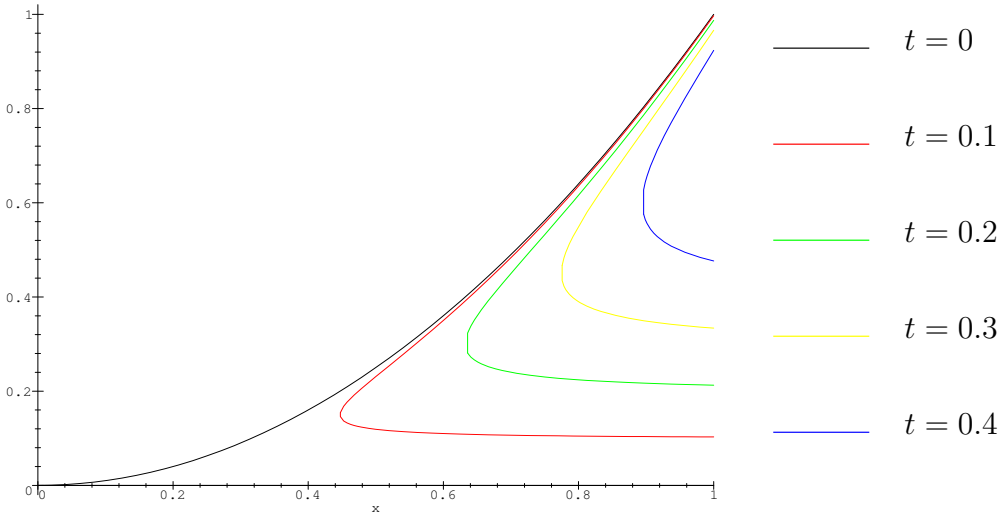

Figure 6.6: The free surface shape for the first codimension-two problem.

6.2.3 The second outer problem

The outer problem in the first disc will be driven by the behaviour of the codimension-two region solution. We must expand the codimension-two solution (6.4) in outer spatial variables to determine the singular behaviour that the outer solution must exhibit, for small time, at the point of contact. To leading order, in outer variables, we obtain

$$p \;\sim\; \frac{\epsilon^2 \hat{t} y}{2(x^2 + y^2)} \qquad \text{as} \quad x^2 + y^2 \to 0 \quad .$$

Thus the second outer problem to be solved is

$$\nabla^2 p \;=\; 0 \qquad \text{in} \quad x^2 + \left(y - \frac{1}{2}\right)^{\frac{1}{2}} < \frac{1}{4}$$

$$p = 0 \qquad \text{on} \quad x^2 + \left(y - \frac{1}{2}\right)^{\frac{1}{2}} = \frac{1}{4} \quad , \quad x \neq 0 \quad , \quad y \neq 0$$

$$p \sim \frac{\epsilon^2 \hat{t} y}{2(x^2+y^2)} \qquad \text{as} \quad x^2 + y^2 \to 0 \ .$$

The solution to this problem is simply

$$p = \frac{\epsilon^2 \hat{t}}{2}\left(\frac{y}{x^2+y^2} - 1\right) \ . \tag{6.7}$$

To use this solution in the next codimension-two region we shift the coordinate origin to $(0,1)$ by setting $y = \tilde{y} + 1$ which, on dropping the tilde, gives

$$p = \frac{\epsilon^2 \hat{t}}{2}\left(\frac{y+1}{x^2+(y+1)^2} - 1\right) \ .$$

6.2.4 The second codimension-two region

An enlargement of the full problem, near the second codimension-two region, with the relevant full equation is shown in Figure 6.7.

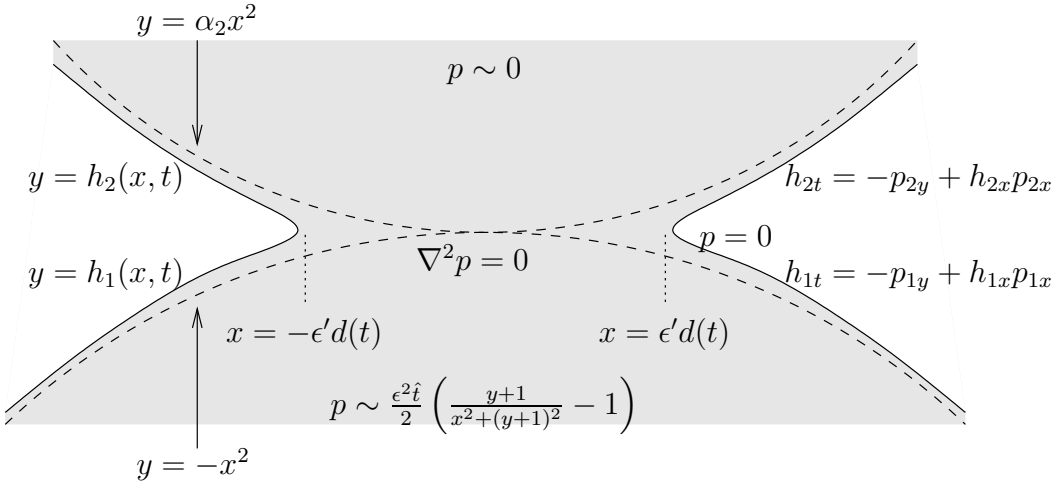

Figure 6.7: The full problem near the second codimension-two region.

We shall again consider the problem in two halves and hence the free boundary has again been split into two pieces, one above the turnover point and one below. The discs have not been assumed to be identical hence the second disc has the local form $y = \alpha_2 x^2$. We define the contact set to be of width order ϵ' which we shall relate to ϵ through the consistent small time. At $y = \infty$, $p \sim 0$ for the same reason as before.

Time is an absolute of the problem and hence $t = \epsilon^2 \hat{t}$ as before. Since the order of the contact width is ϵ' the length scalings are

$$x = \epsilon' \hat{x} \quad , \quad y = \epsilon' \hat{y} \quad , \quad h = \epsilon'^2 \hat{h} \ .$$

Expanding the far field condition as $y \to -\infty$ to leading order in these inner variables gives

$$p_1 \sim -\frac{\epsilon^2\epsilon'\hat{t}\hat{y}}{2} \ .$$

Hence we scale $p = \epsilon^2\epsilon'\hat{p}$. Finally the kinematic condition then implies $\epsilon' = \epsilon^2$. Summarising the scalings are, therefore,

$$x = \epsilon^2\hat{x} \quad , \quad y = \epsilon^2\hat{y} \quad , \quad h = \epsilon^4\hat{h} \quad , \quad t = \epsilon^2\hat{t} \quad , \quad p = \epsilon^4\hat{p} \ .$$

Substituting these scalings into the model shown in Figure 6.7 and expanding p as a regular asymptotic expansion we obtain the leading order codimension-two models, on dropping the hats, shown in Figure 6.8.

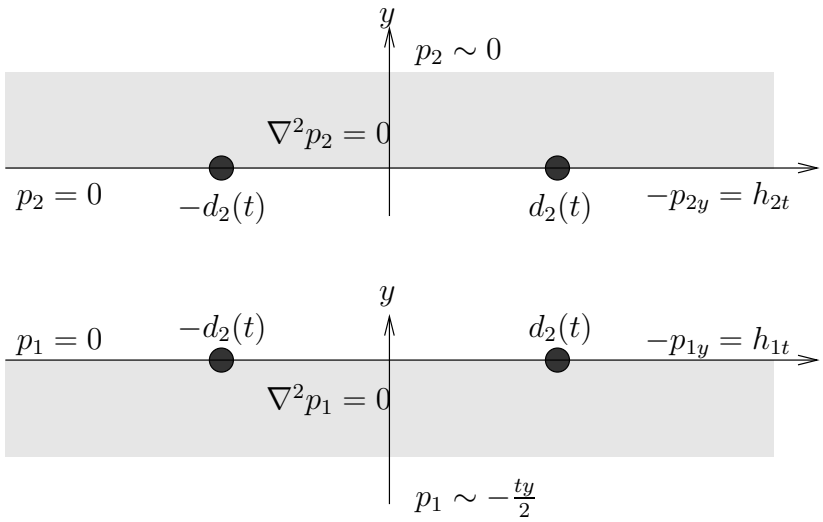

Figure 6.8: The second codimension-two problem.

As with the previous problem the two problems are connected by the continuity of the pressure on the contact region giving the further condition

$$p_1 = p_2 \qquad \text{on} \quad y = 0 \quad , \quad |x| < d_2(t) \ .$$

The problem shown in Figure 6.8 is practically the same as that in Figure 6.5 and has solution

$$\begin{aligned} p_1 &= -\frac{ty}{4} + \frac{t}{4}\Re\left\{(d_2^2 - z^2)^{\frac{1}{2}}\right\} \\ p_2 &= -\frac{ty}{4} + \frac{t}{4}\Re\left\{(d_2^2 - \overline{z}^2)^{\frac{1}{2}}\right\} \ . \end{aligned}$$

6.2.4.1 Determination of the free surface position

To determine the free surface shape we apply the kinematic conditions shown in Figure 6.8. For the lower and upper parts of the boundary we find

$$h_1 = -x^2 + \frac{t^2}{8} + \frac{1}{4}\int_0^t \frac{x\tau}{(x^2 - d_2(\tau)^2)^{\frac{1}{2}}} d\tau \tag{6.8}$$

$$h_2 = \alpha_2 x^2 + \frac{t^2}{8} - \frac{1}{4}\int_0^t \frac{x\tau}{(x^2 - d_2(\tau)^2)^{\frac{1}{2}}} d\tau \ . \tag{6.9}$$

6.2.4.2 The law of motion of the free point

At the turnover point $x = d_2(t)$ these two free boundaries must intersect which gives us the necessary condition

$$h_2 = h_1 \qquad \text{at} \quad x = d_2(t)$$

from which we can determine the law of motion of the free point. Applying this condition produces the integral problem

$$2(\alpha_2 + 1)d_2(t) = \int_0^t \frac{\tau}{(d_2(t)^2 - d_2(\tau)^2)^{\frac{1}{2}}} d\tau \ .$$

Inverting this in the same manner as for the first problem we obtain

$$\begin{aligned} d_2^{-1}(x)^2 &= \frac{8(\alpha_2 + 1)}{\pi}\int_0^x \frac{\xi^2}{(x^2 - \xi^2)^{\frac{1}{2}}} d\xi \\ &= 2(\alpha_2 + 1)x^2 \ . \end{aligned}$$

Further inverting this solution for $d_2^{-1}(x)$ we find

$$d_2(t) = \frac{t}{\sqrt{2(\alpha_2 + 1)}}$$

which on substituting into (6.8) and (6.9) gives

$$\begin{aligned} h_1 &= -x^2 + \frac{t^2}{8} - \frac{(\alpha_2 + 1)x}{2}\left\{\left[x^2 - \frac{t^2}{2(\alpha_2 + 1)}\right]^{\frac{1}{2}} - x\right\} \\ h_2 &= \alpha_2 x^2 + \frac{t^2}{8} + \frac{(\alpha_2 + 1)x}{2}\left\{\left[x^2 - \frac{t^2}{2(\alpha_2 + 1)}\right]^{\frac{1}{2}} - x\right\} \ . \end{aligned}$$

A plot of the surface shape at increasing times, for $\alpha_2 = 1.5$ is shown in Figure 6.9.

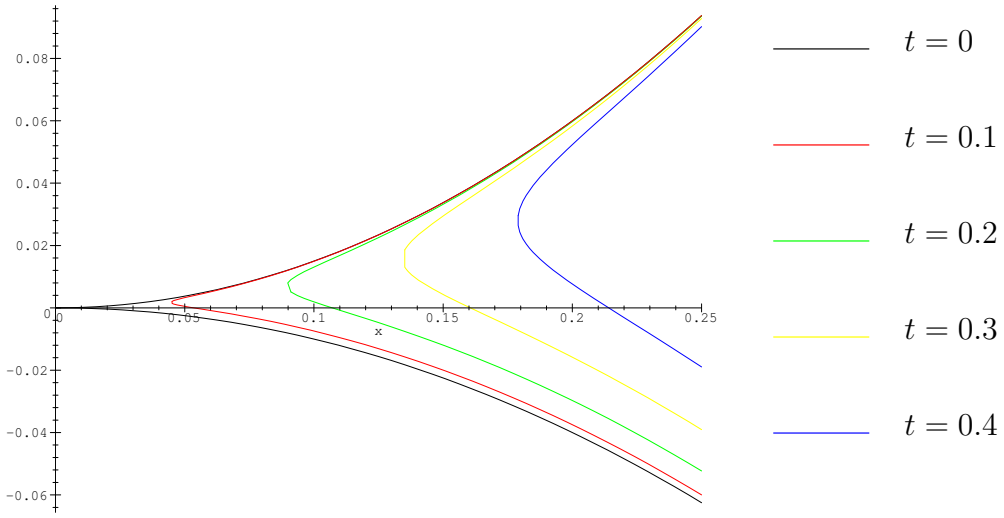

Figure 6.9: The free surface shape for the second codimension-two problem.

6.2.5 The third outer problem

The outer problem in the second disc will be driven by the behaviour of the second codimension-two region solution. We thus expand it in outer spatial variables, for small time to obtain

$$p \sim \frac{\epsilon^6 \hat{t}^3 y}{16(\alpha_2+1)(x^2+y^2)} .$$

The third outer problem to solve is, therefore, of the same form as the previous one as we would expect and hence by analogy with (6.7) we see the solution is

$$p = \frac{\epsilon^6 \alpha_2 \hat{t}^3}{16(\alpha_2+1)} \left(\frac{y}{\alpha_2(x^2+y^2)} - 1 \right) .$$

As before we now shift the origin to the centre of the new codimension-two region by making the change of coordinates $y = \tilde{y} + 1/\alpha_2$, which, on dropping the tilde, gives

$$p = \frac{\epsilon^6 \alpha_2 \hat{t}^3}{16(\alpha_2+1)} \left(\frac{y + \frac{1}{\alpha_2}}{\alpha_2 \left(x^2 + \left(y + \frac{1}{\alpha_2} \right)^2 \right)} - 1 \right) .$$

6.2.6 The third codimension-two region

An enlargement of the full problem, near the third codimension-two region, with the relevant full equation is shown in Figure 6.10.

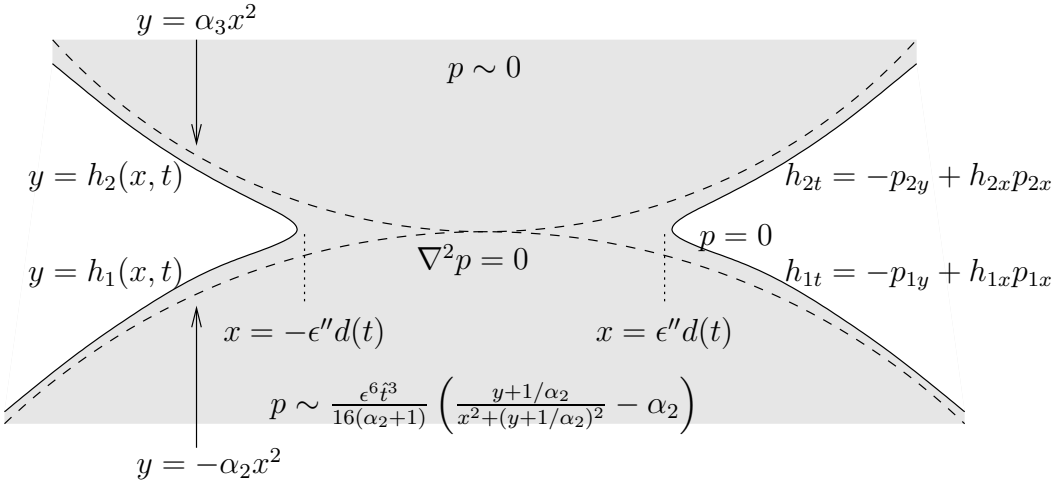

Figure 6.10: The full problem near the third codimension-two region.

This time we define the contact set to be of width order ϵ'' which we shall again relate to ϵ through the consistent small time. At $y = \infty$, $p \sim 0$ for the same reason as before.

Since the order of the contact width is ϵ'' the length scalings are

$$x = \epsilon'' \hat{x} \quad , \quad y = \epsilon'' \hat{y} \quad , \quad h = \epsilon''^2 \hat{h} \ .$$

Expanding the far field condition as $y \to -\infty$ to leading order in these inner variables gives

$$p_1 \ \sim \ -\frac{\epsilon^6 \epsilon'' \alpha_2^2 \hat{t}^3 \hat{y}}{16(\alpha_2 + 1)} \ .$$

Hence we scale $p = \epsilon^6 \epsilon'' \hat{p}$. Finally the kinematic condition then implies $\epsilon'' = \epsilon^4$. Summarising the scalings are, therefore,

$$x = \epsilon^4 \hat{x} \quad , \quad y = \epsilon^4 \hat{y} \quad , \quad h = \epsilon^8 \hat{h} \quad , \quad t = \epsilon^2 \hat{t} \quad , \quad p = \epsilon^{10} \hat{p} \ .$$

Substituting these scalings into the model shown in Figure 6.10 and expanding p as a regular asymptotic expansion we obtain the leading order codimension-two models, on dropping the hats, shown in Figure 6.11.

As with both the previous problems the two problems are connected by the continuity of the pressure on the contact region giving the further condition

$$p_1 \ = \ p_2 \qquad \text{on} \quad y = 0 \quad , \quad |x| < d_3(t) \ .$$

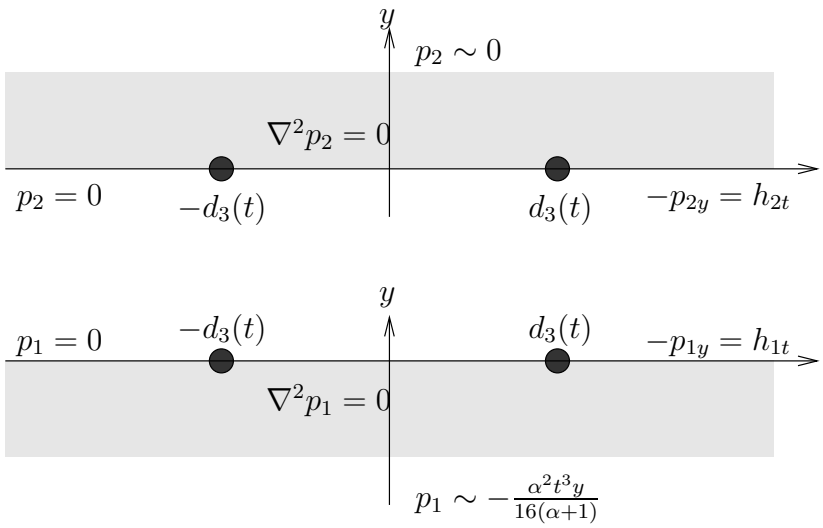

Figure 6.11: The third codimension-two problem.

The problem shown in Figure 6.11 is practically the same as the two considered before and has solution

$$\begin{aligned} p_1 &= -\frac{\alpha_2^2 t^3 y}{32(\alpha_2+1)} + \frac{\alpha_2^2 t^3}{32(\alpha_2+1)} \Re\left\{(d_3^2 - z^2)^{\frac{1}{2}}\right\} \\ p_2 &= -\frac{\alpha_2^2 t^3 y}{32(\alpha_2+1)} + \frac{\alpha_2^2 t^3}{32(\alpha_2+1)} \Re\left\{(d_3^2 - \overline{z}^2)^{\frac{1}{2}}\right\} \quad . \end{aligned}$$

6.2.6.1 Determination of the free surface position

To determine the free surface shape we apply the kinematic conditions shown in Figure 6.11. For the lower and upper parts of the boundary we find

$$h_1 = -\alpha_2 x^2 + \frac{\alpha_2^2 t^4}{128(\alpha_2+1)} + \frac{\alpha_2^2}{32(\alpha_2+1)} \int_0^t \frac{x\tau^3}{(x^2 - d_3(\tau)^2)^{\frac{1}{2}}} d\tau \qquad (6.10)$$

$$h_2 = \alpha_3 x^2 + \frac{\alpha_2^2 t^4}{128(\alpha_2+1)} - \frac{\alpha_2^2}{32(\alpha_2+1)} \int_0^t \frac{x\tau^3}{(x^2 - d_3(\tau)^2)^{\frac{1}{2}}} d\tau \quad . \qquad (6.11)$$

6.2.6.2 The law of motion of the free point

At the turnover point $x = d_3(t)$ these two free boundaries must intersect which gives us the necessary condition

$$h_2 = h_1 \qquad \text{at} \quad x = d_3(t)$$

from which we can determine the law of motion of the free point. Applying this condition produces the integral problem

$$16(\alpha_2+1)(\alpha_2+\alpha_3) d_3(t) = \alpha_2^2 \int_0^t \frac{\tau^3}{(d_3(t)^2 - d_3(\tau)^2)^{\frac{1}{2}}} d\tau \quad .$$

Inverting this in the same manner as for the previous problems we obtain

$$\begin{aligned} d_3^{-1}(x)^4 &= \frac{128(\alpha_2+1)(\alpha_2+\alpha_3)}{\pi\alpha_2^2}\int_0^x \frac{\xi^2}{(x^2-\xi^2)^{\frac{1}{2}}}d\xi \\ &= \frac{32(\alpha_2+1)(\alpha_2+\alpha_3)x^2}{\alpha_2^2} \quad . \end{aligned}$$

Further inverting this solution for $d_3^{-1}(x)$ we find

$$d_3(t) = \frac{\alpha_2 t^2}{4\sqrt{2(\alpha_2+1)(\alpha_2+\alpha_3)}} \quad .$$

Substituting back into (6.10) and (6.11) we find

$$\begin{aligned} h_1 &= -\alpha_2 x^2 + \frac{\alpha_2^2 t^4}{128(\alpha_2+1)} - \frac{(\alpha_2+\alpha_3)x}{2}\left\{\left[x^2 - \frac{\alpha_2^2 t^4}{32(\alpha_2+1)(\alpha_2+\alpha_3)}\right]^{\frac{1}{2}} - x\right\} \\ h_2 &= \alpha_3 x^2 + \frac{\alpha_2^2 t^4}{128(\alpha_2+1)} + \frac{(\alpha_2+\alpha_3)x}{2}\left\{\left[x^2 - \frac{\alpha_2^2 t^4}{32(\alpha_2+1)(\alpha_2+\alpha_3)}\right]^{\frac{1}{2}} - x\right\} \quad . \end{aligned}$$

Plots of this surface shape at increasing times, for $\alpha_2 = 1.5$ and $\alpha_3 = 2$ are shown in Figure 6.12.

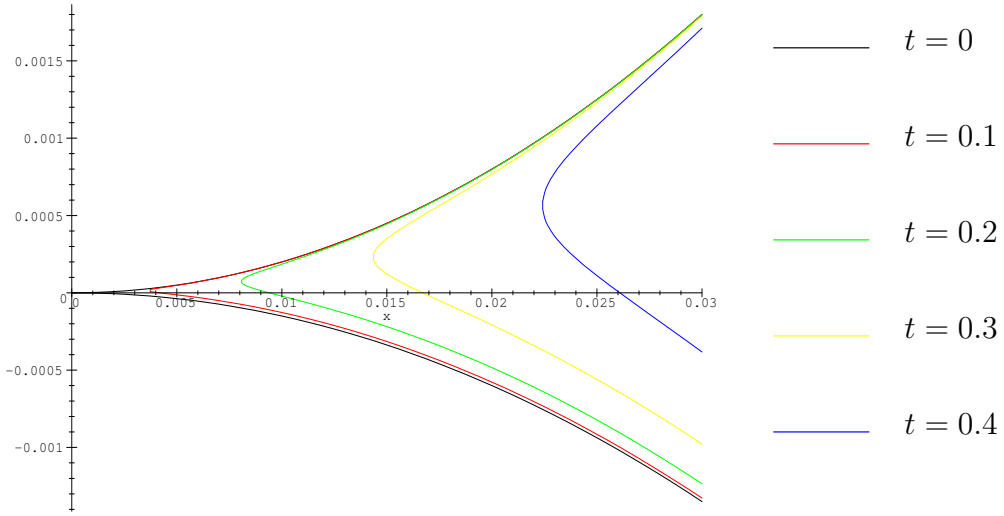

Figure 6.12: The free surface shape for the third codimension-two problem.

6.2.7 Extension to n discs

Clearly we can repeat the process above as many times as we like. Since the procedure is essentially iterative it is possible to derive a general set of formulae for the n'th such problem.

We define constants

$$p_n = 2^{n-1} \quad , \quad r_n = p_{n-1} + r_{n-1} \quad , \quad q_n = p_n + 2r_n \quad , \quad \lambda_n = \frac{\alpha_{n-1}^2 d_{n-1}^2}{4t^{(r_{n-1}+1)}}$$

$$\alpha_0 = 0 \quad , \quad \alpha_1 = 1 \quad , \quad r_1 = 0 \quad , \quad \lambda_1 = \frac{1}{2} \ .$$

Then the solution to the n'th outer problem ($n \geq 2$) can be expressed as

$$p \ = \ \epsilon^{2r_n} 2 \prod_{i=1}^{n} \lambda_i \frac{t_{r_n}}{\alpha_{n-1}^2} \left[\frac{y + \frac{1}{\alpha_{n-1}}}{x^2 + \left(y + \frac{1}{\alpha_{n-1}} \right)^2} - \alpha_{n-1} \right]$$

in appropriate coordinates. This gives the required behaviour for the codimension-two region as $y \to -\infty$ as

$$p \ \sim \ -\epsilon^{q_n} 2 \prod_{i=1}^{n} \lambda_i t^{r_n} y \ .$$

The scalings for the codimension-two region are found to be

$$x = \epsilon^{p_n} \hat{x} \quad , \quad y = \epsilon^{p_n} \hat{y} \quad , \quad h = \epsilon^{2p_n} \hat{h}$$

$$t = \epsilon^2 \hat{t} \quad , \quad p = \epsilon^{q_n} \hat{p} \ .$$

The pressure and free surface shapes in the codimension-two region are given by

$$\begin{aligned}
p_1 &= \prod_{i=1}^{n} \lambda_i t^{r_n} \left(-y + \Re \left\{ (d_n^2 - z^2)^{\frac{1}{2}} \right\} \right) \\
p_2 &= \prod_{i=1}^{n} \lambda_i t^{r_n} \left(-y + \Re \left\{ (d_n^2 - \overline{z}^2)^{\frac{1}{2}} \right\} \right) \\
h_1 &= -\alpha_{n-1}^2 x^2 - \prod_{i=1}^{n} \lambda_i \frac{t^{r_n+1}}{r_n+1} + \prod_{i=1}^{n} \lambda_i \int_0^t \frac{x \tau^{r_n}}{(x^2 - d_n(\tau)^2)^{\frac{1}{2}}} d\tau \\
h_2 &= +\alpha_n^2 x^2 - \prod_{i=1}^{n} \lambda_i \frac{t^{r_n+1}}{r_n+1} - \prod_{i=1}^{n} \lambda_i \int_0^t \frac{x \tau^{r_n}}{(x^2 - d_n(\tau)^2)^{\frac{1}{2}}} d\tau \ .
\end{aligned}$$

Applying the condition at the free point we obtain

$$(\alpha_{n-1} + \alpha_n) d_n(t) \ = \ 2 \prod_{i=1}^{n} \lambda_i \int_0^t \frac{\tau^{r_n}}{(d_n(t)^2 - d_n(\tau)^2)^{\frac{1}{2}}} d\tau$$

which we can invert to yield

$$d_n^{-1}(x) \left[\frac{\alpha_{n-1} + \alpha_n}{2 \prod_{i=1}^{n} \lambda_i} (r_n + 1) \frac{x^2}{2} \right]^{\frac{1}{r_n+1}} \ .$$

Further inverting this we obtain

$$d_n(t) \ = \ \left[\frac{2}{r_n + 1} \frac{2 \prod_{i=1}^{n} \lambda_i}{\alpha_{n-1} + \alpha_n} \right]^{\frac{1}{2}} t^{\frac{r_n+1}{2}} \ .$$

6.3 Muskat problems

A variation on the Hele–Shaw problem is the Muskat problem, named so after the author of the original paper [60]. As remarked at the beginning of the chapter this is a notorious free boundary problem about which very little is known. Muskat was modelling the encroachment of water into an oil sand for the Gulf Research and Development Corporation to try to understand better how oil could be extracted from a porous medium by injecting water to displace it. In his original paper, Muskat solved the one-dimensional, cylindrically symmetric and radially symmetric problems. We shall consider two versions which can be modelled as codimension-two problems. In order for them to fall into this category we clearly require one of the fluids to occupy a long thin region.

Since the problem models the flow of two immiscible liquids in a porous medium the fluid velocities in the two liquids are given by Darcy's law

$$\mathbf{u}_i \;=\; -k_i \nabla p_i$$

where p is the pressure and the subscript i is either 1 or 2 according to the region. The fluid is incompressible and hence in each region the field equation is

$$\nabla^2 p_i \;=\; 0 \qquad \text{in fluid } i \quad . \tag{6.12}$$

To produce a codimension-two problem we shall take one of the regions to be long and thin so that the free boundary has equation $y = \epsilon h(x,t)$. At the free boundary between the two fluids the pressure and velocity are continuous and a kinematic condition holds giving

$$\begin{aligned} p_1 \;&=\; p_2 \qquad \text{on} \quad y = \epsilon h(x,t) \\ -v_n \;=\; k_1 p_{1n} \;&=\; k_2 p_{2n} \qquad \text{on} \quad y = \epsilon h(x,t) \end{aligned}$$

where v_n is the normal velocity of the boundary. The equations so far given are for the general problem, that is they are equally valid for any ϵ, not just $\epsilon \ll 1$.

We shall restrict ourselves to problems with up-down symmetry and so have the further condition that $p_{iy} = 0$ on $y = 0$ (note we have made this restriction for ease of demonstration but it could be easily relaxed). Putting these conditions together we have a problem as shown in Figure 6.13.

Looking at the flow of information in this problem, at first glance it would appear to be similar to the other Hele–Shaw problems where a driving mechanism at infinity is going to drive the codimension-two region which in turn drives the flow in the inner

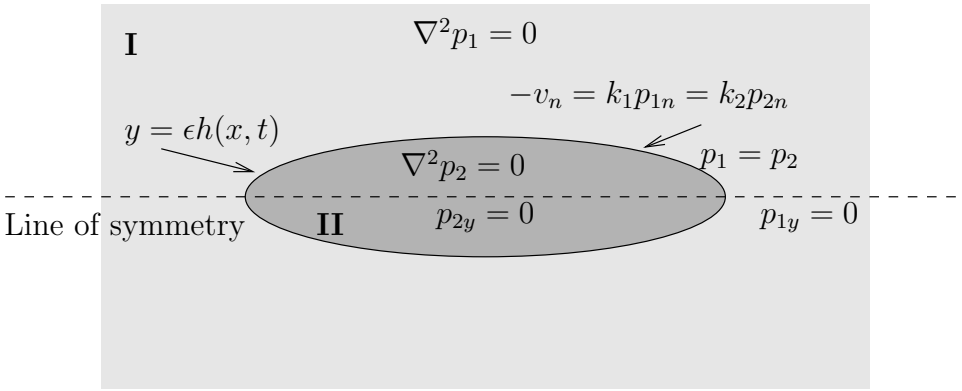

Figure 6.13: The Muskat problem.

regions around the codimension-two free points. However, this is a two-phase problem in which the solution in region II is non-trivial which changes things slightly. With appropriate scalings for the codimension-two region the free boundary condition will remain coupled to the solution of the problem in region II. Thus we cannot begin to solve the codimension-two problem without having at least an expansion solution in region II which we can substitute into the boundary conditions that are currently coupling the problems. Hence we must begin by finding an approximate solution in that region which can then be substituted into the free boundary conditions.

In region II we define $y = \epsilon Y$ and so the field equation 6.12 becomes

$$\epsilon^2 p_{2xx} + p_{2YY} = 0 \qquad \text{in} \quad Y < h(x,t) \ .$$

Looking for an asymptotic expansion solution of the form

$$p_2 \sim p_{21} + \epsilon^2 p_{22} + \ldots$$

and applying the symmetry boundary condition $p_{2Y} = 0$ on $Y = 0$ we find

$$\begin{aligned} p_2 &\sim b(x,t) - \frac{\epsilon^2 Y^2}{2} b_{xx}(x,t) + O(\epsilon^4) \\ &= b(x,t) - \frac{y^2}{2} b_{xx}(x,t) + O(y^4) \ . \end{aligned}$$

The normal to the free boundary is

$$\mathbf{n} = \frac{1}{(1+\epsilon^2 h_x^2)^{\frac{1}{2}}}(-\epsilon h_x, 1)$$

and hence

$$\begin{aligned} p_{2n} = \mathbf{n}.\nabla p_{2n} &= \frac{1}{(1+\epsilon^2 h_x^2)^{\frac{1}{2}}}(p_{2y} - \epsilon h_x p_{2x}) \\ &\sim -\epsilon (h b_x)_x + O(\epsilon^3) \end{aligned}$$

on the free boundary. Substituting back into the free boundary conditions we obtain to leading order

$$\begin{aligned} p_1 &= b(x) \qquad \text{on } y = 0 \quad x \text{ in non-contact region} \\ h_t = -\frac{k_1}{\epsilon} p_{1y} &= k_2 (h b_x)_x \qquad \text{on } y = 0 \quad x \text{ in non-contact region} \quad . \end{aligned}$$

From the second condition we see that the most interesting balance, which will neither lead to a decoupling of the problems nor a return to the one phase Hele–Shaw type problem, is when $k_1 = \epsilon K_1$ where K_1 is an order one constant. In this case the leading order codimension-two problem for p_1 in the upper half plane (for the case of symmetric free points at $x = \pm d(t)$) takes the form shown in figure 6.14.

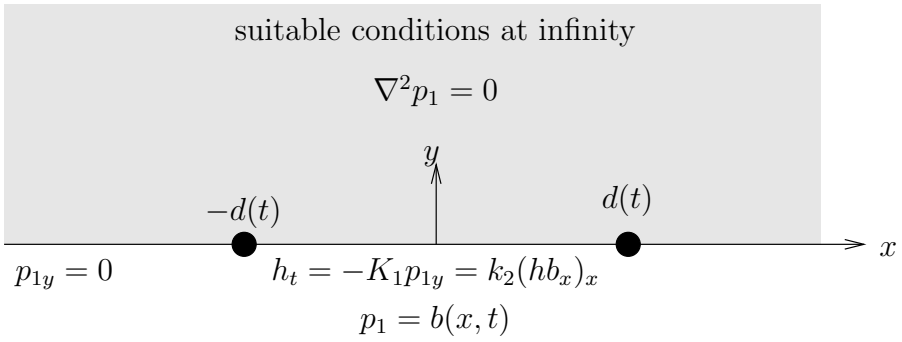

Figure 6.14: The codimension-two Muskat problem.

The fact that the problem has two phases also complicates the usual local analysis at the free point that we use to determine the appropriate singularity that the codimension-two solution should have there. A local analysis by Morgan [58] shows that no single power singularity can satisfy the local problem. Instead what is required is a local solution of the form

$$p_1 \sim A r \cos\theta + B r^{\frac{n}{2}} \cos\frac{n\theta}{2} \qquad \text{for} \quad n \in \mathbb{N} \quad .$$

Such a solution is further indicated by the solution of a two fluid Ivantsov parabola problem as is carried out in Appendix D. This suggests that a possible inner solution is to have the fluid in region II moving at a constant velocity and the fluid in region I moving with the usual sort of Ivantsov parabola velocity superimposed on a uniform flow, that is in the far field it has the form above with $n = 1$.

The solution can be written in the form

$$p_1 = \Im\{P(z)\}$$

where $z = x + iy$. Note that in this case $p_{1x} = \Im\{P'(z)\}$ and $p_{1y} = \Re\{P'(z)\}$. Thus if we define a function

$$G(z) \;=\; \begin{cases} P'(z) \;=\; u(x,y) + iv(x,y) & \text{in} \quad y > 0 \\ -\overline{P'}(\overline{z}) \;=\; -u(x,-y) + iv(x,-y) & \text{in} \quad y < 0 \end{cases}$$

then in the upper half plane the real and imaginary parts of $G(z)$ are related to the velocity components of the fluid. Applying the boundary conditions results in the following Riemann boundary value problem

$$\begin{aligned} G^+(x) + G^-(x) &= 2ib_x \qquad \text{on} \quad |x| < d \\ G^+(x) - G^-(x) &= 0 \qquad \text{on} \quad |x| > d \ . \end{aligned}$$

To solve the above Riemann problem we must also specify some behaviour at infinity.

6.3.1 Problem 1: Circular source at infinity

In this first problem we shall specify that

$$P'(z) \;\sim\; \frac{i}{z} \qquad \text{as} \quad z \to \infty$$

which corresponds to having a circular source at some large distance from the thin region. This condition is enough to allow us to solve the Riemann problem.

Using the results from Appendix B we find that the solution must be unbounded at the end points and takes the form

$$P'(z) \;=\; \frac{i}{(z^2-d^2)^{\frac{1}{2}}} + \frac{1}{\pi(z^2-d^2)^{\frac{1}{2}}} \int_{-d}^{d} \frac{(\tau^2-d^2)^{\frac{1}{2}} b_\tau(\tau,t)}{\tau - z} d\tau \ .$$

Substituting into the kinematic free boundary condition we obtain

$$h_t \;=\; -\frac{K_1}{(d^2-x^2)^{\frac{1}{2}}} - \frac{K_1}{x(d^2-x^2)^{\frac{1}{2}}} \int_{-d}^{d} \frac{(d^2-s^2)^{\frac{1}{2}} b_s(s,t)}{s-x} ds \ ,$$

where the integral is interpreted in a principal value manner. This is an equation relating h and b. The other equation we have relating h and b is

$$h_t \;=\; k_2 (h b_x)_x \ .$$

Lastly we have the usual condition

$$h \;=\; 0 \qquad \text{at} \quad x = d \ .$$

Together these are three equations for the three unknowns h, b and d. However, as yet we have been unable to find an analytical solution to them.

We should also note that using a Hilbert transform it is possible to produce an integral equations purely in terms of h and d. We have

$$p_{1x}(x,0,t) \;=\; \frac{1}{\pi}\int_{-\infty}^{\infty}\frac{p_{1y}(\xi,0,t)}{x-\xi}d\xi$$

which when combined with the boundary conditions gives

$$h_t \;=\; -\frac{k_2}{\pi K_1}\frac{\partial}{\partial x}\left[h\int_{-d}^{d}\frac{h_t}{x-\xi}d\xi\right] \quad . \tag{6.13}$$

6.3.2 Problem 2: Contact and non-contact regions interchanged

The second case we shall consider is when the long thin region now lies outside of $x \in (-d, d)$. That is we shall consider a problem analogous to a two fluid Hele–Shaw problem, where the driving mechanism is uniform flow down at $y = +\infty$ and uniform flow up at $y = -\infty$, as shown in Figure 6.15. Thus in the upper half plane

$$P'(z) \;\sim\; A \qquad \text{as} \quad z \to \infty \;\;,$$

where A is a constant determined by the solution to a particular outer problem.

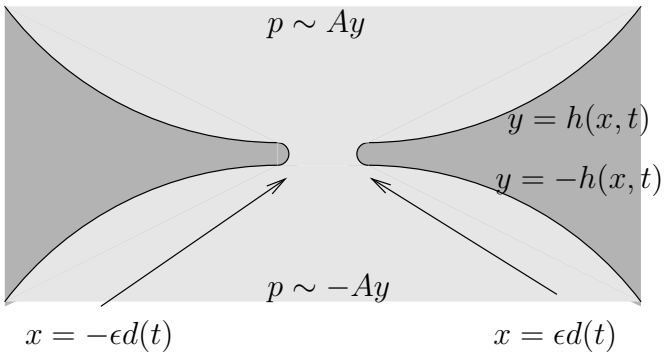

Figure 6.15: The geometry of the second Muskat problem.

For this case the Riemann boundary value problem becomes

$$\begin{aligned} G^+(x) + G^-(x) &= 2ib_x \qquad \text{on} \quad |x| > d \\ G^+(x) - G^-(x) &= 0 \qquad \text{on} \quad |x| < d \;\;. \end{aligned}$$

The only possible solution is one which is unbounded at the end points and takes the form

$$\begin{aligned} P'(z) &= \frac{Az}{(z^2-d^2)^{\frac{1}{2}}} \\ &\quad + \frac{1}{\pi(z^2-d^2)^{\frac{1}{2}}}\left[\int_{-\infty}^{-d}\frac{(\tau^2-d^2)^{\frac{1}{2}}b_\tau(\tau,t)}{\tau-z}d\tau + \int_d^{\infty}\frac{(\tau^2-d^2)^{\frac{1}{2}}b_\tau(\tau,t)}{\tau-z}d\tau\right] \quad . \end{aligned}$$

Substituting into the kinematic free boundary condition we obtain

$$h_t = -K_1 A\frac{x}{(x^2-d^2)^{\frac{1}{2}}} - \frac{K_1}{\pi(x^2-d^2)^{\frac{1}{2}}}\left(\int_{-\infty}^{-d}+\int_d^{\infty}\right)\frac{(s^2-d^2)^{\frac{1}{2}}b_s(s,t)}{s-x}ds \quad ,$$

where again the integral term is interpreted in a principal value manner. As before we also have the equations

$$\begin{aligned} h_t &= k_2(hb_x)_x \\ h &= 0 \qquad \text{at} \quad x=d \end{aligned}$$

but again as with the previous problem no analytic solution of them has yet been obtained. Again using a Hilbert transform and the boundary conditions an integral equation relating h and d can be obtained

$$h_t = -\frac{k_2}{\pi K_1}\frac{\partial}{\partial x}\left[h\left(\int_{-\infty}^{-d}\frac{h_t}{x-\xi}d\xi + \int_d^{\infty}\frac{h_t}{x-\xi}d\xi\right)\right] \quad .$$

As a last remark we again note the reverse problems of suction, where the free boundary is opening rather than closing, can be formally written as the time reversal of the injection problem but is again an ill-posed process just like the water exit and other suction problems.

Chapter 7

Conclusions and further work

7.1 Summary

In Chapter 1 we illustrated in broad terms what defining properties a free boundary problem was usually required to have in order that it could be studied using the codimension-two framework. In particular we drew attention to the type of geometry usually required and how such a geometry is exploited to formulate the codimension-two problem. We further gave a list of some of the typical problems that have previously been considered using a codimension-two approach. From that list it is clear to see that codimension-two problems can arise in many different real world applications. The difference between one- and two-phase problems was also highlighted and a distinction made between those types of two phase problems which would yield a codimension-two problem and those that would not. The key mathematical techniques that would be used were outlined and the methodology discussed. In particular we set out how the solution procedure should follow the flow of information through the problem.

Chapter 2 began with a review of the water entry problem as a means of demonstrating clearly the codimension-two methodology. That is, how the codimension-two problem is first formulated from the full free boundary problem, and then solved. In particular an emphasis was made on the careful solution procedure by means of the formulation as a Riemann boundary value problem which can prove to be a valuable tool for the systematic solution of a codimension-two problem. The different regions of the problem and how the information flowed from one to the next were discussed. It was shown that the water entry problem can be formulated in a variational form which allows existence and uniqueness to be proved as well as giving a convenient form for use in a numerical solution. A local stability analysis was performed which showed clearly that the codimension-two water entry problem is stable whilst the

time reversal problem is unstable and ill-posed. The differences and similarities to other types of stability analyses were discussed. The techniques used for the stability analysis should be applicable to other codimension-two problems and should show that in general problems in which the contact region grows are stable whilst those with decreasing contact region are unstable. Perturbations to a single free boundary problem were also considered in the form of an initial value problem and also showed that the time reversal problem was unstable. The difficulties associated with a water exit problem were discussed. Possible extensions to the basic problem were briefly considered. In particular the new extension of a non-constant body force due to a free falling body was considered.

In Chapter 3 we reviewed some classic contact and crack problems in linear elasticity. We first considered a dynamic type-III crack problem whose field equation could be reduced to Laplace's equation. We began by reviewing the basic problem where the crack face was assumed to be stress free along its entire face. By means of a conformal map the problem was mapped onto the upper half plane and then subsequently formulated as a Riemann problem. The speed of propagation of the crack tip was then predicted using the dynamic stress intensity factor approach. This problem exhibited a minus one half power singularity in the stress at the crack tip which, as discussed, is not physically acceptable. For this reason we proceeded to investigate the effect of including a cohesive zone near the tip of the crack. This also lead to a Riemann problem. The inclusion of the cohesive zone was seen to change the singularity at the crack tip from a minus one half power to a plus one half power. The inclusion of a cohesive zone on its own, however, lead to no prediction of the crack tip velocity. The recovery of such a result was indicated to be possible with the additional inclusion of a viscous resistance force along the entire crack face.

Secondly we considered the contact of two identical bodies. We began by reviewing the case of a purely normal contact which is the classic Hertz problem. We showed how this could be solved using both a superposition technique and the more elegant Muskhelishvili potential method. Including friction we considered the effect of a further tangential force applied after the initial normal loading. The addition of such a load was seen to give rise to regions of slip at the edges of the contact region. These slip regions grew inward with increasing load until they met at which point sliding would begin. Lastly we presented a means of considering the incremental loading of the problem.

In the next section of the chapter we saw how a simple type-I crack problem was also solvable using the techniques and results developed for the contact problems. The

results of the solution to the type-I crack problem were then developed, by means of an incremental loading technique similar to that used in the contact problem, to address the problem of the closing mechanism of an aperture used to deliver ink for a printing process. For three examples it was shown how the particular variation of the pressure with crack width lead to the crack zipping shut as required, being cusp shaped near the ends. The inverse problem of finding the particular loading necessary to close a given initial crack shape was also solved.

The contact problems and type-I crack problem all demonstrated how we can solve codimension-two problems whose field equation is the biharmonic equation whilst the water entry problem and type-III crack problem demonstrated the solution of codimension-two problems whose field equation was Laplace's equation.

In Chapter 4 we considered a different type of codimension-two problem. All the other problems had arisen by exploiting a naturally occurring small parameter which allowed the free boundary to be linearised onto a known boundary meaning that the only undetermined characteristic of the domain was the positions of the resulting free points, that is the codimension-two free boundaries. The problem of a rectangular elastic plate simply supported at its edges was seen to naturally give rise to a codimension-two problem without the need to exploit any naturally occurring small parameter. The variational formulation of such a problem was discussed in view of its use in proving the existence and uniqueness of a solution and for generating an efficient numerical solution. The reasoning why simply supported plates can lift at the corners was clearly analysed with the single corner problem of Section 4.2 and the rectangular problem of Section 4.3. A numerical solution using dynamic relaxation was formulated and used to solve the problems of a clamped plate, a simply supported plate, and a simply supported plate free to lift at the corners for three different plate sizes. The numerical results showed how the plate shape and edge forces differed in each of the cases.

Chapter 5 began with a consideration of an injection problem for a Stokes flow. Using this problem we introduced the important solution procedure analogous to the Muskhelishvili potential method previously used in the elastic contact problems of Chapter 3. Using this formulation gave a systematic method for obtaining the codimension-two solution. We further noted the ill-posedness of the suction problem and the fact that it cannot be simply viewed as the time reversal of the injection problem.

Following on from the injection problem we considered the more complicated problem of viscous sintering due to surface tension effects. The relevance of such a

problem to the glass industry was discussed. Following our careful solution procedure of following the flow of information through the problem we showed that the necessary matching conditions for the codimension-two region came from matching to an inner problem. The inner problem had previously been solved by Hopper and was shown to give the desired matches allowing us to solve the problem in the codimension-two region. Having obtained the codimension-two solution we further showed how the necessary information from the inner region required for matching could be extracted by considering the far field problem for the inner problem which was much easier to solve than the full inner problem. The section was concluded by showing how the results could be easily extended to different initial free boundary shapes in the codimension-two region which allows us to consider other initial geometries for which no exact solution is available.

The third problem of the chapter we considered was the closure of a long thin channel at an ice-till interface. Using the Muskhelishvili potential method and exploiting the fact that the problem is defined on a half-space we were able to derive the solution easily for both the case of an impermeable bed and also the case when the till motion was also modelled as a slow flow.

In Chapter 6 we addressed several problems in Hele–Shaw flow. The chapter began with a recap of the Hele–Shaw injection problem previously done by Morgan which showed that it was equivalent to the water entry problem of Chapter 2. As a consequence, the suction problem was also noted to be ill-posed.

The second problem considered was the mathematically entertaining three discs problem. Working through the problem we showed how formulation as a Riemann problem was again a sound methodological approach. The problem further demonstrated the value of following the flow of information through the problem to give a well ordered solution procedure as information flows from the outer region into the codimension-two region and on into the next outer region and so on. The problem was then generalised to give results for an infinite sequence of discs.

The third distinct problem of the chapter was the Muskat problem. The Muskat problem is a two-phase problem and as such its solution shows how the methodology is adapted in this case. Two particular examples were considered. However, in both cases we were unable to find explicit solutions for the free surface shape and hence unable to completely solve the problems. Again the suction problems were noted to be ill-posed.

7.2 General remarks

This thesis should have convinced you that there is a vast array of industrial and applied mathematics problems that can be formulated as codimension-two free boundary problems. Formulation as a codimension-two problem enables progress to be made with a problem in certain parameter regimes which would otherwise be difficult to consider numerically due to the rapid motion and awkward geometries, such as cusp regions at initial contact. Furthermore the resulting codimension-two solution can be used to progress a problem beyond the initial singularities to a point at which a numerical scheme can be more efficiently initiated. We have also seen how exact solutions often only exist for specific initial configurations (if they exist at all) whereas codimension-two formulations can be used for more general initial free boundary shapes.

The stability analysis performed in Chapter 2 has finally shown that a dispersion type relationship is attainable from a codimension-two stability analysis as it is for more traditional stability analyses. Moreover, there is no reason why the method used in that stability analysis could not be applied to other codimension-two problems to show that the problems with growing contact region are in general stable whilst those with shrinking contact region are unstable. The discussion on water exit also clearly explained why although the codimension-two exit problem can be formally posed as the time reversal of the entry problem it is actually an ill-posed process. Throughout the thesis the ill-posedness of other time reversal problems relating to suction was stressed. It is certainly a truism that for a codimension-two problem in which the free boundary is closing the process is well posed and stable, but in the case of an opening free boundary (when surface is being created not destroyed) the problem is both ill-posed and unstable.

A key tool in solving many of the codimension-two problems considered was the use of the Riemann problem formulation which should be seen as a powerful approach which allows the problem to be considered in a very systematic fashion. The other key methodological idea used throughout is to follow the flow of information through the problem even if it means starting from an inner problem and working out. Proceeding in this way will save many a sleepless night when it comes to getting the solution to match correctly. Break this rule at your peril — the results of trying to avoid this approach were seen to produce misleading results and generally cause problems.

7.3 Two open problems

7.3.1 Hele-Shaw flow with non-zero surface tension

Having successfully solved the similar Stokes flow problem in Section 5.2 (for which an exact solution exists) we wish to consider the Hele–Shaw version (for which no exact solution has been found).

The full problem has the same configuration as the Stokes flow case. The equations become

$$\begin{aligned}
\nabla^2 p &= 0 \qquad \text{in fluid} \\
h_t &= -p_y + p_x h_x \qquad \text{on} \quad y = h(x,t) \\
p &= -\frac{h_{xx}}{(1+h_x^2)^{\frac{3}{2}}} \qquad \text{on} \quad y = h(x,t) \\
h &> 0 \\
p_y &= 0 \qquad \text{on} \quad y = 0 \quad , \quad |x| < \epsilon d \\
p &> 0 \qquad \text{on} \quad y = 0 \quad , \quad |x| < \epsilon d \\
h &= 0 \qquad \text{at} \quad |x| = \epsilon d \ ,
\end{aligned}$$

where p is the pressure and h is the free boundary shape. By analogy with the Stokes flow problem we expect the codimension-two scalings to take the form

$$x = \epsilon \hat{x} \quad , \quad y = \epsilon \hat{y} \quad , \quad h = \epsilon^2 \hat{h} \quad , \quad t = \epsilon^a \hat{t} \quad , \quad p = p_0 + \epsilon^{3-a} p_1$$

where $O(p_0) \gg O(\epsilon^{3-a})$. The resulting codimension-two problems (on dropping the hats) are

$$\begin{aligned}
\nabla^2 p_0 &= 0 \qquad \text{in} \quad y > 0 \\
p_{0y} &= 0 \qquad \text{on} \quad y = 0 \quad , \quad |x| < d \\
p_0 &= 0 \qquad \text{on} \quad y = 0 \quad , \quad |x| > d
\end{aligned}$$

and

$$\begin{aligned}
\nabla^2 p_1 &= 0 \qquad \text{in } y > 0 \\
h_t &= -p_{1y} \qquad \text{on} \quad y = 0 \quad , \quad |x| > d \\
p_1 &= 0 \qquad \text{on} \quad y = 0 \quad , \quad |x| > d \\
h &> 0 \\
p_{1y} &= 0 \qquad \text{on} \quad y = 0 \quad , \quad |x| < d
\end{aligned}$$

$$
\begin{aligned}
p &> 0 \qquad \text{on} \quad y = 0 \quad , \quad |x| < d \\
h &= 0 \qquad \text{at} \quad |x| = d \\
h &= \frac{1}{2}x^2 \qquad \text{at} \quad t = 0 \ .
\end{aligned}
$$

p_0 will be determined by the solution to an inner problem in which the curvature term comes back in. The matching between the solution to the inner and codimension-two problems should fix the codimension-two time scale (i.e. a) and the free point position $d(t)$. The solution for p_1 should be of the same form as the injection case, namely

$$
\begin{aligned}
p_1 &= B(t)\Re\left\{\left[d^2 - (x - iy)^2\right]^{\frac{1}{2}}\right\} \\
h &= \frac{x^2}{2} - x\int_0^t \frac{B(\tau)}{(x^2 - d(\tau)^2)^{\frac{1}{2}}}d\tau \ .
\end{aligned}
$$

Applying $h(d) = 0$ we find

$$
B(t) = \frac{1}{2}d(t)\dot{d}(t)
$$

which we can substitute back in to get

$$
h = \frac{1}{2}\left(x^2 - d(t)^2\right)^{\frac{1}{2}} \ . \tag{7.1}
$$

Hence if we can solve the inner problem and perform the matching we can pin down the time scale, d, and p_0 and thus have a complete solution to the codimension-two problem.

A first thought might be to try to solve the far field of the inner problem by again putting in a point force to mimic the force due to the high curvature in the inner region. Unfortunately this technique proves fruitless for the Hele–Shaw case. A second thought might be to try to solve the full inner problem. As was remarked for the injection case an inner solution is easily found for zero surface tension (see Appendix D). However, it is not possible to extend that solution procedure to the case of non-zero surface tension.

A source of possible progress is to try to use the results of Lacey et al. [51] who have put forward a model for 'crack' propagation in a Hele–Shaw cell for non-zero surface tension. Their model gives a parabolic free boundary shape near the crack tip which is consistent with the above free boundary shape when expanded locally near the free points.

At this point, therefore, there is still much work to be done on this inner problem before the codimension-two region solution can be found.

7.3.2 A note on inviscid sintering

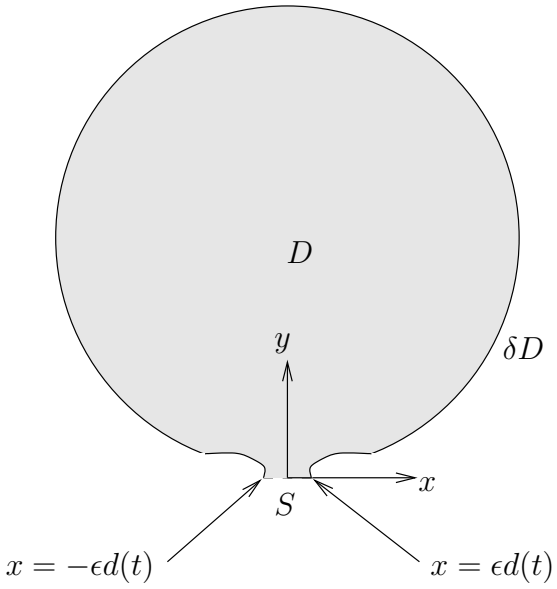

Figure 7.1: The inviscid sintering problem.

Having considered viscous sintering it is not unreasonable to wonder what happens in a corresponding inviscid regime. Such a problem can be simply expressed, in terms of a velocity potential ϕ and a free boundary shape h, as

$$\begin{aligned} \nabla^2\phi &= 0 \qquad \text{in } D \\ \phi_t + \frac{1}{2}\left(\phi_x^2+\phi_y^2\right) - \frac{h_{xx}}{(1+h_x^2)^{\frac{3}{2}}} &= -1 \qquad \text{on } \partial D \\ h_t + \phi_x h_x - \phi_y &= 0 \qquad \text{on } \partial D \\ \phi_y &= 0 \qquad \text{on } S \end{aligned}$$

where the domain and boundary labels are defined in Figure 7.1 and everything has already been nondimensionalised using the scalings

$$x = L\hat{x} \quad , \quad y = L\hat{y} \quad , \quad h = L\hat{h} \quad , \quad t = \left(\frac{\rho L}{\sigma}\right)^{\frac{1}{2}} L\hat{t} \quad , \quad \phi = \left(\frac{\sigma}{\rho L}\right)^{\frac{1}{2}} L\hat{\phi}$$

where as usual we have immediately dropped the hats.

To obtain a codimension-two model we adopt the scalings

$$x = \epsilon\hat{x} \quad , \quad y = \epsilon\hat{y} \quad , \quad h = \epsilon^2\hat{h} \quad , \quad t = \epsilon^a\hat{t} \quad , \quad \phi = \epsilon^{3-a}\hat{\phi}$$

which results in the leading order model

$$\nabla^2\phi = 0 \qquad \text{in } y > 0$$

$$\begin{aligned}
\epsilon^{3-2a}\phi_t + \frac{\epsilon^{4-2a}}{2}\left(\phi_x^2 + \phi_y^2\right) - h_{xx} &= -1 \qquad \text{on} \quad |x| > d(t) \quad , \quad y = 0 \\
h_t &= \phi_y \qquad \text{on} \quad |x| > d(t) \quad , \quad y = 0 \\
\phi_y &= 0 \qquad \text{on} \quad |x| < d(t) \quad , \quad y = 0 \ .
\end{aligned}$$

We have scaled time to some general power of ϵ since we do not yet know on what time scale the codimension-two problem occurs only that it will exist for small time (i.e. $a > 0$). The choice of scaling for ϕ has been chosen to balance terms in the kinematic condition to obtain an equation which will determine the free surface shape. a will only be determined at the matching stage.

If the flow were being driven by injection at the centres of the discs or if the two discs were colliding at high speed (rather than the driving mechanism being surface tension) a would be determined by matching to an outer solution and would lead to a leading order codimension-two problem which was essentially the same as the water entry problem and would have a solution of the form $\phi = A(t)\Re\left\{\sqrt{d^2 - z^2}\right\}$.

However since the flow is being driven by surface tension the information which will determine a will come from an inner region near the moving tip and the expansion for ϕ will be a two term expansion, along the same lines as the Stokes flow and Hele–Shaw problems, where the first term satisfies a simpler problem than that above and it is the second term which satisfies a problem similar to the water entry problem.

As in the Stokes flow case we might hope to be able to extract the information we need from the inner region without actually solving the full inner problem but by instead solving the outer limit of the inner problem. However, we suspect that the inner problem may be fraught with danger. Unlike in the viscous case where the inner free boundary was parabolic there is some evidence to suggest that it will be more complicated than that in this case. In [71] the problem of incompressible, inviscid sintering with surface tension is considered on a simplified geometry with cylindrical symmetry, the simplified geometry being two slits closed at the ends by half tori. The result of their numerical calculations is that capillary waves can form on the free boundary and then lead to pinch off. At the pinch off point the whole problem essentially begins again on a smaller scale.

7.4 Further work

The stability of other codimension-two problems is an obvious area for further work. The next step could be to work through the stability analysis, following the method from the water entry problem, for the Stokes flow problems of Chapter 5.

The other clear area for further work that this thesis has highlighted is to solve the two open problems of sintering due to surface tension in a Hele–Shaw cell or an inviscid flow. In particular both these problems require an inner solution, or at least a far field solution of the inner problem. Once such a solution has been obtained solving the problem in the codimension-two region should be a simple extension of the injection solutions.

We finally conclude by listing clearly several open problems/areas of further work

- Stability analysis of Stokes flow problems
- Hele–Shaw cell sintering problem
- Inviscid sintering problem
- Three-dimensional axisymmetric versions of Stokes flow problems
- Numerical solution of the skimming stone problem
- Formulate and solve a codimension–three problem.

Appendix A

Sobolev and Hilbert spaces

We begin by making some basic definitions. For a vector $\mathbf{x} \in \mathbb{R}^n$ we define

$$\mathbf{x}^\alpha \;=\; \prod_{j=1}^{n} x_j^{\alpha_j} \tag{A.1}$$

where $\mathbf{x} = (x_1, x_2, \ldots, x_n)^t$. $\alpha = (\alpha_1, \alpha_2, \ldots, \alpha_n)^t$ is known as the multi-index and we define the length of α to be $|\alpha| = \alpha_1 + \alpha_2 + \ldots + \alpha_n$. We next define a differential operator $\mathbf{D}$ by

$$\mathbf{D} \;=\; (D_1, D_2, \ldots, D_n)^t \;=\; \left(\frac{\partial}{\partial x_1}, \frac{\partial}{\partial x_2}, \ldots, \frac{\partial}{\partial x_n}\right)^t \quad .$$

Hence by definition (A.1)

$$\mathbf{D}^\alpha \;=\; \prod_{j=1}^{n} D_j^{\alpha_j} \;=\; \frac{\partial^{\alpha_1}}{\partial x_1}\frac{\partial^{\alpha_2}}{\partial x_2}\cdots\frac{\partial^{\alpha_n}}{\partial x_n} \quad .$$

A Sobolev space consists of functions $\mathbf{u} \in \mathcal{L}^p(\Omega)$ (note $\mathbf{u}$ is in $\mathcal{L}^p(\Omega)$ if $\int_\Omega |\mathbf{u}(\mathbf{x})|^p d\mathbf{x} < \infty$) whose weak derivatives $\mathbf{D}^\alpha\mathbf{u}$ are also elements of $\mathcal{L}^p(\Omega)$. In order to give a precise definition of a Sobolev space we must, therefore, first define a weak derivative. Suppose $\mathbf{u} \in \mathcal{C}^k(\Omega)$ and let $\mathbf{v} \in \mathcal{C}_0^\infty(\Omega)$. Then from integration by parts we have the formula

$$\int_\Omega \mathbf{v}(\mathbf{x})\mathbf{D}^\alpha\mathbf{u}(\mathbf{x})d\mathbf{x} \;=\; (-1)^{|\alpha|}\int_\Omega \mathbf{u}(\mathbf{x})\mathbf{D}^\alpha\mathbf{v}(\mathbf{x})d\mathbf{x} \qquad \text{for} \quad |\alpha| \le k \quad , \quad \forall\, \mathbf{v} \in \mathcal{C}_0^\infty(\Omega) \quad .$$

However, often we may be considering a function $\mathbf{u}$ which does not possess the smoothness hypothesised above yet we may require it to be differentiable in some sense, and thus we introduce a weak derivative. Suppose $\mathbf{u} \in \mathcal{L}^1(\omega)$ for each bounded open set ω, with $\overline{\omega} \subset \Omega$. Suppose further there also exists a function w_α, locally integrable on Ω such that

$$\int_\Omega \mathbf{w}_\alpha(\mathbf{x})\mathbf{v}(\mathbf{x})d\mathbf{x} \;=\; (-1)^{|\alpha|}\int_\Omega \mathbf{u}(\mathbf{x})\mathbf{D}^\alpha\mathbf{v}(\mathbf{x})d\mathbf{x} \qquad \forall\, \mathbf{v} \in \mathcal{C}_0^\infty(\Omega) \tag{A.2}$$

then we say $\mathbf{w}_\alpha$ is the weak derivative of $\mathbf{u}$ of order $|\alpha|$ and write $\mathbf{w}_\alpha = \mathbf{D}^\alpha \mathbf{u}$. Clearly if $\mathbf{u}$ is a smooth function then its weak derivatives are the ordinary pointwise derivative. Another way of defining the weak derivative would be to say it is the derivative in a distributional sense which is exactly what is being stated in (A.2). Thus with the definitions all in place we can now define a Sobolev space. Let k be a non-negative integer, then we define

$$\mathcal{W}^{k,p}(\Omega) \;=\; \{\mathbf{u} \in \mathcal{L}^p(\Omega) : \mathbf{D}^\alpha \mathbf{u} \in \mathcal{L}^p(\Omega), |\alpha| \leq k\} \tag{A.3}$$

where $\mathcal{W}^{k,p}$ is called a Sobolev space of order k in the $\mathcal{L}^p$ framework. It is equipped with the Sobolev norm

$$||\mathbf{u}||_{\mathcal{W}^{k,p}(\Omega)} \;=\; \left(\sum_{|\alpha| \leq k} ||\mathbf{D}^\alpha \mathbf{u}||^p_{\mathcal{L}^p(\Omega)} \right)^{\frac{1}{p}}$$

where

$$||\mathbf{u}||_{\mathcal{L}^p(\Omega)} \;=\; \left(\int_\Omega |\mathbf{u}(\mathbf{x})|^p d\mathbf{x} \right)^{\frac{1}{p}} \quad .$$

In the case $p = 2$ it can also be equipped with the inner product

$$(\mathbf{u}, \mathbf{v})_{\mathcal{W}^{k,2}(\Omega)} \;=\; \sum_{|\alpha| \leq k} (\mathbf{D}^\alpha \mathbf{u}, \mathbf{D}^\alpha \mathbf{v})$$

where

$$(\mathbf{f}, \mathbf{g}) \;=\; \int_\Omega \mathbf{f}(\mathbf{x}) \cdot \overline{\mathbf{g}(\mathbf{x})} d\mathbf{x} \quad .$$

With this inner product $\mathcal{W}^{k,2}$ is a Hilbert space. In this case the notation $\mathcal{H}$ is more common than $\mathcal{W}$. In general a vector space V equipped with an inner product and an associated norm is called a Hilbert space if, whenever $\{\mathbf{u}_m\}_{m=1}^\infty \in V$ satisfy

$$\lim_{n,m \to \infty} ||\mathbf{u}_n - \mathbf{u}_m||_V = 0$$

then there exists a $\mathbf{u} \in V$ such that

$$\lim_{m \to \infty} ||\mathbf{u} - \mathbf{u}_m||_V = 0 \quad ,$$

that is the sequence converges to $\mathbf{u} \in V$.

We define the Fourier transform over $\mathbb{R}^n$ to be

$$\mathcal{F}\mathbf{u}(\mathbf{s}) \;=\; \hat{\mathbf{u}}(\mathbf{s}) \;=\; \int_{\mathbb{R}^n} \mathbf{u}(\mathbf{x}) e^{i\mathbf{x}\cdot\mathbf{s}} d\mathbf{x} \qquad \text{for} \quad \mathbf{s} \in \mathbb{R}^n$$

and the Fourier inverse to be

$$\mathcal{F}\mathbf{v}(\mathbf{x}) \quad = \quad (2\pi)^{-n}\int_{\mathbb{R}^n}\mathbf{v}(\mathbf{s})e^{-i\mathbf{x}\cdot\mathbf{s}}d\mathbf{s} \qquad \text{for} \quad \mathbf{x}\in\mathbb{R}^n \quad .$$

Two standard results for Fourier transforms are

$$\begin{aligned}\mathcal{F}(\mathbf{D}^\alpha\mathbf{u}) &= (-i\mathbf{s})^\alpha\mathcal{F}\mathbf{u}(\mathbf{s}) \\ (\mathbf{u}_1,\mathbf{u}_2) &= (2\pi)^{-n}(\mathcal{F}\mathbf{u}_1,\mathcal{F}\mathbf{u}_2) \quad .\end{aligned}$$

The second of these is known as Plancherel's formula from which we can see that if $\mathbf{v}(\mathbf{x})\in\mathcal{L}^2(\Omega)$ its Fourier transform $\mathcal{F}\mathbf{v}(\mathbf{s})\in\mathcal{L}^2(\Omega)$ also. Using both these results together we see

$$||\mathbf{u}||_{\mathcal{H}^k(\mathbb{R}^n)} \quad = \quad \left(\sum_{|\alpha|\leq k}(2\pi)^{-n}||(-i\mathbf{s})^\alpha\mathcal{F}\mathbf{u}(\mathbf{s})||^2_{L^2(\mathbb{R}^n)}\right)^{\frac{1}{2}}$$

which provides us with an alternative definition of the Sobolev space. Further defining the semi-norm to be

$$|\mathbf{u}|_{\mathcal{H}^k(\mathbb{R}^n)} \quad = \quad \left(\sum_{|\alpha|=k}||\mathbf{D}^\alpha\mathbf{u}||^2_{L^2(\mathbb{R}^n)}\right)^{\frac{1}{2}} \quad = \quad \left(\sum_{|\alpha|=k}(2\pi)^{-n}||(-i\mathbf{s})^\alpha\mathcal{F}\mathbf{u}(\mathbf{s})||^2_{L^2(\mathbb{R}^n)}\right)^{\frac{1}{2}}$$

it is possible to extend our definition to include non-integer orders. It can be shown for $0<\gamma<1$ that the semi-norm is given by the formula

$$|\mathbf{u}|^2_{\mathcal{H}^\gamma(\mathbb{R}^n)} \quad = \quad ||\mathbf{D}^\gamma\mathbf{u}||^2_{\mathcal{L}^2(\mathbb{R}^n)} \quad = \quad C(\gamma,n)\int_{\mathbb{R}^n}|\mathbf{s}|^{2\gamma}|\mathcal{F}\mathbf{u}(\mathbf{s})|^2d\mathbf{s}$$

which allows us to interpret differentiation of a fractional order. We can easily hence define a Sobolev space of non-integer order in the $\mathcal{L}^2$ framework by defining the norm to be

$$||\mathbf{u}||^2_{\mathcal{H}^{k+\gamma}(\mathbb{R}^n)} \quad = \quad ||\mathbf{u}||^2_{\mathcal{H}^k(\mathbb{R}^n)} + |\mathbf{u}|^2_{\mathcal{H}^{k+\gamma}(\mathbb{R}^n)} \quad .$$

Now that we have defined a Sobolev space in the $\mathcal{L}^2$ framework with a non-integer order we are in a position to state the *trace theorem*. The trace theorem states [81] that if $\mathbf{u}\in\mathcal{H}^1(\mathbb{R}^n)$ then $\mathbf{u}|_{x_n=0}\in\mathcal{H}^{\frac{1}{2}}(\mathbb{R}^{n-1})$. Thus if we can define a coordinate system in which the boundary of Ω is given by $x_n=0$ then the solution to the mixed boundary value problem evaluated on the boundary is in $\mathcal{H}^{\frac{1}{2}}(\mathbb{R}^{n-1})$.

Now for a function $u(x)$ defined on $\mathbb{R}$ such that $u(x) \sim |x|^m$ as $x \to 0$ and $u(x)$ decays rapidly at infinity its approximate Fourier transform is given by Watson's lemma as

$$\mathcal{F}u(s) \quad \sim \quad \frac{2\Gamma(m+1)}{s^{m+1}}$$

where Γ is the Gamma function. From our definition above if $u \in \mathcal{H}^{\frac{1}{2}}(\mathbb{R})$ the integrand must decay quickly enough at infinity giving the condition $1 - 2(m+1) < -1$ which implies $m > 0$. This yields the important result that a function belonging to $\mathcal{H}^{\frac{1}{2}}(\mathbb{R})$ cannot have any negative power singularities. In particular if we combine this with the trace theorem we can state that for a two-dimensional problem, if the solution is assumed to be in $\mathcal{H}^1(\mathbb{R}^2)$ then it cannot have any negative power singularities.

A second useful result based on Hilbert spaces concerns the existence and uniqueness of a solution to a variational inequality. Suppose V is a real Hilbert space with an inner product and associated norm. Further suppose $a(.,.) : V \times V \to \mathbb{R}$ is a continuous bilinear form and there exists a constant $\beta \geq 0$ such that

$$|a(u,v)| \quad \leq \quad \beta||u||||v|| \qquad \forall\, u, v \in V \quad .$$

Then we say $a(.,.)$ is coercive if there exists an $\alpha > 0$ such that

$$a(v,v) \quad \geq \quad \alpha||v||^2 \quad .$$

Next we define $l : V \to \mathbb{R}$ to be a continuous linear mapping so that there exists a γ such that

$$|l(v)| \quad \leq \quad \gamma||v|| \qquad \forall\, v \in V \quad .$$

Lastly we say W, a non-empty subset of V, is closed if any convergent sequence in W has its limit in W.

Then if $u \in W$ such that

$$a(u, v-u) \quad \geq \quad l(v-u) \qquad \forall\, v \in W \tag{A.4}$$

where $a(.,.)$ is a continuous coercive bilinear form, $l(.)$ is a continuous linear mapping and W is a closed convex non-empty subset of V then there exists a unique solution to (A.4). For the proof of this result see [17].

Appendix B

Riemann boundary value problems and index

The index of a function will prove to be a valuable tool in the solution of a Riemann problem. The index of a function $G(t)$ with respect to a contour L is defined to be the change in the argument of G on traversing L, divided by 2π. That is the index is given by

$$\kappa \;=\; \mathrm{Ind}G(t) \;=\; \frac{1}{2\pi}[\arg G(t)]_L \;=\; \frac{1}{2\pi i}[\ln G(t)]_L \;\; .$$

If $G(t)$ denotes the boundary value of a function analytic in L and $G(t)$ is differentiable then it can be shown that

$$\kappa \;=\; \frac{1}{2\pi i}\int_L \frac{G'(t)}{G(t)}dt \;\; .$$

Also if $G(t)$ is analytic in L, where L is now a closed curve, then its index is simply given by the number of zeros inside L. If, however, $G(t)$ is only analytic inside L except for a finite number of poles then the index becomes the difference between the number of zeros and number of poles, where each is counted according to multiplicity. Another useful fact is that the index of the product of two functions is equal to the sum of the indices of both functions. Lastly we note that if $G(t)$ is defined outside a closed contour L then its index is simply the number of poles minus the number of zeros.

In the solution of the Riemann problem we shall continually call upon the concept of analytic continuation. Suppose two domains D_1 and D_2 have a common smooth boundary L and functions $f_1(z)$ and $f_2(z)$ are defined in D_1 and D_2, respectively. If as z tends to L from both sides f_1 and f_2 tend to the same continuous function then f_1 and f_2 are said to be the analytic continuations of each other. Another useful

result will be Liouville's theorem which concerns functions $f(z)$ analytic in the entire plane except at the points $a_0 = \infty$, $a_1, \ldots, a_n$ where it has poles. If we suppose that near these poles $f(z)$ takes the form

$$\begin{aligned} G_0(z) &= c_1^0 z + c_2^0 z^2 + \ldots + c_{n_0}^0 z^{n_0} \qquad \text{near} \quad a_0 \\ G_k\left(\frac{1}{z-a_k}\right) &= \frac{c_1^k}{z-a_k} + \frac{c_2^k}{(z-a_k)^2} + \ldots + \frac{c_{m_k}^k}{(z-a_k)^{m_k}} \quad \text{near} \quad a_k \quad , \quad k = 1, \ldots, n \end{aligned}$$

then the function $f(z)$ is a rational function and is representable in the form

$$f(z) = C + G_0(z) + \sum_{k=1}^{n} G_k\left(\frac{1}{z-a_k}\right) \quad .$$

In particular, if the only singularity of $f(z)$ is a pole of order m at infinity then $f(z)$ is a polynomial of degree m.

B.1 The Riemann problem for a simply connected domain

Suppose L is a simple smooth curve dividing the complex plane into an interior domain D^+ and an exterior domain D^-. A function $\psi(t)$ satisfies a Hölder condition on a curve L if there are constants A and λ such that

$$|\psi(t_2) - \psi_(t_1)| < A|t_2 - t_1|^\lambda \tag{B.1}$$

for two arbitrary points t_1 and t_2 on L where A and λ are positive numbers. A is called the Hölder constant and λ the Hölder index. If λ were greater than one (B.1) would imply that $\psi'(t) = 0$ on L and hence ψ would be a constant on L. Consequently we take $0 \leq \lambda \leq 1$ where if $\lambda = 1$ we have the familiar Lipschitz condition. The smaller λ is the wider the class of functions this condition allows. Further suppose two functions of position on L, $G(t)$ and $g(t)$ satisfy the Hölder condition, and $G(t)$ does not vanish.

We must determine the two functions $\Phi^+(z)$ and $\Phi^-(z)$ analytic in D^+ and D^-, respectively (alternatively this can be thought of as one sectionally analytic function $\Phi(z)$), which satisfy on L one of the following conditions:

$$\Phi^+(t) = G(t)\Phi^-(t) \qquad \text{homogeneous problem} \tag{B.2}$$

$$\Phi^+(t) = G(t)\Phi^-(t) + g(t) \qquad \text{non-homogeneous problem.} \tag{B.3}$$

The function $G(t)$ is called the coefficient of the Riemann problem and the function $g(t)$ its free term.

For the particular problem of Φ vanishing at infinity and satisfying

$$\Phi^+(t) - \Phi^-(t) \;=\; \psi(t) \qquad \text{on} \quad L$$

we have the well known Plemelj formulae (see [24] p25, sometimes called the Sokhotski formulae) giving

$$\Phi(z) \;=\; \frac{1}{2\pi i}\int_L \frac{\psi(\tau)}{\tau - z}d\tau \;\; .$$

This solution is clearly unique since considering the difference of two such solutions gives a function with a zero jump on L and so it is analytic in the entire complex plane and zero at infinity. Hence by Liouville's theorem the solution is identically zero. If the condition that $\Phi^-(\infty) = 0$ is dropped then a constant is simply added to the solution above.

B.1.1 Solution of the homogeneous problem

Denoting the number of zeros of $\Phi^+(z)$ and $\Phi^-(z)$ by N^+ and N^- then taking the index of (B.2) we see

$$N^+ + N^- \;=\; \mathrm{Ind}G(t) \;=\; \kappa \;\; .$$

The index κ of the coefficient of the Riemann problem is called the index of the problem. Clearly from above $\kappa > 0$, thus for the homogeneous Riemann boundary value problem to be solvable the index of the problem must be non-negative (having assumed $\Phi^+(z)$ and $\Phi^-(z)$ have no poles). Also we can see that if $\kappa = 0$, $\Phi^+(z)$ and $\Phi^-(z)$ have no zeros.

Case $\kappa = 0$

In this case $\ln G(t)$ is a singled valued function and $\ln \Phi^+(z)$ and $\ln \Phi^-(z)$ are analytic. Thus taking the logarithm of (B.2) yields

$$\ln \Phi^+(t) - \ln \Phi^-(t) \;=\; \ln G(t) \;\; .$$

The problem is now of the form already solved and so if $\ln \Phi^-(\infty) = 0$ the solution is

$$\Gamma(z) \;=\; \ln \Phi(z) \;=\; \frac{1}{2\pi i}\int_L \frac{\ln G(\tau)}{\tau - z}d\tau \;\; . \tag{B.4}$$

Hence for $\Phi^-(\infty) = 1$

$$\Phi^+(z) \;=\; e^{\Gamma^+(z)} \qquad , \qquad \Phi^-(z) \;=\; e^{\Gamma^-(z)} \;\; .$$

If the condition at infinity is not imposed the solution contains an arbitrary constant multiplying the exponentials. Since $\Gamma^-(\infty) = 0$ this constant is simply the value of $\Phi^-(z)$ at infinity. Thus in the case $\kappa = 0$ if $\Phi^-(\infty) \neq 0$ the solution contains one arbitrary constant and in the case that $\Phi^-(\infty) = 0$ only the trivial solution of zero exists. A corollary of this is that in the case of $G(t)$ having zero index $G(t) = \Phi^+(t)/\Phi^-(t) = e^{\Gamma^+(z)}/e^{\Gamma^-(z)}$.

Case $\kappa > 0$

We assume the origin of the coordinate system lies in D^+ and write the boundary condition as

$$\Phi^+(t) \;=\; t^\kappa [t^{-\kappa} G(t)] \Phi^-(t) \;\; .$$

Since t^κ has index κ, $G_1(t) = t^{-\kappa} G(t)$ has index zero and thus from above we can write

$$G_1(t) \;=\; \frac{e^{\Gamma^+(t)}}{e^{\Gamma^-(t)}}$$

where

$$\Gamma(z) \;=\; \frac{1}{2\pi i} \int_L \frac{\ln[\tau^{-\kappa} G(t)]}{\tau - z} d\tau \;\; . \tag{B.5}$$

Consequently we can write the boundary condition as

$$\frac{\Phi^+(t)}{e^{\Gamma^+(t)}} \;=\; t^\kappa \frac{\Phi^-(t)}{e^{\Gamma^-(t)}} \;\; .$$

This implies $\Phi^+(z)/e^{\Gamma^+(z)}$ is analytic in D^+ and $z^\kappa \Phi^-(z)/e^{\Gamma^-(z)}$ is analytic in D^- except for a pole of order at most κ, and that they are each others analytic continuations through L. They are, therefore, branches of a unique analytic function which can only have a pole singularity at infinity of at most order κ. From Liouville's theorem we can hence state that this function is a polynomial of degree at most κ. The general solution is, therefore,

$$\Phi^+(z) \;=\; e^{\Gamma^+(z)} P_\kappa(z) \qquad , \qquad \Phi^-(t) \;=\; e^{\Gamma^-(z)} P_\kappa(z) z^\kappa \;\; .$$

From this result we can see that if the index of the problem is $\kappa > 0$ then the problem has $\kappa + 1$ linearly independent solutions, namely

$$\Phi^+(z) \;=\; z^k e^{\Gamma^+(z)} \quad , \quad \Phi^-(t) \;=\; z^{k-\kappa} e^{\Gamma^-(z)} \quad \text{for} \quad k = 0, \ldots, \kappa \;. \tag{B.6}$$

The solution is hence completely determined if $\kappa + 1$ independent conditions are imposed on $\Phi^+(z)$ and $\Phi^-(z)$. From (B.6) it follows that if we have the condition $\Phi^-(z) = 0$ then the coefficient of z^κ in $P_\kappa(z)$ is zero. Thus in this case the problem only has κ independent solutions.

The order of an analytic function at z_0 is the exponent of the lowest power in the expansion of $\Phi(z)$ as a power series in $(z - z_0)$. In the vicinity of infinity we form the expansion in powers of $1/z$. In this case the order at infinity is taken to be the exponent of the lowest power of $1/z$ in the expansion. The total order of an analytic function is defined to be the sum of its orders at all points in the domain. Thus the total order is the difference between the number of zeros and number of poles counted according to multiplicity. If we now admit solutions of the Riemann problem to have poles then the total order of the solution of the homogeneous solution is equal to the index of the problem.

The canonical function of the homogeneous Riemann problem is defined to be a sectional analytic function satisfying (B.2) and having zero order everywhere in the finite plane. At infinity its order is therefore κ. For $\kappa \geq 0$ the canonical function has no poles and so is a solution of the boundary value problem called the canonical solution. For $\kappa < 0$ the canonical function has a pole at infinity and is hence not a solution of the homogeneous Riemann problem. The canonical function is

$$X^+(z) \;=\; e^{\Gamma^+(z)} \quad , \quad X^-(z) \;=\; z^{-\kappa} e^{\Gamma^-(z)}$$

where Γ is as defined in (B.5). For $\kappa \geq 0$ the general solution of the homogeneous problem can therefore be expressed as $\Phi(z) = X(z)P_\kappa(z)$.

B.1.2 Solution of the non-homogeneous problem

Replacing $G(t)$ in (B.3) by the ratio of the boundary values of the homogeneous problem gives

$$\frac{\Phi^+(t)}{X^+(t)} \;=\; \frac{\Phi^-(t)}{X^-(t)} + \frac{g(t)}{X^+(t)}$$

where $g(t)/X^+(t)$ satisfies a Hölder condition. We further define

$$\Psi(z) \;=\; \frac{1}{2\pi i} \int_L \frac{g(\tau)}{X^+(\tau)(\tau - z)} d\tau \tag{B.7}$$

and hence

$$\frac{g(t)}{X^+(t)} = \Psi^+(t) - \Psi^-(t)$$

on the boundary. The boundary condition can therefore be expressed as

$$\frac{\Phi^+(t)}{X^+(t)} - \Psi^+(t) = \frac{\Phi^-(t)}{X^-(t)} - \Psi^-(t) \ .$$

Note for $\kappa \geq 0$ the function $\Phi^-(z)/X^-(z)$ has at infinity a pole and for $\kappa < 0$ a zero of order κ. Using similar arguments to those used for the homogeneous case we can say

Case $\kappa \geq 0$

$$\frac{\Phi^+(t)}{X^+(t)} - \Psi^+(t) = \frac{\Phi^-(t)}{X^-(t)} - \Psi^-(t) = P_\kappa(z)$$

and hence

$$\Phi(z) = X(z)[\Psi(z) + P_\kappa(z)] \ .$$

Case $\kappa < 0$

$$\frac{\Phi^+(t)}{X^+(t)} - \Psi^+(t) = \frac{\Phi^-(t)}{X^-(t)} - \Psi^-(t) = 0$$

which implies

$$\Phi(z) = X(z)\Psi(z) \ .$$

The expression for $\Phi^-(z)$ can have at worst a pole of order $-\kappa - 1$ at infinity since $X^-(z)$ has a pole of order $-\kappa$ there and $\Psi^-(z)$ has a zero of order one there. Thus if $\kappa < -1$ the non-homogeneous problem is in general insolvable. In order for it to possess a solution in this case certain solvability conditions must be satisfied. To determine these conditions we expand $\Psi^-(z)$ as a series valid near infinity,

$$\Psi^-(z) = \sum_{k=1}^{\infty} c_k z^{-k}$$

where

$$c_k = \frac{1}{2\pi i} \int_L \frac{g(\tau)\tau^{k-1}}{X^+(\tau)} d\tau \ .$$

For analyticity of $\Phi^-(z)$ at infinity it is necessary that the first $-\kappa - 1$ coefficients of the expansion of $\Psi^-(z)$ be zero. Hence we have $-\kappa - 1$ necessary and sufficient conditions for the non-homogeneous problem to possess an analytic solution when the index is negative, namely that $c_k = 0$ for $k = 1, \ldots, -\kappa - 1$.

B.2 Solution of the Riemann problem with discontinuous coefficients

As was the case for the continuous problem L is taken to be a closed contour. We now however suppose that the functions $G(t)$ and $g(t)$ satisfy a Hölder condition everywhere on L except at the points $t_1, \ldots, t_m$ where they have discontinuities. Defining $G(t_k+)$ to be the limit of G as t approaches t_k from above and similarly defining $G(t_k-)$ in the same manner, then we assume neither of these limits is zero. A solution will be sought in the class of functions which are integrable on the contour L, and hence solutions will be continuous in the Hölder sense everywhere except possibly $\{t_k\}_{k=1}^m$. At these points we may require the solution to be bounded, unbounded or a combination of both.

As with the continuous case we begin by considering the simplest case of $G(t) = 1$, such that the boundary condition is

$$\Phi^+(t) \;=\; \Phi^-(t) + g(t) \;\; . \tag{B.8}$$

We suppose $g(t)$ may have discontinuities of the first kind (that is jump discontinuities) or singularities of the form

$$g(t) \;=\; \frac{g^*(t)}{(t-t_k)^\gamma} \qquad \text{for} \quad \alpha = \Re\gamma < 1 \tag{B.9}$$

where $g^*(t)$ satisfies a Hölder condition. The solution is sought in the class of functions which vanish at infinity with the property that

$$|\Phi^\pm(t)| \;<\; \frac{C}{|t-t_k|^\alpha} \qquad \text{for} \quad \alpha < 1 \quad \text{on} \quad L \;\; .$$

By the Plemelj formulae the solution is

$$\Phi(z) \;=\; \frac{1}{2\pi i}\int_L \frac{g(z)}{(\tau - z)} d\tau \;\; .$$

At the points of discontinuities of the first kind of g, Φ has a logarithmic singularity and at points with singularities of the type (B.9) it has a singularity of the same type. This solution can be shown to be unique in a similar manner to the continuous case (see Gakhov [24]). If a solution is sought in a class of functions having at infinity a pole of order κ then a term $P_\kappa(z)$ is added to the above solution. In order to solve the general problem we shall convert it into a problem of the above form.

B.2.1 Reduction to a problem with continuous coefficients

Consider the homogeneous problem where $G(t)$ has only one point of discontinuity t_1. Setting

$$\gamma \;=\; \frac{1}{2\pi i}\ln\frac{G(t_1-)}{G(t_1+)} \tag{B.10}$$

we define

$$w^+(z) \;=\; (z-t_1)^\gamma \qquad , \qquad w^-(z) \;=\; \left(\frac{z-t_1}{z-z_0}\right)^\gamma$$

where the complex plane has been cut from z_0 to infinity going through t_1. The section of the cut from z_0 to t_1 lies completely in D^+. We next introduce functions $\Phi^\pm(z)$ satisfying

$$\Phi^\pm(z) \;=\; w^\pm(z)\Phi_1^\pm(z) \tag{B.11}$$

such that the boundary condition can be written in the form

$$\Phi_1^+(t) \;=\; G_1(t)\Phi_1^-(t) \tag{B.12}$$

where

$$G_1(t) \;=\; \frac{w^-(t)}{w^+(t)}G(t) \;\; .$$

Defining $\Omega(t) = w^-(t)/w^+(t) = (t-z_0)^{-\gamma}$ then $G_1(t) = \Omega(t)G(t)$. $G_1(t)$ is continuous on L including the point t_1 which can be seen from

$$\frac{G_1(t_1-)}{G_1(t_1+)} \;=\; \frac{\Omega_1(t_1-)}{\Omega_1(t_1+)}\frac{G(t_1-)}{G(t_1+)} \;=\; e^{-2i\pi\gamma}\frac{G(t_1-)}{G(t_1+)} \;=\; 1 \;\; ,$$

having made use of (B.10) and the fact that $\Omega(t_1-)$ and $\Omega(t_1+)$ lie on opposite sides of the cut for the function $(z-z_0)^\gamma$. We have therefore converted the discontinuous problem into a continuous one for which we already know the solution.

The behaviour of the solution of the homogeneous problem near the point of discontinuity t_1 depends on the behaviour of $w^+(z)$ and $w^-(z)$ which can be seen from (B.11). The behaviour of the functions $w^\pm(z)$ near t_1 is given by

$$(z-t_1)^\gamma \;=\; e^{\gamma\ln(z-t_1)} \;=\; r^\alpha e^{-\beta\theta}e^{i(\beta\ln r+\alpha\theta)}$$

where $z-t_1 = re^{i\theta}$ and $\gamma = \alpha + i\beta$. For $\alpha \neq 0$ the order of this expression depends only on α. If $\alpha > 0$ it has a zero of order α and if $\alpha < 0$ a pole of order $-\alpha$. For $\alpha = 0$

this quantity is bounded, but as $z \to t_1$ it does not tend to any limit. For $-1 < \alpha < 0$ the infinity at t_1 is of an integrable order. Since γ is defined by (B.10) the behaviour of $w^{\pm}(z)$ near t_1 depends upon the choice of the branch of the logarithm. This choice is made depending on the admissible class of solutions. If the solution is bounded near t_1 we require

$$0 \leq \Re\gamma \leq 1 \tag{B.13}$$

but if it is to have an integrable infinity we require

$$-1 < \Re\gamma < 0 \ . \tag{B.14}$$

If we denote by θ the increment of a branch of $G(t)$ in describing the contour L then we can see immediately that θ is the jump of the argument of $G(t)$ at the point of discontinuity, taken with positive sign. Hence, set

$$\frac{G(t_1-)}{G(t_1+)} = \rho e^{i\theta} \ .$$

Then from (B.10)

$$\gamma = \frac{1}{2\pi i} \ln \frac{G(t_1-)}{G(t_1+)} = \frac{\theta}{2\pi} - \kappa - \frac{i}{2\pi} \ln \rho$$

where the integer κ is chosen such that either (B.13) or (B.14) are satisfied. That is

$$\begin{aligned} 0 &\leq \frac{\theta}{2\pi} - \kappa < 1 \\ -1 &< \frac{\theta}{2\pi} - \kappa < 0 \ . \end{aligned}$$

Thus for the class of bounded solutions

$$\kappa = \left[\frac{\theta}{2\pi} \right] \tag{B.15}$$

and for the class of solutions unbounded near t_1

$$\kappa = \left[\frac{\theta}{2\pi} \right] + 1 \tag{B.16}$$

where $[x]$ denotes the greatest integer not exceeding x. Now the index of the problem defined by (B.12) is

$$\begin{aligned} \mathrm{Ind} G_1(t) &= \frac{1}{2\pi} [\arg G_1(t)]_L = \frac{1}{2\pi} \left([\arg \Omega(t)]_L + [\arg G(t)]_L \right) \\ &= \frac{1}{2\pi} \left(-2\pi \left(\frac{\theta}{2\pi} - \kappa \right) + \theta \right) \\ &= \kappa \ . \end{aligned}$$

κ is, therefore, the index of the problem and can be found from (B.15) or (B.16). Note if $\theta/2\pi$ is an integer only (B.15) can be satisfied and so t_1 must be a point at which the solution is to be bounded.

B.2.2 Solution of the homogeneous problem

Suppose that $G(t)$ has discontinuities at $t_1, \ldots, t_n$. Then we split the contour L into sections between t_k and t_{k+1}. We define arbitrarily at each point of the section the branch of $\arg G(t_k+)$ and at the end point of each section $\arg G(t_{k+1}+)$ will be obtained from the selected branch of $\arg G(t_k+)$ by a continuous change.

As in the previous section we set

$$\frac{G(t_k-)}{G(t_k+)} = \rho_k e^{i\theta_k} \qquad \text{for} \quad k = 1, \ldots, n$$

where θ_k is the jump of the argument at the point of discontinuity t_k taken with opposite sign. Again we set

$$\gamma_k = \frac{1}{2\pi i} \ln \frac{G(t_k-)}{G(t_k+)} = \frac{\theta_k}{2\pi} - \kappa_k - \frac{i}{2\pi} \ln \rho_k \ ,$$

where κ_k are given by (B.13) or (B.14), and define

$$\Phi^+(z) = \prod_{k=1}^{n} (z - t_k)^{\gamma_k} \Phi_1^+(z) \quad , \quad \Phi^-(z) = \prod_{k=1}^{n} \left(\frac{z - t_k}{z - z_0} \right)^{\gamma_k} \Phi_1^-(z) \ , \tag{B.17}$$

the cuts for the functions $(z - z_0)^{\gamma_k}$ passing through the points t_k of the contour. Substituting this into the homogeneous boundary condition we obtain

$$\Phi_1^+(t) = \prod_{k-1}^{n} (t - z_0)^{-\gamma_k} G(t) \Phi_1^-(t) \tag{B.18}$$

in which by definition the function $(t - z_0)^{-\gamma_k}$ has a jump in passing through the point t_k. It can be shown that the coefficient $G_1(t) = \prod_{k=1}^{n} (t - z_0)^{-\gamma_k} G(t)$ is continuous and hence we have again manipulated the problem into one with a continuous coefficient. Noting

$$\frac{((t_k-) - z_0)^{\gamma_k}}{((t_k+) - z_0)^{\gamma_k}} = e^{2\pi i \gamma_k}$$

then

$$\begin{aligned}
\mathrm{Ind} G_1(t) &= \frac{1}{2\pi} [\arg G_1(t)]_L = \frac{1}{2\pi} \sum_{k=1}^{n} [\arg G_1(t)]_{t_k}^{t_{k+1}} \\
&= \frac{1}{2\pi} \sum_{k=1}^{n} \left([\arg (t - z_0)^{\gamma_k}]_{t_k}^{t_{k+1}} + [\arg G(t)]_{t_k}^{t_{k+1}} \right) \\
&= \frac{1}{2\pi} \sum_{k=1}^{n} \left(-2\pi \left(\frac{\theta_k}{2\pi} - \kappa_k \right) + \theta_k \right) \\
&= \sum_{k=1}^{n} \kappa_k
\end{aligned}$$

and this is known as the index of the problem. To derive the general solution of the problem we must determine $\Phi_1(z)$ using the solution of the continuous problem developed earlier.

B.2.3 Solution of the non-homogeneous problem

Introducing functions $\Phi_1^{\pm}(z)$ as defined in (B.17) the boundary condition can be written as

$$\Phi_1^+(t) \;=\; \prod_{k=1}^{n}(t-z_0)^{-\gamma_k}G(t)\Phi_1^-(t) + \prod_{k=1}^{n}(t-t_k)^{-\gamma_k}g(t) \;\;.$$

Replacing the continuous coefficient by the ratio of the canonical functions we obtain

$$\frac{\Phi_1^+(t)}{X_1^+(t)} - \frac{\Phi_1^-(t)}{X_1^-(t)} \;=\; \frac{\prod_{k=1}^{n}(t-t_k)^{-\gamma_k}g(t)}{X_1^+(t)} \;\;.$$

But this is the same as problem (B.8) and so has solution

$$\frac{\Phi_1(z)}{X_1(z)} \;=\; \frac{1}{2\pi i}\int_L \frac{\prod_{k=1}^{n}(\tau-t_k)^{-\gamma_k}g(\tau)}{X_1^+(\tau)(\tau-z)}d\tau + P_\kappa(z)$$

where $P_\kappa = 0$ if $\kappa < 0$. Hence the solution to the current problem is

$$\Phi^+(z) \;=\; \prod_{k=1}^{n}(z-t_k)^{\gamma_k}X_1^+(z)[\Psi^+(z)+P_\kappa(z)] \tag{B.19}$$

$$\Phi^-(z) \;=\; \prod_{k=1}^{n}\left(\frac{z-t_k}{z-z_0}\right)^{\gamma_k}X_1^+(z)[\Psi^-(z)+P_\kappa(z)] \tag{B.20}$$

where

$$X_1^+(z) \;=\; e^{\Gamma^+(z)} \tag{B.21}$$

$$X_1^-(z) \;=\; (z-z_0)^{-\kappa}e^{\Gamma^-(z)} \tag{B.22}$$

$$\Gamma(z) \;=\; \frac{1}{2\pi i}\int_L \frac{\ln[(\tau-z_0)^{-\kappa}\prod_{k=1}^{n}(\tau-z_0)^{-\gamma_k}G(\tau)]}{\tau-z}d\tau \tag{B.23}$$

$$\Psi(z) \;=\; \frac{1}{2\pi i}\int_L \frac{\prod_{k=1}^{n}(\tau-t_k)^{-\gamma_k}g(\tau)}{X_1^+(\tau)(\tau-z)}d\tau \;\;. \tag{B.24}$$

As usual if we further require $\Phi^-(\infty)=0$ then P_κ is replaced by $P_{\kappa-1}$. Further note when $\kappa<0$ we have $-\kappa$ consistency conditions

$$\int_L \frac{\prod_{k=1}^{n}(\tau-t_k)^{-\gamma_k}g(\tau)}{X_1^+(\tau)}\tau^{j-1}d\tau \;=\; 0 \qquad \text{for} \;\; j=1,\ldots,-\kappa \;\;.$$

Also note that although z_0 appears explicitly in the solution it can be shown that any z_0 may be taken in general without changing the overall solution.

If we also have discontinuities in g as well as G then we must consider the case when they are distinct points from those of G and when they are not.

Suppose near $t_1^{'}, \ldots, t_m^{'}$ $g(t)$ takes the form

$$g(t) \;=\; \frac{g^*(t)}{(t-t_k^{'})^{\gamma_k^{'}}} \qquad \gamma_k^{'} = \alpha_k^{'} + i\beta_k^{'} \;\;,\;\; 0 \leq \alpha_k^{'} < 1$$

and near $t_1^{''}, \ldots, t_p^{''}$ it has discontinuities of the first kind. Then when they are all distinct from $t_1, \ldots, t_n$ the solution is as above except it has further singularities at the points of discontinuity of $g(t)$ of a logarithmic type at $t_i^{''}$ and at $t_i^{'}$ of the same type as the discontinuity. When some of these points of discontinuity coincide with some of the t_i we need to consider them further. Points of discontinuity of the first kind don't complicate the solution any more but when points of type $t_i^{'}$ coincide with points of type t_i more complicated singularities may occur which shall not be discussed here.

B.3 The Riemann problem for open contours

Let the contour L consist of the union of m simple, smooth, non-intersecting curves $L_1, \ldots, L_m$ the ends of which are a_k and b_k. As usual we must find Φ analytic in the entire plane except on L where it satisfies

$$\Phi^+(t) \;=\; G(t)\Phi^-(t) + g(t) \;\;.$$

We can formulate this problem as one of a closed curve with discontinuities and use the results of the previous section. We complete L with m arbitrary lines $L_1^{'}, \ldots, L_m^{'}$ so that one closed curve C is constructed. On the additional curves we require $\Phi^+(t) = \Phi^-(t)$. Hence the problem of an open contour can be regarded as that of the closed contour C such that

$$\Phi^+(t) \;=\; G_1(t)\Phi^-(t) + g_1(t)$$

where

$$G_1(t) \;=\; \begin{cases} G(t) & \text{on } L_k \\ 1 & \text{on } L_k^{'} \end{cases}$$

$$g_1(t) \;=\; \begin{cases} g(t) & \text{on } L_k \\ 0 & \text{on } L_k^{'} \end{cases} \;\;.$$

Now all we need do is apply the solution of the previous section. Set $G(a_k) = \rho_k e^{i\theta_k}$ and $G(b_k) = \rho_k^{'} e^{i(\theta_k + \Delta_k)}$ where Δ_k denotes the change of $\arg G(t)$ on L_k. θ_k, therefore, denotes the jump in $\arg G_1(t)$ at a_k and $\theta_k + \Delta_k$ the jump at b_k, taken with negative sign. Then

$$\begin{aligned} G_1(a_k-) &= 1 \quad , \quad G_1(a_k+) = \rho_k e^{i\theta_k} \\ G_1(b_k-) &= \rho_k^{'} e^{i(\theta_k+\Delta_k)} \quad , \quad G_1(b_k+) = 1 \end{aligned}$$

which implies

$$\frac{G_1(a_k-)}{G_1(a_k+)} = \frac{e^{-i\theta_k}}{\rho_k} \quad , \quad \frac{G_1(b_k-)}{G_1(b_k+)} = \rho_k^{'} e^{i(\theta_k+\Delta_k)} \ . \tag{B.25}$$

The value of θ_k at a_k will be taken in the range $-2\pi \leq \theta_k \leq 0$ if a solution bounded at a_k is required, and in the range $0 < \theta_k < 2\pi$ if the solution is required to be unbounded at a_k.

Setting

$$\begin{aligned} \gamma_k &= \frac{1}{2\pi i} \ln\left(\frac{e^{-i\theta_k}}{\rho_k}\right) = -\frac{\theta_k}{2\pi} + \frac{i}{2\pi} \ln \rho_k \\ \gamma_k^{'} &= \frac{1}{2\pi i} \ln\left(\rho_k^{'} e^{-i\theta_k}\right) = \frac{\theta_k + \Delta_k}{2\pi} - \kappa_k + \frac{i}{2\pi} \ln \rho_k^{'} \end{aligned}$$

where

$$\begin{aligned} \kappa_k &= \left[\frac{\theta_k + \Delta_k}{2\pi}\right] \qquad \text{if solution is bounded} \\ \kappa_k &= \left[\frac{\theta_k + \Delta_k}{2\pi}\right] + 1 \qquad \text{if solution is unbounded,} \end{aligned}$$

then the index of the problem is

$$\kappa = \sum_{k=1}^{m} \kappa_k \ .$$

As before we convert the problem into one with continuous coefficients by defining

$$\begin{aligned} \Phi^+(z) &= \prod_{k=1}^{m} (z-a_k)^{\gamma_k} (z-b_k)^{\gamma_k^{'}} \Phi_1^+(z) \\ \Phi^-(z) &= \prod_{k=1}^{m} \left(\frac{z-a_k}{z-z_0}\right)^{\gamma_k} \left(\frac{z-b_k}{z-z_0}\right)^{\gamma_k^{'}} \Phi_1^-(z) \end{aligned}$$

such that the boundary condition becomes

$$\Phi_1^+(t) = \prod_{k=1}^{m} (t-z_0)^{-\gamma_k} (t-z_0)^{-\gamma_k^{'}} G_1(t) \Phi_1^-(t) + \prod_{k=1}^{m} (t-a_k)^{-\gamma_k} (t-b_k)^{-\gamma_k^{'}} g_1(t) \tag{B.26}$$

The solution can now be generated in the usual way. It can be shown that the choice of additional curves L' does not affect the solution.

We shall next consider a simple example which will have the added benefit of providing results which will enable us to invert a Cauchy type integral.

Example

This example is the kind of problem which may occur in a codimension-two problem and the inversion results that we yield from it will be used regularly.

Suppose we have a contour L composed of m open curves on which $G(t) = -1$; then we can formulate the problem as

$$\Phi^+(t) \;=\; G_1(t)\Phi^-(t) + g_1(t)$$

where

$$\begin{aligned} G_1(t) &= \begin{cases} -1 & \text{on } L_k \\ 1 & \text{on } L_k' \end{cases} \\ g_1(t) &= \begin{cases} g(t) & \text{on } L_k \\ 0 & \text{on } L_k' \end{cases} \end{aligned}$$

and L' is the contour consisting of those curves used to close L. We shall consider the case of a solution unbounded at all the ends, bounded at some ends and unbounded at others and bounded at all ends.

Beginning with the solution unbounded at all ends we have

$$\begin{aligned} G_1(a_k-) &= 1 \quad , \quad G_1(a_k+) = -1 = e^{i\pi} \\ G_1(b_k-) &= -1 = e^{i\pi} \quad , \quad G_1(b_k+) = 1 \end{aligned}$$

from which we obtain

$$\frac{G_1(a_k-)}{G_1(a_k+)} \;=\; e^{-i\pi} \quad , \quad \frac{G_1(b_k-)}{G_1(b_k+)} \;=\; e^{i\pi} \;\; .$$

Hence

$$\gamma_k \;=\; \frac{1}{2\pi i}\ln e^{-i\pi} \;=\; -\frac{1}{2} \;\; .$$

From (B.25) we see that $\Delta_k = 0$ and hence $\kappa_k = [1/2] + 1 = 1$ and $\gamma_k' = -1/2$. Consequently the index

$$\kappa = \sum_{k=1}^{m} \kappa_k \;=\; m \;\; .$$

Thus from (B.26) the problem on the closed contour with a continuous coefficient is

$$\Phi_1^+(t) \;=\; \prod_{k=1}^{m}(t-z_0)^{\frac{1}{2}}(t-z_0)^{\frac{1}{2}}G_1(t)\Phi_1^-(t) + \prod_{k=1}^{m}(t-a_k)^{\frac{1}{2}}(t-b_k)^{\frac{1}{2}}g_1(t) \quad \text{(B.27)}$$

By definition one of the functions $(t-z_0)^{\frac{1}{2}}$ changes sign at a_k or b_k at which points $G_1(t)$ also changes sign. Hence we can see the discontinuity has been removed and hence

$$\prod_{k=1}^{m}(t-z_0)^{\frac{1}{2}}(t-z_0)^{\frac{1}{2}}G_1(t) \;=\; (t-z_0)^m \quad .$$

Defining

$$\begin{aligned} R(z) &= \prod_{k=1}^{m}(z-a_k)^{\frac{1}{2}}(z-b_k)^{\frac{1}{2}} \\ R_a(z) &= \prod_{k=1}^{m}(z-a_k)^{\frac{1}{2}} \\ R_b(z) &= \prod_{k=1}^{m}(z-b_k)^{\frac{1}{2}} \end{aligned}$$

then condition (B.27) can be written

$$\Phi_1^+(t) \;=\; (t-z_0)^m\Phi_1^-(t) + R(t)g_1(t) \quad .$$

Also using (B.21), (B.22) and (B.23) we obtain

$$X_1^+(z) \;=\; 1 \qquad , \qquad X_1^- \;=\; (z-z_0)^{-m} \quad .$$

Then from (B.19) and (B.20) the solution is

$$\Phi^+(z) \;=\; \Phi^-(z) \;=\; \frac{1}{R(z)}[\Psi(z) + P_m(z)]$$

where

$$\Psi(z) \;=\; \frac{1}{2\pi i}\int_L \frac{R(\tau)g(\tau)}{\tau - z}d\tau \quad .$$

As usual if we further require the solution to tend to zero at infinity then the polynomial of degree m is replaced by one of degree $m-1$.

If at any given ends the solution is instead required to be bounded the corresponding exponents γ are taken to be $1/2$ and the index of the problem decreases by one for each such point.

The solution bounded at the points a_k and unbounded at b_k takes the form

$$\Phi(z) \;=\; \frac{R_a(z)}{R_b(z)}\frac{1}{2\pi i}\int_L \frac{R_b(\tau)}{R_a(\tau)}\frac{g(\tau)}{\tau - z}d\tau$$

and has index zero while the solution bounded at all ends is

$$\Phi(z) \;=\; \frac{R(z)}{2\pi i}\int_L \frac{g(\tau)}{R(\tau)(\tau - z)}d\tau$$

and has index $-m$. In this case we require the consistency conditions

$$\int_L \frac{g(\tau)}{R(\tau)}\tau^{j-1}d\tau \;=\; 0 \qquad \text{for} \quad j = 1, \ldots, m$$

to all be satisfied.

B.4 Inversion of a Cauchy integral

In many codimension-two problems we will often be presented with a need to invert integral equations of the form

$$\frac{1}{\pi}\int_L \frac{\psi(\tau)}{\tau - t}d\tau \;=\; f(t) \tag{B.28}$$

where the contour L will be taken to be of the most general form of a collection of open curves. We can solve this problem by exploiting the results of the previous example.

First we define the analytic function

$$\Phi(z) \;=\; \frac{1}{2\pi i}\int_L \frac{\psi(\tau)}{\tau - z}d\tau \;\;.$$

From the Plemelj formulae we know

$$\frac{1}{\pi i}\int_L \frac{\psi(\tau)}{\tau - z}d\tau \;=\; \Phi^+(t) + \Phi^-(t)$$

which when we substitute (B.28) in we obtain the boundary value problem

$$\Phi^+(t) \;=\; -\Phi^-(t) - if(t) \;\;.$$

The solution of (B.28) can be deduced from the second of the Plemelj formulae

$$\psi(t) \;=\; \Phi^+(t) - \Phi^-(t) \;\;.$$

The branch of the function $R(z)$ defined in the previous section is chosen such that on the boundary

$$R^-(t) \;=\; -R^+(t) \;=\; -R(t)\ .$$

Consequently one last application of the Plemelj formulae yields

$$\begin{aligned}\Phi^+(t) &= \frac{1}{R(t)}\left[-\frac{i}{2}R(t)f(t) - \frac{1}{2\pi}\int_L \frac{R(\tau)f(\tau)}{\tau - t}d\tau + P_{m-1}(t)\right]\\ \Phi^-(t) &= -\frac{1}{R(t)}\left[\frac{i}{2}R(t)f(t) - \frac{1}{2\pi}\int_L \frac{R(\tau)f(\tau)}{\tau - t}d\tau + P_{m-1}(t)\right]\end{aligned}$$

from which we obtain

$$\psi(t) \;=\; -\frac{1}{\pi R(t)}\int_L \frac{R(\tau)f(\tau)}{\tau - t}d\tau + \frac{P_{m-1}(t)}{R(t)}\ . \tag{B.29}$$

Similarly it can be shown that in the case of a solution bounded at a_k and unbounded at b_k the solution is

$$\psi(t) \;=\; -\frac{R_a(t)}{\pi R_b(t)}\int_L \frac{R_b(\tau)}{R_a(t)}\frac{f(\tau)}{\tau - t}d\tau$$

while the solution bounded at all ends takes the form

$$\psi(t) \;=\; -\frac{R(t)}{\pi}\int_L \frac{f(\tau)}{R(\tau)(\tau - t)}d\tau$$

provided the conditions

$$\int_L \frac{f(\tau)}{R(\tau)}\tau^{j-1}d\tau \;=\; 0 \qquad \text{for} \quad j = 1, \ldots, m$$

are all satisfied.

B.5 The Riemann problem for a non-Hölder free term

All the different problems considered so far have a solution which relies upon the free term, $g(t)$, satisfying a Hölder condition (B.1), or possibly the modified condition (B.9) if it is discontinuous. When $g(t)$ doesn't satisfy either (B.1) or (B.9) the method can be easily modified provided there exists an integer $m > 0$ such that $g^{(-m)}(t)$ satisfies (B.9), where $g^{(-m)}(t)$ denotes the integral of g m times. Thus if we have the problem

$$\Phi^+(t) - \Phi^-(t) \;=\; g(t)$$

then we can integrate this condition m times to yield the new problem

$$\Phi^{+(-m)}(t) - \Phi^{-(-m)}(t) \;=\; g^{(-m)}(t) \;\; .$$

This is now a Riemann problem for $\Phi^{(-m)}(z)$ which has a free term which satisfies the necessary condition and hence the solution is

$$\Phi^{(-m)}(z) \;=\; \frac{1}{2\pi i}\int_L \frac{g^{(-m)}(\tau)}{\tau - z}d\tau \;\; .$$

Finally we can differentiate this m times to give

$$\Phi(z) \;=\; \frac{m!}{2\pi i}\int_L \frac{g^{(-m)}(\tau)}{(\tau - z)^{m+1}}d\tau \;\; .$$

We note further that if $\Phi(\infty) = 0$ then $\Phi^{(-m)}(\infty) \sim z^{m-1}$. That is it can have a pole at infinity of order $m-1$. Thus if we have an inversion problem to determine $g^{(-m)}$ we must take this into account by replacing $P_{\kappa-1}$ with $P_{\kappa-1+m}$.

Appendix C

The Stokes flow sintering matching condition

As mention in Section 5.2 the inner problem for the non-zero surface tension Stokes flow is somewhat complicated. As a consequence Morgan [58] suggested the following method to determine instead a condition that the codimension-two solution should match out to rather than one it should match in to.

He conjectures that the singular nature of the outer flow will be governed by some sort of dipole at the origin due to the two cusps and that this can be solved for by considering first the problem of a single cusp in Stokes flow at $(\epsilon d(t), 0)$, then adding to it an image at $(-\epsilon d(t), 0)$ and finally expanding the resulting formulae for small ϵ. His solution to his hypothetical problem is incorrect. Below we have systematically followed the method he suggests in a carefully considered asymptotic framework to determine the correct solution to the problem he posed which shows that this is not a valid method (i.e gives the wrong matching condition) for determining the matching condition between the outer and codimension-two regions.

C.1 Solution of Stokes flow with a cusp

C.1.1 Solution following the procedure suggested by Morgan

Morgan proposes that the singularity at the cusp can be included in the model by including a term $2\mathbf{i}\delta(x)\delta(y)$ in (5.1) to give

$$\nabla p \;=\; \nabla^2\mathbf{u} + 2\mathbf{i}\delta(x)\delta(y) \;\; .$$

To understand this reasoning consider the force in the x direction on a surface like that shown in Figure C.2.

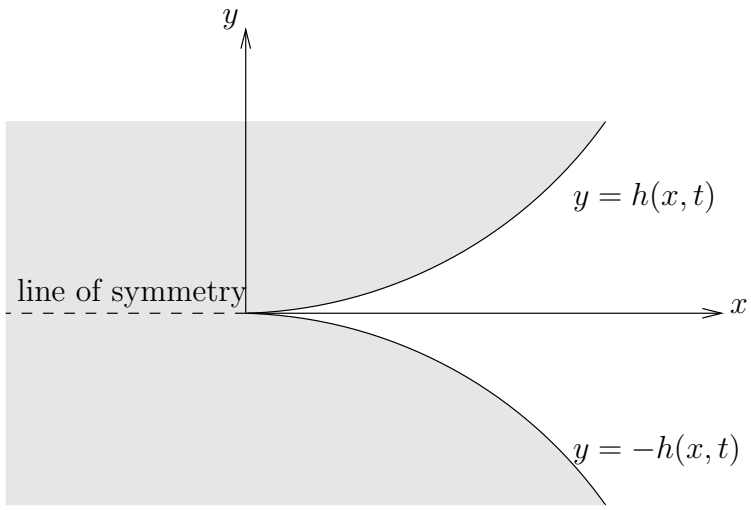

Figure C.1: The geometry of the cusp problem.

The force in the x direction is given by

$$\begin{aligned} F_x &= \int_{\text{tip}} -\kappa dy \\ &= \left[\frac{g_y}{\sqrt{1+g_y^2}}\right]_{\text{tip}} . \end{aligned}$$

Now Morgan considers the case $g(y) = y\tan\gamma$, where γ is the angle between the surface and y axis, which results in $F_x = 2\sin\gamma$. Taking the limit as $\gamma \to \pi/2$ closes up the wedge into a crack, which is the local shape of the free boundary as we scale in to the cusp, and results in a force $F_x = 2$ and hence the delta function term used. One could worry that considering a wedge shape which tends to a crack in the limit is not the same as our cusp. However, putting $g(y) = \sqrt{y/\alpha}$ instead and taking the limit for small y turns out to give the same result of $F_x = 2$ at the origin.

The resulting model we now have is

$$\nabla^4\psi + 2\delta(x)\delta'(y) = 0 \quad \text{in} \quad x<0\ ,\ y>0 \quad \text{and} \quad x>0\ ,\ y>h(x,t) \tag{C.1}$$

$$p_x - \psi_{xxy} - \psi_{yyy} = 0 \quad \text{in} \quad x<0\ ,\ y>0 \quad \text{and} \quad x>0\ ,\ y>h(x,t) \tag{C.2}$$

$$p_y + \psi_{xxx} + \psi_{xyy} = 0 \quad \text{in} \quad x<0\ ,\ y>0 \quad \text{and} \quad x>0\ ,\ y>h(x,t) \tag{C.3}$$

$$-p - 2\psi_{xy} + \frac{h_{xx}}{(1+h_x^2)^{\frac{3}{2}}} = h_x(\psi_{yy} - \psi_{xx}) \quad \text{on} \quad x>0\ ,\ y=h(x,t) \tag{C.4}$$

$$\left(-p + 2\psi_{xy} + \frac{h_{xx}}{(1+h_x^2)^{\frac{3}{2}}}\right) h_x = \psi_{yy} - \psi_{xx} \quad \text{on} \quad x>0\ ,\ y=h(x,t) \tag{C.5}$$

$$\psi_{xxx} + \psi_{xyy} = 0 \quad \text{on} \quad x<0\ ,\ y=0 \tag{C.6}$$

$$\psi_x = 0 \quad \text{on} \quad x<0\ ,\ y=0\ . \tag{C.7}$$

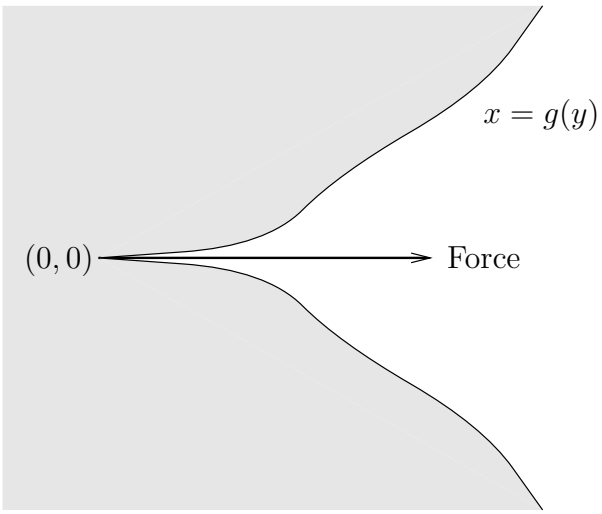

Figure C.2: The general geometry to explain the force at the cusp.

The last two boundary condition ensure that the solution is symmetrical in the y axis. We are interested in the solution locally near the cusp and thus scale our coordinates by defining $x = \hat{\epsilon}\hat{x}$ and $y = \hat{\epsilon}\hat{y}$, where $\hat{\epsilon} \ll 1$. In order for all terms to balance as in (C.1), (C.2) and (C.3), as Morgan implies they do, we scale $\psi = \hat{\epsilon}\hat{\psi}$ and $p = \hat{p}/\hat{\epsilon}$. The equation of the free boundary becomes $y = \alpha\hat{\epsilon}\hat{x}^2$, where α is a constant. With these scalings the model becomes, on dropping the hats,

$$\begin{aligned}
\nabla^4\psi + 2\delta(x)\delta'(y) &= 0 \qquad \text{in} \quad x<0 \;,\; y>0 \quad \text{and} \quad x>0 \;,\; y>\alpha\epsilon x^2 \\
p_x - \psi_{xxy} - \psi_{yyy} &= 0 \qquad \text{in} \quad x<0 \;,\; y>0 \quad \text{and} \quad x>0 \;,\; y>\alpha\epsilon x^2 \\
p_y + \psi_{xxx} + \psi_{xyy} &= 0 \qquad \text{in} \quad x<0 \;,\; y>0 \quad \text{and} \quad x>0 \;,\; y>\alpha\epsilon x^2 \\
-p - 2\psi_{xy} - 2\alpha\epsilon x(\psi_{yy} - \psi_{xx}) &= -2\alpha\epsilon(1 - 6\alpha\epsilon^2 x^2 + \ldots) \quad \text{on} \quad x>0 \;,\; y=\alpha\epsilon x^2 \\
\psi_{yy} - \psi_{xx} + \epsilon p - 2\epsilon\psi_{xy} &= 4\alpha^2\epsilon^2(1 - 6\alpha\epsilon^2 x^2 + \ldots) \quad \text{on} \quad x>0 \;,\; y=\alpha\epsilon x^2 \\
\psi_{xxx} + \psi_{xyy} &= 0 \qquad \text{on} \quad x<0 \;,\; y=0 \\
\psi_x &= 0 \qquad \text{on} \quad x<0 \;,\; y=0 \;.
\end{aligned}$$

Writing ψ and p as regular power series in ϵ and formally Taylor expanding the boundary conditions on the free surface we obtain the following leading order model:

$$\begin{aligned}
\nabla^4\psi_0 + 2\delta(x)\delta'(y) &= 0 \qquad \text{in} \quad y>0 \\
p_{0x} - \psi_{0xxy} - \psi_{0yyy} &= 0 \qquad \text{in} \quad y>0 \\
p_{0y} + \psi_{0xxx} + \psi_{0xyy} &= 0 \qquad \text{in} \quad y>0 \\
p_0 + 2\psi_{0xy} &= 0 \qquad \text{on} \quad y=0 \;,\; x>0 \\
\psi_{0yy} - \psi_{0xx} &= 0 \qquad \text{on} \quad y=0 \;,\; x>0
\end{aligned}$$

$$\begin{aligned}
\psi_{0xxx} + \psi_{0xyy} &= 0 \qquad \text{on} \quad y = 0 \quad , \quad x < 0 \\
\psi_{0x} &= 0 \qquad \text{on} \quad y = 0 \quad , \quad x < 0 \ .
\end{aligned}$$

The solution to this is found using separation of variables in polar coordinates or by taking a two-dimensional Fourier transform. The resulting solution when written back in cartesian coordinates is

$$\psi_0 = -\frac{1}{4\pi} y \log(x^2 + y^2) \tag{C.8}$$

$$p_0 = -\frac{1}{\pi} \frac{x}{x^2 + y^2} \ . \tag{C.9}$$

The next order problem is then

$$\begin{aligned}
\nabla^4 \psi_1 &= 0 \qquad \text{in} \quad y > 0 \\
p_{1x} - \psi_{1xxy} - \psi_{1yyy} &= 0 \qquad \text{in} \quad y > 0 \\
p_{1y} + \psi_{1xxx} + \psi_{1xyy} &= 0 \qquad \text{in} \quad y > 0 \\
p_1 + 2\psi_{1xy} &= 2\alpha \qquad \text{on} \quad y = 0 \quad , \quad x > 0 \\
\psi_{1yy} - \psi_{1xx} &= \frac{3\alpha}{\pi} \qquad \text{on} \quad y = 0 \quad , \quad x > 0 \\
\psi_{1xxx} + \psi_{1xyy} &= 0 \qquad \text{on} \quad y = 0 \quad , \quad x < 0 \\
\psi_{1x} &= 0 \qquad \text{on} \quad y = 0 \quad , \quad x < 0 \ .
\end{aligned}$$

The solution to this problem can also be found by separation of variables and is found to be

$$\begin{aligned}
\psi_1 &= -\frac{1}{4\pi} \left[4C\pi xy \log(x^2 + y^2) - 6\alpha y^2 - 4C\pi(1 - x^2 + y^2) \tan^{-1}\left(\frac{y}{x}\right) - 8D\pi xy \right] \\
p_1 &= 2C \log(x^2 + y^2) + 2\alpha + 4C - 4D \ ,
\end{aligned}$$

where C and D are constants. It is at this point we realise that our expansion in simple powers of ϵ was naive. We expect that on unscaling our variables the logarithmic terms should not involve ϵ. For this to happen we need $D = -C \log \epsilon$ which is equivalent to having chosen an expansion for ψ and p which included terms of order $\epsilon \log \epsilon$. Hence we have the solution

$$\begin{aligned}
\psi_1 &= -\frac{1}{4\pi} \left[4C\pi xy \log[\epsilon^2(x^2 + y^2)] - 6\alpha y^2 - 4C\pi(1 - x^2 + y^2) \tan^{-1}\left(\frac{y}{x}\right) \right] \\
p_1 &= 2C \log[\epsilon^2(x^2 + y^2)] + 2\alpha + 4C \ .
\end{aligned}$$

The solution shown is not that implied by Morgan and we therefore expect that if we continue with Morgan's method we will not generate the expected matching

condition for the codimension-two region. Continuing anyway we must rewrite the solution in outer variables, recentre the cusp at $x = \epsilon d(t)$, $y = 0$, add to it an image cusp at $x = -\epsilon d(t)$, $y = 0$, expand the resulting expression for small ϵ and then change back to inner variables to determine the implied matching condition. The result of all this is

$$\psi \;=\; -\frac{\epsilon d(t)}{\pi}\frac{xy}{x^2+y^2} - 4C\epsilon d(t)\epsilon^2 \log \epsilon y + O(\epsilon^2)$$

which is not the condition we know to be correct from the exact solution.

C.1.2 Direct method of obtaining the same result

The above solution can also be generated much more simply as follows. Simply start by putting the two cusp behaviour force at $x = \pm\epsilon d(t)$ into (5.1). That is the force term is

$$[\delta(x - \epsilon d(t))\delta(y) - \delta(x + \epsilon d(t))\delta(y)]\,\mathbf{i} \;\; .$$

This force term is then expanded for small ϵ yielding the leading order force

$$-2\epsilon d(t)\delta'(x)\delta(y)\mathbf{i}$$

from which we determine the field equation (in outer variables) to be solved is

$$\nabla^4\psi \;=\; 2\epsilon d(t)\delta'(x)\delta'(y) \;\; .$$

This is easily solved by taking a Fourier transform in both x and y. The resulting solution (in inner spatial variables) on inversion is

$$\psi \;=\; -\frac{\epsilon d(t)}{\pi}\frac{xy}{x^2+y^2}$$

which is the same as the leading order behaviour determined above.

This is essentially the technique used by Morgan [58] for an inviscid sintering problem and thus it seems curious that he used the more verbose method initially proposed.

Appendix D

The Ivantsov parabola

One of the problems considered by Ivantsov [41] is that shown in Figure D.1.

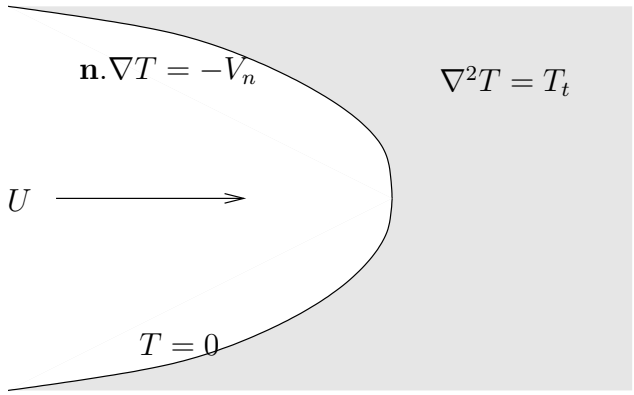

Figure D.1: The Ivantsov parabola problem.

To solve this problem is a simple matter of separating variables in parabolic coordinates. Firstly we move into a frame in which the parabola is stationary by defining $X = x - Ut$. Thus the field equation becomes

$$T_{XX} + T_{yy} + UT_X = 0 \ .$$

Defining new parabolic coordinates by

$$\begin{aligned} X &= \xi^2 - \eta^2 \\ y &= 2\xi\eta \end{aligned}$$

the field equation becomes

$$T_{\xi\xi} + T_{\eta\eta} + 2U(\xi T_\xi - \eta T_\eta) = 0 \ .$$

Looking for a solution of the form $T = T(\xi)$ this further simplifies to

$$T_{\xi\xi} + 2U\xi T_\xi = 0 \ .$$

Integrating twice we obtain

$$T(\xi) \;=\; A\int_{\xi_0}^{\xi} e^{-U\zeta^2}d\zeta$$

where the boundary has been taken to be the parabola $\xi = \xi_0$. All that remains is to find A by applying the kinematic condition, namely

$$\begin{aligned} -\mathbf{n}.\nabla T &= U\mathbf{i}.\mathbf{n} \qquad \text{on} \quad \xi = \xi_0 \\ \Rightarrow \quad -(\xi_0\ ,\ \eta).\frac{1}{2(\xi_0^2+\eta^2)}\left(A\xi_0 e^{-U\xi_0^2}\ ,\ A\eta e^{-U\xi_0^2}\right) &= U\xi_0 \\ \Rightarrow \quad A &= -2U\xi_0 e^{U\xi_0^2}\ . \end{aligned}$$

Hence the solution is

$$T \;=\; -2U\xi_0 e^{U\xi_0^2}\int_{\xi_0}^{\xi} e^{-U\zeta^2}d\zeta\ .$$

The Hele–Shaw cell problem is even easier. The problem is the same as that shown in Figure D.1 without the T_t term and with $T = p$ the pressure. Thus performing the same steps of changing to a moving frame and then further changing to parabolic coordinates yields the field equation

$$p_{\xi\xi} + p_{\eta\eta} \;=\; 0\ .$$

We again look for a solution of the form $p = p(\xi)$ which yields

$$p(\xi) \;=\; A(\xi - \xi_0)\ .$$

Applying the kinematic condition then gives $A = -2U\xi_0$ and hence

$$p(\xi) \;=\; -2U\xi_0(\xi - \xi_0)\ .$$

To change back into cartesian coordinates note

$$X \;=\; \xi^2 - \frac{y^2}{4\xi^2}$$

and hence

$$\xi \;=\; \frac{1}{\sqrt{2}}\left[X + (X^2+y^2)^{\frac{1}{2}}\right]^{\frac{1}{2}}$$

where the positive square root has been taken since as $\xi \to \infty$, $X \sim \xi^2$. Thus

$$p \;=\; -2\xi_0 U\left[\frac{1}{\sqrt{2}}\left[X + (X^2+y^2)^{\frac{1}{2}}\right]^{\frac{1}{2}} - \xi_0\right]$$

where

$$X = x - Ut$$

and the free boundary is given by

$$X = \xi_0^2 - \frac{y^2}{4\xi_0^2} \ .$$

The solution for p can be written neatly in terms of $z = X + iy$ by noting that for $X = r\cos\theta$ and $y = r\sin\theta$

$$\begin{aligned} \left[X + (X^2 + y^2)^{\frac{1}{2}}\right]^{\frac{1}{2}} &= \sqrt{2} r^{\frac{1}{2}} \cos\frac{\theta}{2} \\ &= \Re\sqrt{2z} \end{aligned}$$

and, therefore,

$$p = -2\xi_0 U \left[\Re\{\sqrt{z}\} - \xi_0\right] \ .$$

This is equivalent to solving the problem by using the simple complex variable map $z = \zeta^2$ which maps the domain to a half space with the boundary at $\Re\zeta = \xi_0$.

The above solution procedure is easily modified to include a second fluid lying inside the parabola moving at a constant velocity. In this case the problem is as shown in Figure D.2.

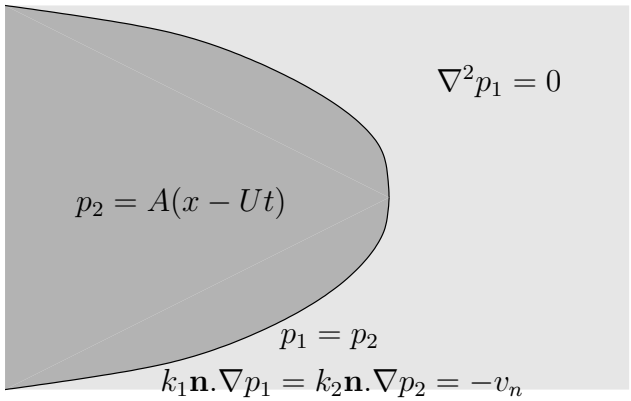

Figure D.2: The Ivantsov parabola problem with two fluids.

In parabolic coordinates we can write the solution as

$$\begin{aligned} p_1 &= A(\xi^2 - \eta^2) + B(\xi - \xi_0) \\ p_2 &= A(\xi^2 - \eta^2) \end{aligned}$$

which naturally satisfies the field equation and the continuity of pressure condition on the boundary. Further applying the other condition on the free boundary we obtain

$$\frac{1}{2}k_1 B + k_1 A\xi_0 \;=\; k_2 A\xi_0 \;=\; -U\xi_0$$

which we can solve for A and B to find

$$\begin{aligned} p_1 &= -\frac{U}{k_2}(\xi^2-\eta^2) - 2U\xi_0\left(\frac{1}{k_1}-\frac{1}{k_2}\right)(\xi-\xi_0) \\ p_2 &= -\frac{U}{k_2}(\xi^2-\eta^2)\ . \end{aligned}$$

Bibliography

[1] J.M. Aitchison. Percolation in gently sloping beaches. *IMA J. Appl. Math.*, **33**:17–31, 1984.

[2] G.I. Barenblatt. Concerning equilibrium cracks forming during brittle fracture: The stability of isolated cracks, relationship with energetic theories. *PMM Applied Mathematics and Mechanics*, **23**:1273–1282, 1959.

[3] G.I. Barenblatt. The formation of equilibrium cracks during brittle fracture: General ideas and hypotheses, axially symmetric cracks. *PMM Applied Mathematics and Mechanics*, **23**:622–636, 1959.

[4] G.I. Barenblatt. *Scaling, self-similarity, and intermediate asymptotics.* Cambridge texts in applied mathematics. Cambridge University Press, 1996.

[5] G.I. Barenblatt, R.L. Salganik, and G.P. Cherepanov. On the non-steady motion of cracks. *PMM Applied Mathematics and Mechanics*, **26**:469–477, 1962.

[6] G.K. Batchelor. *An Introduction to Fluid Mechanics.* Cambridge University Press, 1967.

[7] M.L. Blanpied and T.E. Tullis. The stability of a frictional system with a two state variable constitutive law. *Pageoph*, **124**:413–433, 1986.

[8] A. Bossavit, A. Damlamian, and M Frémond, editors. *Free Boundary Problems: Applications and Theory, Pitman Research Notes Math.*, **120,121**, London, 1985. Pitman.

[9] S.L. Ceccio and C.E. Brennen. Observations of the dynamics and acoustics of travelling bubble cavitation. *J. Fluid Mech.*, **233**:633–660, 1991.

[10] J.M. Chadam and M. Rasmussen, editors. *Emerging Applications in Free Boundary Problems, Pitman Reseacrch Notes Math.*, **280,281**. Longman, Harlow, 1993.

[11] R. Cointe and J.L. Armand. Hydrodynamic impact analysis of a cylinder. *J. Off. Mech. Arc. Eng.*, **107**:237–243, 1987.

[12] J. Crank. *Free and Moving Boundary Problems.* Clarendon Press, Oxford, 1984.

[13] C.W. Cryer. A bibliography of free boundary problems, technical summary report. Technical report, Math. Research Centre, N. 1793 Wisconsin, 1977.

[14] L. Cummings. The three cylinder problem in Hele–Shaw flow. private communication, 1997.

[15] J.H. Dieterich. Modeling of rock friction, 1. Experimental results and constitutive equations. *J. Geophys. Res.*, **84**:2161–2168, 1979.

[16] D.C. Dugdale. Yielding of steel sheets containing slits. *J. Mech. Phys. Solids*, **8**:100–104, 1960.

[17] C.M. Elliott and J.R. Ockendon. *Weak and Variational Methods*, **59**. Pitman Research Notes, London, 1982.

[18] A. Fasano and M. Primercero, editors. *Free Boundary Problems: Theory and Applications, Pitman Reseacrch Notes Math.*, **78,79**. Pitman, London, 1983.

[19] E. Fontaine and R. Cointe. A slender body approach to nonlinear bow waves. *Phil. Trans. Roy. Soc. Lon. A*, **355**:565–574, 1997.

[20] L. E. Fraenkel and J.B. McLeod. Some results for the entry of a blunt wedge into water. *Phil. Trans. Roy. Soc. Lon. A*, **355**:523–535, 1997.

[21] L.E. Fraenkel. On the method of mathced asymptotic expansions (parts I–III). In *Proceedings of the Cambridge Philosophical Society*, **65**, pages 209–284, 1969.

[22] L.B. Freund. *Dynamic Fracture Mechanics.* CUP, 1990.

[23] A. Friedman. *Variational Principles and Free Boundary Problems.* J. Wiley, New York, 1982.

[24] G.F. Gakhov. *Boundary Value Problems*, **85** of *International series of monographs in pure and applied mathematics.* Pergamon, 1966.

[25] J.W. Glasheen and T.A. McMahon. A hydrodynamic model of locomotion in the basilisk lizard. *Nature*, **380**:340–342, 1996.

[26] A.E. Green and W. Zerna. *Theoretical Elasticity.* Dover, 19668.

[27] M. Greenhow and S. Mayo. Water entry and exit of horizontal circular cylinders. *Phil. Trans. Roy. Soc. Lon. A*, **355**:551–563, 1997.

[28] A.A. Griffith. The phenomenon of rupture and flow in solids. *Phil. Trans. Roy. Soc. Lon. A*, **221**:163–198, 1920.

[29] H. Hertz. Über die berührung fester elastischer körper (On the contact of elastic solids). *J. reine und angewandte Mathematik*, **92**:156–171, 1882.

[30] H. Hertz. Über die berührung fester elastischer körper und über die harte (On the contact of elastic solids and on hardness). *Verhandlungen des Vereins zur Beförderung des Gewerbefleisses, Leipzig, Nov*, 1882.

[31] K.-H. Hoffman and J. Sprekels, editors. *Free Boundary Problems: Theory and Applications, Pitman Reseacrch Notes Math.*, **185,186**. Pitman, London, 1990.

[32] R.W. Hopper. Plane Stokes flow driven by capillarity on a free surface. *J. Fluid Mech.*, **213**:349–375, 1990.

[33] R.W. Hopper. Stokes flow of a cylinder and half-space driven by capillarity. *J. Fluid Mech.*, **243**:171–181, 1992.

[34] R.W. Hopper. Capillary-driven plane Stokes flow exterior to a parabola. *Q. J. Mech. Appl. Math.*, **46**:193–210, 1993.

[35] S.D. Howison. Codimension-two free boundary problems. In J. Chadam and H. Rasmussen, editors, *Proc. Int'l Colloquium on Free Boundary Problem.* Pitman, London, 1991.

[36] S.D. Howison, J.D. Morgan, and J.R. Ockendon. Codimension-two free boundary problems. *SIAM Review*, **39**(2):221–253, 1997.

[37] S.D. Howison, J.R. Ockendon, and S.K. Wilson. Incompressible water-entry problems at small deadrise angle. *J. Fluid Mech.*, **222**:215–230, 1991.

[38] S.D. Howison and S. Richardson. Cusp development in free boundaries, and two–dimensional slow viscous flows. *Euro. J. Appl. Math.*, **6**:441–454, 1995.

[39] B.J. Hunton. *Vortex Dynamics*. DPhil thesis, Oxford, 1994.

[40] G.R. Irwin. Analysis of stresses and strains near the end of a crack traversing a plate. *J. Appl. Mech.*, **24**:361–364, 1957.

[41] G.P. Ivantsov (Г. П. Иванцов). The temperature field around a spherical, cylindrical, or point crystal growing in a cooling solution (Температурное поле вокруг шарообразного, цилиндрического и иглообразного кристалла, растущего в переохлажденом расплаве). *Doklady Akademii Nauk SSSR (*Доклады Академии Наук СССР*)*, **58**:567–569, 1947. (In Russian).

[42] A. Jagota and P.R. Dawson. Simulation of the viscous sintering of particles. *J. Am. Ceramic Soc.*, **73**:173–77, 1990.

[43] K.L. Johnson. *Contact Mechanics*. Cambridge University Press, 1985.

[44] J.R. King, H. Ockendon, and J.R. Ockendon. The Laplace–Young equation near a corner. Submitted to Quart. J. Mech. Appl. Math., 1998.

[45] A.A. Korobkin. Formulation of penetration problem as a variational inequality. *Din. Sploshnoi Sredy*, **58**:73–79, 1982.

[46] A.A. Korobkin. Asymptotic theory of liquid–solid impact. *Phil. Trans. Roy. Soc. Lon. A*, **355**:507–522, 1997.

[47] A.A. Korobkin and V.V. Pukhnachov. Initial stages of water impact. *Ann. Rev. Fluid Mech.*, **20**:159–185, 1988.

[48] D.D. Kosloff and H.P. Liu. Reformulation and discussion of mechanical behaviour of the velocity dependent friction law proposed by Dieterich. *Geophys. Res. Lett.*, **7**:913–916, 1980.

[49] H.K. Kuiken. Viscous sintering: the surface–tension–driven flow of a liquid form under the influence of curvature gradients at its surface. *J. Fluid Mech.*, **214**:503–515, 1990.

[50] M.K. Kuo. Transient stress intensity factors for a cracked plane strip under anti-plane point forces. *Int. J. Eng. Sci.*, **30**:199–211, 1992.

[51] A.A. Lacey, S.D. Howison, J.R. Ockendon, and P. Wilmott. Irregular morphologies in unstable Hele-Shaw free-boundary problems. *Quart. J. Mech. Appl. Math.*, **43**:387–405, 1990.

[52] A.A. Lacey and A.B. Tayler. A mushy region in a Stefan problem. *IMA J. Appl. Math.*, **30**:303–313, 1983.

[53] H.W. Liepmann and A. Rosko. *Elements of Gas Dynamics*. Wiley, 1957.

[54] M.F. Linker and J.H. Dieterich. Effects of variable normal stress on rock friction: Observations and constitutive equations. *J. Geophys. Res.*, **97**:4923–4940, 1992.

[55] J.I. Martinez-Herrera and J.J. Derby. Analysis of capillary–driven viscous flows during the sintering of ceramic powders. *AIChE Journal*, **40**:1794–1803, 1994.

[56] R.D. Mindlin and H. Deresiewicz. Elastic spheres in contact under varying oblique forces. *J. Appl. Mech.*, **20**:327–344, 1953.

[57] M. Moghisi and P.T. Squire. An experimental investigation of the initial force of impact on a sphere striking a liquid surface. *J. Fluid Mech.*, **108**:133–146, 1981.

[58] J.D. Morgan. *Codimension-two free boundary problems*. DPhil thesis, Oxford, 1994.

[59] J.D. Morgan, D.L. Turcotte, and J.R. Ockendon. Models for earthquake rupture propagation. *Tectonophysics*, **277**:209–217, 1997.

[60] M. Muskat. Two fluid systems in porous media. The enchroachment of water into an oil sand. *Physics*, **5**:250–264, 1934.

[61] N.I. Muskhelishvili. *Some Basic Problems of the Mathematical Theory of Elasticity*. P. Noordhoff Ltd, 1953. (English translation by J.R.M. Radok).

[62] H. Nakanishi. Continuum model of mode-III crack propagation with surface friction. *Physics Review E*, **49**:5412–5419, 1994.

[63] F. Ng. *Mathematical Modelling of Subglacial Drainage and Erosion*. DPhil thesis, Oxford, 1998.

[64] M. Niezgodka and I. Pavlow. Recent advances in free boundary problems. *Control Cybernetics*, **14**:1–307, 1985.

[65] F. Nilsson. Dynamic stress-intensity factors for finite strip problems. *Int. J. Fract. Mech.*, **8**:403–411, 1972.

[66] D. Nowell, D.A. Hills, and A. Sackfield. Contact of dissimilar elastic cylinders under normal and tangential loading. *J. Mech. Phys. Solids*, **36**:59–75, 1988.

[67] J.R. Ockendon. A class of moving boundary problems arising in industry. In *Proc. Venice Conf. Appl. Ind. Math.* Kluwer Academic Publishers, 1991.

[68] J.R. Ockendon and W.R. Hodgkins. *Moving Boundary Problems in Heat Flow and Diffusion*. Clarendon Press, Oxford, 1975.

[69] P.G. Okubo. Dynamic rupture modeling with laboratory-derived constitutive relations. *J. Geophys. Res.*, **94**:12321–12335, 1989.

[70] K. O'Malley, A.D. Fitt, T.V. Jones, J.R. Ockendon, and P. Wilmott. Models for high Reynolds number flow down a step. *J. Fluid Mech.*, **222**:139–155, 1991.

[71] A. Prosperetti and H.N. Oguz. Surface-tension effects in the contact of liquid surfaces. *J. Fluid Mech.*, **203**:149–171, 1989.

[72] J.N. Reddy. *Applied Functional Analysis and Variational Methods in Engineering*. Keiger publishing company, 1991.

[73] R.L. Ricca. Rediscovery of da Rios equations. *Nature*, **352**:561–562, 1992.

[74] S. Richardson. Some Hele-Shaw flows with time-dependent free boundaries. *J. Fluid Mech.*, **102**:263–278, 1981.

[75] S. Richardson. Two–dimensional slow viscous flows with time–dependent free boundaries driven by surface tension. *Euro. J. Appl. Math.*, **3**:193–207, 1992.

[76] S. Richardson. Hele–Shaw flows with free boundaries driven along infinite strips by a pressure difference. *Euro. J. Appl. Math.*, **7**:345–366, 1996.

[77] J.C.W. Rogers and W.G. Szymczak. Computation of violent surface motion: comparison with theory and experiment. *Phil. Trans. Roy. Soc. Lon. A*, **355**:649–664, 1997.

[78] K.R. Rushton. Dynamic–relaxation solutions of elastic–plate problems. *J. Strain Anal.*, **3**:23–32, 1968.

[79] K.R. Rushton. Simply supported plates with corners free to lift. *J. Strain Anal.*, **4**:307–311, 1969.

[80] P.G. Saffman. *Vortex Dynamics*. CUP, 1992.

[81] N. Shimakura. *Partial Differential Operators of Elliptic Type*. American Mathematical Society, 1992.

[82] G.C. Sih, editor. *Methods of analysis and solution of crack problems*. Noordhoff Int., 1973.

[83] G.C. Sih and E.P. Chen. Moving cracks in a finite strip under tearing action. *J. Franklin Inst.*, **290**:25–35, 1970.

[84] I.N. Sneddon and D.S. Berry. *The classical theory of elasticity*. Springer–Verlag, 1958.

[85] I.N. Sneddon and R. Hill, editors. *Progress in Solid Mechanics*. North-Holland, 1963.

[86] I.N. Sneddon and M. Lowengrub. *Crack Problems in the classical theory of elasticity*. Wiley, 1969.

[87] I.S. Sokolnikoff. *Mathematical theory of elasticity*. McGraw–Hill, 1956.

[88] D.A. Spence. Self similar solutions to adhesive contact problems with incremental loading. *Proc. Roy. Soc.*, **305A**:55–80, 1968.

[89] D.A. Spence. The Hertz contact problem with finite friction. *J. Elasticity*, **5**:297–319, 1975.

[90] D.A. Spence. Frictional contact with transverse shear. *Quart. J. Mech. Appl. Math.*, **39**:233–253, 1986.

[91] D.A. Tarzia. A bibliography of moving-free boundary problems for the heat diffusion equation, 1988.

[92] S. Timoshenko and S. Woinowski-Kreiger. *Theory of Plates and Shells*. McGraw-Hill Book Co. Inc., 2nd edition, 1959.

[93] S.P. Timoshenko and J.N. Goodier. *Theory of elasticity*. McGraw–Hill, 3rd edition, 1970.

[94] W. Tollmien. Zum landestoß von seeflugzeugen. *Zeitschrift Für Angewandte Mathematik Und Mechanik*, **14**:251, 1934.

[95] J.R. Turner. The frictional unloading problem on linear elastic half-space. *J. Inst. Maths Applics*, **24**:439–469, 1979.

[96] G.A.L. Van de Vorst. Integral method for a two–dimensional Stokes flow with shrinking holes applied to viscous sintering. *J. Fluid Mech.*, **257**:667–689, 1993.

[97] G.A.L. Van de Vorst. Numerical simulation of axisymmetric viscous sintering. *Eng. Anal. with Boundary Elements*, **14**:193–207, 1994.

[98] G.A.L. Van de Vorst, R.M.M. Mattheij, and H.K. Kuiken. A boundary element solution for two–dimensional viscous sintering. *J. Comp. Phys.*, **100**:50–63, 1992.

[99] M. Van Dyke. *Perturbation methods in fluid dynamics*. Parabolic Press, annotated edition, 1975.

[100] H. Wagner. Über stoß- und gleitvorgänge an der oberfläche von flüssigkeiten (phenomena associated with impacts and sliding on liquid surfaces). *Zeitschrift Für Angewandte Mathematik Und Mechanik*, **12**:193–215, 1932.

[101] D.G. Wilson, A.D. Solomon, and P.T. Roggs, editors. *Moving Boundary Problems*. Academic Press, New York, 1978.

[102] S.K. Wilson. *The Mathematics of ship slamming*. DPhil thesis, Oxford, 1989.